Evaluation of Modified Binders

FINAL REPORT
September 2003

Submitted by

Mr. Thomas Bennert*
Research Engineer

Dr. Ali Maher*
Chairman and Professor

Dr. Nenad Gucunski,* Professor

* Dept. of Civil & Environmental Engineering
Center for Advanced Infrastructure & Transportation (CAIT)
Rutgers, The State University
Piscataway, NJ 08854-8014

NJDOT Research Project Manager
Mr. Anthony Chmiel

Disclaimer Statement

1. Report No.	2. Government Accession No.	3. Recipient's Catalog No.
FHWA-NJ-2003-017		

4. Title and Subtitle	5. Report Date
Evaluation of the Modified Binders	March, 2003
	6. Performing Organization Code
	CAIT/Rutgers

7. Author(s) Mr. Thomas Bennert, Dr. Ali Maher Dr. Nenad Gucunski	8. Performing Organization Report No.
	FHWA-NJ-2003-017

9. Performing Organization Name and Address	10. Work Unit No.
New Jersey Department of Transportation CN 600 Trenton, NJ 08625	
	11. Contract or Grant No.

12. Sponsoring Agency Name and Address	13. Type of Report and Period Covered
Federal Highway Administration U.S. Department of Transportation Washington, D.C.	Final Report 2/1/2000 – 1/31/2003
	14. Sponsoring Agency Code

15. Supplementary Notes

16. Abstract

The report pertains to the laboratory evaluation of hot mix asphalt modifiers (HMA-M). These modifiers are defined as materials that are added to hot mix asphalt (HMA) to improve its working capacity, whether for permanent deformation, fatigue/low temperature cracking, or both. The HMA-M is not a standard, approved material for the NJDOT. They are typically materials that customers bring to the NJDOT, with the understanding that the HMA-M would improve the working capacity of the HMA. However, the extent of the improvement is unknown. Therefore, a methodology to evaluate the extent of the improvement was necessary. And since the additives involved in this study claimed to aid in the rut resistance of the HMA, the performance testing focused on the mixes resistance to permanent deformation.

A total of six binders were evaluated in the study. Three of the binders were NJDOT approved materials and were used as baseline comparisons. They were a PG64-22 from Citgo, and a PG76-22 from both Citgo and Koch Materials. The three HMA-M evaluated in the study were; 1) Eastman's EE-2 polymer additive, 2) Creanova's Vestoplast polymer additive, and 3) Hydrocarbon Technology's Carbon Black. The HMA-M were added to the PG64-22 baseline sample by using the manufacturer's recommended procedures. This allowed for the direct comparison between the initial mix (PG64-22) and the modified mix. The two PG76-22 mixes were used as a high end comparison. All additives and binders were mixed to make a 12.5mm Coarse Superpave mix designed for heavy traffic (3 to 30 million ESAL's).

The compacted samples were tested in the APA (Asphalt Pavement Analyzer), Superpave Shear Tester (SST) under the Repeated Shear (RSCH), Frequency Sweep (FSCH), and Simple Shear (SSCH) test modes. The results showed that the SST test was extremely useful at evaluating the HMA-M for stiffness, creep, and permanent deformation. RSCH and APA results compared favorably, as did the FSCH and binder test results. The Creanova Vestoplast HMA-M ranked as the best HMA-M tested, however, the Vestoplast did not perform as well as the either of the PG76-22 mixes. An evaluation procedure and test parameters are recommended for future the use of evaluating HMA-M.

17. Key Words	18. Distribution Statement
Superpave Shear Tester, Asphalt Pavement Analyzer, Modified Binders, Short Term Oven Aged, Long Term Oven Aged	

19. Security Classif (of this report)	20. Security Classif. (of this page)	21. No of Pages	22. Price
Unclassified	Unclassified	213	

Form DOT F 1700.7 (8-69)

TABLE OF CONTENTS

LIST OF FIGURES

LIST OF SYMBOLS/ABBREVIATIONS

APA – Asphalt Pavement Analyzer
ESAL – Equivalent Single Axle Load
FSCH – Frequency Sweep at Constant Height
HMA – Hot Mix Asphalt
HMA-M – Hot Mix Asphalt Modifiers
LTOA – Long Term Oven Aged
NJDOT – New Jersey Department of Transportation
RAPL – Rutgers Asphalt/Pavement Laboratory
RSCH – Repeated Shear at Constant Height
SSCH – Simple Shear at Constant Height
SST – Superpave Shear Tester
STOA – Short Term Oven Aged
G* - Dynamic Shear Modulus
G' – Dynamic Shear Storage Modulus
G" – Dynamic Shear Loss Modulus
δ – Phase Angle of Asphalt Binder
ϕ – Phase Angle of Hot Mix Asphalt

ABSTRACT

This report pertains to the laboratory evaluation of hot mix asphalt modifiers (HMA-M). These modifiers are defined as materials that are added to hot mix asphalt (HMA) to improve its working capacity, whether for permanent deformation, fatigue/low temperature cracking, or both. The HMA-M is not a standard, approved material for the NJDOT. They are typically materials that customers bring to the NJDOT, with the understanding that the HMA-M would improve the working capacity of the HMA. However, the extent of the improvement is unknown. Therefore, a methodology to evaluate the extent of the improvement is necessary. And since the additives involved in this study claimed to aid in the rut resistance of the HMA, the performance testing focused on the mixes resistance to permanent deformation.

A total of six binders were evaluated in the study. Three of the binders were NJDOT approved materials and were used as baseline comparisons. They were a PG64-22 from Citgo, and a PG76-22 from both Citgo and Koch Materials. The three HMA-M evaluated in the study were; 1) Eastman's EE-2 polymer additive, 2) Creanova's Vestoplast polymer additive, and 3) Hydrocarbon Technology's Carbon Black. The HMA-M were added to the PG64-22 baseline sample by using the manufacturer's recommended procedures. This allowed for the direct comparison between the initial mix (PG64-22) and the modified mix. The two PG76-22 mixes were used as a high end comparison. All additives and binders were mixed to make a 12.5mm Coarse Superpave Mix designed for heavy traffic loads (3 to 30 million ESAL's). Individual mix designs were not conducted for each additive. The aim of the research was to evaluate materials that could be added directly into a pre-determined mix design.

The compacted samples were tested in the APA (Asphalt Pavement Analyzer), Superpave Shear Tester (SST) under the Repeated Shear (RSCH), Frequency Sweep (FSCH), and Simple Shear (SSCH) test modes, and Indirect Tensile test (IDT). The results showed that the SST test was extremely useful at evaluating the HMA-M for stiffness, creep, and permanent deformation. RSCH and APA results compared favorably, as did the FSCH and binder test results. The Creanova Vestoplast HMA-M ranked as the best HMA-M tested, however, the Vestoplast did not perform as well as the either of the PG76-22 mixes. The Hydrocarbon Technology's Carbon Black material performaed the worst, actually performing worse than the baseline PG64-22. A reason for this may be that the carbon black provided an over-asphalting affect on the mix. Therefore, if any future evaluation is to be necessary with carbon black material, it is recommended that the material not be used as an add-in additive, and a specific mix design be conducted for this material. The Superpave Shear Tester (SST) is recommended as the ideal evaluation tool since one sample can be evaluated for stiffness (FSCH), creep (SSCH), and permanent deformation (RSCH), although triplicate samples are recommended for proper analysis.

INTRODUCTION

The use of modified asphalt can serve a number purposes. It can target a specific improvement in the asphalt, such as permanent deformation (rutting) or low temperature cracking. The modified asphalt can also be aimed at improving the overall performance by increasing both the high and low performance grade of the asphalt. However, there needs to be a way to evaluate whether the performance of the modified asphalt is cost effective.

RESEARCH OBJECTIVES

The main goal of the research reported here was to evaluate the use of modified binders in a pre-determined hot mix asphalt design. The modified hot mix asphalt blends (HMA-M) were evaluated using a number of performance tests, while the binders were evaluated separately to determine a true performance grade. The testing was conducted on a total of six different binder types:

1. Citgo PG64-22
2. Citgo PG76-22
3. Koch Material PG76-22
4. Creanova's Vestoplast polymer added to a Citgo PG64-22
5. Eastman's EE-2 polymer added to a Citgo PG64-22
6. Hydrocarbon Technology's Carbon Black added to a Citgo PG64-22

All HMA-M were used and mixed according to the respective manufacturer's suggested procedures. After mixing and compaction in the Superpave gyratory compactor, the samples were tested at the Rutgers University Asphalt/Pavement Laboratory (RAPL) using the following:

1. Asphalt Pavement Analyzer (APA)
2. Superpave Shear Tester (SST) under the Repeated Shear at Constant Height (RSCH) test mode
3. Superpave Shear Tester (SST) under the Frequency Sweep at Constant Height (FSCH) test mode
4. Superpave Shear Tester (SST) under the Simple Shear at Constant Height (SSCH) test mode

In all, a total of 162 samples were tested under different temperature and loading configurations (constant, static, and cyclic). Also, samples were sent to the binder laboratory at Citgo Refinery in Paulsboro, NJ for performance grading. Based on the results from the testing, a test recommendation, as well as a test parameter recommendation, is to be made for future implementation for the evaluation of HMA-M materials in New Jersey.

LITERATURE SEARCH

A search of literature was conducted to define rutting and summarize the testing equipment and procedures used in this study. Also, typically used parameters from the individual tests are also included within this scope.

Permanent Deformation in Hot Mix Asphalt (Rutting)

Permanent deformation or rutting in hot mix asphalt (HMA) usually develops gradually as the number of loading applications increases. The rutting is a combination of the HMA compacting, or its decrease in volume, as well as deforming due to shear strain. Research conducted on test tracks by Hofstra and Klomp (1972) showed that rutting is more due to the shear deformation than volume change. Work performed by Eisenmann and Hilmer (1987) and revisited by Sousa et al. (1994) described the phenomena of rutting to be a two stage condition:

1) The first stage consists of irreversible deformation below the wheel loads being larger than the upheaval zones. This stage therefore is mainly due to increased compaction (decrease in air voids) under the wheel loads.
2) After stage 1, the volume decrease beneath the wheel loads equalizes with the volume increase in the upheaval zones. This illustrates that the air void decrease has essentially stopped and the HMA is being displaced with constant volume (any volume loss below wheel loads moves into the upheaval zones).

The general progression of rutting can be illustrated by following the decrease in air void content (Figure 1). As discussed before, stage 1 is mainly due to the compaction of the HMA. This is represented by the large curved section in figure 1. Stage 2 is represented by the linear portion of the figure. Stage 3, although not discussed earlier, is called tertiary flow. This is a condition when the air voids decreases approximately below 3% and the binder starts to act as a lubricant between the aggregates, reducing the contact pressures. At this point, the HMA has ultimately failed and the rutting will occur at a much quicker rate. Therefore, once compaction has finished in the pavement under the wheel loads, shear strains, caused primarily by large shear stresses in the upper portion of the HMA are dominant (Sousa et al., 1991). Since the compaction of the HMA is a natural phenomena that is inevitable in most HMA, it is the shear strains that a properly designed HMA must withstand. Actual field data from the WesTrack accelerated loading facility (Witzcak et al., 2002) also show this three stage evolution of rutting (Figure 2).

Asphalt Binder Influence on HMA

HMA is essentially a two part material consisting of both the asphalt binder and the aggregate skeleton. Each part, as well as the asphalt binder-aggregate interface, contributes to the HMA's resistance to permanent deformation. However, each part influences differently, and the asphalt binder's influence also changes with time.
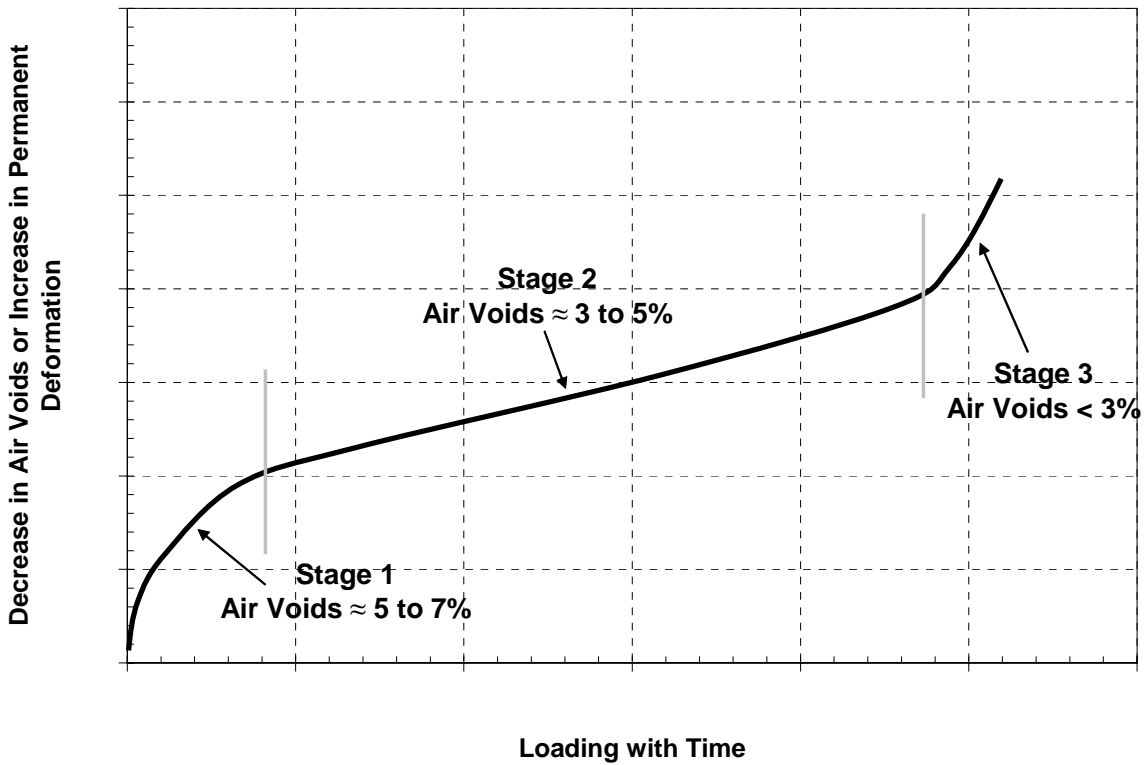
Figure 1 – Evolution of Permanent Deformation (Rutting) in HMA
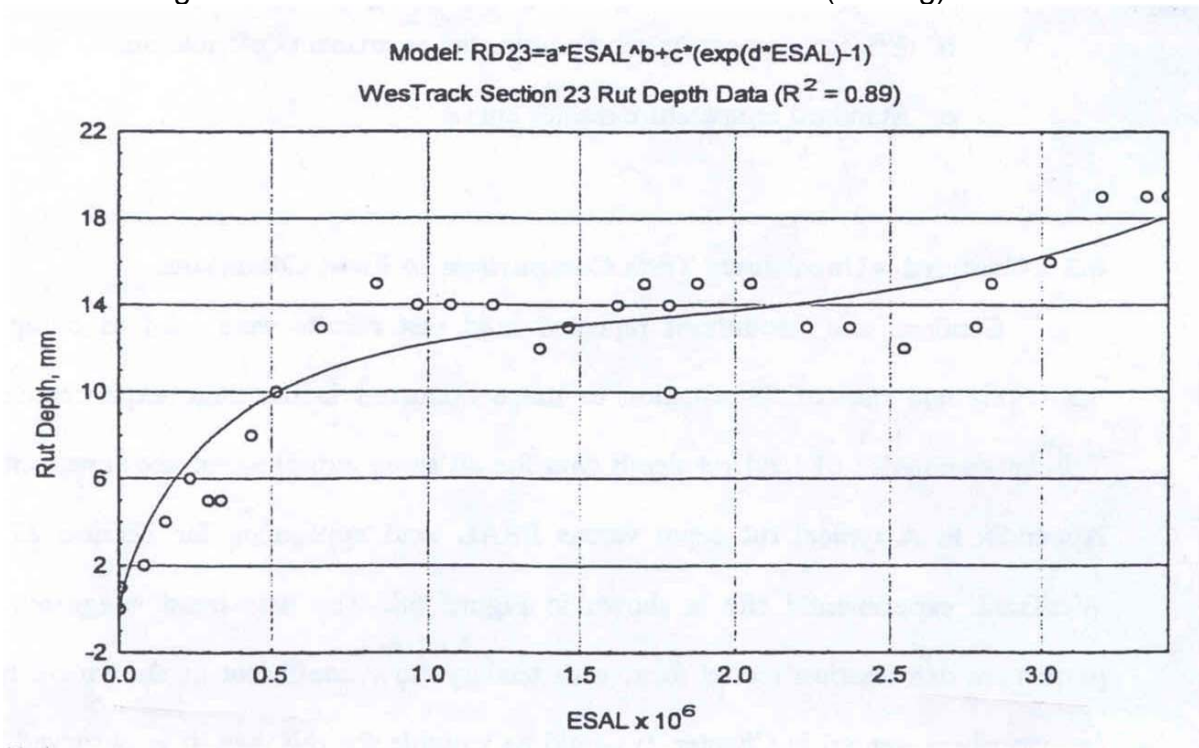
Figure 2 – Permanent Deformation at WesTrack

Temperature and Rate of Loading

It is well understood that the HMA is affected by both temperature and the rate of loading. Rutting is usually greatest when temperatures are at its highest and traffic is moving its slowest. This can be presented in master curves for dynamic modulus from a frequency sweep type test. However, by modifying the high temperature end binder grade, the effects on rutting can be minimized, or greatly reduced.

Asphalt Binder Age Hardening

The first significant type of hardening that occurs in the asphalt binder occurs at the plant during the mixing process. However, this can generally be simulated in the laboratory by allowing the loose mix to be conditioned in an oven for 2 hours prior to compaction, called Short Term Oven Aging (STOA). Original procedures developed by SHRP-A003A used 4 hours at 135 ^{o}C, however, this has recently been changed to 2 hours. Unfortunately, what is very difficult to simulate is the aging that occurs while the HMA is in service. Procedures for this, called Long Term Oven Aging (LTOA), were also developed under SHRP-A003A, however, attempts to correlate laboratory oven aging to field aging were not successful. Some of the factors that contribute to age hardening are (Roberts et al., 1994):

1. Oxidation
2. Volatilization
3. Polymerization
4. Thixotropy
5. Syneresis
6. Separation

Figure 3 show the affects of aging on the asphalt binder from the SHRP-A003A study. It is very clear that the stiffness (called dynamic modulus) increases with aging.

Aggregate Influence

The aggregate amount, as well as type, can significantly influence the permanent deformation characteristics. The SHRP researchers put a large emphasis on evaluating the different aggregates typically used for HMA design and construction and developed a number of different quality control tests. Reviewing these tests are beyond the scope of this report, however, more information on the quality control testing can be found in the FHWA publication FHWA-SA-95-003 entitled, "Background of Superpave Asphalt Mixture Design and Analysis. However, what will be reviewed are the direct influences that quality aggregates have on a properly designed HMA.

Dilation

The phenomenon of dilation accounts for the tendency of the HMA to develop confining stresses when subjected to shear strains (Figure 4). The dilation will actually aid in
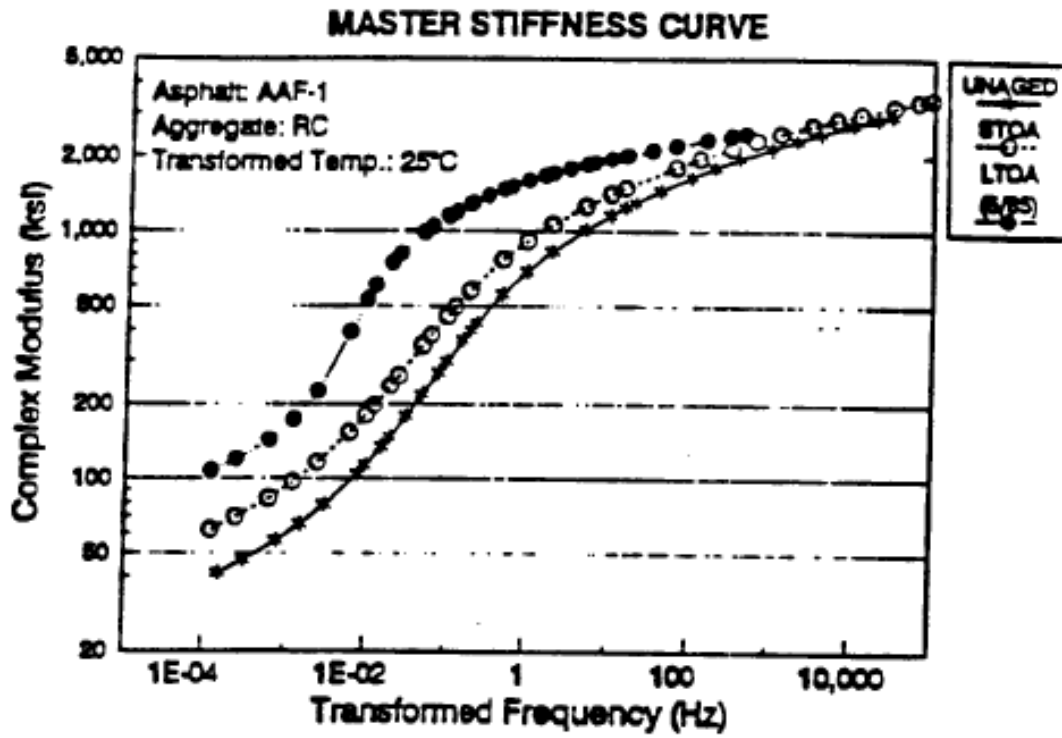
Figure 3 – Effect of Aging (Short Term and Long Term) on the Master Curve (Stiffness) of HMA
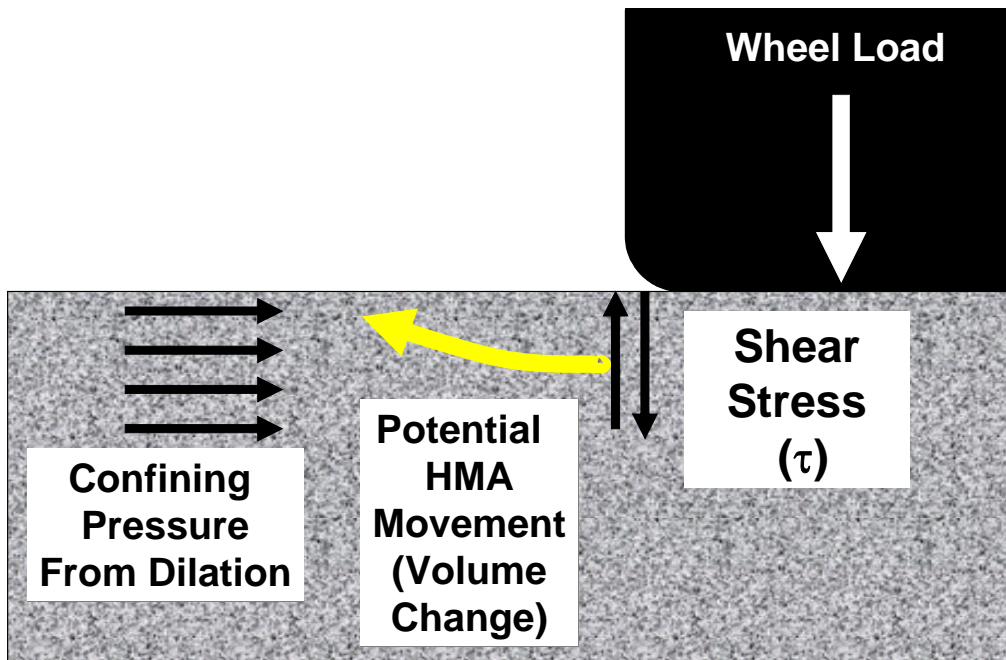
Figure 4 – Mechanism for Dilation to Occur in HMA

increasing the shear stiffness of the HMA by reducing some of the permanent deformation due to confinement. The dilatency can be mainly contributed to the aggregate particles trying to "roll" over or past one another during movement. Dilation can also be attributed to modified binders that exhibit rate dependent dilatency, however, it is mainly attributed to the aggregate structure (Sousa, et al. 1991).

Stress Hardening

Aggregates undergo stress hardening when a confining pressure is applied to the aggregate structure. As the confining pressure applied to the aggregate structure increases, the stiffness of the aggregate structure also increases, ultimately reducing the permanent deformation. The coupling behavior between the dilation and stress hardening is the primary cause of mix stability due to aggregate interlock (Sousa et al., 1994).

Air Void Content Influence

As discussed earlier, the permanent deformation of HMA can be traced along with the change in air voids. The reduction of air void content significantly increases the permanent deformation resistance in HMA. Figure 5 shows the results of an on-going research project at the Rutgers University Asphalt/Pavement Laboratory (RAPL). The results show rutting in the Asphalt Pavement Analyzer vs Air Void Content for a fine Superpave mix with a PG64-22 binder. It can clearly be seen that as the air void content of the samples increased, so did the rutting. What can also be seen from the figure is that stage 1 (densification of HMA) is greatly affected by the air voids. The samples of 2.4%, 6.0% and 8.9% air voids have almost identical slopes within stage 2. This provides evidence that once the initial compaction finishes, the samples accumulate permanent deformation at comparable rates. Meanwhile, the 10.3% air void sample seemed to still be undergoing densification at the end of the 20,000 loading cycles. Although the 2.4% air void achieved the lowest amount of rutting in the APA testing, one would not want to place the HMA at that air void content since the material would be highly susceptible to both bleeding and tertiary flow in the future.

A national study conducted by NCAT (Brown and Cross, 1992) evaluated the rutting of 42 in-service pavements in 14 states. A summary of the conclusions from the study are:
1) An in-place air void content of 3% or more is needed to decrease the probability of rutting due to the potential of tertiary flow occurring; and
2) Asphalt mixes must be placed in a void content significantly higher than 3% (usually 5 to 7%) since the HMA will naturally compact. After the compaction stage has completed, the HMA needs to be above 3% for stability.

The work of Wambura et al. (1999) is also in agreement with the 3% limit after secondary compaction by traffic (Stage 1).
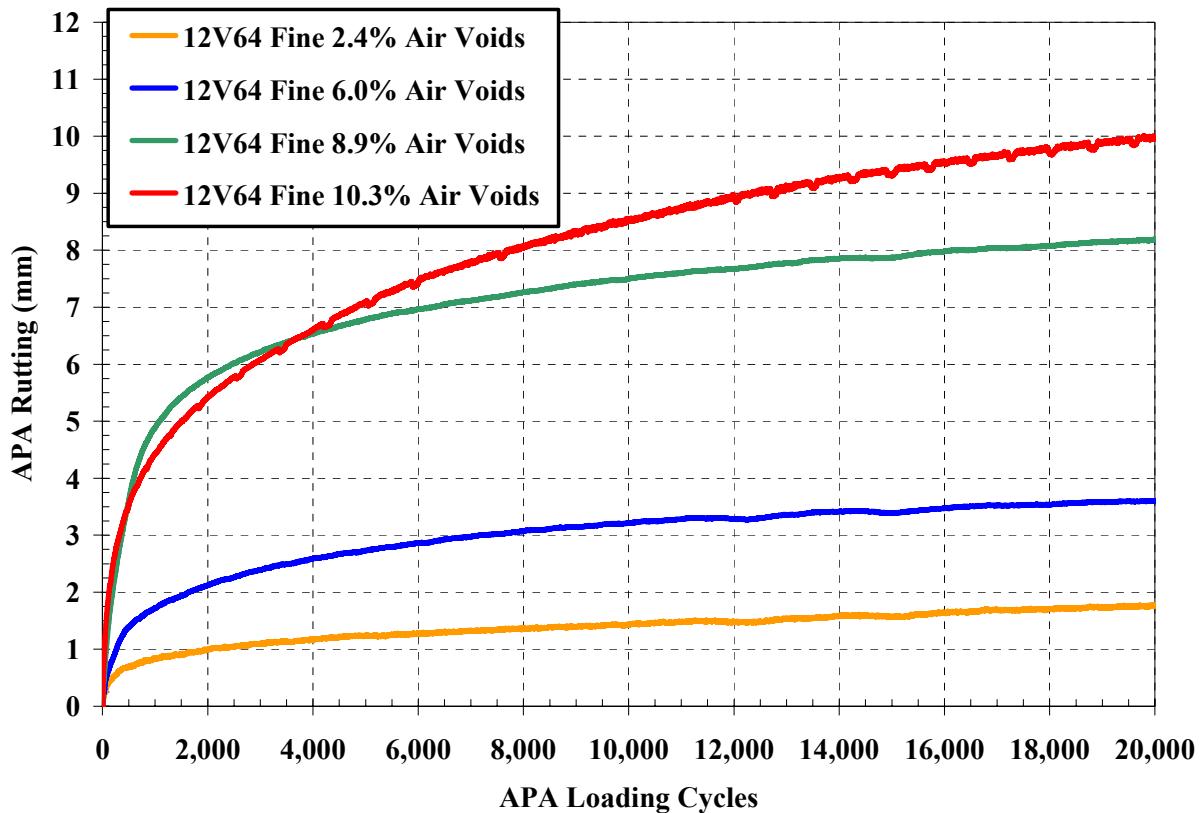
Figure 5 – Rutting vs Air Void Content from Laboratory Testing in the Asphalt Pavement Analyzer

Further work conducted at NCAT (Hanson et al., 1994) looked at the densification (change of air voids over time) of five in-service pavements five year after construction. Conclusions from their work showed:

1) The densification of the pavement continued beyond two years after construction;
2) Sections with higher initial (at construction) air voids had a higher rate of void change (rutting); and
3) Most cases showed that after five years, the in-place air voids were less than the design air voids (4%);

It can be seen that the air void content plays a significant role in the development of permanent deformation during the life of the pavement.

HMA Tests Used in Study

A comparison and correlation of various parameters, such as permanent strain, creep strain, stiffness', slopes and intercepts from log and power law regressions, from a number of different tests were used to aid in evaluating the influence of modified binders on HMA. The tests used were fundamental, simulative, and empirical in nature. A

fundamental test is one that evaluates the properties of the material that are known to influence its behavior. The test utilized in this manner was the Superpave Shear Tester (SST), under 3 different test modes:

1. Repeated Shear at Constant Height
2. Frequency Sweep at Constant Height
3. Simple Shear at Constant Height

Simulative tests are tests that mimic the type of loading for which the material typically experiences. The test utilized in this manner was the Asphalt Pavement Analyzer (APA). The previous two types of tests are in contrast to the empirical type of test. This test does not evaluate the true material properties nor does it mimic the actual loading the material undergoes. The empirical test is typically a test that measures a strength index of the material, such as the Marshall Stability or Flow. However, in this report, the Indirect Tensile Test, which is almost identical to the Marshall Stability, was used for conditioned and unconditioned samples.

Superpave Shear Tester (SST)

In 1987, SHRP began a 5 year, $50 million study to address and provide solutions to the performance problems of HMA pavements in the United States (FHWA-SA-95-003, 1995). As part of the study, the Superpave Shear Tester (SST) was developed to become the performance test used in the mix design process. The initial testing required a total of 6 different test (AASHTO M-003, Determining the Shear and Stiffness Behavior of Modified and Unmodified Hot Mix Asphalt in the Superpave Shear Test). The tests included:

1. Uniaxial
2. Hydrostatic
3. Frequency Sweep at Constant Height (FSCH)
4. Simple Shear at Constant Height (SSCH)
5. Repeated Shear at Constant Stress Ratio (RSCSR)
6. Repeated Shear at Constant Height (RSCH)

The first two tests, as well as the Simple Shear, were mainly used for modeling purposes within the Superpave modeling program. However, inaccuracies within the results of the computer analysis, as well test complexities, resulted in eliminating three of the tests. The test now only utilizes the SSCH, FSCH, and RSCH modes (AASHTO TP7-01).

The development and selection of the Superpave Shear Tester (SST) by the SHRP researchers was based on the device having the capability of measuring properties under states of stress that are encountered within the entire rutting zone of the pavement, particularly near the surface. Since there are an infinite number of states of stress that could exist within the pavement, it would be impossible to truly simulate all of

them considering the non-linear and viscous behavior of HMA. Realizing this (Sousa et al., 1993) the SHRP researchers concentrated on the most important aspects and simulative conditions of the HMA behavior.

The following summary of factors which significantly affect the behavior of HMA was taken from the SHRP research product entitled, *Accelerated Performance-Related Tests for Asphalt-Aggregate Mixes and Their Use in Mix Design and Analysis Systems, SHRP-A-417.*

1. Specimen Geometry: a) A six inch by 2 inch specimen can easily be obtained from any pavement section by coring, or from any typical compaction method; b) the state of stress is relatively uniform for the loads applied; c) the magnitude of loads needed to be applied can easily be achieved by the use of normal hydraulic equipment.
2. Rotation of Principle Axis: The test set-up permits the controlled rotation of principal axes of strain and stress which represent the conditions that impact rutting.
3. Repetitively Applied Loads: Work by the SHRP researchers has indicated that to accurately capture the rutting phenomena, repetitive loads are required. This type of loading is needed given the viscous nature of the binder (load frequency dependent) and also granular nature of the aggregate (aggregates behave differently under static and dynamic loading).
4. Dilation: As discussed earlier, the dilation plays an important role in the rutting behavior of HMA. The SST constrains the dilation, and by doing so, confining stresses are developed. It is in part due to the development of these confining stresses that a mix derives most of its stability against rutting. The SST allows this by implying a constant height on the specimen while under going a shear stress. In the constant height regime, the development of axial stresses (confining stress in the SST) is fully dependent on the dilatency characteristics of the HMA. A vertical LVDT is positioned on the specimen to measure the dilation. This in turn props the axial actuator to either create a compressive or tensile force on the sample, depending on the volume change characteristic of the specimen. In this configuration, the HMA will either resist permanent deformation by relying on the high binder stiffness to minimize shear strains or the aggregate structure stability developed by the axial stresses from the dilation. In the constant height test, these two mechanisms are free to fully develop their relative contribution to the resistance of permanent deformation.

The SST system used in the testing was fabricated by Interlaken Technologies Corp. It consists of two orthogonal tables which are mounted on bearing. The tables are connected to two hydraulic actuators which are controlled using servo-values under a feedback closed-loop system (Figure 6, 7, and 8). To insure that the shear and axial forces are transmitted to the specimen, aluminum caps are glued to the parallel faces of the specimen. The gluing device used with this system was again fabricated by Interlaken Technologies Corp. Hydraulic clamps are then used to securely fasten the glued caps to SST test platens.
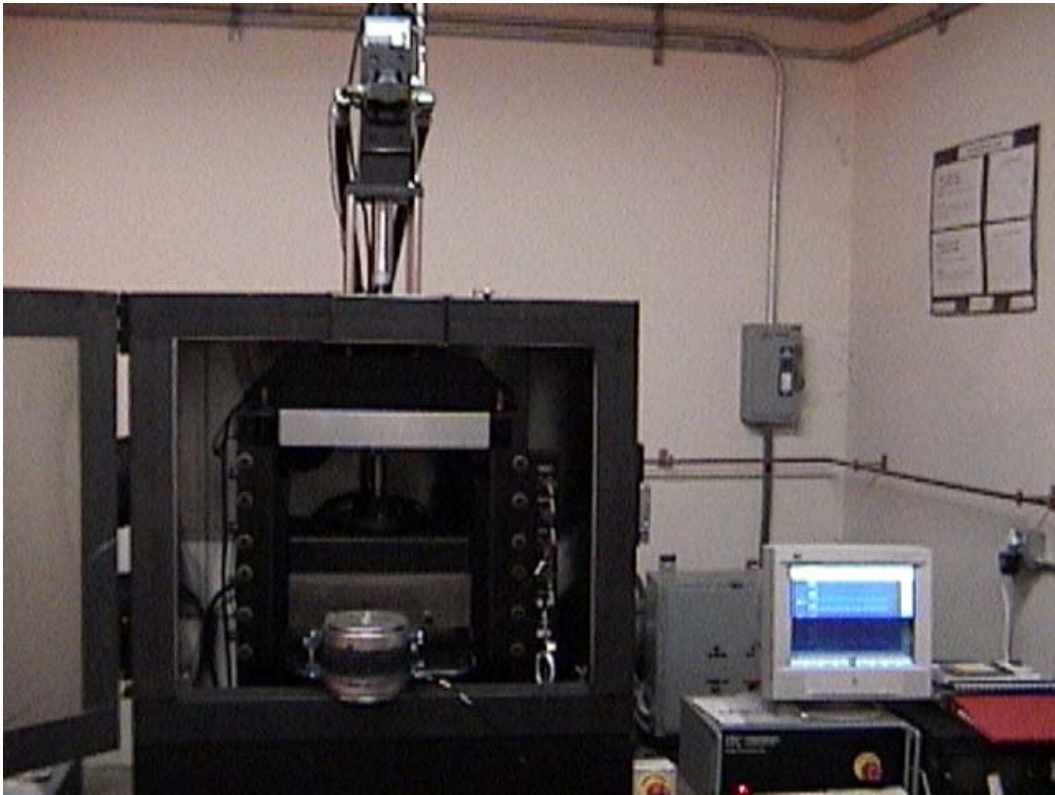
Figure 6 – Superpave Shear Tester (SST) at the Rutgers Asphalt/Pavement Laboratory
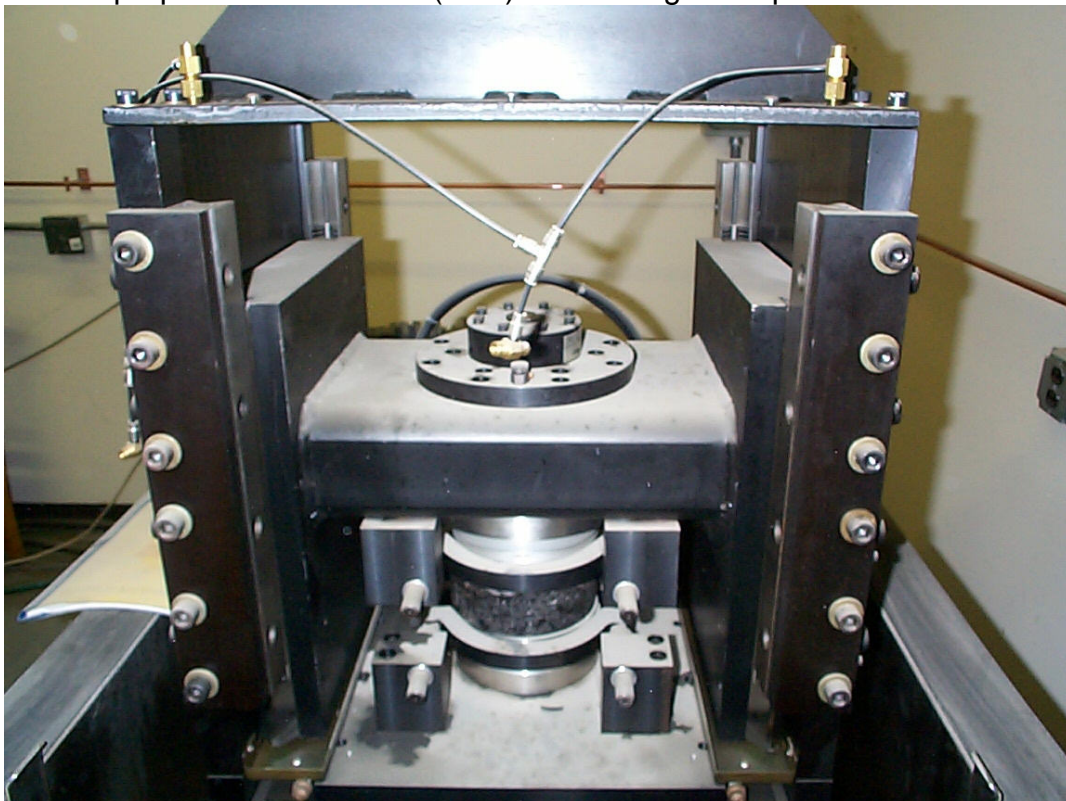
Figure 7 – Looking Into SST (No Environmental Chamber Attached)

Figure 8 – SST Specimen Glued to Caps with LVDT's Attached

The tests conducted with the SST for this project were specific in evaluating the different fundamental parameters of the HMA. The tests conducted and the description of the test is discussed below.

Repeated Shear at Constant Height (RSCH)

The RSCH test involves applying a repeated haversine shear stress of 10 psi a sample that has the dimensions of 150 mm in diameter and 50 mm in height. The applied load has a duration of 0.1 seconds, with an unload time of 0.6 seconds. An axial load is applied to the sample during the test to insure a constant height is applied at all times. The test procedure followed for this test was AASHTO TP7-01, test procedure C. The HMA sample is tested at a test temperature that corresponds to local pavement temperatures. In New Jersey, this is approximately 52°C. For this study, samples were tested at both 52°C, and also at the high temperature performance grade used in the New Jersey, 64°C. The shear stress is applied to the sample for 5,000 loading cycles, or until the sample reaches 5% permanent shear strain. Work conducted by a number of researchers (Harvey et al., 1994; Monismith et al., 2000; Witzcak et al., 2002) has indicated the RSCH to be an excellent tool in determining rut susceptible HMA mixes.

For this study, the test was only constrained to 6,000 cycles. Therefore, based on the AASHTO specs, the parameter used for evaluation from the test is the % permanent

shear strain that has occurred at 5,000 loading cycles. However, for this research, the parameters that were evaluated were expanded. A discussion of the parameters evaluated from the RSCH test is below.

Permanent Shear Strain at 3,000 Cycles – Research work conducted by Witzcak et al., (2002) has shown that the permanent shear strain at 3,000 cycles from the RSCH test correlated well with rutting at a number of accelerated loading locations. The 3,000 cycles was evaluated in the work of Witzcak et al. (2002) to try to quicken the RSCH test. By reducing the test 2,000 cycles, approximately 24 minutes in testing time can be saved. Although not sounding like a lot, if a large number of tests need to be conducted for evaluation, this could significantly shorten the evaluation time. Therefore, this value was evaluated.

Slope of Regression Analysis – Permanent deformation is typically expressed as one of two different regression models. The first is the Log Model shown as equation (1). The second is the Power Model shown as equation (2). The models generally have three parameters. The first parameter is a regression constant that pertains to an intercept, the second parameter is a sloping parameter, and the third parameter in the number of loading cycles. For this analysis, the sloping parameter from both the Log and Power regression models were evaluated. The sloping parameter would pertain to the accumulating permanent strain occurring during the test. Therefore, the sloping parameter should be able to discriminate between samples of varying accumulated permanent strain.

$$\varepsilon_P(N) = \varepsilon_P(N=1) + S\log(N) \qquad\qquad (1)$$

where,
   $\varepsilon_P(N)$ – permanent deformation at N cycles
   $\varepsilon_P(N=1)$ – permanent deformation a N = 1 cycle
   S – sloping parameter
   N – number of loading cycles

$$\varepsilon_P(N) = [\varepsilon_P(N=1)]N^b \qquad\qquad (2)$$

where,
   $\varepsilon_P(N)$ – permanent deformation at N cycles
   $\varepsilon_P(N=1)$ – permanent deformation a N = 1 cycle
   b – sloping parameter
   N – number of loading cycles

Frequency Sweep at Constant Height (FSCH)

The FSCH test involves applying a sinusoidal shear strain of 0.0001 mm/mm (0.01 %) at each of the following loading frequencies – 10, 5, 1, 0.5, 0.2, 0.1, 0.05, 0.02, and 0.01 Hz. Fifty cycles are tested for 10 and 5 Hz, twenty cycles are used for 2 and 1 Hz,

seven cycles are used for 0.5, 0.2, and 0.1 Hz, and four cycles are used for 0.05, 0.02, and 0.01 Hz. This follows the test procedure used for the testing (AASHTO TP7-01, test procedure A). The tests were conducted at 20, 40, and 52°C, as recommended in the AASHTO procedures. Due to the nature of HMA, the test produces a value known as the dynamic shear modulus, G*. As the load is applied, there is a small delay in the actual movement of the HMA. This delay is called the phase angle, ϕ, and is schematically shown in Figure 9.
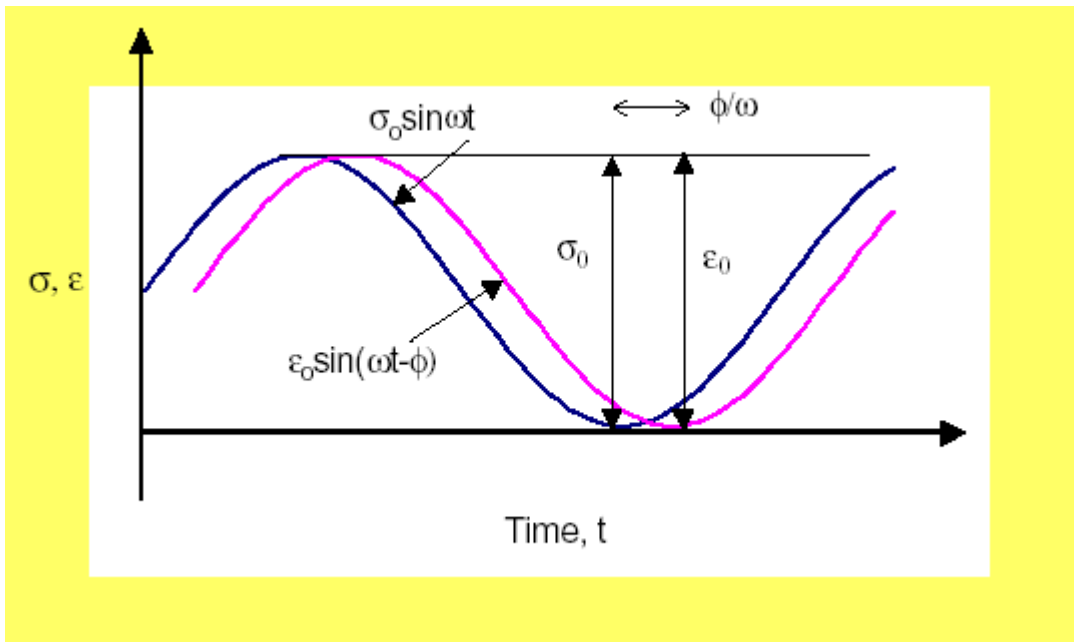
Figure 9 – Development of the Phase Angle in the FSCH Test

After the sample has been tested over a range of temperatures, a master stiffness curve can be developed. The master stiffness curve of HMA allows for the comparison of visco-elastic materials when testing has been conducted using different loading frequencies and temperatures. The master curve can be constructed using the time-temperature superposition principle. This principle suggests that the temperature and loading frequency of visco-elastic materials can be interchangeable.

The data from the FSCH tests can be "shifted" relative to the time of the frequency, so that the various curves can be aligned to form a single "master curve" (Pellinen, 2001). The shifting is theoretically allowed because the HMA material will act differently under the loading frequency and temperature. What actually occurs is that a G* at a temperature of 40°C and a loading frequency of 5 Hz may equal the G* at a temperature of 20°C and a loading frequency of 0.5 Hz. An example of this from work conducted at RAPL is shown as Figure 10.

Figure 10 shows the results of FSCH tests conducted at 20, 40, 52, and 64°C on a coarse Superpave mix with a PG64-22 asphalt binder. As can be seen from the figure, a similar G* value can be achieved at different temperatures and at different frequencies. The G* value of 4,000 psi was marked on the figure. This value for

14

temperatures of 40, 52, and 64°C corresponds to approximate loading frequencies of 0.065, 1, and 5.5, respectively.
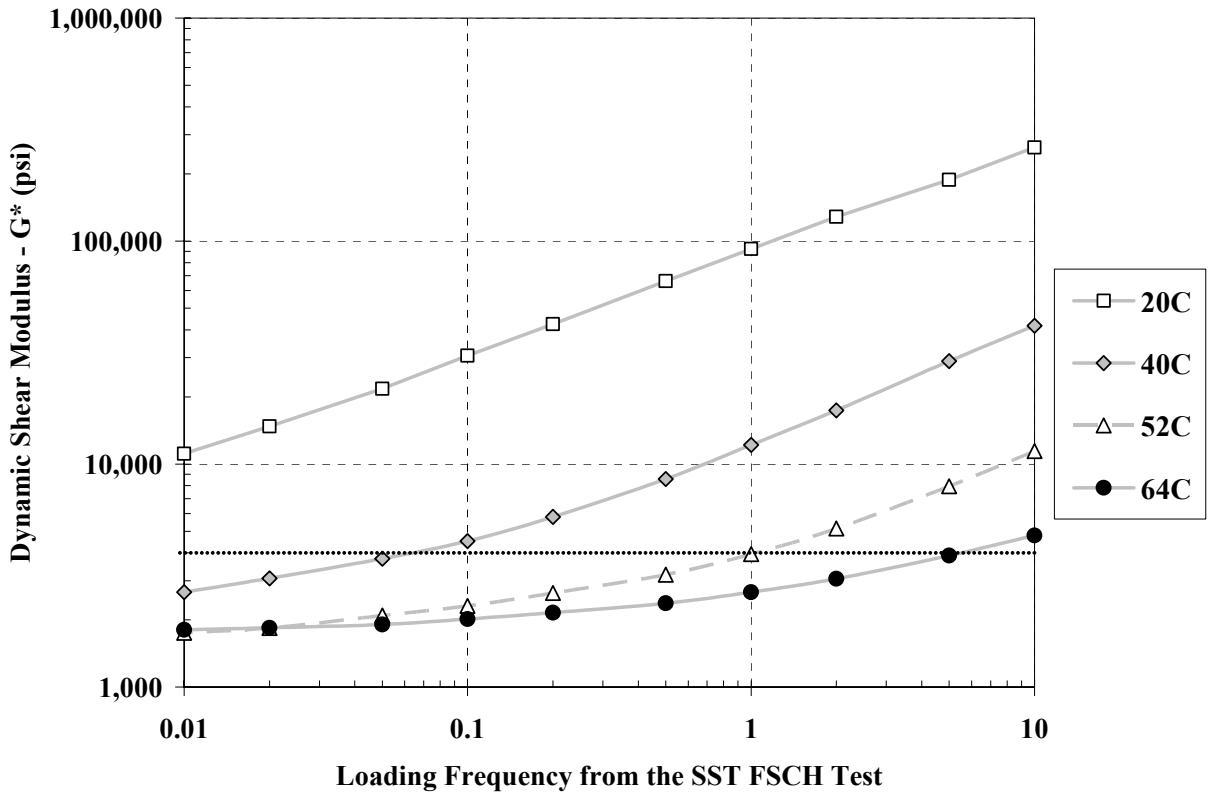
Figure 10 – FSCH Results from Testing Conducted at RAPL

The "shifting" of the curves necessitates the determination of a "shifting factor". The shift factor, a(T), defines the required shift at a given temperature (i.e. a constant by which the frequency must be multiplied or divided by to get an increased or reduced frequency (t_r) for the master curve (equation 3).

$$t_r = \frac{t}{a(T)} \quad \text{or} \quad t[a(T)] \tag{3}$$

The master curve can be developed using any arbitrarily selected reference temperature to which all of the data are fitted. For a more detailed explanation of the time-temperature superposition principle, refer to Painter and Coleman (1997).

A new method for developing master curves of HMA mixtures was utilized in this report. The method was developed at the University of Maryland (Pellinen, 1998). In this method, the master curves are constructed by fitting a sigmoidal function to the measured dynamic modulus test data using a non-linear least squares regression procedure. The shifting factors, a(T), are solved simultaneously with the coefficients of the sigmoidal function, without assuming an functional for the relationship of a(T) versus

15

temperature (Pellinen, 2001). The fitting function for the master curve construction is defined by equation (4).

$$y = \delta + \frac{\alpha}{1 + \exp^{(\beta - \gamma x)}}$$

(4)

where,
y = criterion variable (predicted value of modulus)
δ = location parameter for y (minimum value for modulus)
α = range of possible values to be added to the minimum modulus
β/γ = location parameter for the x corresponding to y = d + a/2
x = predictor variable (loading frequency)

The master curve is then constructed using the Solver Function in the Excel spreadsheet. Figure 11 illustrates the master curve developed based on the data in Figure 10 when shifted to 52°C.
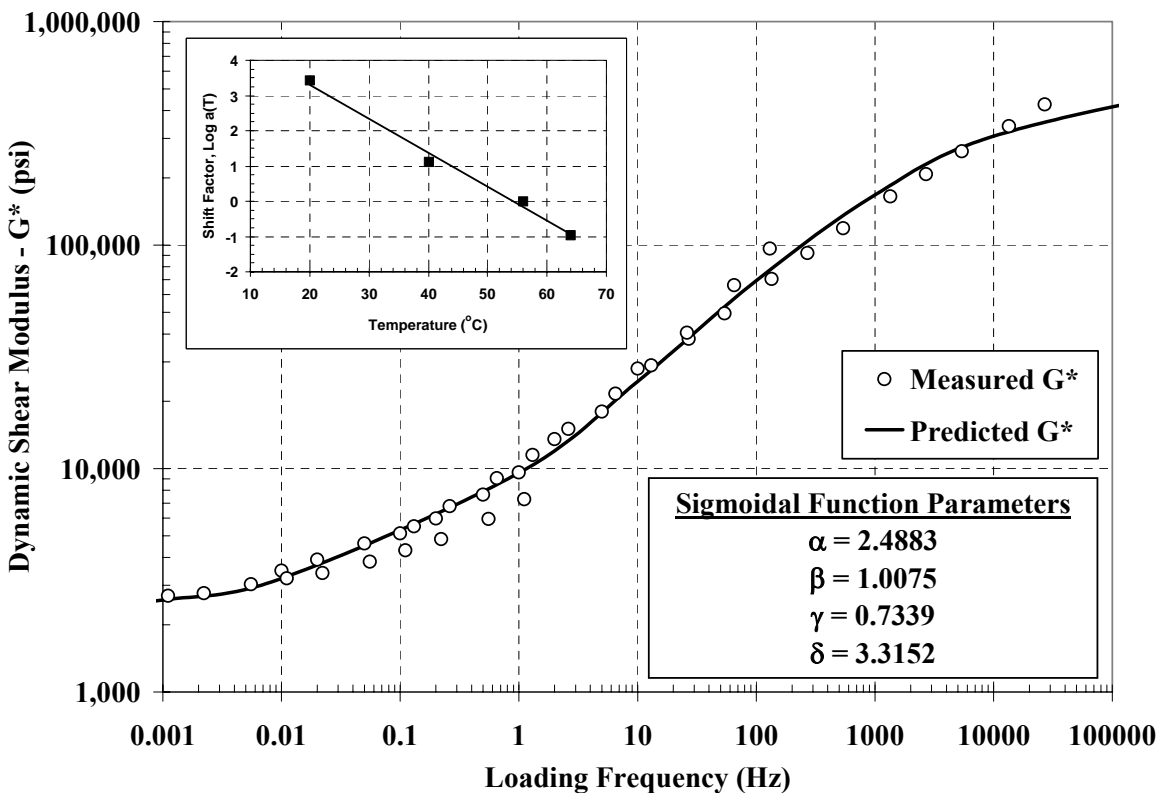
Figure 11 – Master Curve Developed from Testing Conducted at RAPL

Williams et al. (1998) analyzed a number of FSCH and RSCH tests that were conducted on samples from the WesTrack site. Comparing the results to binder testing and also the mix performance on the test track itself, the authors concluded that FSCH related to the binder stiffness, while the RSCH results related to the mixture performance. Others

have also recommended the FSCH to be used in evaluating the effects of HMA-Modifiers (Buncher et al., 2000). Therefore, this test was used to evaluate the HMA-M effects on stiffness, particularly the dynamic shear modulus (G*).

The results were compared using the graphing shown in figure 10, although the results of each sample was plotted at that particular temperature for a direct comparison. The analysis also included the following parameters.

G/sin ϕ* - The G*/sinϕ of the HMA mix is similar to G*/sinδ (rutting parameter) of PG graded asphalt binder. It is a measure of HMA stiffness at high pavement temperature (40 and 52°C) at a slow rate of loading (0.1 cycle/second). Higher values of G*/sinϕ indicate an increased stiffness of HMA mixtures and, therefore, increased resistance to rutting. G* is the complex modulus and δ is the phase angle when HMA is tested under dynamic loading.

Slope m of the G vs Frequency plot* – The m value is obtained from the frequency sweep at constant height conducted by the Superpave shear tester (SST) at high effective temperature (40 and 52°C) for permanent deformation with frequencies ranging from 0.01 hertz to 10 hertz. In other words, G* (stiffness) of the compacted HMA specimen is measured at different frequencies. The slope (m) of the best fit line on the frequency vs G* plot is calculated. This slope represents the rate of development of rutting for the tested mix and is used in the Superpave model as such. The lower the m slope, the better is the mix's resistance to rutting.

G(sin ϕ)* – G*sinϕ of the HMA mix is similar to G*sinδ (fatigue factor) of the asphalt binder. It is a measure of the stiffness at intermediate effective pavement temperatures for fatigue cracking or Teff(FC). G*sinϕ was measured at 1.0 hertz to represent fast moving traffic. A Teff(FC) of 20°C was used. High values of G*sinϕ at 1.0 hertz indicate high stiffness at intermediate temperatures and, therefore, low resistance to fatigue cracking according to Superpave.

Work conducted by Kandhal et al. (1998) had suggested that the above three parameters, which were meant to be used in the intermediate (Level II) Superpave analysis, could be used to determine the tendency for permanent deformation and fatigue cracking in HMA materials. Therefore, the above three parameters, as well as the actual stiffness plots of the samples were evaluated using the FSCH data.

Simple Shear at Constant Height (SSCH)

The SSCH test is essentially a shear creep test. The specimen is loaded at a stress rate of 70 kPa/sec until a pre-determined creep load is obtained. The creep load is based on the temperature for which it is tested. The creep loads used in this study conform to those recommended in AASHTO TP7-01 test procedure B, and are; 345 ± 5 kPa for 4°C, 105 ± 5 kPa for 20°C, and 35 ± 5 kPa for 40°C. The creep load is applied for 10 seconds and then the load is reduced to zero at a rate of 25 kPa/sec. Once the

stress reaches zero, the shear strain is measured for another 10 seconds. The test is complete after these final 10 seconds at zero stress.

AASHTO TP7-01, test procedure B recommends the calculation of the maximum shear strain that occurs during the test and also the permanent shear strain at the end of the test. Therefore, these two parameters were used in the evaluation of the HMA-M. However, two other parameters were also evaluated from the SSCH test.

SSCH Creep Curve – The data from the creep load portion of the SSCH test was extrapolated and used as an evaluation parameter. The data focused on the shear strain that occurred only when the creep load was applied. The results for each sample for the particular temperature tested was plotted along side one another for analysis. This type of analysis is similar to the creep compliance test.

SSCH Creep Curve Slope – The slope of the SSCH creep curve was determined by using a linear regression relationship. Although the SSCH creep curves are not a straight line, by fixing the linear regression to the origin, only one regression constant is determined and can be used for a direct comparison. The R^2 value (coefficient of correlation) for each of the regressions was not less than 0.85, indicating that even by using the fixed linear regression, a good correlation was able to be achieved.

The SSCH is not commonly used for this type of analysis, however, the creep performance of the mix would surely changed if some type of modifier has been applied to the asphalt binder. Work conducted by Buncher et al. (2000) recommended using the SSCH to estimate a mixture's susceptibility to permanent deformation since the test measures the mixes ability to resist shear strain. Lytton et al (1993) also used the creep compliance test to predict fatigue-cracking and low-temperature cracking. So, although the SSCH and the creep compliance test are performed differently, the creep information from both tests can be an important indicator of performance.

Asphalt Pavement Analyzer (APA)

The first loaded wheel tester was the Georgia Loaded Wheel Tester. This device was developed by the Georgia Department of Transportation and the Georgia Institute of Technology (Georgia Tech University) in 1985. It was developed in response to a belief in the industry that Marshal stability tests were inadequate to accurately predict rutting potential in asphalt pavement mixes (Collins, 1996). Since then, several loaded wheel-testing devices have been developed, including the Hamburg Wheel Tracking Device and Purdue University's PURwheel device.

The APA is a second-generation loaded wheel tester (Figure 12 and 13). It has the capability of testing compacted brick or pill samples under various environmental conditions in both rutting (high temperature permanent deformation) and fatigue (low temperature cracking). This project utilized the rutting feature of the APA. The device can also be linked to a computer and data acquisition system so the user can measure the rutting of the HMA for each load cycle. However, this feature of the APA was not

available yet at RAPL during this portion of the study. The APA has since then been modified for data acquisition.

Figure 12 – Asphalt Pavement Analyzer

Basically, a moving wheel load is applied at a rate of about one cycle per second to a ¾ inch pressurized hose that rests atop the HMA samples. This simulates (on a small scale) the loading of the standard 80 kN (18 kip) wheel loads on actual road sections. However, as to date, there have been no successful attempts at directly comparing the results of the APA to an actual roadway in the field. Therefore, the major use of the device is as a comparative tool for mixture selection (i.e. one would select the mix that ruts the least from the APA testing).
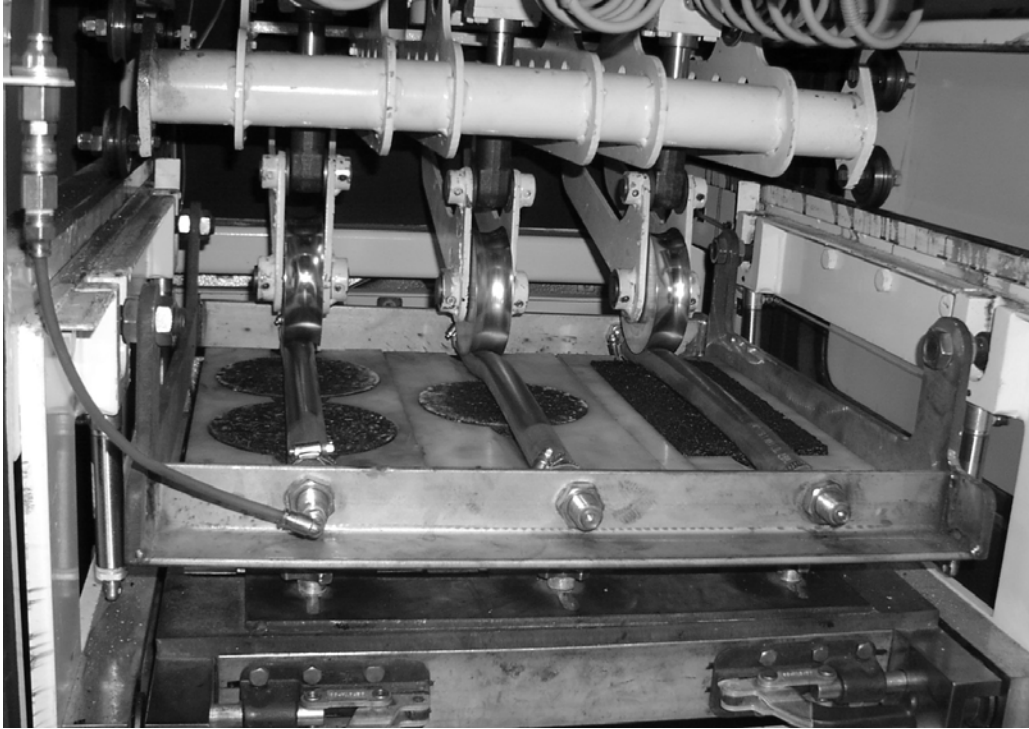
Figure 13 – Inside the Asphalt Pavement Analyzer

The APA is typically run at a test temperature of 64°C. The samples are conditioned under this temperature for minimum of 4 hours prior to testing. The loading configurations typically used within the APA are a wheel load of 100 lbs and a hose pressure of 100 psi, although some other researchers have had success with increased loads and pressures (Williams and Prowell, 1999). However, both the APA User's Group (2000) and the National Center for Asphalt Technology (Kandhal and Cooley, 2002) have recommended using 100 psi hose pressure with 100 lbs wheel load. Once conditioned, the samples under-go a 25 cycle seating load. Once the 25 cycles have completed, the initial rut depths are measured. Testing then usually continues until a minimum of 8,000 cycles are completed. The difference between the initial and final rut depth measurements is calculated as the APA rut depth.

Brown et al (2001) evaluated a number of different performance tests as a result of the immediate need for a simple performance test in the asphalt industry. Table 1 is taken directly from that report. Brown et al. (2001) evaluated 26 different tests that were in current use throughout the United States. The conclusion from the study is that the APA was recommended for immediate use as a means of evaluating permanent deformation in HMA.

The main disadvantage found in the SST testing, either the FSCH or the RSCH, was that the device was very expensive and it was difficult to find a testing facility that had an SST device. However, since RAPL owns a SST, this was not a problem in the study.

Table 1 – HMA Tests Evaluated by NCAT with Their Respective Advantages and Disadvantages (Brown et al., 2001)

	Test Method	Sample Dimension	Advantages	Disadvantages
Fundamental: Diametral Tests	Diametral Static (creep)	4 in. diameter × 2.5 in. height	• Test is easy to perform • Equipment is generally available in most labs • Specimen is easy to fabricate	• State of stress is nonuniform and strongly dependent on the shape of the specimen • Maybe inappropriate for estimating permanent deformation • High temperature (load) changes in the specimen shape affect the state of stress and the test measurement significantly • Were found to overestimate rutting • For the dynamic test, the equipment is complex
	Diametral Repeated Load	4 in. diameter × 2.5 in. height	• Test is easy to perform • Specimen is easy to fabricate	
	Diametral Dynamic Modulus	4 in. diameter × 2.5 in. height	• Specimen is easy to fabricate • Non destructive test	
	Diametral Strength Test	4 in. diameter × 2.5 in. height	• Test is easy to perform • Equipment is generally available in most labs • Specimen is easy to fabricate • Minimum test time	
Fundamental: Uniaxial Tests	Uniaxial Static (Creep)	4 in. diameter × 8 in. height & others	• Easy to perform • Test equipment is simple and generally available • Wide spread, well known • More technical information	• Ability to predict performance is questionable • Restricted test temperature and load levels does not simulate field conditions • Does not simulate field dynamic phenomena • Difficult to obtain 2:1 ratio specimens in lab
	Uniaxial repeated Load	4 in. diameter × 8 in. height & others	• Better simulates traffic conditions	• Equipment is more complex • Restricted test temperature and load levels does not simulate field conditions • Difficult to obtain 2:1 ratio specimens in lab
	Uniaxial Dynamic Modulus	4 in. diameter × 8 in. height & others	• Non destructive tests	• Equipment is more complex • Difficult to obtain 2:1 ratio specimens in lab
	Uniaxial Strength Test	4 in. diameter × 8 in. height & others	• Easy to perform • Test equipment is simple and generally available • Minimum test time	• Questionable ability to predict permanent deformation

Table 1 (continued) – HMA Tests Evaluated by NCAT with Their Respective
Advantages and Disadvantages (Brown et al., 2001)

	Test Method	Sample Dimension	Advantages	Disadvantages
Fundamental: Triaxial Tests	Triaxial Static (creep confined)	4 in. diameter × 8 in. height & others	• Relatively simple test and equipment • Test temperature and load levels better simulate field conditions than unconfined • Potentially inexpensive	• Requires a triaxial chamber • Confinement increases complexity of the test
	Triaxial Repeated Load	4 in. diameter × 8 in. height & others	• Test temperature and load levels better simulate field conditions than unconfined • Better expresses traffic conditions • Can accommodate varied specimen sizes • Criteria available	• Equipment is relatively complex and expensive • Requires a triaxial chamber
	Triaxial Dynamic Modulus	4 in. diameter × 8 in. height & others	• Provides necessary input for structural analysis • Non destructive test	• At high temperature it is a complex test system (small deformation measurement sensitivity is needed at high temperature) • Some possible minor problem due to stud, LVDT arrangement. • Equipment is more complex and expensive • Requires a triaxial chamber
	Triaxial Strength	4 or 6 in. diameter × 8 in. height & others	• Relative simple test and equipment • Minimum test time	• Ability to predict permanent deformation is questionable • Requires a triaxial chamber

Table 1 (continued) – HMA Tests Evaluated by NCAT with Their Respective Advantages and Disadvantages (Brown et al., 2001)

	Test Method	Sample Dimension	Advantages	Disadvantages
Fundamental: Shear Tests	SST Frequency Sweep Test – Shear Dynamic Modulus	6 in. diameter × 2 in. height	• The applied shear strain simulate the effect of road traffic • AASHTO standardized procedure available • Specimen is prepared with SGC samples • Master curve could be drawn from different temperatures and frequencies • Non destructive test	• Equipment is extremely expensive and rarely available • Test is complex and difficult to run, usually need special training • SGC samples need to be cut and glued before testing
	SST Repeated Shear at Constant Height	6 in. diameter × 2 in. height	• The applied shear strains simulate the effect of road traffic • AASHTO procedure available • Specimen available from SGC samples	• Equipment is extremely expensive and rarely available • Test is complex and difficult to run, usually need special training • SGC samples need to be cut and glued before testing • High COV of test results • More than three replicates are needed
	Triaxial Shear Strength Test	6 in. diameter × 2 in. height	Short test time	• Much less used • Confined specimen requirements add complexity
Empirical Tests	Marshall Test	4 in. diameter × 2.5 in. height or 6 in. diameter × 3.75 in. height	• Widespread, well known, standardized for mix design • Test procedure standardized • Easiest to implement and short test time • Equipment available in all labs.	• Not able to correctly rank mixes for permanent deformation • Little data to indicate it is related to performance
	Hveem Test	4 in. diameter × 2.5 in. height	• Developed with a good basic philosophy • Short test time • Triaxial load applied	• Not used as widely as Marshall in the past • California kneading compacter needed • Not able to correctly rank mixes for permanent deformation
	GTM	Loose HMA	• Simulate the action of rollers during construction • Parameters are generated during compaction • Criteria available	• Equipment not widely available • Not able to correctly rank mixes for permanent deformation
	Lateral Pressure Indicator	Loose HMA	• Test during compaction	• Problems to interpret test results • Not much data available

Table 1 (continued) – HMA Tests Evaluated by NCAT with Their Respective Advantages and Disadvantages (Brown et al., 2001)

Test Method		Sample Dimension	Advantages	Disadvantages
Simulative Tests	Asphalt Pavement Analyzer	Cylindrical 6 in. × 3.5 or 4.5 in. or beam	• Simulates field traffic and temperature conditions • Modified and improved from GLWT • Simple to perform • 3-6 samples can be tested at the same time • Most widely used LWT in the US • Guidelines (criteria) are available • Cylindrical specimens use SGC	• Relatively expensive except new table top version
	Hamburg Wheel-Tracking Device	10.2 in. × 12.6 in. × 1.6 in.	• Widely used in Germany • Capable of evaluating moisture-induced damage • 2 samples tested at same time	• Less potential to be accepted widely in the United States
	French Rutting Tester	7.1 in. × 19.7 in. × 0.8 to 3.9 in.	• Successfully used in France • Two HMAs labs can be tested at one time	• Not widely available in U.S.
	PURWheel	11.4 in. × 12.2 in.× 1.3, 2, 3 in.	• Specimen can be from field as well as lab-prepared	• Linear compactor needed • Not available
	Model Mobile Load Simulator	47 in. × 9.5 in.× thickness	• Specimen is scaled to full-scaled load simulator	• Extra materials needed • Not suitable for routine use • Standard for lab specimen fabrication needs to be developed
	RLWT	6 in. diameter × 4.5 in. height	• Use SGC sample • Some relationship with APA rut depth	• Not widely used in the United States • Very little data available
	Wessex Device	6 in. diameter × 4.5 in. height	• Two specimens could be tested at one time • Use SGC samples	• Not widely used or well known • Very little data available

Factors Affecting APA Results

Recent work at the RAPL (Bennert et al., 2001) looked at the factors that may affect the rutting measurements in the APA. Factors that were evaluated were: 1) Temperature ($60^{o}C$ vs $64^{o}C$), 2) Sample type (Brick vs Gyratory), 3) Compaction method (Vibratory vs Gyratory), and 4) Position of the rut measurement (location of sample). The study also looked at determining if the gradation of Superpave mixes had an affect on the rutting performance when tested in the APA. Conclusions that were drawn from the study were:

> 1) The temperature increase from $60^{o}C$, which was the previous recommended test temperature, to $64^{o}C$ can cause a 30 to 100% increase in the rutting results when tested in the APA.

2) Rutting is typically slightly greater when tested in brick samples than gyratory samples.   This is most likely due to larger area for the material to flow. However, the differences between the bricks and pills were not large enough to warrant concern.

3) The compaction type, vibratory vs gyratory, showed to have a small effect on the rutting performance in the APA. Some increase in rutting can be seen for the vibratory compacted samples when compared to the gyratory compacted samples. This is most likely due to different aggregate alignment from the two different means of sample compaction. Figure 14 shows the overall results from the testing.

4) The location of the sample, center cut mold vs double mold, again showed to have a small effect on the rutting performance in the APA. The center cut mold samples tended to rut less than the double mold. However, this is most likely due to the location of the measurements on the samples. The same template was used for both types of molds. This caused the measurements of the center cut mold samples to be much closer to the edge of the mold. Lateral confinement of the sample is much greater at this location than for the double molds. As a result, this may have led to lower measured rutting.
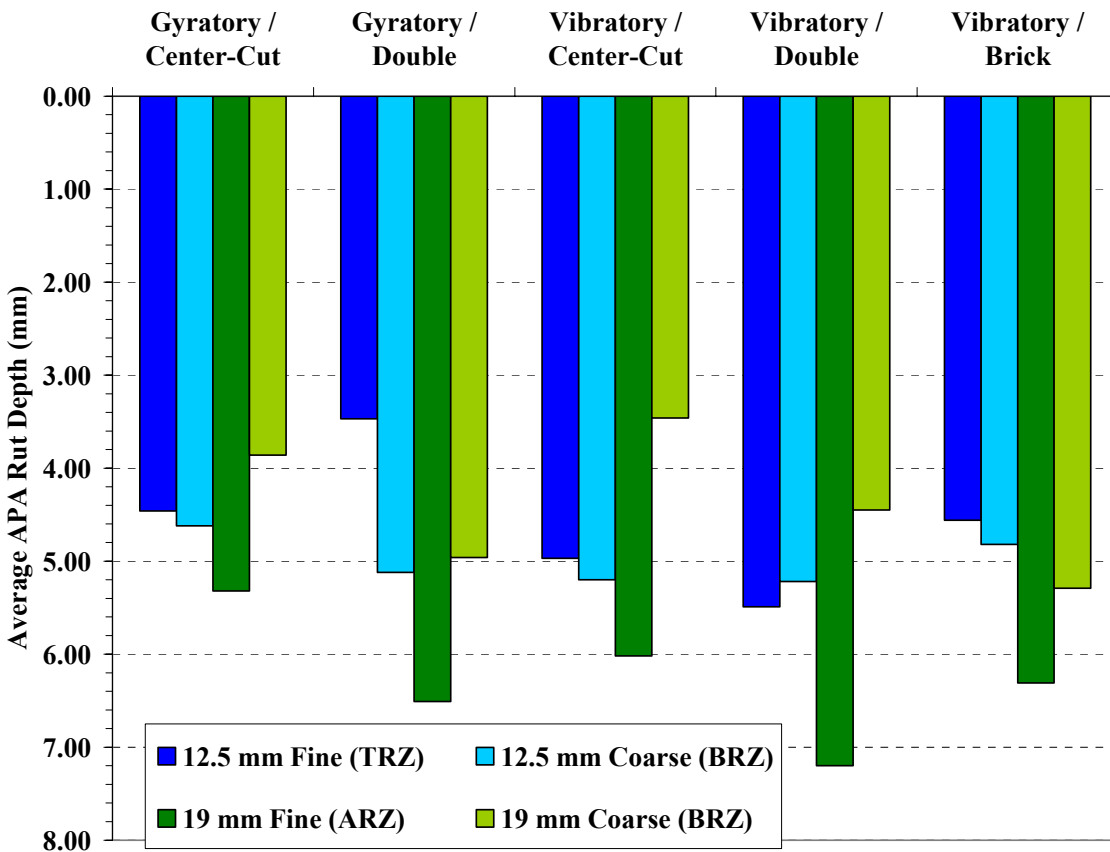
Figure 14 – Results of Evaluation of the Effects of Sample Compaction and Location on APA Test Results (Bennert et al., 2001)

Therefore, the work by Bennert et al., (2001) recommended the use of double pill sample molds with samples compacted from the gyratory compactor. The gyratory compactor is preferred since it is the industry standard, and the user has more control over compaction than the vibratory compactor. A summary of the test configurations recommended from the testing are listed below.

Test Temperature = 64°C
Loading Cycles = 8,000 Cycles
Wheel Load = 100 lbs
Hose Pressure = 100 psi
Compaction Method = Gyratory Compactor
Mold Type/Sample Location = Double Pill Mold

MIX DESIGN

The asphalt mix used in the testing program was a 12.5 mm, coarse gradation, Superpave mix using a PG64-22 asphalt binder from Citgo. The design of the mix was based on ESAL's of 0.3 to 3.0 million. This was decided by NJDOT representatives under the theory that this type of design would be prone to permanent deformation. Therefore, the addition of an asphalt binder modifier would surely enhance the permanent deformation properties of the HMA mix. The HMA mix specifications are shown in Table 2 and Table 3. The gradation of the mix is shown in figure 15.

Table 2 – Gyratory Compaction Effort

Design ESAL's (Million)	N_{ini}	N_{des}	N_{max}
< 0.3 (Low - L)	6	50	75
0.3 to 3.0 (Medium - M)	7	75	115
3.0 to 30 (Heavy - H)	8	100	160
> 30 (Very Heavy - V)	9	125	205

Table 3 – Superpave Hot Mix Asphalt Design Requirements

Design ESAL's (millions)	Required Density (% of Theoretical Max. Specific Gravity)			VMA % (minimum) Nom. Max. Agg. Size (mm)					Voids Filled with Asphalt	Dust-to-Binder Ratio[#]
	N_{ini}	N_{des}	N_{max}	37.5	25.0	19.0	12.5	9.5	(VFA) %	
< 3 (L,M)	90.5	96.0	98.0	11.0	12.0	13.0	14.0	15.0	65 – 78	0.6 – 1.2
> 3 (H,V)	89.0	96.0	98.0	11.0	12.0	13.0	14.0	15.0	65 – 75*	0.6 – 1.2

* For 9.5mm nominal maximum size mixtures the specified VFA range shall be 73% to 76% of design traffic levels of 30 million ESAL's
* For 37.5mm nominal maximum size mixtures the specified lower limit of the VFA shall be 64% for all design traffic levels
[#] For production, the upper limit is 1.3

The asphalt content determined from the mix design and used throughout the study was 4.9%. Results of the mix design process are shown in Appendix A. Since the goal
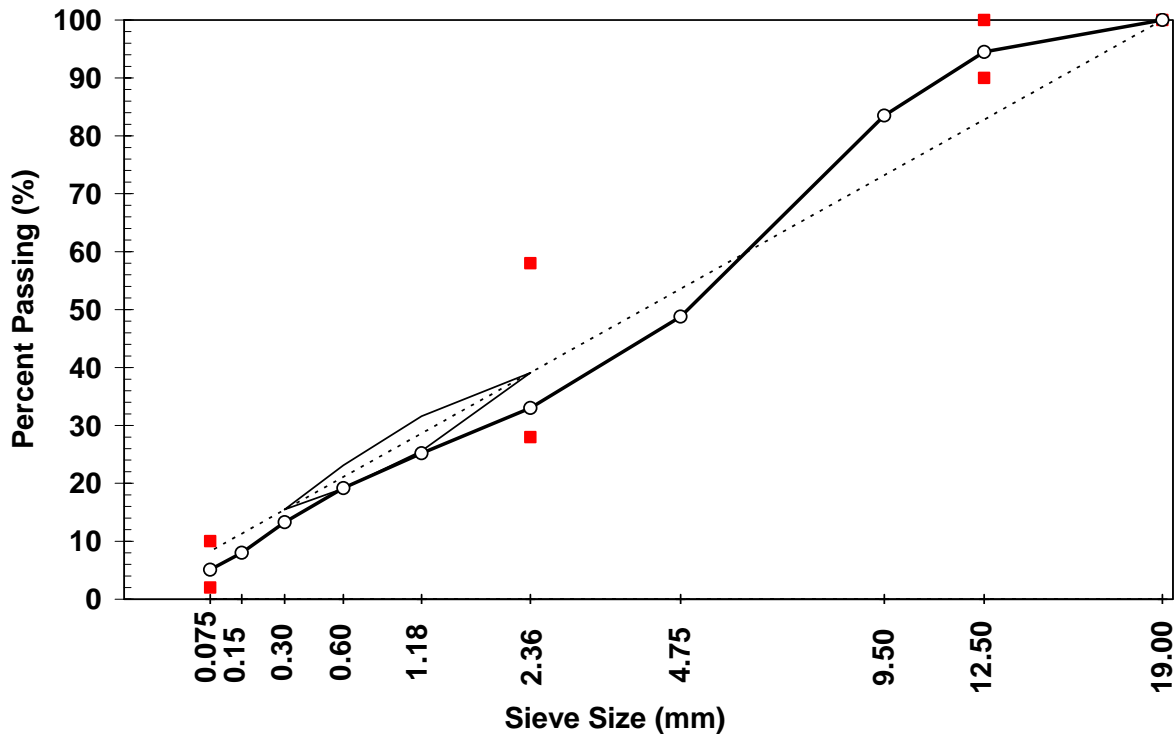
Figure 15 – Mix Design Gradation Used for 12.5mm Superpave Design

of the research project was to evaluate modifiers as add-in admixtures, mix designs were not conducted for each modifier. The modifiers were added either in a dry process or a wet process, as specified by the manufacturer.

Sample Preparation

All asphalt mixes tested were prepared at the Rutgers University Asphalt/Pavement Laboratory (RAPL). Samples were produced in lots of 6 to 12. The aggregates were blended based on the percentages to replicate the gradation shown in figure 15. The aggregates were heated to 148 ^{o}C, and once the aggregates reached temperature, the appropriate amount of asphalt binder (either the neat or modified) was added. The batch was then mixed in a rotating 5-gallon stainless steel mixing bucket for a minimum of 5 minutes (Figure 16). Immediately after mixing, the batch was transferred to a pan and cured for 2 hours at the compaction temperature of 144 ^{o}C. This is said to model the aging of the mix that occurs at the mixing plant and in the truck in route from the asphalt plant to the construction site. After the samples had been 'short termed aged', the mix was transferred to the corresponding compaction mold and compacted.

Figure 16 - Rotating 5-gallon Stainless Steel Mixing Bucket

Most of the samples tested were compacted in the Superpave Gyratory Compactor (Figure 17). This produced a sample of 150 mm in diameter and 77 mm in height. The gyratory compactor applies a constant stress of 600 kPa (87 psi) while the mold is gyrated at a contact angle of 1.25^{o} at a rate of 30 gyrations per minute. The gyratory compactor automatically stops compacting when the sample reaches its design height of 77 mm.

The other compactor used in the study was the Vibratory Compactor (Figure 18). The vibratory compactor produced the brick sample used in the APA testing. The vibratory compactor applies a 793 kPa vibrating stress, for a duration specified by the user. The stress is applied to the sample until the desired height of the sample has been obtained.

All samples were compacted to a target air void content of 7%. This was chosen because the current APA practice uses this value for all testing. Also, when the SST samples were cut from the gyratory samples, it typically produces a sample having an air void content between 5 and 6%, which is typical for most field placed HMA. For the SST testing, a 50 mm thick sample was cut out of the middle of the 77 mm tall gyratory sample. Triplicate samples were used for all SST testing. For the APA testing, the 77 mm tall sample was placed directly into the APA mold for testing. A total of 6 gyratory samples were used for the APA testing. Vibratory brick samples, 3 for each mix, were also compacted for APA testing.

Figure 17 – Superpave Gyratory Compactor at RAPL (Manufactured by Interlaken Technologies)

Figure 18 – Vibratory Compactor at RAPL (Manufactured by Pavement Technologies Inc.)

Materials

Three asphalt modifiers were evaluated in the research. These modifiers were compared to the performance of a neat asphalt, Citgo PG64-22, and two polymer-modified asphalts, PG76-22 from both Citgo Refineries and Koch Materials. A brief description of the asphalt modifiers and how the manufacturer recommended them to be blended into the asphalt is shown below.

Eastman EE-2 Polymer

The Eastman EE-2 is a functionally modified olefin that is designed to be used as a high temperature modifier for road asphalt. The visual appearance of the material was that of small, clear round pellets. The company advertises the product as:
- Easy to blend
- Compatible with a wide range of asphalts
- Raises high temperature SHRP grade without changing the low temperature grade
- Low viscosity
- Excellent storage stability
- Good workability

According to the manufacturer, the following procedure should be followed for using the product in hot mix asphalt.
1. Heat asphalt to recommended mixing temperature
2. Add 3% EE-2 by total weight of asphalt binder
3. Mix for 5 minutes
4. Add mixture to aggregates and mix for recommended time

Creanova's Vestoplast

The Vestoplast is a typically produced polymer that has a chemical composition of an amorphous poly-alpha-olefin. The visual appearance of the material was that of small, clear round pellets. Creanova advertises the use of their Vestoplast as a high temperature modifier for road construction.

According to the manufacturer, the following procedure should be followed for using the product in hot mix asphalt.
1. Need to premix the Vestoplast with hot aggregate before adding binder
2. Substitute 7% of binder (by weight) with the Vestoplast (93% Binder, 7% Vestoplast by weight)
3. Mix with the aggregate for 10 to 30 seconds
4. Add binder to the aggregates
5. Mix entire mixture until homogeneous

Hydrocarbon Technology Inc. Carbon Black

The carbon black used in this study was from the processing (pyrolysis) of tires and used motor oil. The visual appearance of the material was dark, black powder that was somewhat oily. Preliminary work had shown that this material may enhance the properties of the asphalt binder if properly blended.

According to the manufacturer, the following procedure should be followed for using the product in hot mix asphalt.
1. Add 10% carbon black by total weight to asphalt binder
2. Heat contents to 150^OC for 1 hour (for a quart sized sample)
3. Agitate mixture for five minutes
4. Add mixture to aggregate and mix for recommended time

EXPERIMENTAL PROGRAM

The experimental program consisted of producing approximately thirty gyratory samples and three vibratory brick samples for each mix to be evaluated. The gyratory samples were to be used for the SST testing by cutting a 50 mm sample out of the 77 m gyratory sample. The APA testing used the intact 77 mm tall gyratory sample. Triplicate

samples were tested for all of the SST designated tests, while six gyratory and three brick samples were used for the APA evaluation.

In conjunction to the laboratory testing of the asphalt mixes, binder testing was conducted at the laboratories at Citgo Refineries in Paulsboro. The main goal of the testing was to determine the "true" performance grade of the modified asphalt. All modifiers were mixed with a neat binder according to the manufacturer's specifications. Once blended, the modified asphalt was then tested according to the AASHTO specifications and a "true" asphalt performance grade was assigned. These designations were solely used for comparison purposes.

EXPERIMENTAL PROGRAM – RESULTS

The experimental program results are discussed below. Each section discusses the individual results from that particular test, with a following section that describes any inter-relationships between tests and test parameters.

"True" Performance Grading of Modified Binder

Binder testing was conducted at the Citgo Refinery in Paulsboro, NJ to determine the true performance grade of the asphalt binder after the addition of the asphalt modifiers. Citgo followed the same percentages discussed earlier, as well as evaluating 25% above and below the recommended percentage. This was conducted to evaluate the effect on the binder if quality control varied during the blending of these materials at the mixing plant or refinery. If the binder properties varied significantly, then additional performance testing would be conducted at those percentages.

The asphalt modifiers were blended with a performance graded neat asphalt of PG64-22. However, the true performance grade of the binder was actually a PG66-26. The true performance grade and the results from the respective binder tests are shown as Tables 4, 5 and 6. Table 7 shows the results of the neat binder used for blending.

As shown in the tables, the true performance grades do not vary significantly when the asphalt modifier was 25% above and below the recommended percentage. The Eastman EE-2 had a high temperature increase of 7°C, while raising the low temperature to -24°C. The Eastman EE-2 modified asphalt would be performance graded as a PG70-22 with a true performance grade of PG73-24. The Creanova Vestoplast again had a 7°C increase in the high temperature performance. Unfortunately, the low temperature increased to -18°C. The Creanova Vestoplast would be performance graded as a PG70-16, with a true performance grade of PG73-18. The Hydrocarbon Technologies Carbon Black had a high temperature increase of 2°C, with a low temperature increase of 2°C. This created a performance graded asphalt of PG64-22, with a true performance grade of PG68-24.

Table 4 – Binder Test Results of Eastman EE-2 Asphalt Modifier

	2.25%	3.0%	3.75%
Unaged Asphalt			
Flash Point (^{o}C)	270	275	275
Viscosity @ 135°C	400 cP	440 cP	451 cP
Original DSR @ 70.3^{o}C (G*/sinδ) kPa	1.305	1.35	1.48
Original DSR @ 76.3^{o}C	0.707	0.767	0.864
Aged Asphalt			
RTFO DSR @ 70.1^{o}C	3.023	3.67	3.25
RTFO DSR @ 76.2^{o}C	1.381	1.842	1.54
Mass Change (%)	0.045	0.086	0.090
PAV DSR 22.0^{o}C	5905	5816	5603
PAV DSR 25.0^{o}C	4056	3978	3816
Creep Stiffness (MPa)			
@ -12°C	192	171	160
@ -18°C	417	405	375
Creep m-value (slope)			
@ -12°C	0.342	0.354	0.321
@ -18°C	0.232	0.233	0.279
True Performance Grade	**PG72-24**	**PG73-24**	**PG73-25**

Table 5 – Binder Test Results of Creanova Vestoplast Asphalt Modifier

	5.25%	7.0%	8.75%
Unaged Asphalt			
Flash Point (^{o}C)	270	275	275
Viscosity @ 135°C	702 cP	937 cP	1072 cP
Original DSR @ 70°C (G*/sinδ) kPa	1.421	1.468	1.614
Original DSR @ 76.3^{o}C	0.682	0.747	0.765
Aged Asphalt			
RTFO DSR @ 70°C	3.6	3.994	4.55
RTFO DSR @ 76.2^{o}C	1.648	1.823	2.14
Mass Change (%)	0.12	0.085	0.085
PAV DSR 22.1^{o}C	6393	(25.1^{o}C) 5783	(25.1^{o}C) 6638
PAV DSR 25.0^{o}C	4679	(28.1^{o}C) 4470	(28.1^{o}C) 4945
Creep Stiffness (MPa)			
@ -6°C	122	114	89.2
@ -12°C	245	291	314
Creep m-value (slope)			
@ -6°C	0.326	0.328	0.341
@ -12°C	0.285	0.245	0.233
True Performance Grade	**PG73-18**	**PG73-18**	**PG74-19**

Table 6 – Binder Test Results of Hydrocarbon Technology Inc. Carbon Black Asphalt Modifier

	7.5%	10%	12.5%
Unaged Asphalt			
Flash Point (^{o}C)	294	292	295
Viscosity @ 135°C	532 cP	572 cP	608 cP
Original DSR @ 66.5^{o}C (G*/sinδ) kPa	1.244	1.593	1.307
Original DSR @ 70.1^{o}C	0.819	0.811	0.9
Aged Asphalt			
RTFO DSR @ 66.5^{o}C	2.566	3.781	2.842
RTFO DSR @ 70.0^{o}C	1.676	1.805	1.84
Mass Change (%)	0.111	0.088	0.132
PAV DSR 22.1^{o}C	6369	6079	5875
PAV DSR 25.1^{o}C	4470	4233	4170
Creep Stiffness (MPa)			
@ -12°C	175	185	187
@ -18°C	430	299	393
Creep m-value (slope)			
@ -12°C	0.338	0.327	0.324
@ -18°C	0.220	0.248	0.242
True Performance Grade	**PG67-23**	**PG68-24**	**PG68-23**

Table 7 – Binder Test Results of Benchmark Neat Binder Used for Blending

Unaged Asphalt

Flash Point (^{o}C)	265
Viscosity @ 135°C	392 cP
Original DSR @ 64°C (G*/sinδ) kPa	1.456
Original DSR @ 70.3^{o}C	0.669

Aged Asphalt

RTFO DSR @ 66.5^{o}C	2.857
RTFO DSR @ 70.0^{o}C	1.182
Mass Change (%)	0.136
PAV DSR 22.1^{o}C	5218
PAV DSR 25.0^{o}C	3560
Creep Stiffness (MPa)	
@ -12°C	163
@ -18°C	343
Creep m-value (slope)	
@ -12°C	0.377
@ -18°C	0.306
True Performance Grade	**PG66-26**

Based on the binder testing and the true performance grade of the recommended percentage, the following ranking for permanent deformation resistance can be concluded (Table 8):

Table 8 – Ranking of Asphalt Binders Used in the Study

Modified Asphalt Binder	Ranking
Koch Materials PG76-22	1*
Citgo PG76-22	1*
Creanova Vestolpast	3
Eastman EE-2	4
HTI Carbon Black	5
Citgo PG64-22	6

* - True Performance Grade not given so ranking assumed based on PG grading

Superpave Shear Tester – System Verification

Prior to testing, it was decided that the SST system should be evaluated to ensure that the data determined by the SST was valid. In order to conduct the verification work, a laboratory that had a SST and experience in using the device was needed. Also, a sample that could be tested by both the RAPL and the verification lab was needed. The sample had be of the type that minimal differences in material performance expected during the sample preparation and testing.

The laboratory chosen to conduct the verification work was the Asphalt Institute. The Asphalt Institute has a Superpave Shear Tester built by Cox and Sons and has used the device for a number of projects involved in its precision (Anderson and McGennis, 1998; Anderson et al., 2003).

To ensure that variation of sample performance was not an issue, a synthetic sample was chosen for use in the Frequency Sweep at Constant Height (FSCH). The use of synthetic samples has been applied to soils related work, especially for stiffness evaluation (Stokoe, K.H. et al., 1990; Nazarian, S. and Feliberti, M., 1993). The samples used for the testing were manufactured from urethane by a company in Ohio called Queen City Polymers. This company and material was recommended by Nazarian (2002). The shear stiffness of the urethane sample selected was one that mimicked the shear stiffness of HMA at moderate temperatures (30 to 40°C).

The FSCH test was selected for a number of factors; 1) The testing is conducted over a wide range of loading frequencies, 2) The test is still used as a means of evaluating the performance of HMA, and 3) Since the strain measurements are very small (in the elastic range) the SST must be properly calibrated. Otherwise, large errors could occur in the sample calculations.

Figure 19 shows the results of the verification testing. The samples were tested at 25°C. As can be seen from the figure, the results are very close, with an average standard deviation of 1,223 psi and an average percent difference of 4.7%. This is extremely close when considering that the urethane samples used for the study may have a small variability.

Superpave Shear Tester – Repeated Shear at Constant Height (RSCH)

The Superpave Shear Test (SST) was used with the Repeated Shear at Constant Height (RSCH) mode to evaluate the permanent deformation response of the baseline and modified mixes. The device applies a 10 psi cyclic shear stress on the sample using a haversine-type load. The load is applied for 0.1 seconds and is followed by a rest period of 0.6 seconds. The samples were tested until a total of 6,000 loading cycles were applied to the samples. During the loading, the accumulation of permanent shear strain was continually measured. A HMA with a high resistance to permanent deformation will exhibit a low accumulation of permanent shear strain.
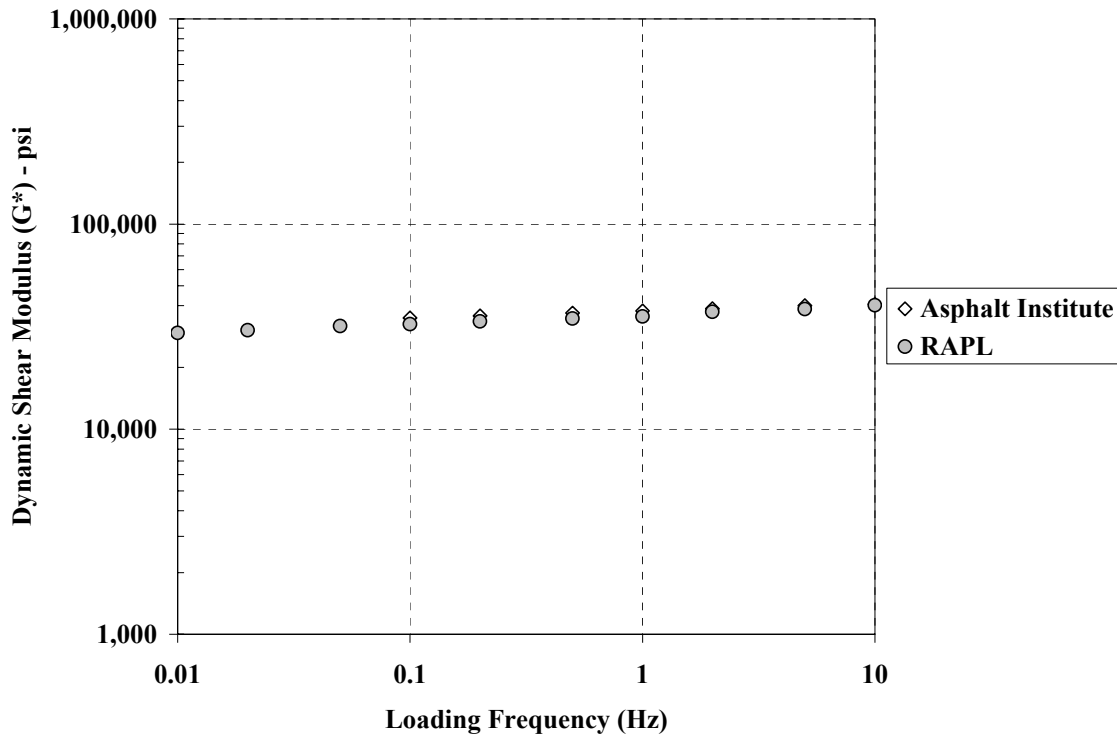
Figure 19 – Superpave Shear Tester Calibration Verification Using the FSCH Test

Typically, the permanent shear strain at 5,000 cycles is used for comparisons (AASHTO TP7-01; Sousa et al., 1994), however recent work has shown that the permanent shear strain at 3,000 cycles correlates well to field rutting (Witzcak et al., 2002).

The results of the RSCH testing are an average of three samples tested. The tests were conducted at both 52 and 64°C. The results of the individual samples tested are shown in Appendix B of the report.

RSCH Permanent Shear Strain - Results

The permanent shear strain versus the number of loading cycles for the RSCH test at 52 and 64°C are shown as figures 19 and 20. As shown in both figures, the PG76-22 samples achieved the lowest permanent shear strain, with the Koch Materials slightly outperforming the Citgo binder. The HTI Carbon Black admixture was typically the worst performing.

Figure 21 shows that the Eastman EE2 and the Creanova Vestoplast provide a slight increase in permanent deformation resistance. However, the differences are very small and statistically insignificant. Figure 20 shows that the Eastman EE2 admixture performed almost identically at 52°C as it did at 64°C. This may indicate that the Eastman EE2 material may not be as temperature sensitive as the other tested materials.
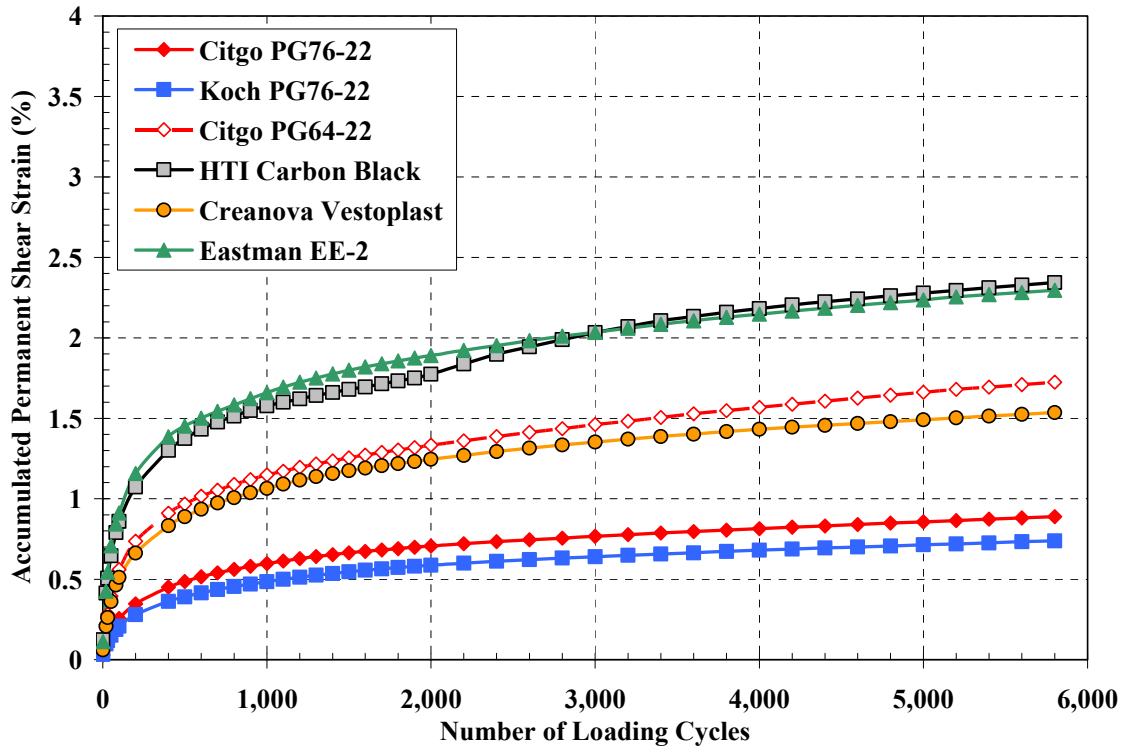
Figure 20 – RSCH Results Tested at 52°C
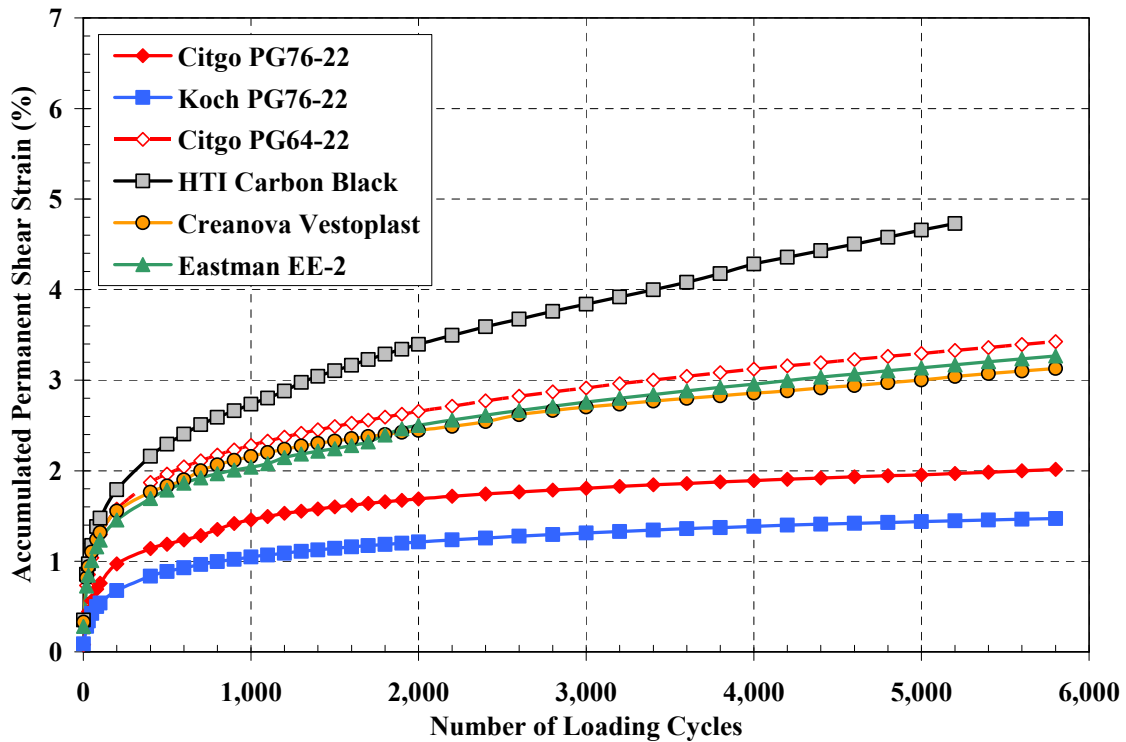
Figure 21 – RSCH Results Tested at 64°C

The RSCH results were further evaluated at different loading cycles. Although research has shown that the more loading cycles applied to the samples the better the comparison to actual field results (Witzcak et al., 2001), quickening any type of evaluation method would be a benefit. Therefore, three different loading cycles (1,000, 3,000, and 5,000) were evaluated for each temperature tested. Table 9 provides a summary of the results, with Figures 22 through 27 graphically depicting the table. Table 10 provides a ranking of the best to worst performing materials, with 1 being the best and 6 being the worst. As shown in the table, as well as the figures, both PG76-22 binders provided the lowest permanent deformation at all loading cycles and temperatures, with the Koch Materials binder slightly out-performing the Citgo PG76-22. The Creanova Vestoplast material was the next best performing additive. The Hydrocarbon Technologies (HTI) Carbon Black performed the worst when averaging the ranking numbers. The Eastman EE2 material performed slightly worse than the neat PG64-22 when averaging the ranking numbers. However, the Eastman EE2 material did perform well at the higher test temperature and loading cycles.

Table 9 – Summary of RSCH Tests at Different Number of Loading Cycles

| Sample Type | Accumulated Permanent Strain from RSCH | | | | | |
| | Temperature = 52C | | | Temperature = 64C | | |
	ε_P @ 1,000	ε_P @ 3,000	ε_P @ 5,000	ε_P @ 1,000	ε_P @ 3,000	ε_P @ 5,000
Citgo PG64-22	1.15	1.46	1.66	2.28	2.91	3.29
Citgo PG76-22	0.60	0.82	0.91	1.46	1.81	1.95
Koch M. PG76-22	0.48	0.67	0.74	1.05	1.31	1.44
Eastman EE2	1.58	2.03	2.24	2.74	2.76	3.14
Creanova Vestoplast	1.06	1.26	1.36	2.16	2.7	3
HTI Carbon Black	1.66	1.88	2.28	2.04	3.84	4.66

Table 10 – Ranking of Materials Based on the RSCH Test

| Sample Type | Ranking of Materials Tested in the RSCH | | | | | |
| | Temperature = 52°C | | | Temperature = 64°C | | |
	ε_P @ 1,000	ε_P @ 3,000	ε_P @ 5,000	ε_P @ 1,000	ε_P @ 3,000	ε_P @ 5,000
Citgo PG64-22	4	4	4	5	5	5
Citgo PG76-22	2	2	2	2	2	2
Koch M. PG76-22	1	1	1	1	1	1
Eastman EE2	5	6	5	6	4	4
Creanova Vestoplast	3	3	3	4	3	3
HTI Carbon Black	6	5	6	3	6	6

Based on the rankings, the 3,000 loading cycles appear to provide similar results to the traditionally used 5,000 loading cycles. Therefore, this parameter may be able to be used for future evaluation to quicken the necessary testing time.
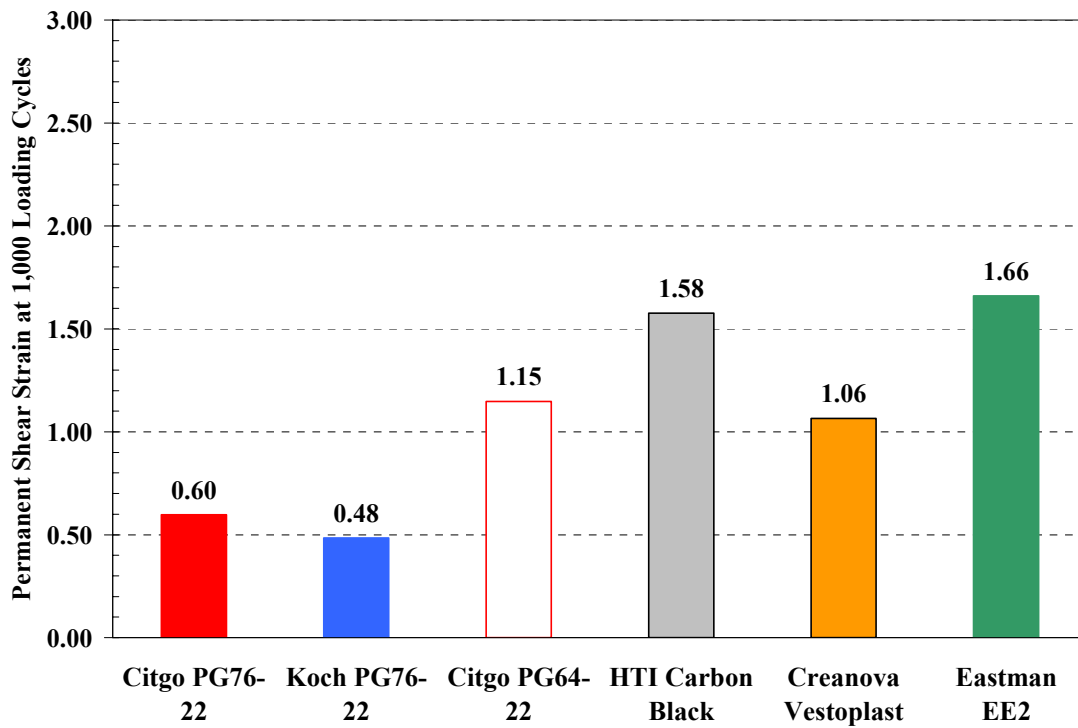
Figure 22 – Permanent Shear Strain at 1,000 Loading Cycles at 52°C from RSCH
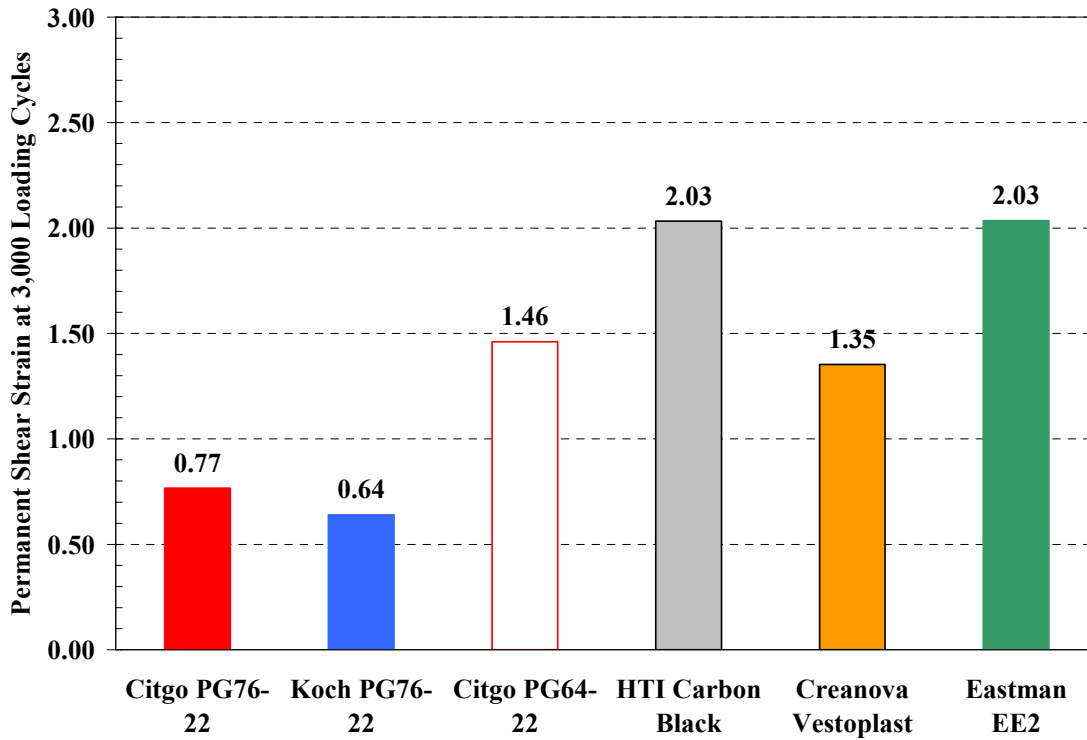
Figure 23 – Permanent Shear Strain at 3,000 Loading Cycles at 52°C from RSCH
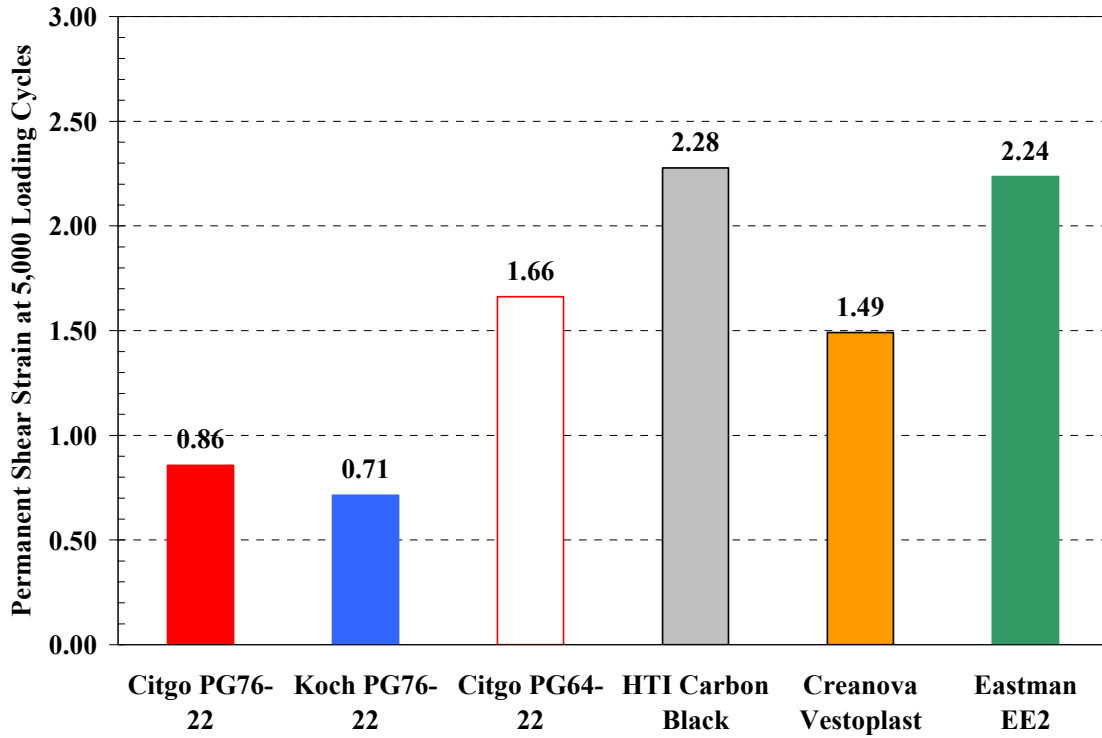
Figure 24 – Permanent Shear Strain at 5,000 Loading Cycles at 52°C from RSCH
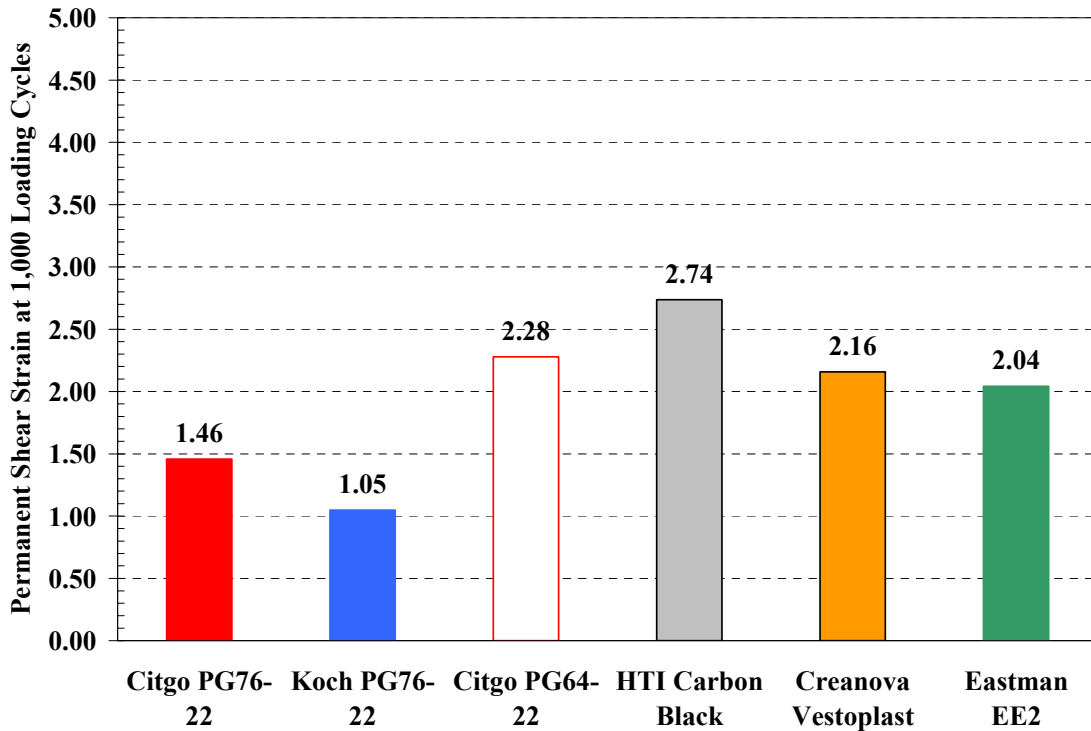
Figure 25 – Permanent Shear Strain at 1,000 Loading Cycles at 64°C from RSCH
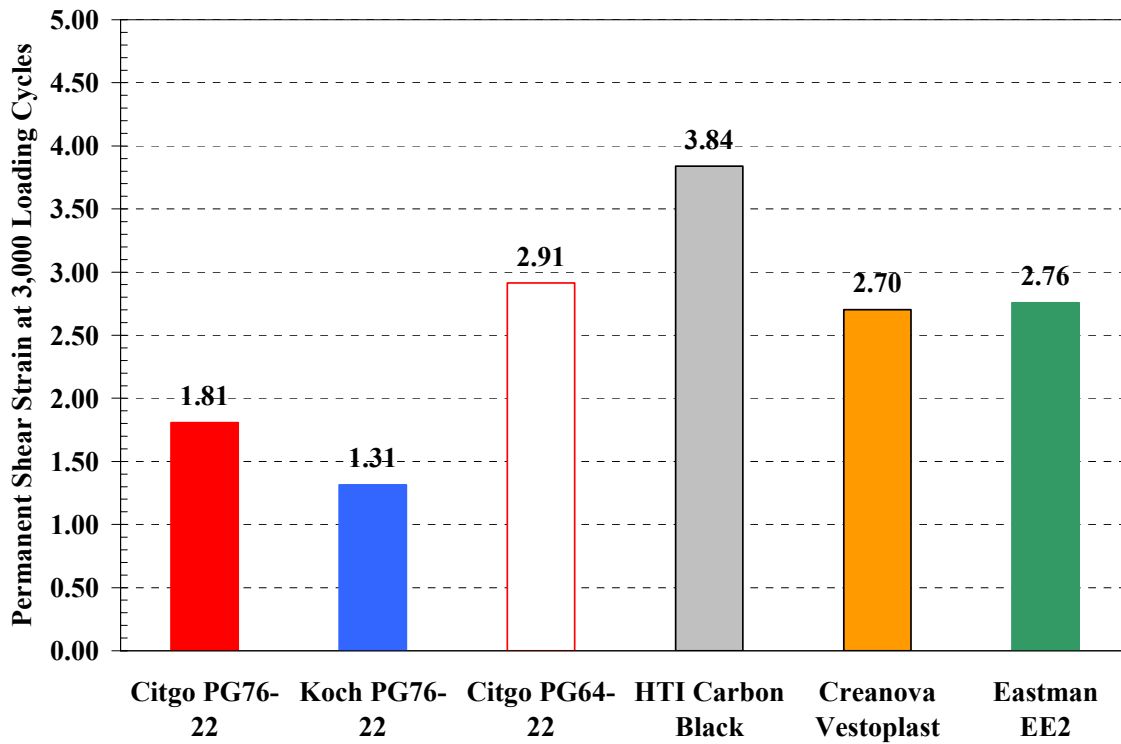
Figure 26 – Permanent Shear Strain at 3,000 Loading Cycles at 64°C from RSCH
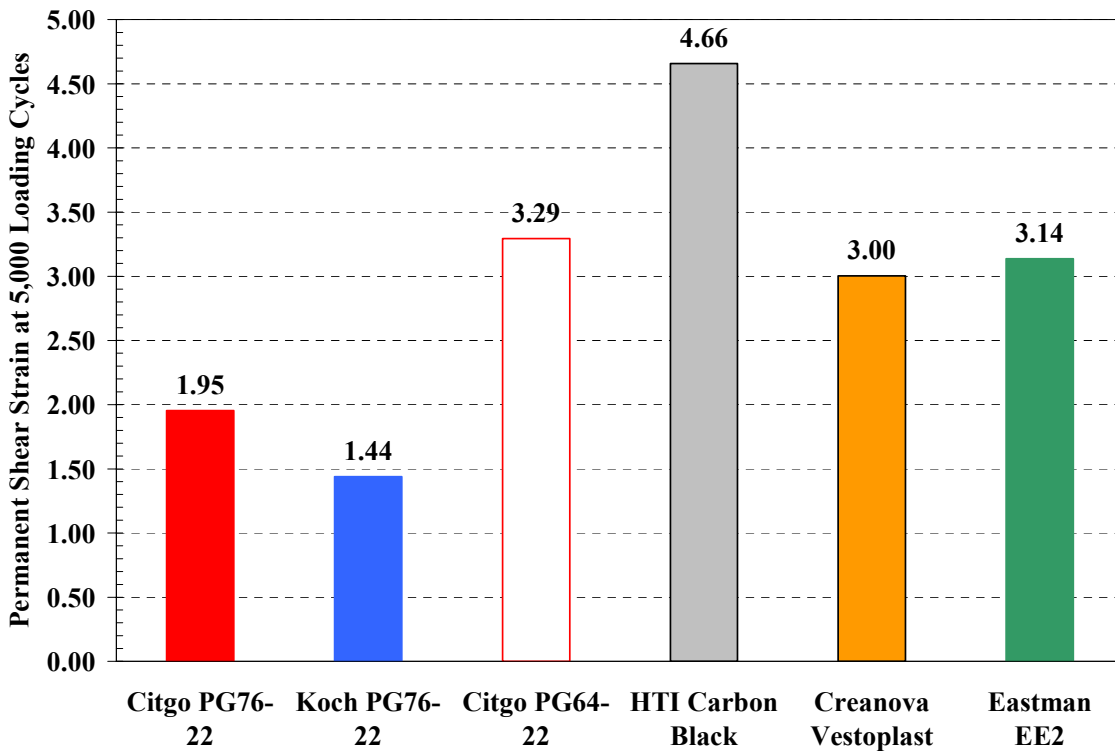
Figure 27 – Permanent Shear Strain at 5,000 Loading Cycles at 64°C from RSCH

Slope of Regression Analysis – Results

As stated earlier, there are typically two statistical models used to predict the accumulation of permanent deformation; the Log Model and the Power Model. Each model is dependent of an intercept parameter and a sloping parameter. The intercept parameter determines the permanent strain at one loading cycle, while the sloping parameter is based on the rate at which the permanent shear strain occurs. The sloping parameter is of particular interest since it is assumed that materials with the highest resistance to permanent deformation will have the lowest rate of permanent strain accumulation. Figure 28 shows the relationship between the two sloping parameters and the accumulated permanent shear strain at 5,000 loading cycles. The 5,000 loading cycles was used since this has been the traditionally accepted number used for the evaluation of permanent shear strain. From the figure it can be shown that the sloping parameter for the Log model (S) increases with the increase in permanent shear strain, while the sloping parameter for the Power model (S*) decreases with increasing permanent shear strain.
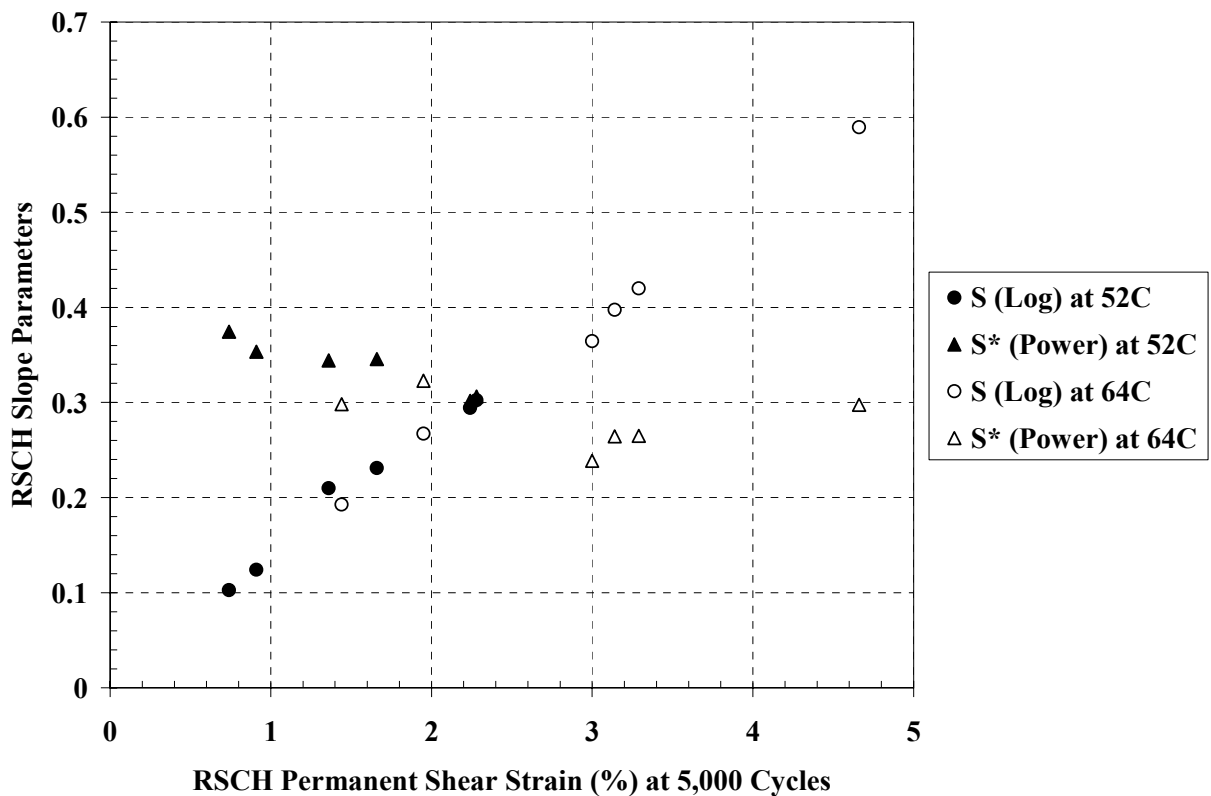
Figure 28 – Relationship Between Sloping Parameters and RSCH Permanent Shear Strain at 5,000 Loading Cycles

The relationship between the Log-sloping parameter (S) is very strong. In fact, a linear trendline can almost be drawn through all points back to the origin. This would suggest that the lower the S sloping parameter, the lower the susceptibility of rutting.

In fact, by drawing the line to the origin, the relationship would suggest that a slope of zero would provide zero permanent shear strain. Meanwhile, the Power sloping parameter (S*) does not have as strong of a relationship to the permanent shear strain at 5,000 loading cycles. However, the relationship does suggest that the Power model sloping parameter would decrease with increasing permanent shear strain at 5,000 loading cycles. Table 11 provides the sloping parameters for both the Log and Power models at both $52^{o}C$ and $64^{o}C$. Table 12 shows the rankings based on both the permanent shear strain at 5,000 loading cycles and the sloping parameters, as well as the rankings from the binder testing. The average rankings for the RSCH using all of the parameters were as follows:

1. Koch PG76-22
2. Citgo PG76-22
3. Creanova Vestoplast
4. Citgo PG64-22
5. Eastman EE-2
6. Hydrocarbon Technologies Carbon Black

Table 11 – Slope Parameters for Both the Log (S) and Power (S*) Models

| Sample Type | Accumulated Permanent Shear Strain Slopes | | | |
| | Temperature = 52C | | Temperature = 64C | |
	S (Log)	S* (Power)	S (Log)	S* (Power)
Citgo PG64-22	0.231	0.3456	0.4198	0.2648
Citgo PG76-22	0.1241	0.3535	0.2672	0.3228
Koch M. PG76-22	0.1027	0.3743	0.1926	0.2983
Eastman EE2	0.2943	0.3018	0.3973	0.2645
Creanova Vestoplast	0.21	0.3443	0.3645	0.2386
HTI Carbon Black	0.3023	0.3062	0.5893	0.2976

Table 12 – Ranking of Asphalt Modifiers from RSCH and Binder Testing

| Sample Type | Ranking of Materials Tested in the RSCH | | | | | | Binder Testing |
| | Temperature = $52^{o}C$ | | | Temperature = $64^{o}C$ | | | |
	S (Log)	S* (Power)	ε_P @ 5,000	S (Log)	S* (Power)	ε_P @ 5,000	
Citgo PG64-22	4	3	5	5	4	5	6
Citgo PG76-22	2	2	2	2	1	2	1
Koch M. PG76-22	1	1	1	1	2	1	1
Eastman EE2	5	6	5	4	5	4	4
Creanova Vestoplast	3	4	3	3	6	3	3
HTI Carbon Black	6	5	6	6	3	6	5

The final average rankings for the RSCH testing were similar to the binder testing. Both of the PG76-22 binders performed the best. However, in the RSCH testing, the HTI carbon black material ranked the worst. In fact, even the Eastman EE2 modifier ranked worse than the neat PG64-22. The Eastman EE2 modifier ranked worse due its poor performance at the 52°C RSCH testing. This particular material may not be sensitive enough to temperature to aid in the resistance to permanent deformation. Meanwhile, the poor performance of the carbon black material was most likely due to the material's inability to be used as a direct add-in modifier. The carbon black modified HMA seemed to act as if it was over-asphalted.

From the RSCH testing, the asphalt modifier that performed the best was the Creanova Vestoplast. Unfortunately, inspection of the permanent shear strain curves shows that the Creanova Vestoplast only increased the shear resistance a slight amount. None of the admixtures were able to capture the rut resistant properties of the two PG76-22 binders.

Summary of RSCH Results – Effect of Loading Cycles

The permanent shear strains at different loading cycles indicate that 1,000 loading cycles may not be long enough to fully evaluate the permanent shear resistance of the mixes. This is based on comparing the rankings of the mixes at 1,000 and 5,000 loading cycles. However, 3,000 loading cycles, as indicated by Witzcak et al. (2002) would be sufficient to properly rank the materials based on the RSCH performance, although there is a small discrepancy at when tested at 52°C. Unfortunately, to take full advantage of RSCH slope parameters, the use of the full 5,000 loading cycles may provide better results. Figure 29 shows the sloping parameters determined when using the full 5,000 loading cycles, as opposed to using only 3,000. As can be seen from the figure, the larger the sloping parameters get, the larger the potential for error.

Summary of RSCH Results – Effect of Test Temperature

As stated earlier, both of the PG76-22 mixes performed the best, with the Koch Materials slightly better than the Citgo PG76-22. This occurred at both 52°C and 64°C. However, the performance of the other mixes changed depending on the temperature tested. At both temperatures, the HTI Carbon Black material performed the worst. However, the largest discrepancy occurred at the 64°C test temperature where the HTI material accumulated a permanent shear strain almost 1.5% higher than the next material, which was the Citgo PG64-22. The Creanova Vestoplast performed in a similar manner in which the material slightly out-performed the neat PG64-22 binder at both 52 and 64°C. The performance of the Eastman EE2 at both 52°C and 64°C were very similar. It appears that this material may not be as sensitive to temperatures as the other modifiers. This insensitivity to temperature may be an example of why both temperatures may need to be incorporated in a testing program. At this point, it was anticipated that New Jersey's seven-day high temperature (approximately 52°C) could be used as the recommended test temperature.

However, based on the RSCH test results, perhaps the better test temperature to evaluate is the neat binder's (blending binder) high performance grade, in this case 64°C.
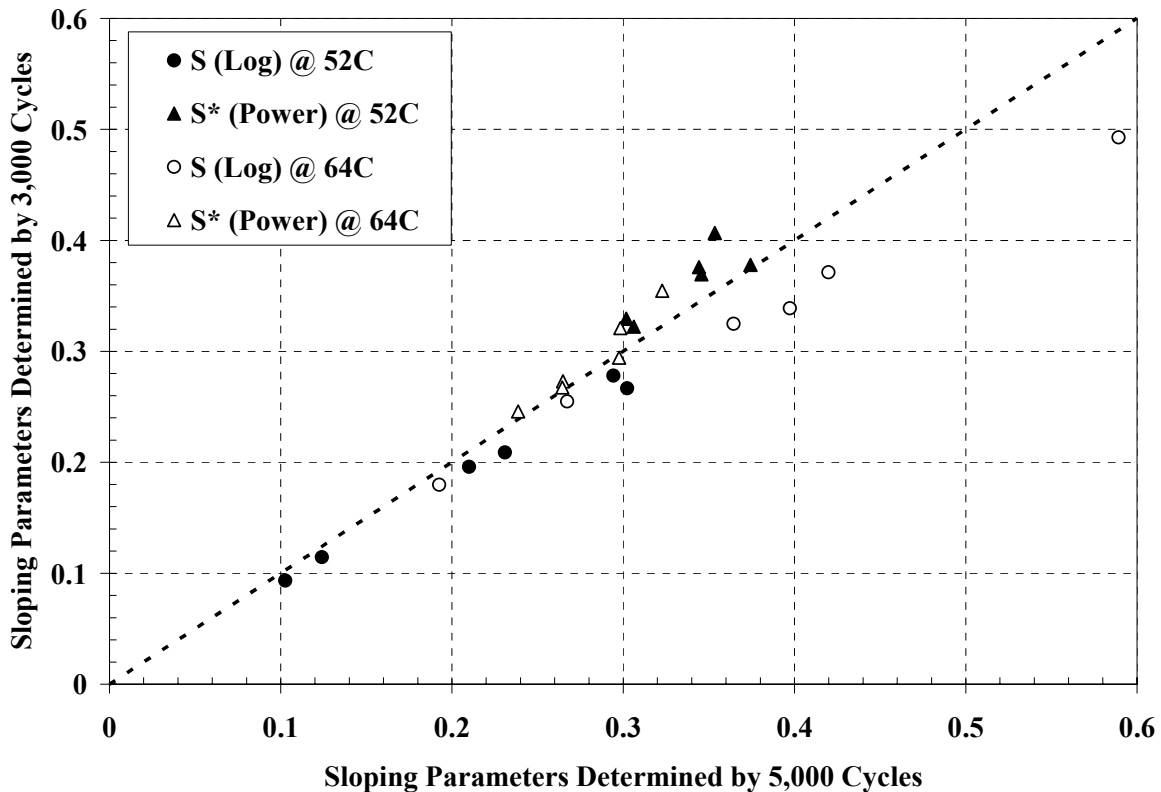
Figure 29 – Comparison of Sloping Parameters When Determined at 3,000 and 5,000 Cycles from the RSCH Test

Superpave Shear Tester – Frequency Sweep at Constant Height (FSCH)

The Superpave Shear Test (SST) was used under the Frequency Sweep at Constant Height (FSCH) test mode. During this test, the asphalt sample is subjected to a haversine wave load at loading frequencies ranging from 10 Hz to 0.01 Hz. The load is applied until a shear stress of 0.01% is obtained. This ensures that the sample is solely tested in the linear elastic range. At each load frequency, the dynamic shear modulus and phase angle are determined. All samples were tested at three temperatures; 20, 40, and 52°C as specified by AASHTO TP7-01. By testing in this manner, a master curve that represents the materials stiffness over a broad range of frequencies can be developed.

The results of the FSCH test were the average of three samples. The individual results for the samples tested are shown in Appendix C.

Dynamic Shear Stiffness (G*)

The dynamic shear stiffness (G*) of the tested materials were determined at three different temperatures as recommended by AASHTO TP7-01 (20, 40, and 52°C). Results of G* at the varying temperatures are shown in Figures 30 through 32.
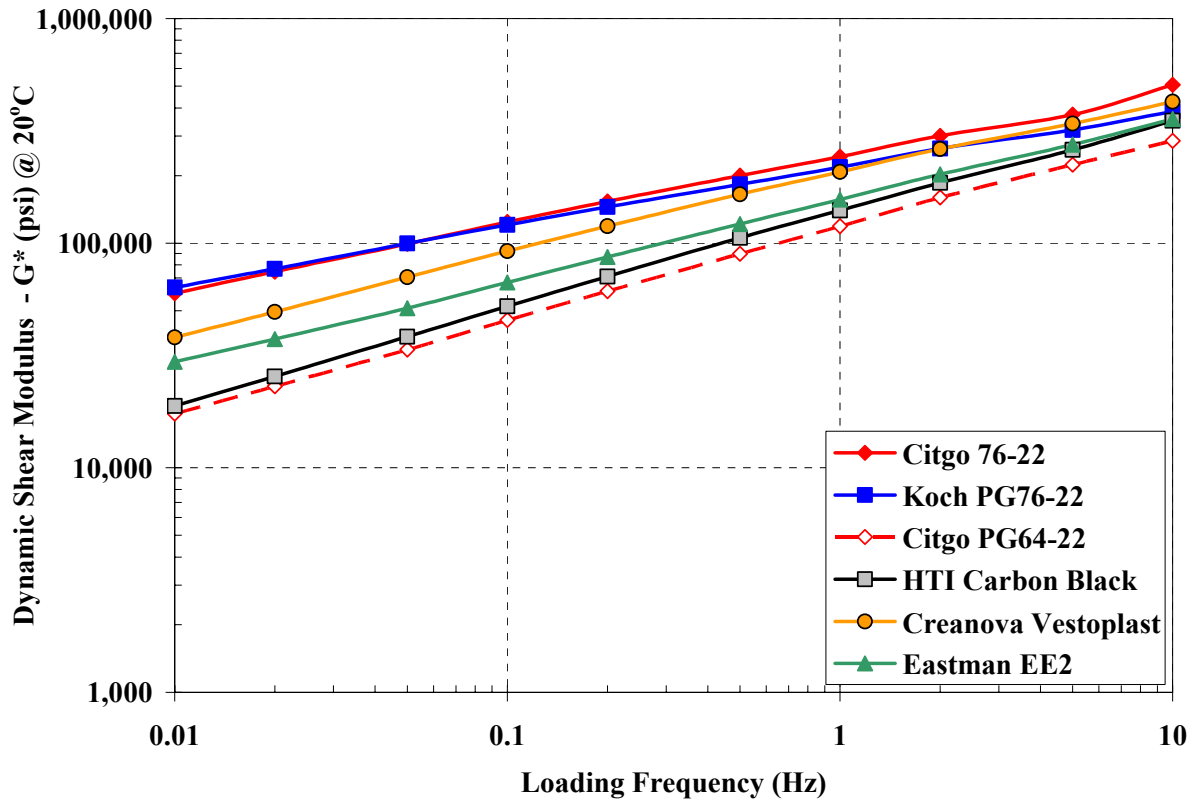
Figure 30 – FSCH Results Tested at 20°C

In general, the two polymer-modified PG76-22 samples obtained the largest stiffness (G*) at all temperatures and frequencies tested. The Creanova Vestoplast obtained the largest stiffness when strictly looking at the add-in modifiers, with the Eastman EE-2 and HTI Carbon Black following, respectively. The HTI carbon black obtained larger stiffness' at the higher loading frequencies. However, as the load frequency went below 0.1 Hz, the stiffness of the carbon black was similar to that of the neat PG64-22. This same trend also existed between the two PG76-22 binders. A higher loading frequencies, the Citgo PG76-22 obtained larger stiffness', especially at temperatures of 20 and 40°C. However, once the loading frequency went below 0.1 Hz, the Koch Materials PG76-22 obtained the larger stiffness. The Koch Material also obtained the largest stiffness at 52°C for all frequencies tested.
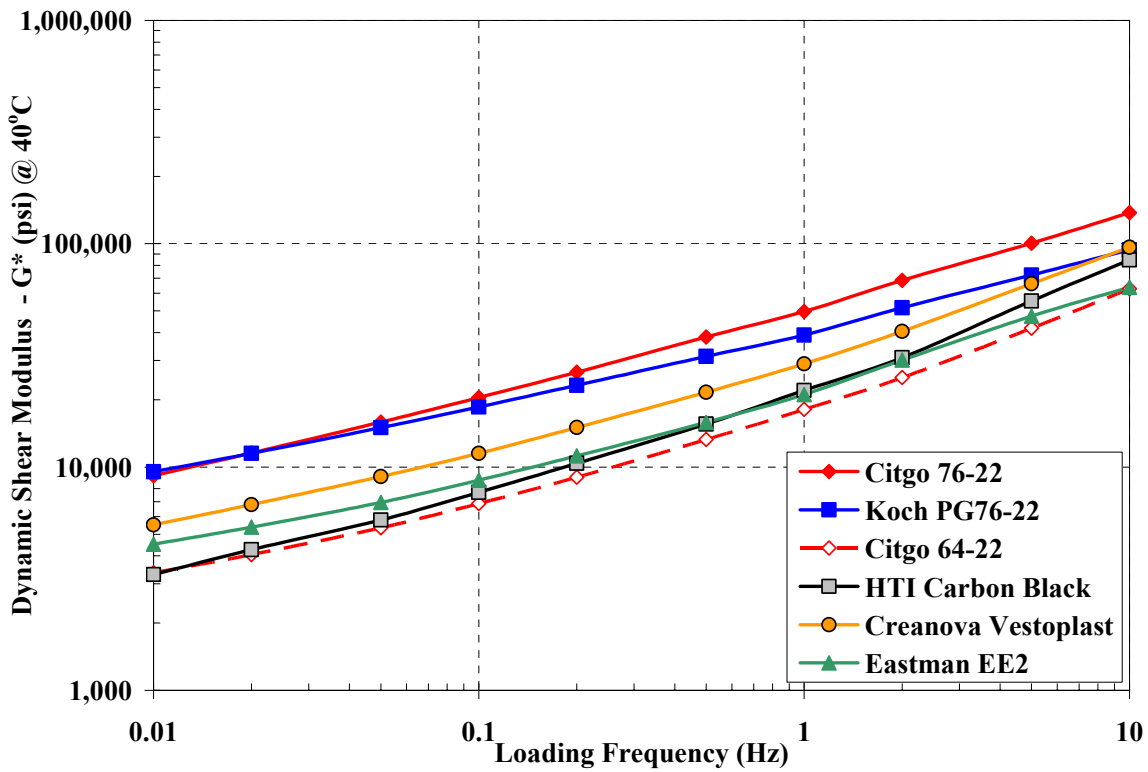
Figure 31 – FSCH Results Tested at 40°C
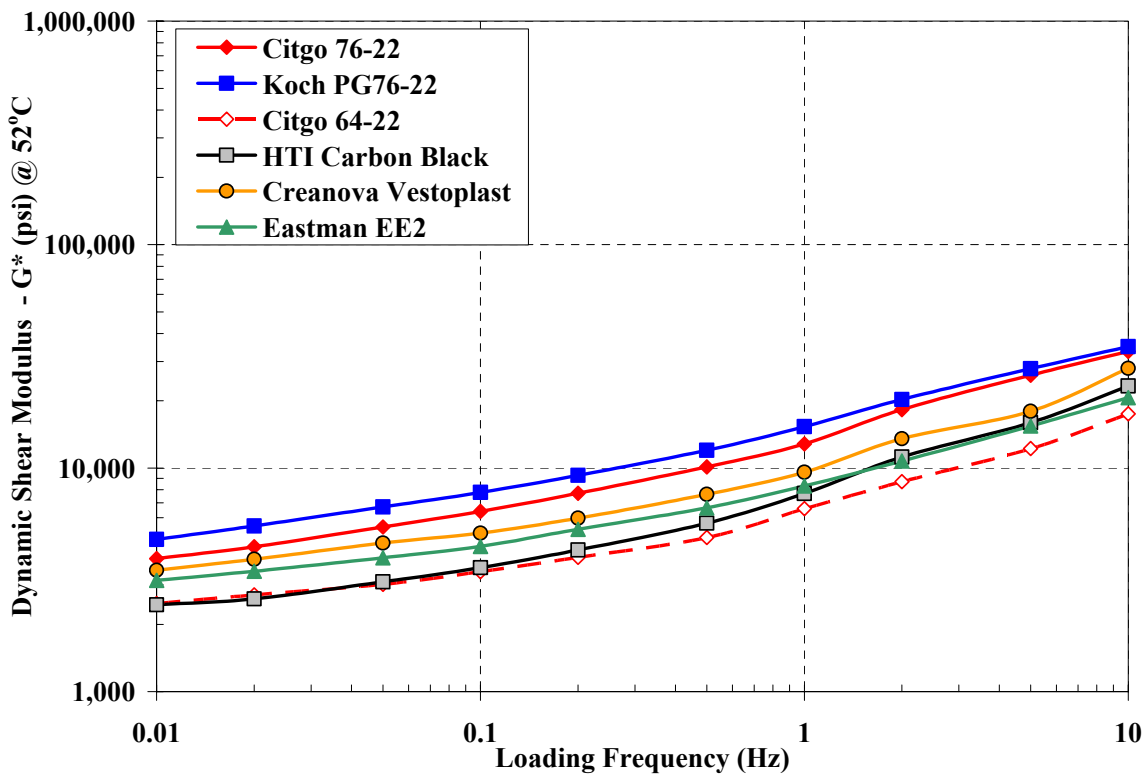
Figure 32 – FSCH Results Tested at 52°C

Figures 33 to 38 show the master curves developed for all of the samples tested. The shifting was conducted using equation (3) and (4), normalized to the test temperature of 20°C.
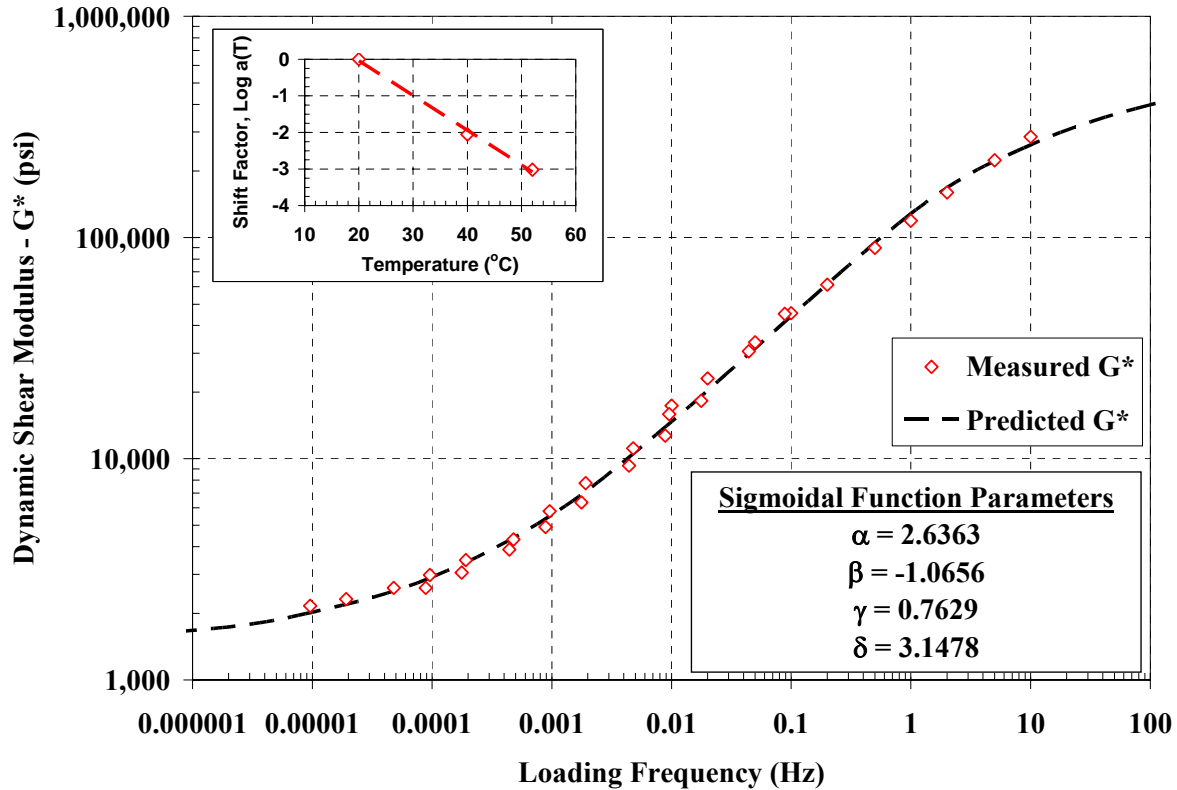
Figure 33 – G* Master Stiffness Curves for Citgo PG64-22

Another factor that is important in the stiffness determination of asphalt-aggregate mixes is the phase angle (ϕ). The phase angle represents the time lag in the strain response to the loading. For totally elastic materials there is no lag between the applied shear stress and the strain response. For this case ϕ is equal to zero. For totally viscous materials, strain response is completely out of phase with the applied stress and ϕ is 90 degrees. For visco-elastic materials like asphalt-aggregate mixes, high temperatures will cause the phase angle to approach 90 degrees with the cold temperatures causing the phase angle to approach zero degrees.

The effect of the phase lag (phase angle, ϕ) can be evaluated by plotting the storage modulus (G'), elastic component, and the loss modulus (G"), viscous component, against one another. The storage modulus is determined using equation (5) and the loss modulus (G") is determined using equation (6).

$$G' = G * (\cos \phi) \tag{5}$$

$$G'' = G * (\sin \phi) \tag{6}$$
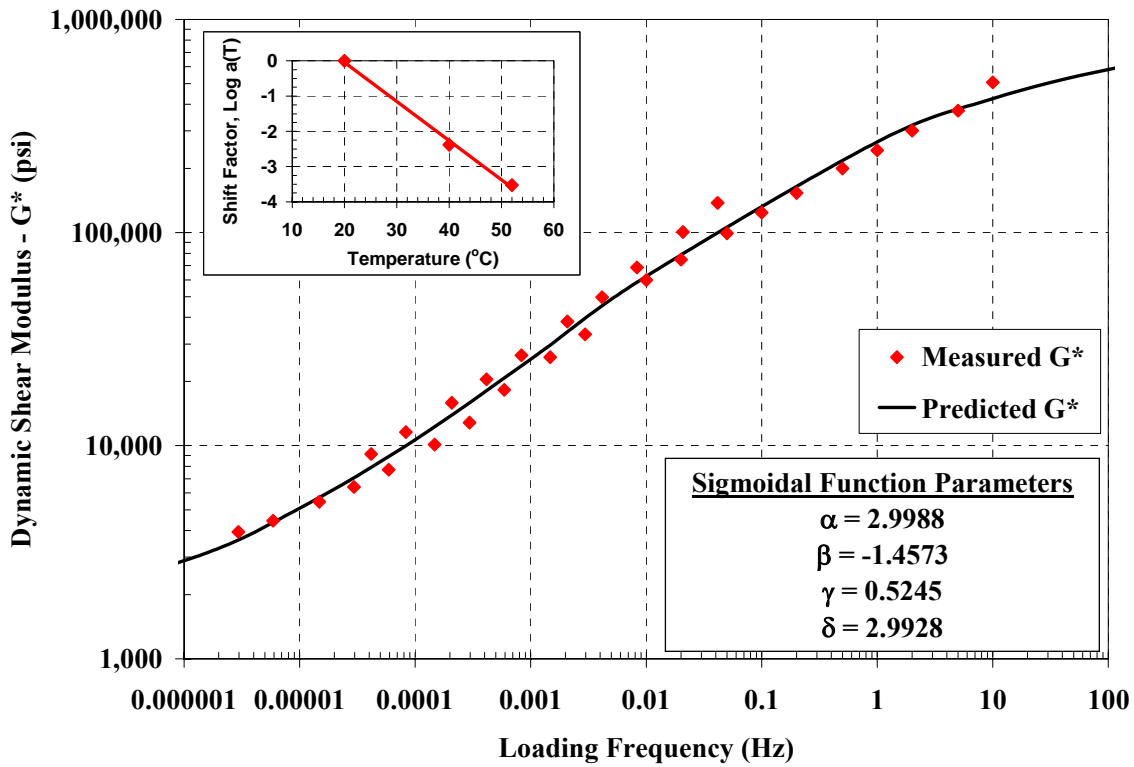
Figure 34 – G* Master Stiffness Curves for Citgo PG76-22
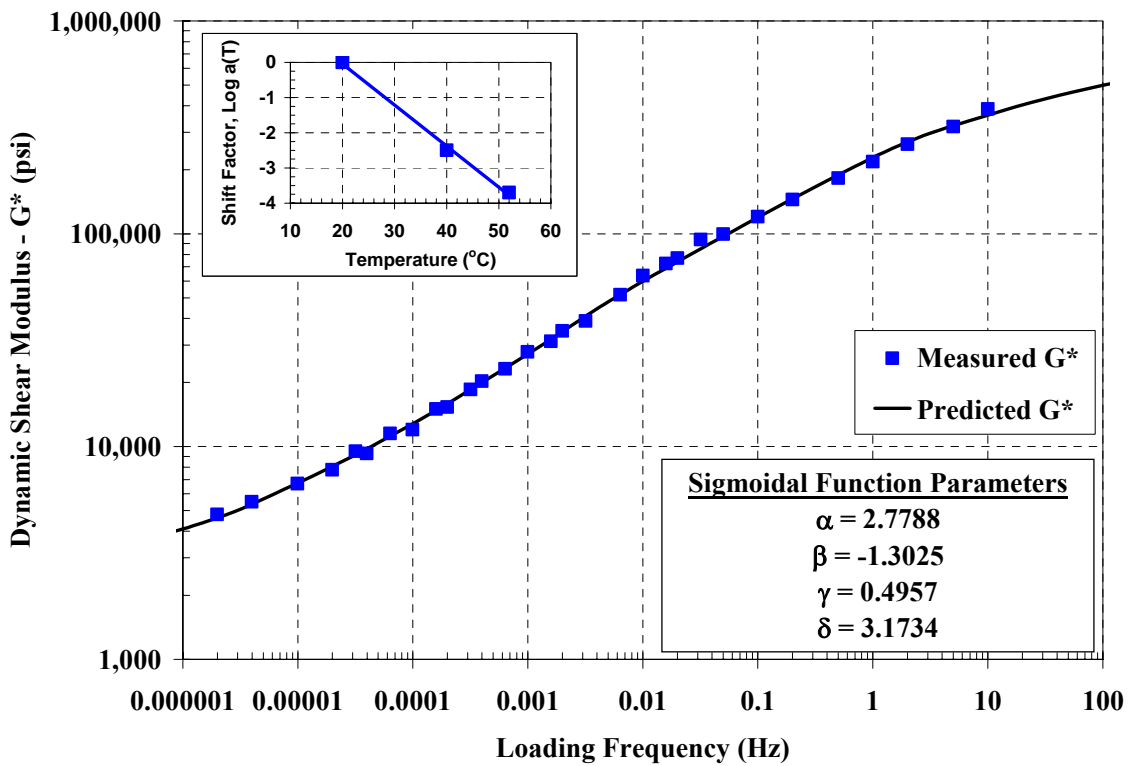
Figure 35 – G* Master Stiffness Curves for Koch Materials PG76-22
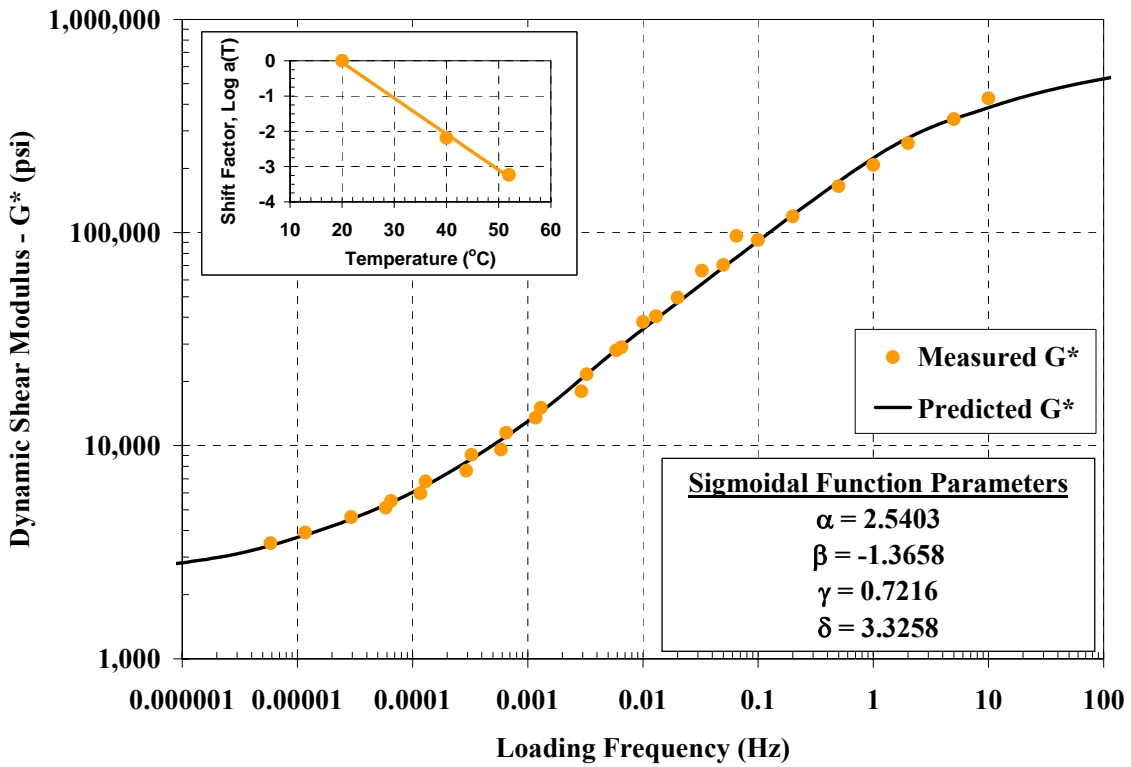
Figure 36 – G* Master Stiffness Curves for Creanova Vestoplast
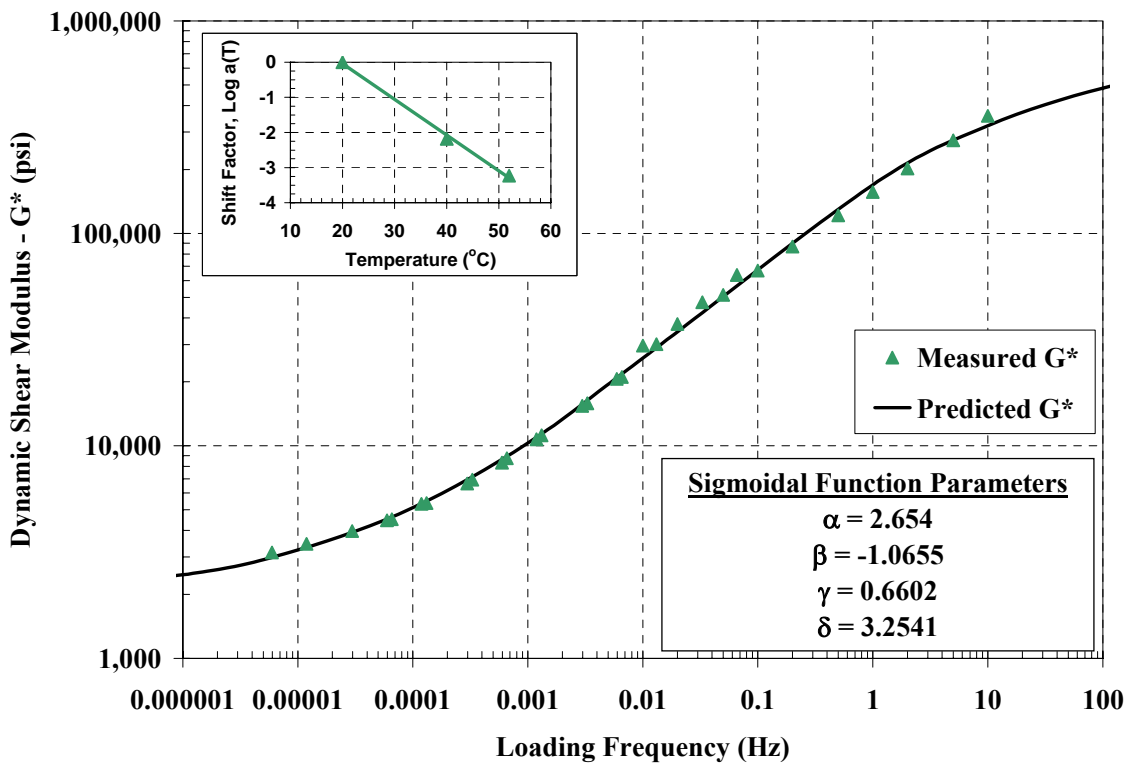
Figure 37 – G* Master Stiffness Curves for Eastman EE-2
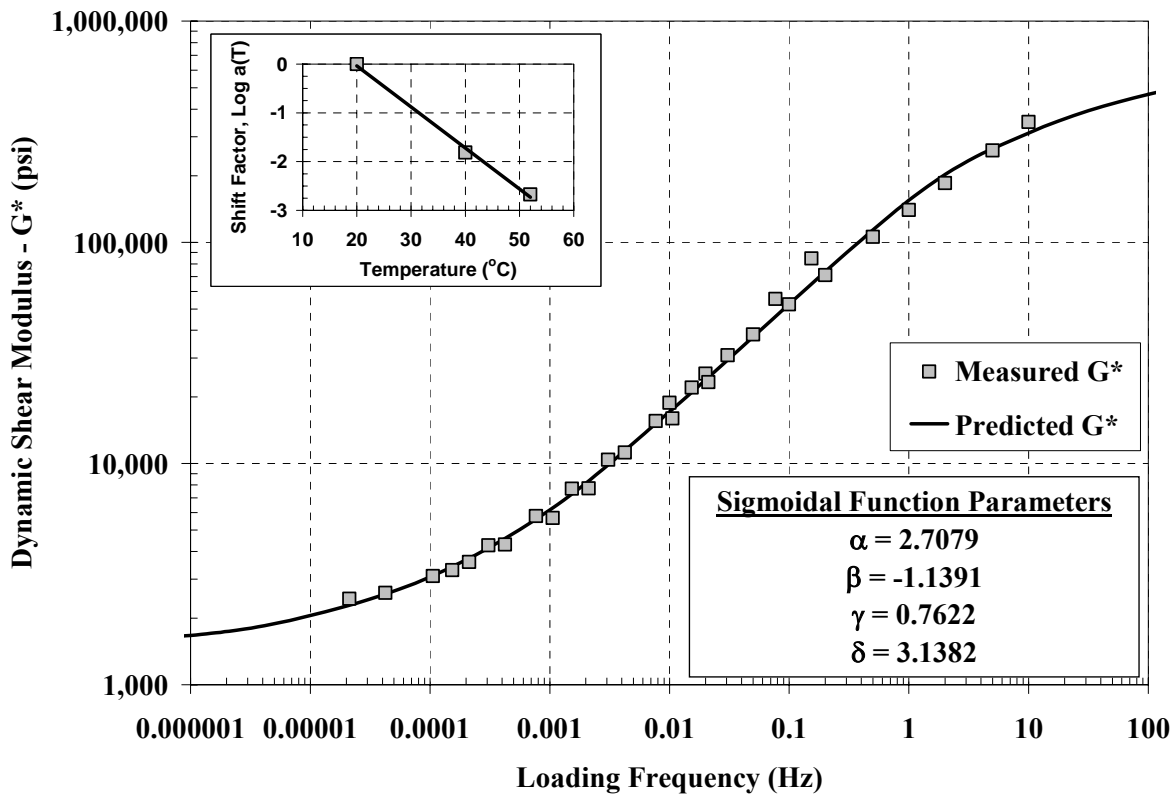
Figure 38 – G* Master Stiffness Curves for HTI Carbon Black

Plotting the G' and G" against one another is called the Cole-Cole Plane or Complex Plane. By plotting the results in this manner, an assessment of the quality of the test data can be accomplished. For good quality data, the values should create one unique curve, which is independent of temperature or frequency (Pellinen, 2001). Figure 39 shows the Cole-Cole Plane for the baseline (PG76-22 and PG64-22) binders and Figure 40 shows the Cole-Cole Plane for the asphalt modifiers. Both figures show a relatively unique curve illustrating the generally good quality of the results.
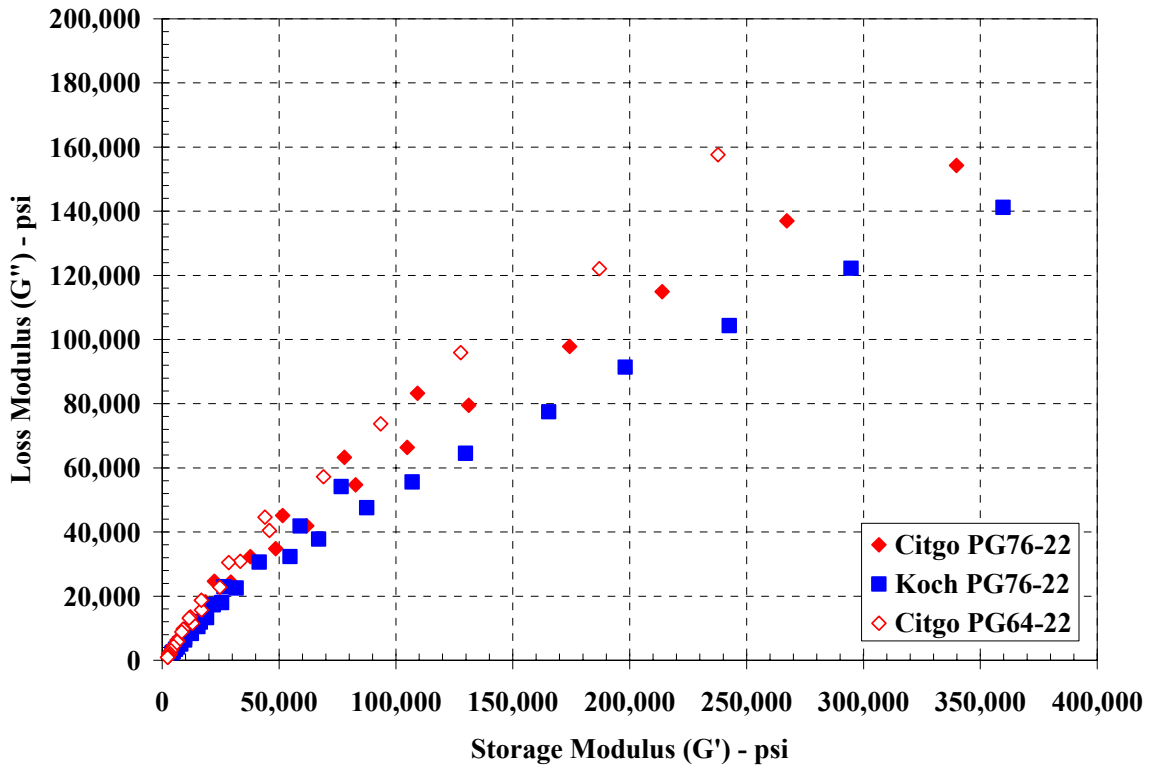
Figure 39 – Cole-Cole Plane for the Baseline Binders
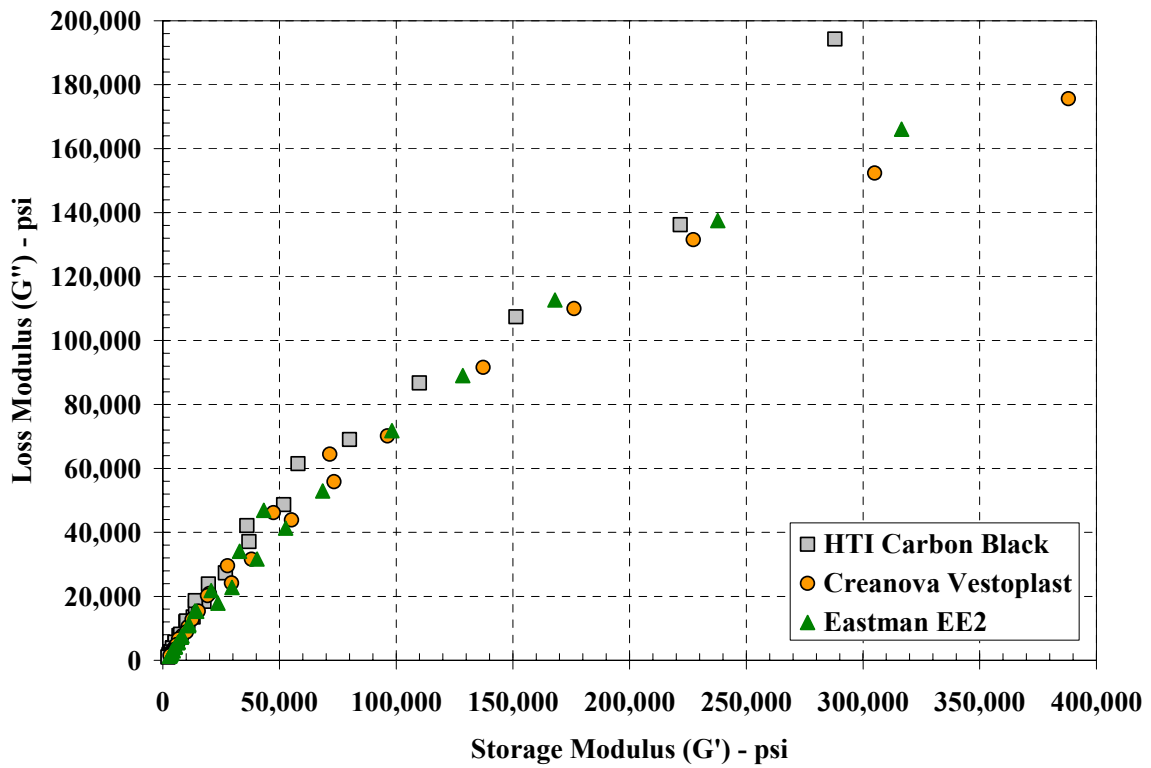
Figure 40 – Cole-Cole Plane for the Asphalt Modifiers

Unfortunately, the Cole-Cole Plane is best used for cold and intermediate temperatures. For high temperatures, the Black Space method is recommended. The Black Space method plots the modulus values in log space and the phase angle values in arithmetic space. Figures 41 and 42 show the Black Space method applied to the baseline binders and the asphalt modifiers, respectively. For good quality data ($R^2 > 0.9$), the kind of data that represents parameters that could be properly incorporated into a performance model, the values should form one unique curve. In the case of the data shown in the figures, the values do not form a unique curve. The non-uniformity is especially evident when going from 20°C to 40°C. This particular problem with FSCH data from the SST was discussed by Witzcak et al. (2000) and can attributed to instrumentation and sample size problems. Therefore, these results can only be categorized as representing index values of the shear modulus of the HMA and not true shear modulus values. Since the same testing problems existed with all of the samples tested, the test procedure can still be used for direct comparisons between one another.
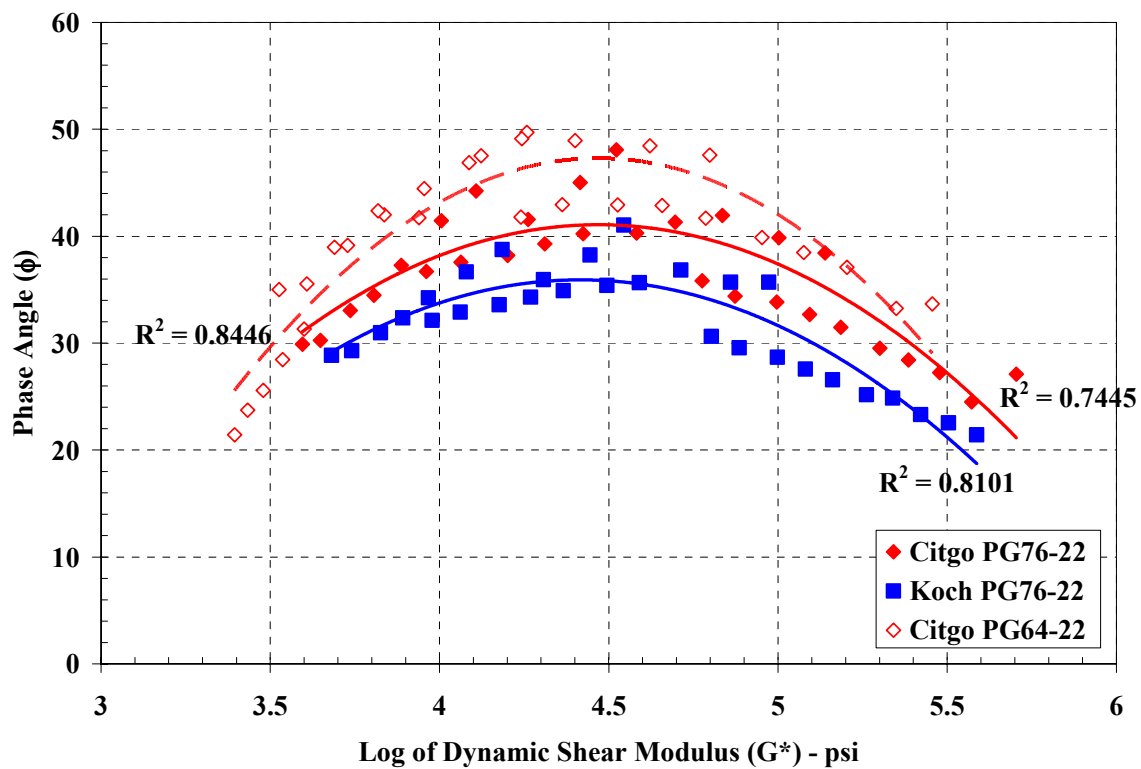
Figure 41 – Black Space Applied to the Baseline Binders
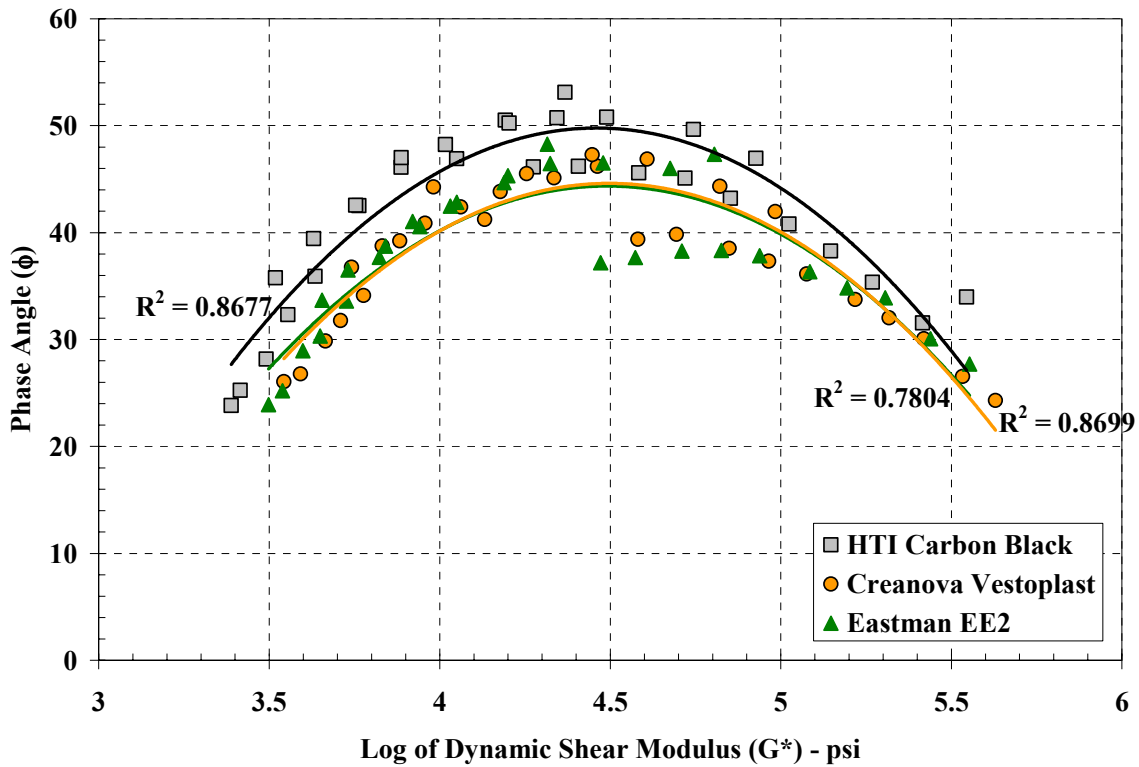
Figure 42 – Black Space Applied to the Asphalt Modifiers

Rutting Parameter (G*/sinφ)

The rutting parameter (G*/sinφ) was determined from the FSCH test at a loading frequency of 0.1 Hz. The rutting parameter was evaluated at both 40 and 52°C. Figures 43 and 44 show the rutting parameter values for all of the samples tested. The rutting parameter results between the 40°C and the 52°C are similar in trend. Both of the PG76-22 binders recorded the largest rutting parameter values, with the Creanova Vestoplast and the Eastman EE2 have the third and fourth largest, respectively. At 40°C, the HTI carbon black obtained a larger rutting parameter than the Citgo PG64-22. However, at the 52°C test temperature, it was the Citgo PG64-22 obtaining a larger rutting parameter than the HTI carbon black.

Earlier binder research showed that binders that obtained larger rutting parameters were less susceptible to permanent deformation. As stated earlier, research has also shown that the FSCH results correlate well with binder performance. Based on this, HMA samples that obtained the largest rutting parameters from the FSCH tests can be assumed to be less rut susceptible than the samples that obtained the lower rutting parameter values. Table 13 shows the rankings of both the binder testing and the rutting parameter results. The table shows a strong relationship between the rankings.
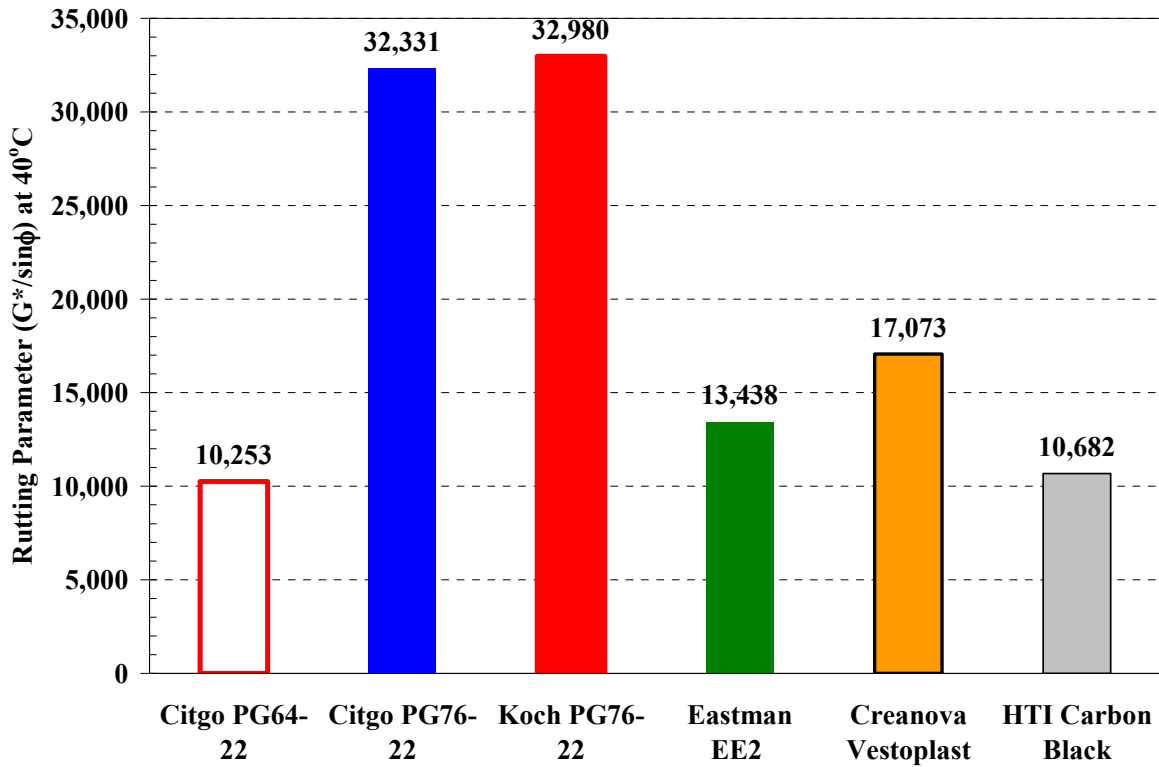
Figure 43 – Rutting Parameter (G*/sinϕ) Determined at 40°C and a Frequency of 0.1 Hz
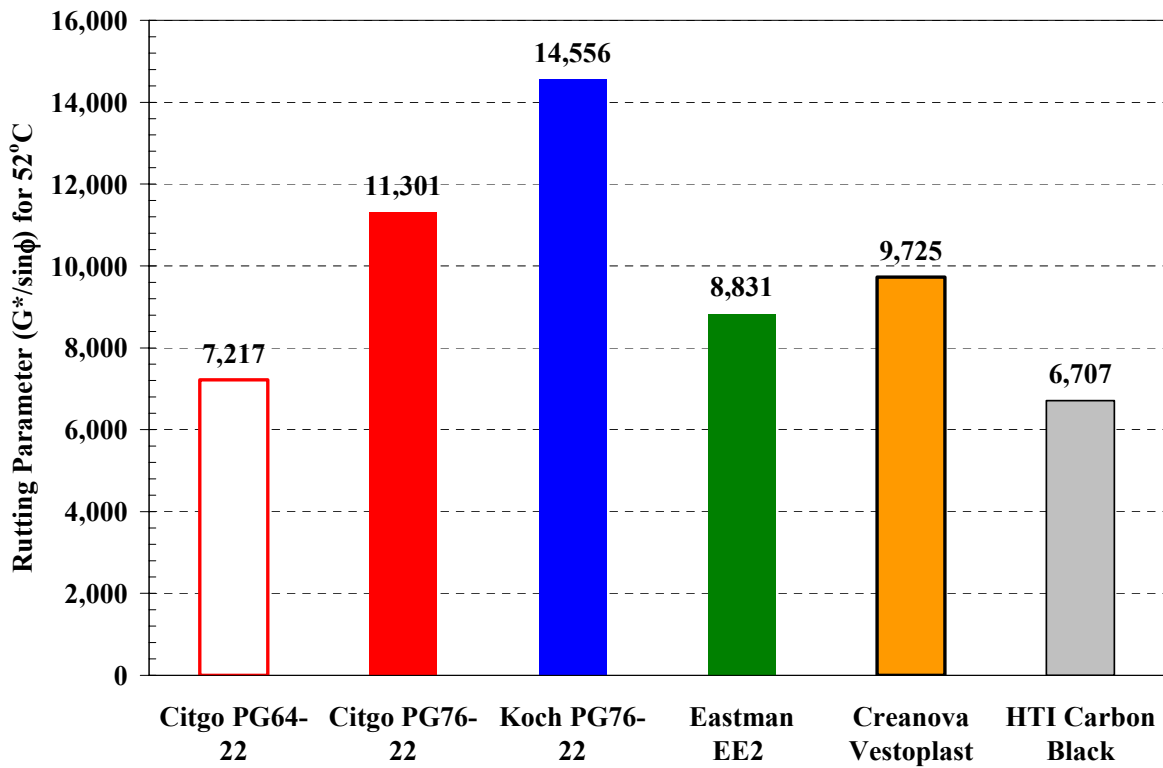
Figure 44 – Rutting Parameter (G*/sinϕ) Determined at 52°C and a Frequency of 0.1 Hz

Table 13 – Performance Ranking of Both Binder Testing and FSCH Rutting Parameter Results

Sample Type	Frequency Sweep Test		Binder Testing
	Rutting Parameter (G*/sinϕ)		
	40°C	52°C	
Citgo PG64-22	6	5	6*
Citgo PG76-22	2	2	1*
Koch M. PG76-22	1	1	1*
Eastman EE2	4	4	4
Creanova Vestoplast	3	3	3
HTI Carbon Black	5	6	5

* - Assumed Based on High Temperature Performance Grade

Slope m of the G* vs Frequency Plot

The m value is obtained from the frequency sweep at constant height conducted by the Superpave shear tester (SST) at high effective temperature (40 and 52°C) for permanent deformation with frequencies ranging from 0.01 hertz to 10 hertz.
This slope represents the rate of development of rutting for the tested mix and is used in the Superpave model as such. The lower the m slope, the better is the mix's resistance to rutting.

The m slope was determined for each mix tested at both 40 and 52°C. Table 14 shows the results from the testing. The table indicates that at 40°C, the m slope is consistent with the rutting parameter, as far as ranking the modifiers. However, at 52°C there is no trend in the m slope. If fact, the Eastman EE2 obtained the lowest m slope, indicating that this material would rut less. Of course, this was not true as the RSCH results showed that this material ranked 4th. Table 15 shows the ranking of materials, with both the rutting parameter and the RSCH test results included. As can be seen, the m slope determined at 52°C is not consistent with the other rankings.

It does not seem that the m Slope parameter is a true measure of the rut susceptibility of the asphalt mixture, although the results from the 40°C are similar to both the rutting parameter and the RSCH rankings. The m Slope parameter is more of an indication of the asphalt mixes response to the loading frequency. The greater the m Slope from the FSCH data, the more the asphalt mixture is influenced by the loading frequency. Although this may not be helpful in the selection of an asphalt modifier to resist rutting, it is a useful parameter to use in deciding between two asphalt modifiers with similar rut resistance. An engineer would want to select an asphalt modifier with a low m Slope since this means that the mix's stiffness would not differ considerably between fast and slow moving traffic.

Table 14 – m Slope Results from FSCH Testing

| Sample Type | FSCH Test Results | |
| | m Slope | |
	40°C	52°C
Koch M. PG76-22	0.3317	0.2916
Citgo PG76-22	0.3925	0.3146
Citgo PG64-22	0.4229	0.2798
Creanova Vestoplast	0.4117	0.2903
Eastman EE2	0.3887	0.2714
HTI Carbon Black	0.4648	0.3302

Table 15 – Ranking of m Slope Parameters for Rut Resistance

| Sample Type | Frequency Sweep Test | | | | RSCH Testing | |
| | Rutting Parameter (G*/sinφ) | | m Slope | | Permanent Shear Strain @ 5,000 | |
	40°C	52°C	40°C	52°C	52°C	64°C
Citgo PG64-22	6	5	5	2	4	5
Citgo PG76-22	2	2	3	5	2	2
Koch M. PG76-22	1	1	1	4	1	1
Eastman EE2	4	4	2	1	5	4
Creanova Vestoplast	3	3	4	3	3	3
HTI Carbon Black	5	6	6	6	6	6

Fatigue Factor (G*sinφ)

Although not specifically needed for the evaluation of permanent deformation, the fatigue factor was evaluated from the FSCH tests. The fatigue factor is a measure of the stiffness at intermediate effective pavement temperatures for fatigue cracking or Teff(FC). G*sinφ was measured at 1.0 hertz to represent fast moving traffic. A Teff(FC) of 20°C was used. High values of G*sinφ at 1.0 hertz indicate high stiffness at intermediate temperatures and, therefore, low resistance to fatigue cracking according to Superpave. Figure 45 shows the Fatigue Factor for the samples tested in the FSCH test. The results show that the Citgo PG76-22 obtained the largest Fatigue factor, with the Creanova Vestoplast obtaining the second largest. The Koch Materials PG76-22 has the third highest. The remaining two modifiers show a slight increase from the baseline PG64-22 mix.

Table 16 shows the final rankings of the FSCH tests. The results of the FSCH rankings are very similar to the binder true performance grading. This verifies the work of Williams et al. (1998). The m Slope was not included in the ranking since it did not provide a true measurement of the rut potential of the mix. It appeared to be more of an indicator of the effect of loading frequency on the material response.
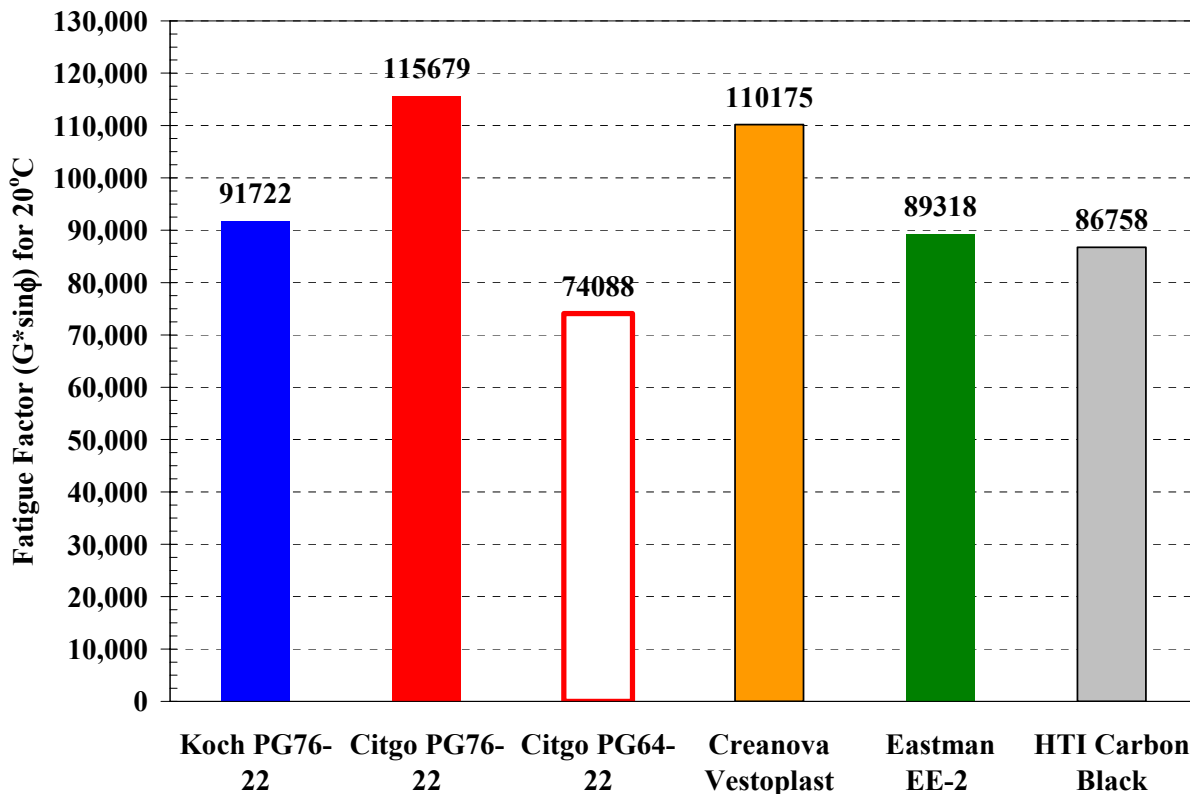
Figure 45 – Fatigue Factors Determined from the FSCH Tests at 20°C

Table 16 – Final Rankings of Tested Materials from the FSCH Test

| Sample Type | Frequency Sweep Test | | | Average Ranking | Binder Testing |
| | Rutting Parameter (G*/sinϕ) | | Fatigue Factor (G*sinϕ) | | |
	40°C	52°C	20°C		
Citgo PG64-22	6	5	5	5	6*
Citgo PG76-22	2	2	1	1	1*
Koch M. PG76-22	1	1	3	1	1*
Eastman EE2	4	4	4	4	4
Creanova Vestoplast	3	3	2	3	3
HTI Carbon Black	5	6	6	6	5

* - Assumed based on the PG grading

Superpave Shear Tester – Simple Shear at Constant Height (SSCH)

The Superpave Shear Tester was used under the Simple Shear at Constant Height (SSCH) test mode to evaluate the creep properties of the modified asphalt samples. The specimen is loaded at a stress rate of 70 kPa/sec until a pre-determined creep load is obtained. The creep load is based on the temperature for which it is tested. The creep loads used in this study conform to those recommended in AASHTO TP7-01 test procedure B, and are; 345 ± 5 kPa for 4°C, 105 ± 5 kPa for 20°C, and 35 ± 5 kPa for

40°C. The creep load is applied for 10 seconds and then the load is reduced to zero at a rate of 25 kPa/sec. Once the stress reaches zero, the shear strain is measured for another 10 seconds. The test is complete after these final 10 seconds at zero stress. Figure 46 shows a schematic of the applied load with a typical SSCH load-deformation curve conducted at 40°C.

The results from the SSCH tests were an average of three samples. The individual results for the samples are in Appendix D.
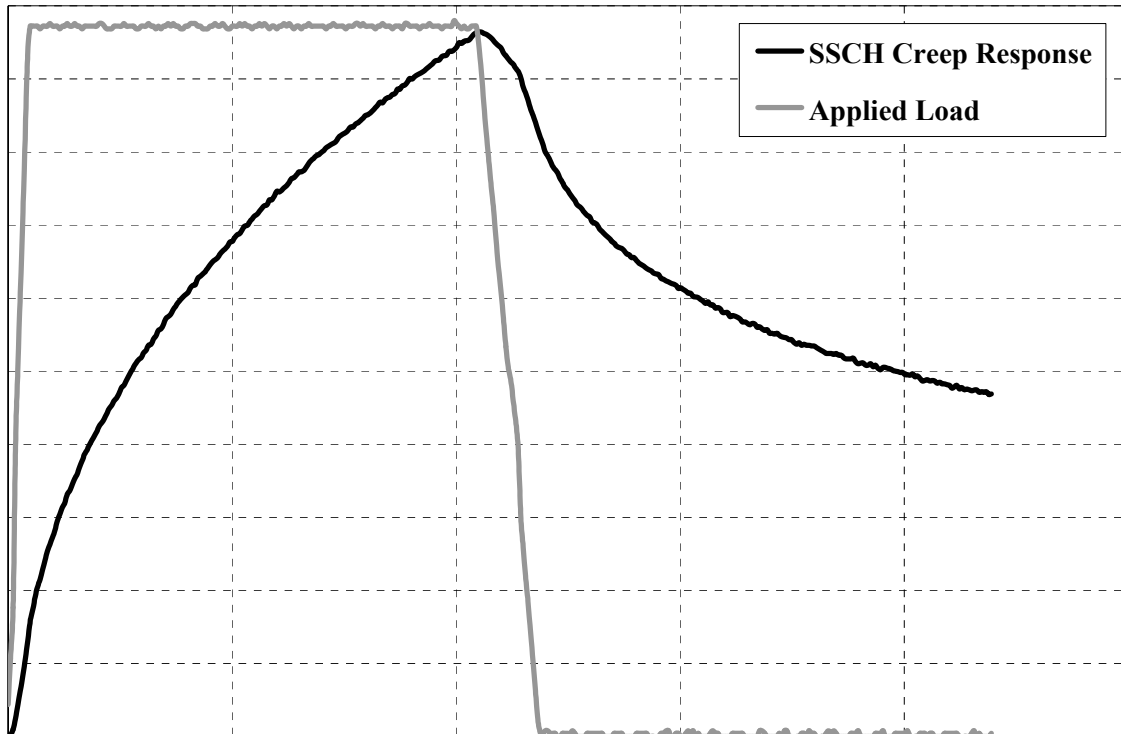
Figure 46 – Typical SSCH Sample Response and Applied Load at 40°C

SSCH Creep Curves

The Simple Shear at Constant Height (SSCH) tests were conducted at three different temperatures (4, 20, and 40°C) as recommended in the AASHTO specifications. The simple shear plots for each temperature are shown as Figures 47, 48, and 49, respectively. The analysis of the results was conducted differently than that recommended by AASHTO. AASHTO recommends that the maximum shear deformation and the permanent shear deformation be used as comparison parameters. However, this is solely based on each sample being of the identical thickness. Due to typical cutting methods, this is almost impossible.

In fact, the AASHTO specifications allows for the sample thickness to be as low as 38 mm, with a recommended thickness of 50 mm. Therefore, to truly compare the deformation of the samples, the shear strain was used for comparisons and not the shear deformation.

Another parameter used to comparison that is not specified in the AASHTO specifications is the SSCH creep curve slope. This slope is based on the creep portion of the curve (the portion of the curve where the applied load is constant). The creep portion has a duration of ten seconds. The slope of the curve was determined using a linear regression that had an origin fixed to zero. By determining the linear regression in this manner, it solely allows for a single number, the slope, for comparison. Without
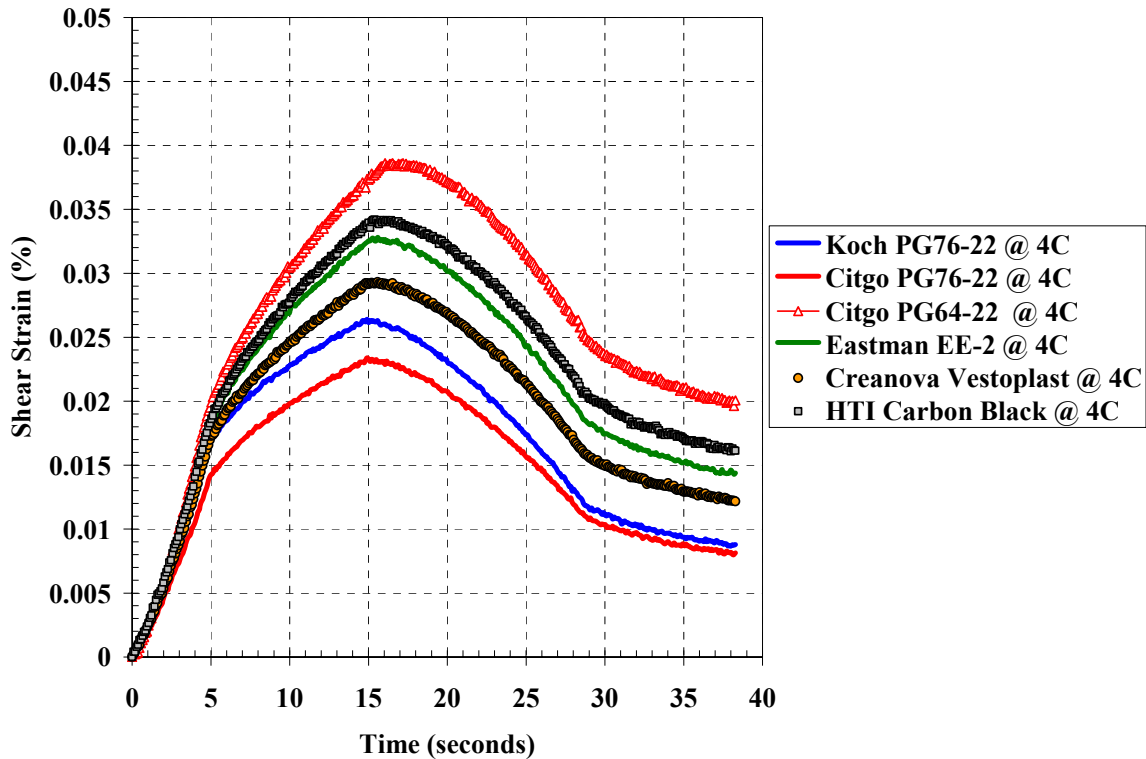
Figure 47 – Simple Shear at Constant Height Tests Conducted at 4°C

fixing the origin to zero, an intercept value would also accompany the regression and not allow for equal comparisons.

Difficulties in testing the Citgo PG64-22 sample at 40°C occurred due to the deformation of the material falling out of the LVDT's range. However, this lesson was learned early and the same mistake was not made again.
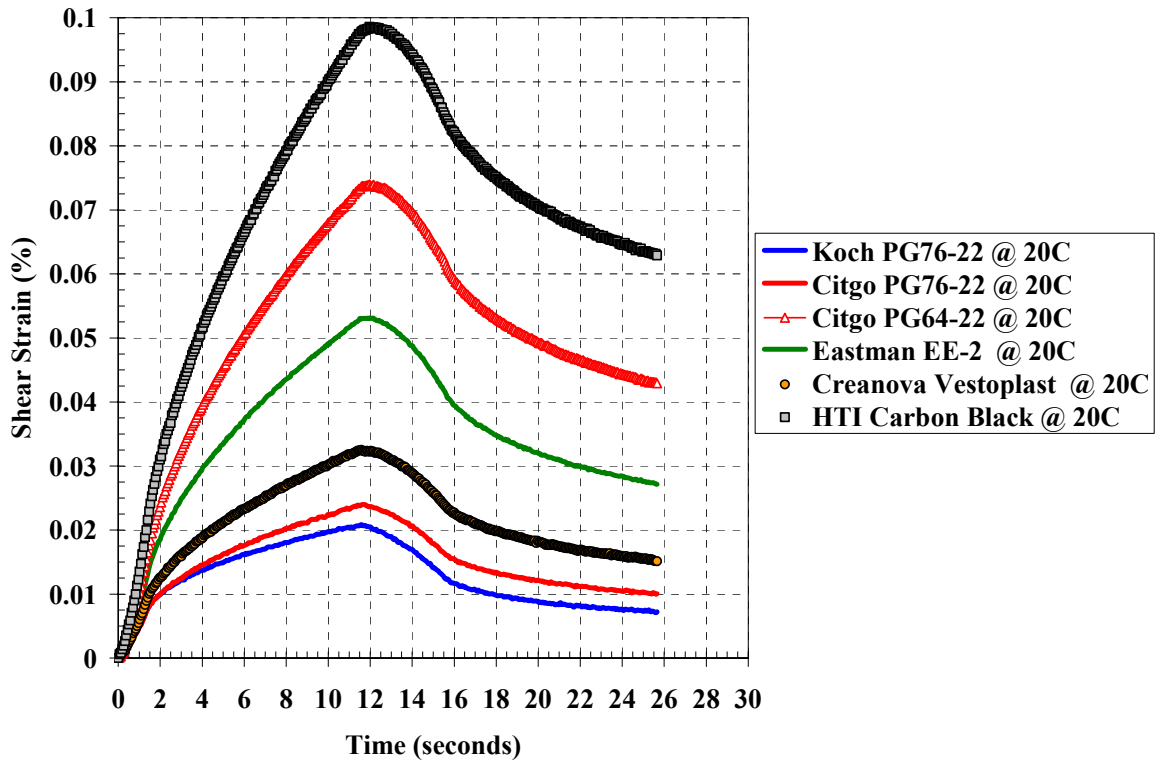
Figure 48 – Simple Shear at Constant Height Tests Conducted at 20°C
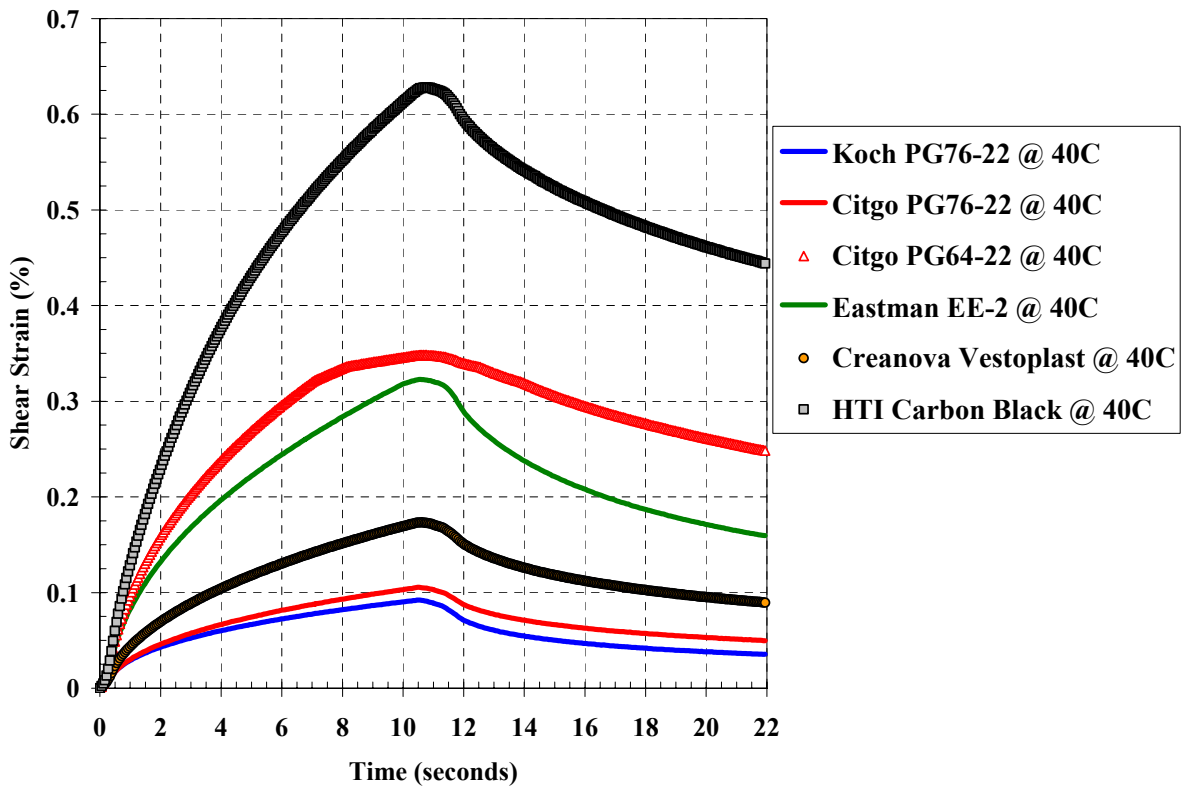
Figure 49 – Simple Shear at Constant Height Tests Conducted at 40°C

SSCH Maximum and Permanent Shear Strain

The maximum and permanent shear strains were determined for each sample and are shown as Figures 50 and 51. The values are also tabulated in Table 17. At 4°C, both the maximum and permanent shear strains are very similar. This was expected since it was assumed that the additives were not materials that would modify the low temperature grade of the asphalt. However, as the test temperature increased, both figures clearly show the two PG76-22 binders obtaining the lowest maximum and permanent shear strain. Meanwhile, the Hydrocarbon Technology's carbon black material typically obtained the largest maximum and permanent shear strain. The best performing asphalt modifier was the Creanova's Vestoplast material.
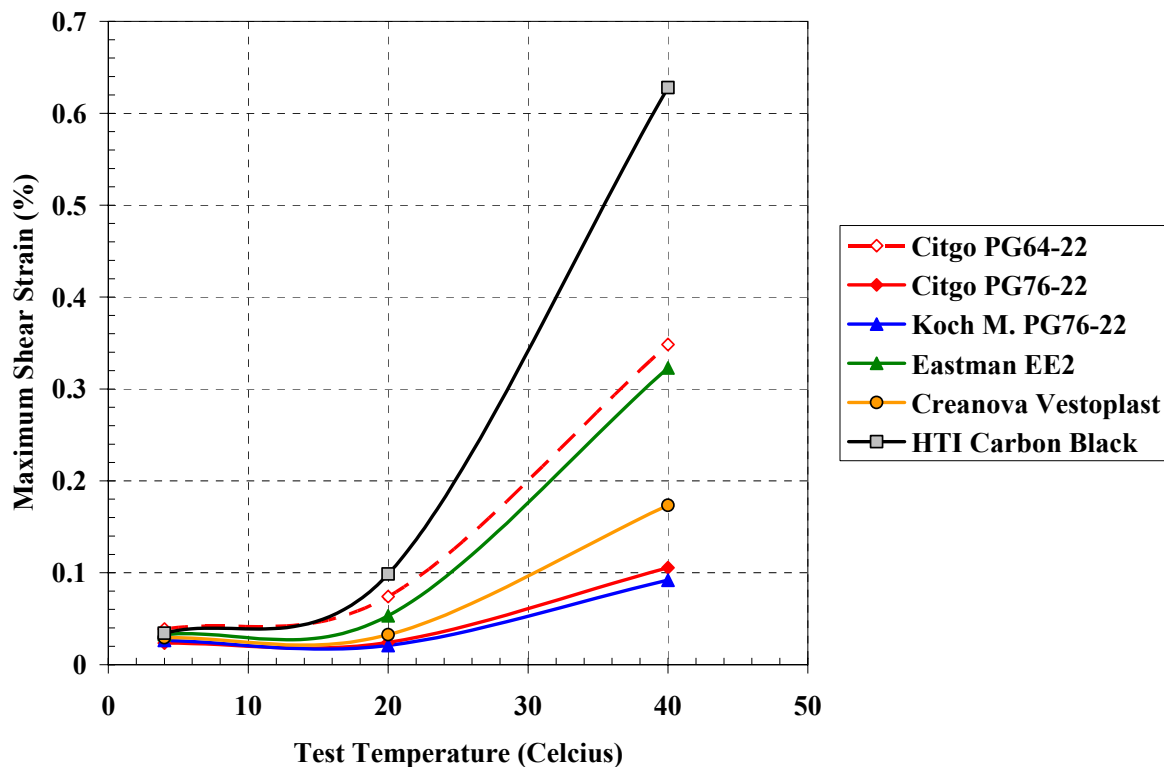
Figure 50 – Maximum Shear Strain from Simple Shear at Constant Height Test
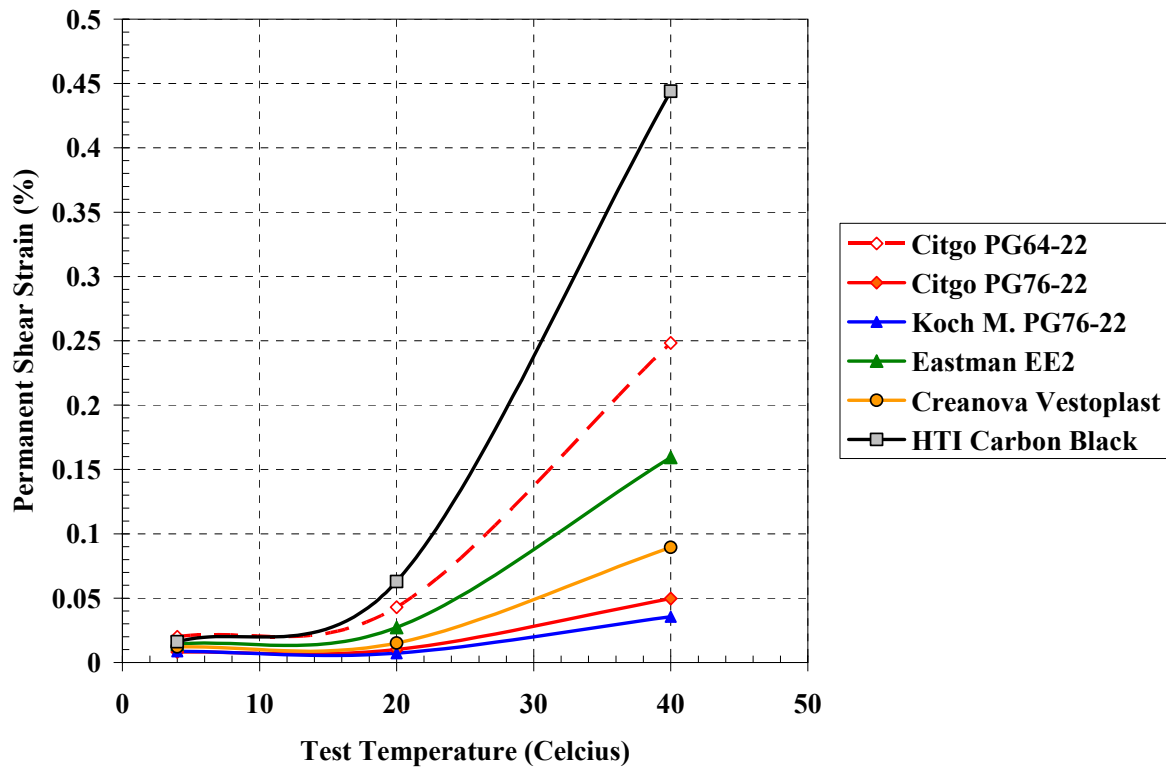
Figure 51 – Permanent Shear Strain from Simple Shear at Constant Height Test

Table 17 – Summary of Results from the Simple Shear at Constant Height Test

Sample Type	Accumulated Strains from SSCH								
	Temperature = 4°C			Temperature = 20°C			Temperature = 40°C		
	ε_{Max} (%)	ε_P (%)	Ranking	ε_{Max} (%)	ε_P (%)	Ranking	ε_{Max} (%)	ε_P (%)	Ranking
Citgo PG64-22	0.0387	0.0200	6	0.0740	0.0429	5	0.3484	0.2483	5
Citgo PG76-22	0.0234	0.0082	1	0.0240	0.0100	2	0.1054	0.0497	2
Koch M. PG76-22	0.0264	0.0087	2	0.0208	0.0073	1	0.0920	0.0355	1
Eastman EE2	0.0328	0.0143	4	0.0531	0.0272	4	0.3229	0.1594	4
Creanova Vestoplast	0.0293	0.0122	3	0.0325	0.0151	3	0.1733	0.0894	3
HTI Carbon Black	0.0342	0.0161	5	0.0986	0.0629	6	0.6280	0.4440	6

* - ε_{MAX} = Maximum Shear Strain

* - ε_P = Permanent Shear Strain

SSCH Creep Curve Slope

The creep portion of the SSCH curve was isolated and used as a comparative parameter. The creep portion of the curve is defined as the shear deformation induced solely by a constant shear load. The constant creep load was applied for ten seconds for each of the temperatures tested as specified in the AASHTO specifications. The slope of the curve was determined by using a linear regression with the intercept set equal to zero. The linear regression then only has a slope component and not an

intercept, allowing for a single parameter comparison. Table 18 provides the creep curve slope and the corresponding R^2 values. As can be seen from the Table, using the set intercept still provides a good correlation.

Table 18 – Summary of Creep Curve Slope Parameters

| Sample Type | Creep Slope from SSCH | | | | | |
| | Temperature = 4C | | Temperature = 20C | | Temperature = 40C | |
	Slope	R^2	Slope	R^2	Slope	R^2
Citgo PG64-22	0.0019	0.96	0.0062	0.93	0.0345	0.87
Citgo PG76-22	0.0010	0.95	0.0018	0.91	0.0103	0.83
Koch M. PG76-22	0.0011	0.95	0.0014	0.86	0.0088	0.80
Eastman EE2	0.0016	0.95	0.0043	0.92	0.0502	0.90
Creanova Vestoplast	0.0013	0.96	0.0025	0.92	0.0172	0.87
HTI Carbon Black	0.0017	0.95	0.0082	0.89	0.0663	0.85

Table 18 also shows what materials respond in more of an elastic manner under a creep-type load. Since the regression used was linear, the higher the R^2 value, the more linearly elastic the behavior. It can be seen that as the test temperature goes up, the materials respond in less of a linear manner. Figures 52, 53, and 54 show the creep curves for the three test temperatures.
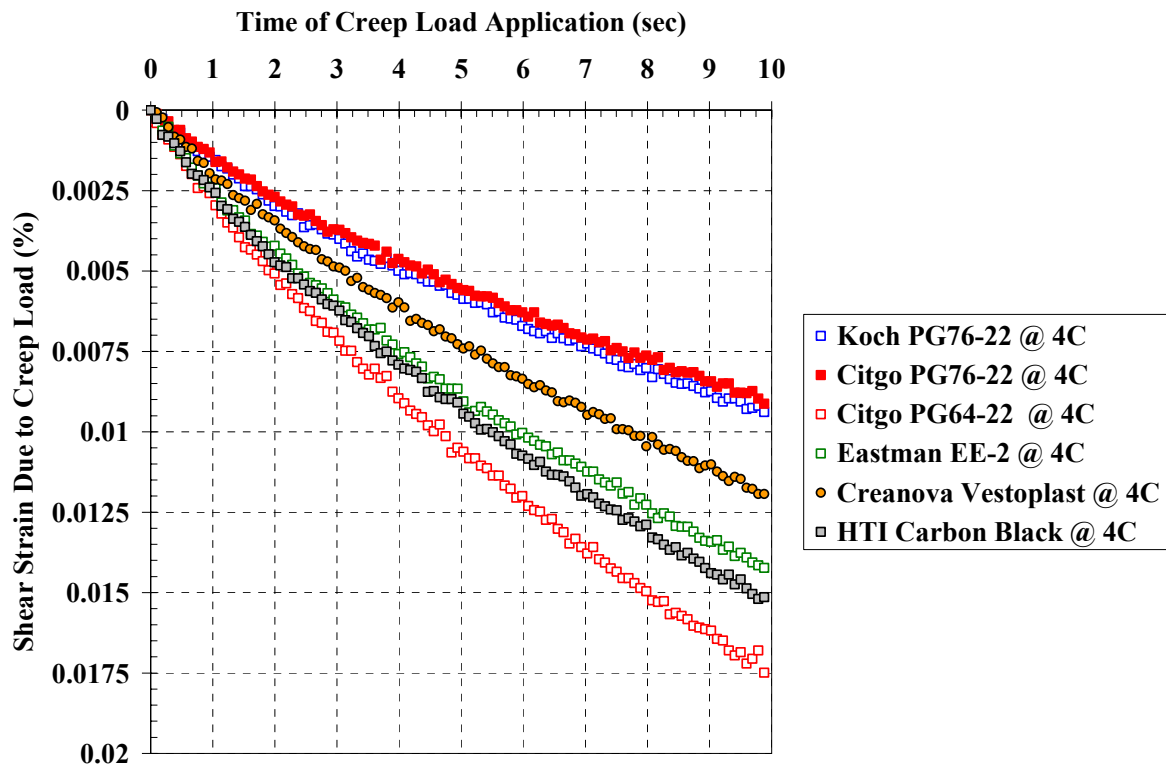
Figure 52 – SSCH Creep Curves Tested at 4°C
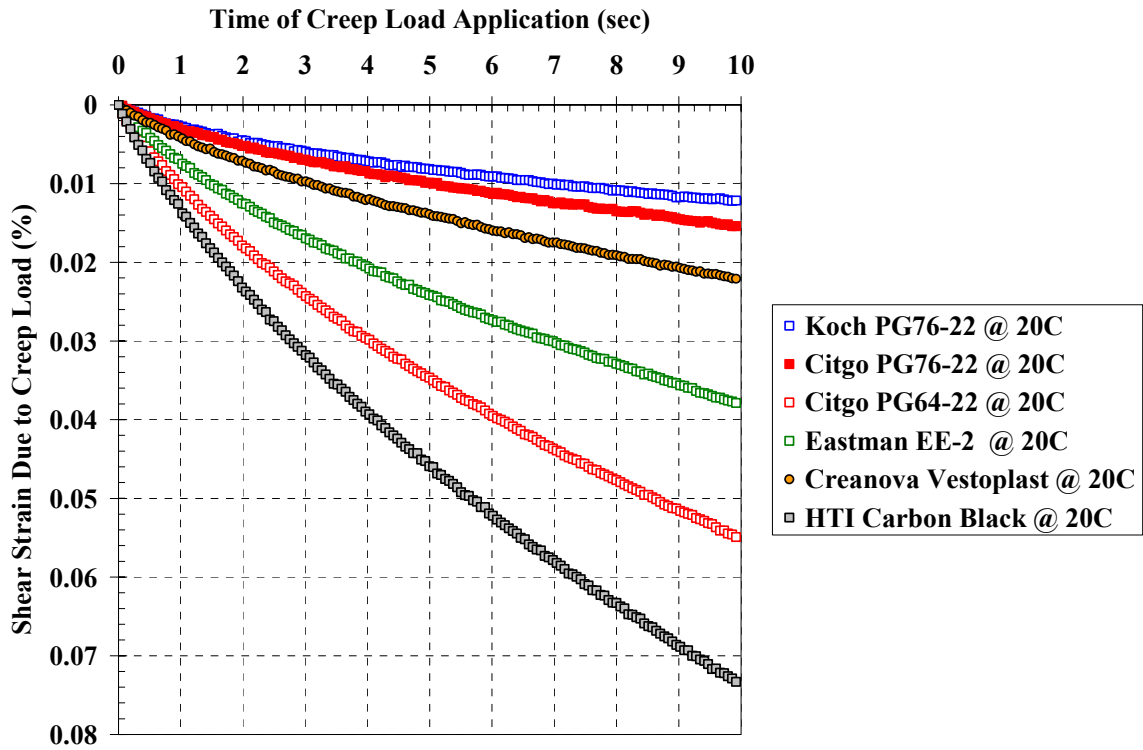
Figure 53 – SSCH Creep Curves Tested at 20°C
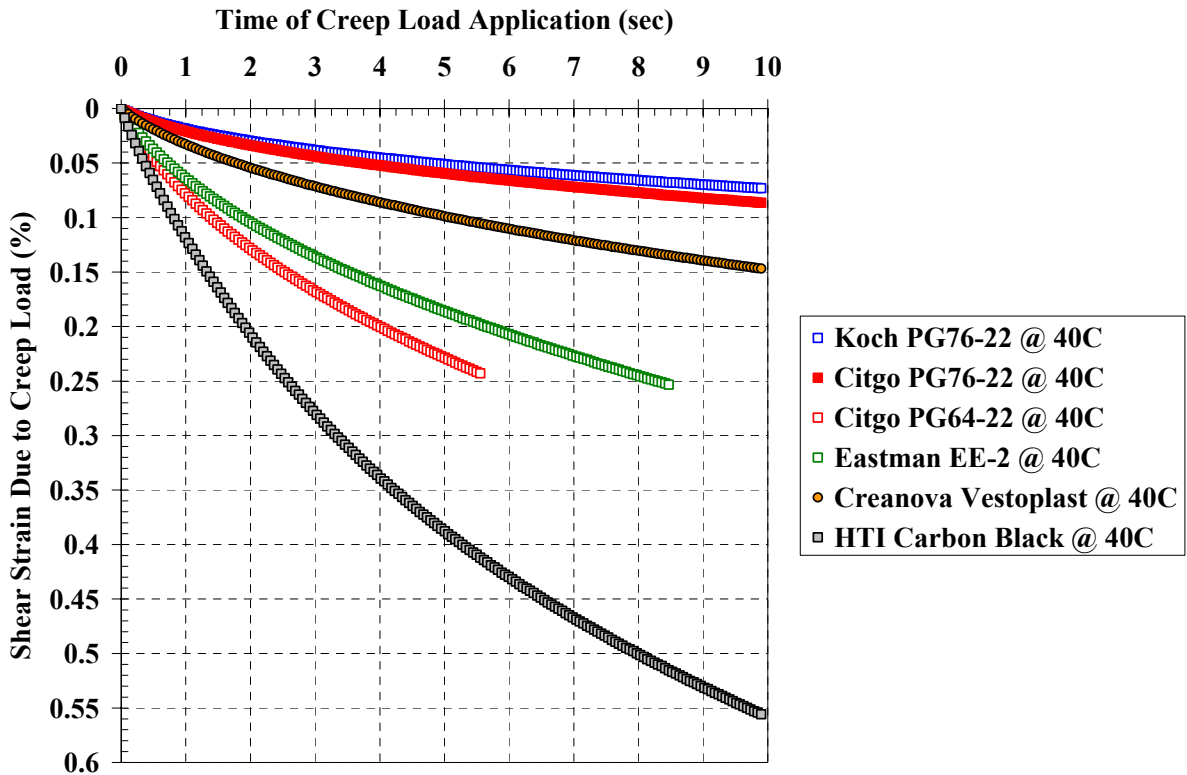
Figure 54 – SSCH Creep Curves Tested at 40°C

The final SSCH rankings are shown in Table 19. Again, the two PG76-22 polymer-modified binders performed the best, with Creanova's Vestoplast ranking the best out of the asphalt modifiers.

Table 19 – Final Ranking for Simple Shear at Constant Height Testing

Sample Type	Accumulated Strains from SSCH									Final Ranking
	Temperature = 4°C			Temperature = 20°C			Temperature = 40°C			
	ε_{Max} (%)	ε_P (%)	Creep Slope	ε_{Max} (%)	ε_P (%)	Creep Slope	ε_{Max} (%)	ε_P (%)	Creep Slope	
Citgo PG64-22	6	6	6	5	5	5	5	5	5	5
Citgo PG76-22	1	1	1	2	2	2	2	2	2	2
Koch M. PG76-22	2	2	2	1	1	1	1	1	1	1
Eastman EE2	4	4	4	4	4	4	4	4	4	4
Creanova Vestoplast	3	3	3	3	3	3	3	3	3	3
HTI Carbon Black	5	5	5	6	6	6	6	6	6	6

Final Rankings from the Superpave Shear Tester (SST)

The rankings from all three SST tests (Repeated Shear, Frequency Sweep, and Simple Shear) were averaged to determine a final ranking on materials based solely on the testing conducted in the SST. Table 20 shows the average test rankings, as well as the overall ranking from the SST. The overall rankings generally follow the trend of binder testing. The best performing asphalt modifier was Creanova's Vestoplast, with Hydrocarbon Technology's carbon black performing the worst, even poorer than the baseline PG64-22.

Table 20 – Summary and Overall Rankings from the Superpave Shear Tester

Sample Type	RSCH Results	FSCH Results	SSCH Results	Overall Ranking	Binder Test Rankings
Citgo PG64-22	4	5	5	**5**	6*
Citgo PG76-22	2	1	2	**2**	1*
Koch M. PG76-22	1	1	1	**1**	1*
Eastman EE2	5	4	4	**4**	4
Creanova Vestoplast	3	3	3	**3**	3
HTI Carbon Black	6	6	6	**6**	5

* - Assumed Based on PG grading

The direct add-in use of the carbon black material seems to "over-asphalt" the mix design. Although the binder testing showed the material to be graded slightly better than the baseline PG64-22, all of the mixture testing ranked the carbon black material the worst. Therefore, it can be concluded that the carbon black material can not be used as a direct add-in material, and should only be used with its own mix design.

Asphalt Pavement Analyzer (APA) Results

The Asphalt Pavement Analyzer (APA) was used to compare the rutting potential of the modified asphalt mixes. Both gyratory pills and vibratory bricks were tested. The samples were cured for four hours at 60°C prior to testing. The reasoning for the 60°C and not the 64°C is that the APA testing was conducted prior to the new testing standards issued by the APA User's Group. Twenty five seating cycles were applied to the samples before the initial rutting measurements were taken. The samples then underwent 8,000 loading cycles with the final rutting measurements taken after the 8,000 cycles had completed.

Figures 55 shows the results of the APA testing for both the gyratory pill and vibratory brick samples. Both of the PG76-22 polymer-modified binders performed the best, with the Koch Materials outperforming the Citgo PG76-22. The Eastman EE-2 was best performing asphalt modifier, with the HTI carbon black material performing even worse than the baseline PG64-22.
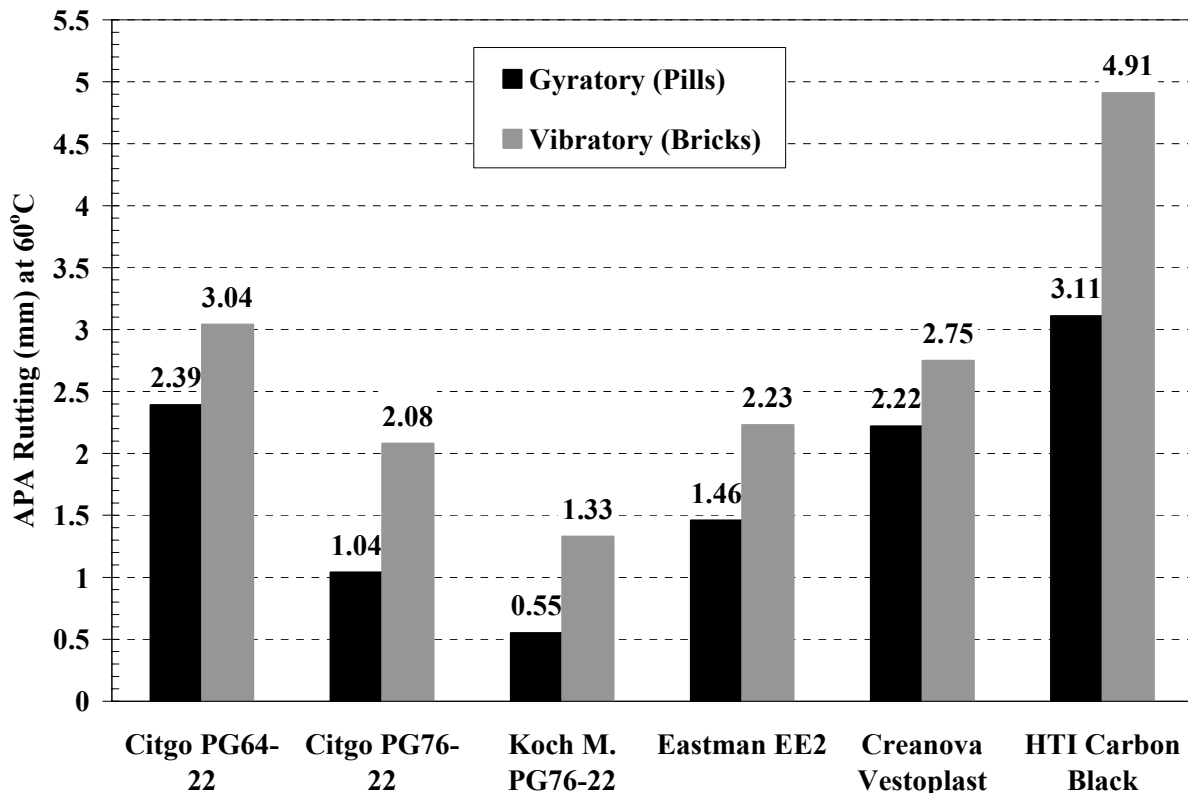
Figure 55 – Asphalt Pavement Analyzer (APA) Rutting Results

Another observation from the APA test results is that the bricks rutted more than the gyratory pills. Figure 56 shows the comparisons between the two different sample types. A linear trendline was fitted to the data with the origin set at zero. This was done

assuming that if there is zero rutting in the gyratory sample, then there should be zero rutting in the brick sample. The trendline equation shows that the rutting of the brick samples is approximately 46% more than the gyratory samples. This may be explained with either or both of the following:

- The compaction methods used aligned the aggregates in a different manner allowing the gyratory samples to be more rut resistant
- There was a greater material volume for the brick samples than the gyratory sample. This may have allowed for a greater volume change (rutting) since the material confinement of the brick samples was greater than that of the gyratory samples.
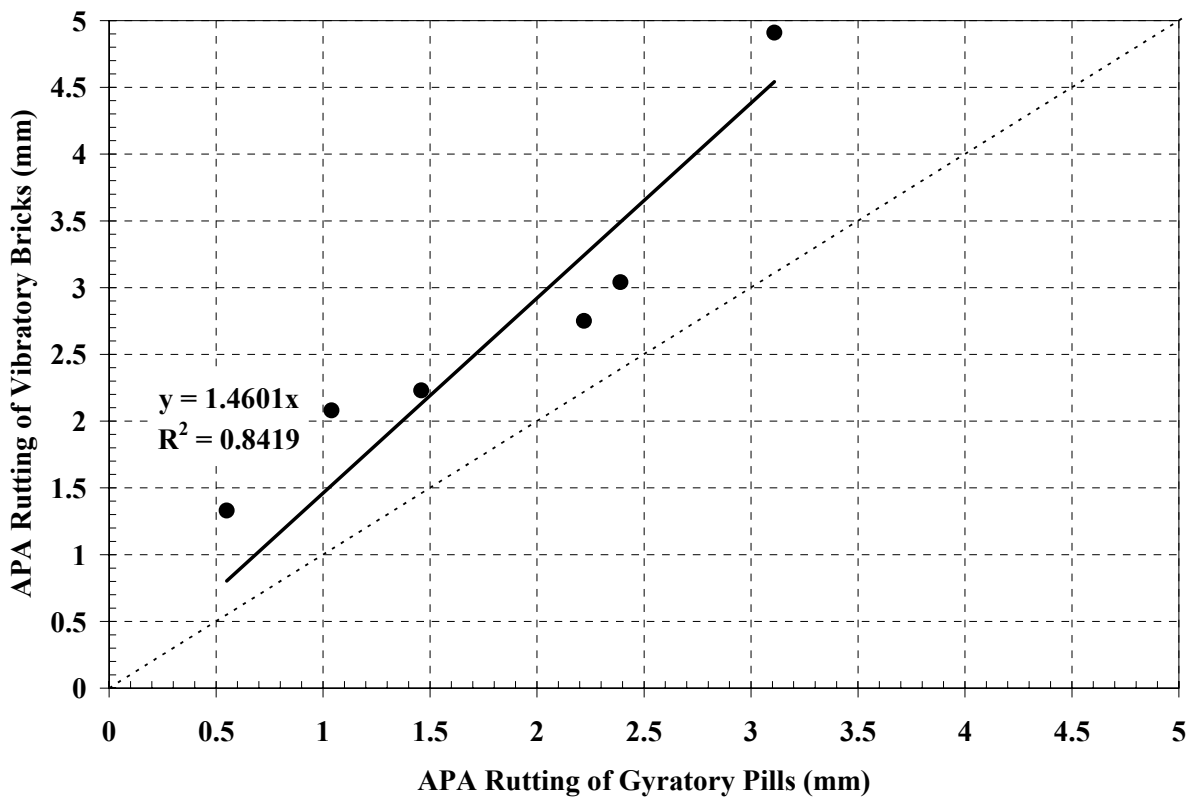
Figure 56 – Comparison Between the APA Results of Gyratory Pill and Vibratory Brick Samples

The ranking of the mixes from the APA testing and also the RSCH tests are shown in Table 21. Since the RSCH test has been known to be able to rank materials based on their rutting performance, it was chosen as a comparison to the APA results. The RSCH results are very similar to that of the APA. However, some discrepancies do exist. This can most likely be explained by the rut measurements that are taken during the APA test. The measurements are constrained to one area and within that area

Table 21 – APA and RSCH Performance Rankings

| Sample Type | Asphalt Pavement Analyzer Rutting Depths | | RSCH Rankings |
| | Rut Depth (mm) | | |
	Gyratory (Pills)	Vibratory (Bricks)	
Citgo PG64-22	5	5	4
Citgo PG76-22	2	2	2
Koch M. PG76-22	1	1	1
Eastman EE2	3	3	5
Creanova Vestoplast	4	4	3
HTI Carbon Black	6	6	6

either aggregate, binder, or surface voids can exist. Therefore, the APA manual measurement method described earlier can provide some erratic results. Since this part of the project testing has been completed, the APA measurements have been automated and are now based on the deformation of the hose. This provides a much smoother measurement without the HMA sample surface problems.

RELATIONSHIPS BETWEEN TEST PARAMETERS

The different test parameters determined during this study were compared to one another to establish relationships among the different test parameters. This was conducted to verify that certain parameters were true measurements of rutting potential and also to see if quicker tests could be substituted for longer tests.

Rutting Potential

Both the Asphalt Pavement Analyzer (APA) and the Repeated Shear at Constant Height (RSCH) are accepted test methods to evaluate the rutting potential of hot mix asphalt (HMA). Therefore, these two tests will be used for the baseline comparisons with the other test parameters discussed in this study. However, before the other test parameters can be evaluated, relationships between the APA and the RSCH test needed to be established. Figures 57 and 58 show the relationships.
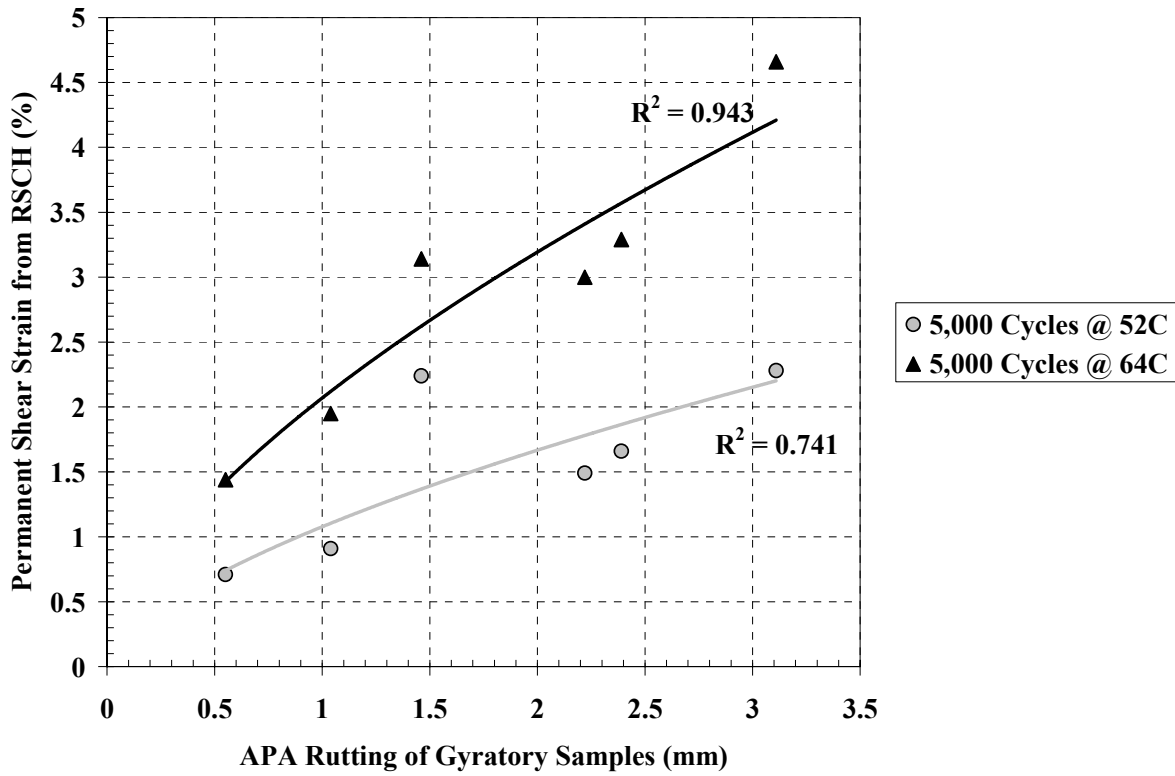
Figure 57 – APA Rutting of Gyratory Samples vs RSCH Test Results
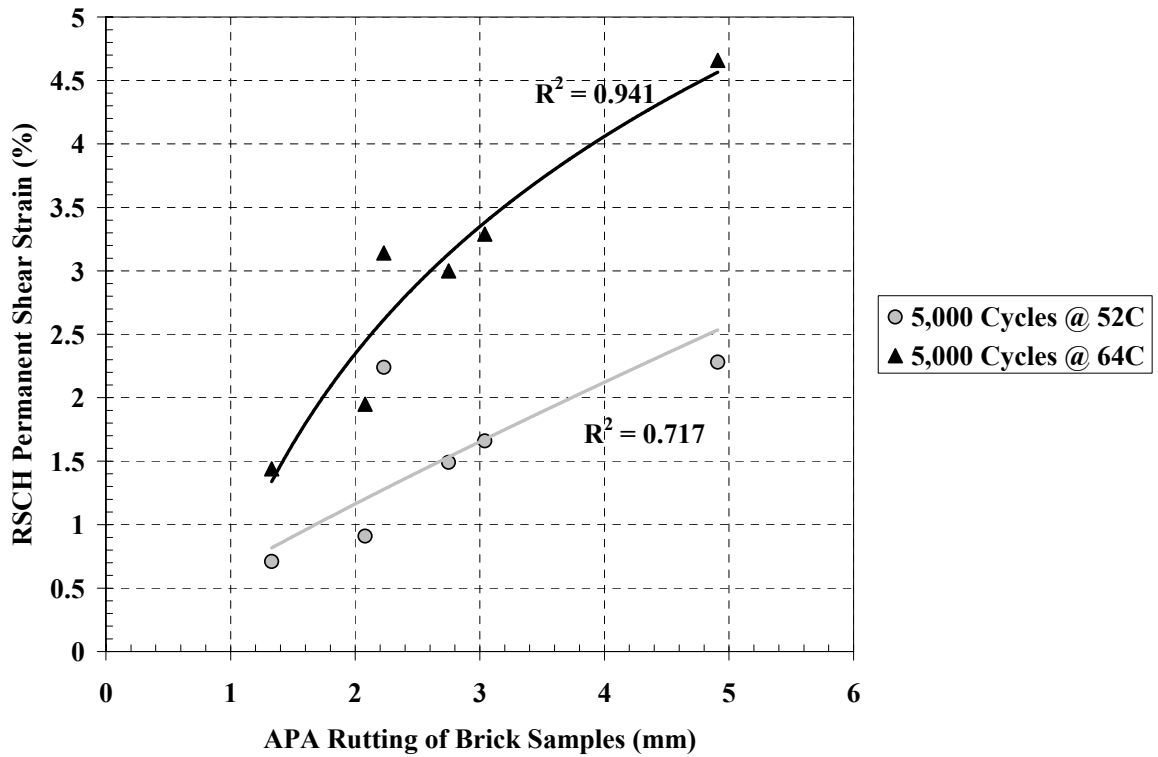
Figure 58 – APA Rutting of Vibratory Brick Samples vs RSCH Test Results

The results show that a very strong relationship exists between the APA rutting and the RSCH tests conducted at 64°C. The RSCH tests conducted at 52°C do not correlate as well to the APA tests mainly due to the difference in test temperatures (52°C for the RSCH and 60°C for the APA). Therefore, it can be concluded that when tested at similar temperatures, the APA and RSCH provide similar test results for the ranking of materials.

Similar analysis was conducted with the Frequency Sweep at Constant Height (FSCH) data, as well as the Simple Shear at Constant (SSCH) Height data. The test parameters from the FSCH and the SSCH tests were compared to the APA rutting at 8,000 cycles and the RSCH permanent shear strain at 5,000 loading cycles. Both the APA and RSCH, and their respective loading cycles, were used as comparisons since each test has been well documented as tests that are able to discriminate between HMA mixes that are and are not rut susceptible.

<u>Frequency Sweep at Constant Height (FSCH) Correlations to Rutting Potential</u>

The results from the FSCH tests were compared to the results of the Asphalt Pavement Analyzer (APA) and also the Repeated Shear at Constant Height (RSCH) to determine if the data from the FSCH can be used to determine if HMA mixes were rut susceptible. The parameters from the FSCH test used were the Rutting Parameter and the m-Slope.

FSCH Rutting Parameter

The Rutting Parameter (G*/sinϕ) of the HMA mix is similar to G*/sinδ (rutting parameter) of PG graded asphalt binder. It is a measure of HMA stiffness at high pavement temperature (40 and 52°C) at a slow rate of loading (0.1 cycle/second). Higher values of G*/sinϕ indicate an increased stiffness of HMA mixtures and, therefore, increased resistance to rutting. G* is the complex modulus and ϕ is the phase angle when HMA is tested under dynamic loading.

Figures 59 and 60 show the FSCH Rutting Parameter values versus the results of the APA testing for the gyratory and brick samples, respectively. The results a fairly good correlation between the Rutting Parameter values and the rutting values for both the gyratory and brick samples. In both cases, a better correlation exists when the Rutting Parameter was determined at the higher temperatures. It can also be seen that the correlation is better when gyratory samples are used. This may indicate a stiffness dependency on sample compaction methods (gyratory versus vibratory).

73
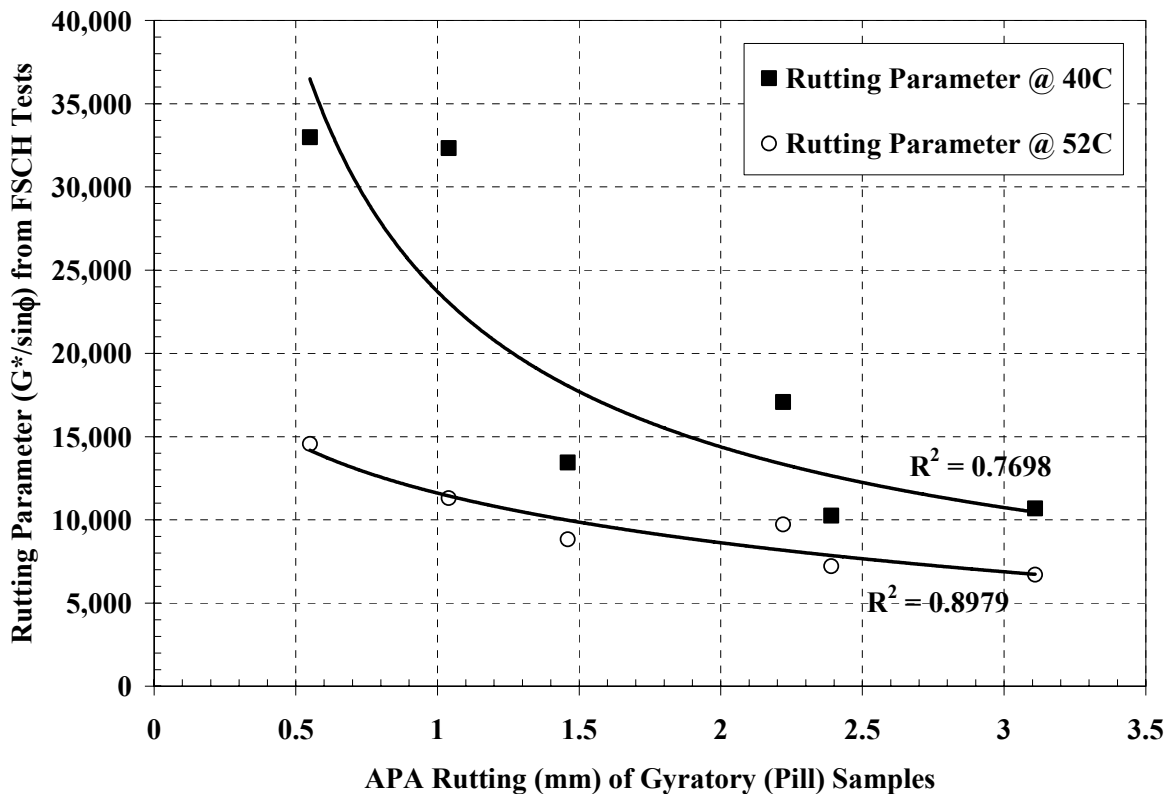
Figure 59 – FSCH Rutting Parameter vs APA Rutting of Gyratory Samples

The RSCH comparisons are shown as Figures 61 and 62. The results again show a good correlation, although slightly better than the APA results. Based on both the APA and RSCH comparisons, it can be concluded that the Rutting Parameter from the FSCH tests provides an alternative method for determining the rutting susceptibility of HMA mixes. The rankings of materials are shown in Table 22. The mixture rankings from the FSCH Rutting Parameter are very similar to the rankings of both the APA and RSCH.
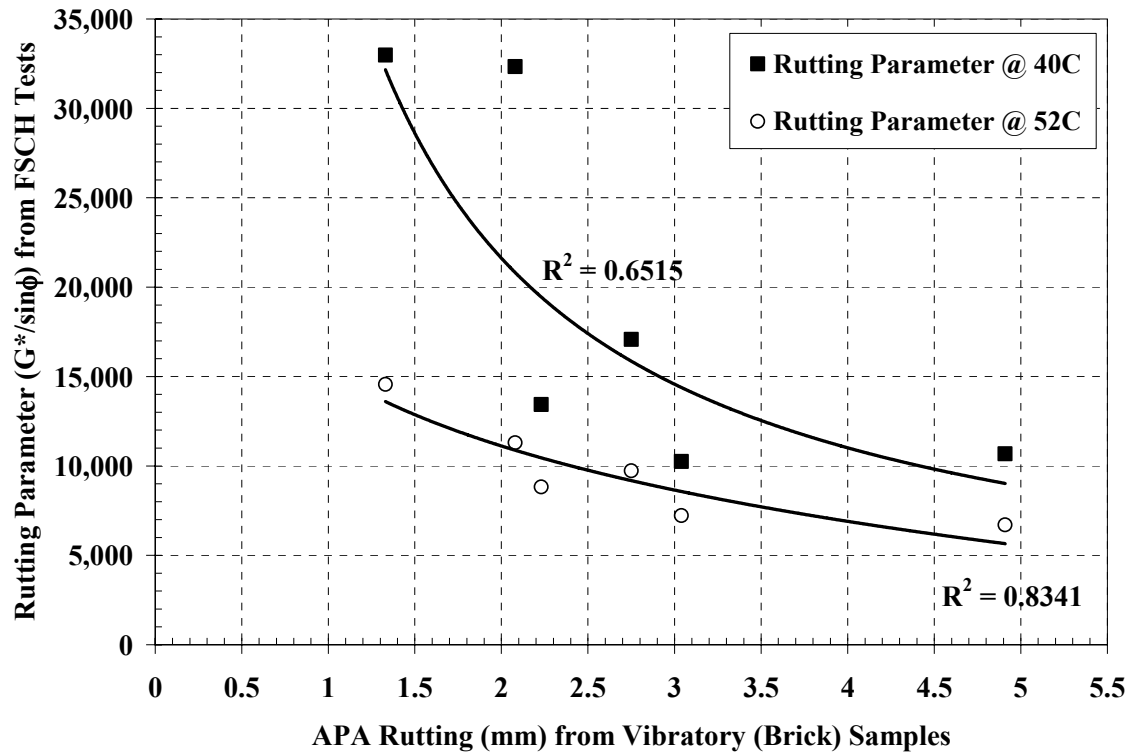
Figure 60 – FSCH Rutting Parameter vs APA Rutting of Brick Samples

Table 22 – HMA Mix Rankings Based on APA, RSCH, and FSCH Rutting Parameter

Sample Type	Frequency Sweep Test Rutting Parameter (G*/sinφ)		APA Testing	RSCH Testing
	40°C	52°C		
Citgo PG64-22	6	5	5	5
Citgo PG76-22	2	2	2	2
Koch M. PG76-22	1	1	1	1
Eastman EE2	4	4	3	4
Creanova Vestoplast	3	3	4	3
HTI Carbon Black	5	6	6	6
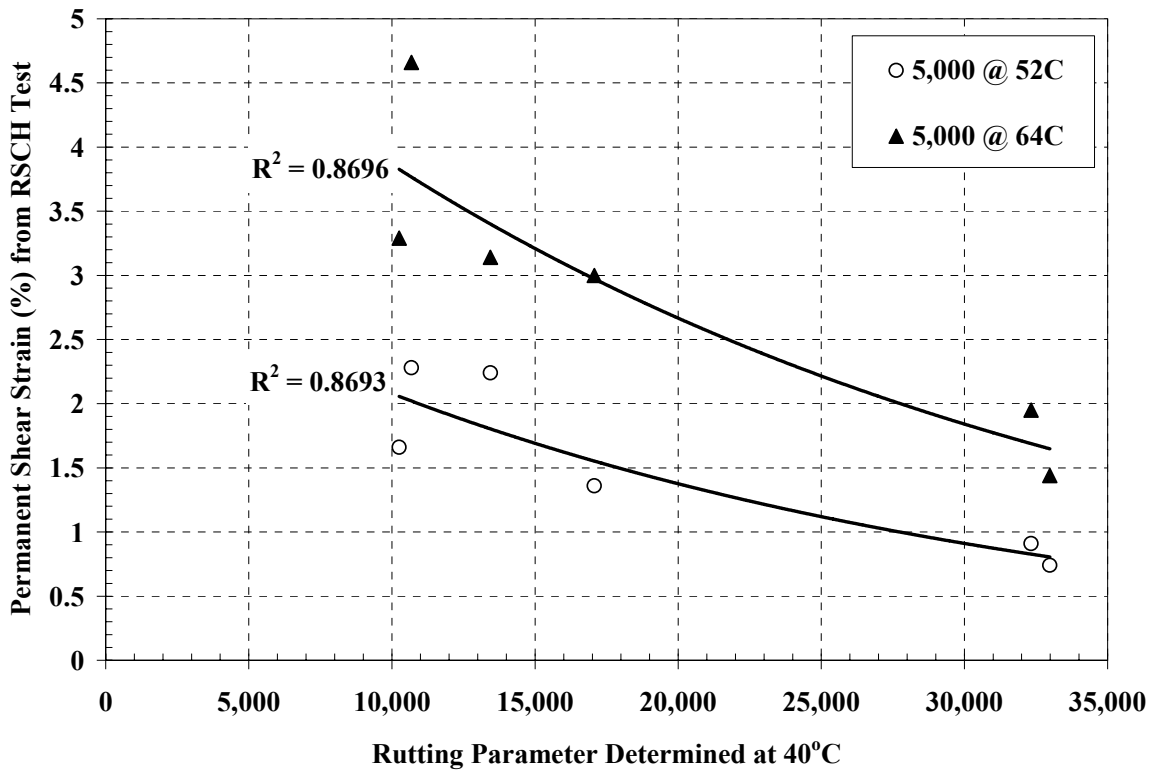
Figure 61 – FSCH Rutting Parameter @ 40°C vs RSCH Permanent Shear Strain
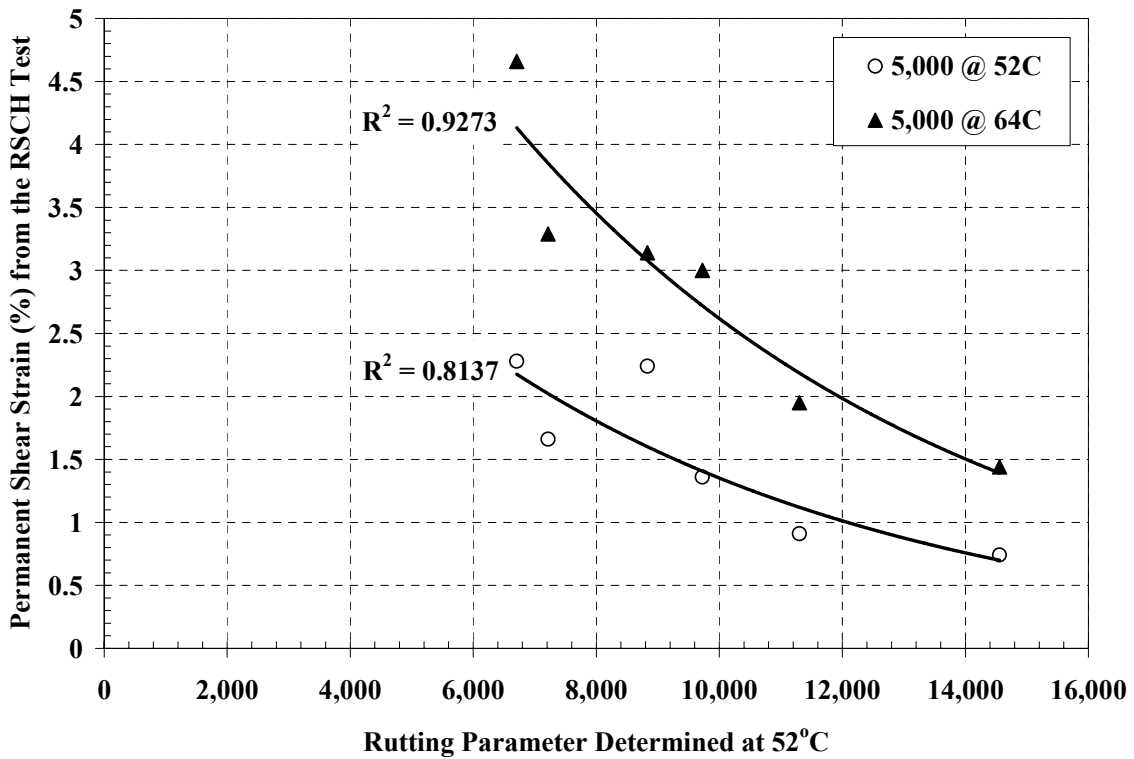
Figure 62 – FSCH Rutting Parameter @ 52°C vs RSCH Permanent Shear Strain

FSCH m-Slope

The m value is obtained from the frequency sweep at constant height conducted by the Superpave shear tester (SST) at high effective temperature (40 and 52°C) for permanent deformation with frequencies ranging from 0.01 hertz to 10 hertz. In other words, G* (stiffness) of the compacted HMA specimen is measured at different frequencies. The slope (m) of the best fit line on the frequency vs G* plot is calculated. This slope represents the rate of development of rutting for the tested mix and is used in the Superpave model as such. The lower the m slope, the better is the mix's resistance to rutting.

Figures 63 and 64 show the FSCH m-Slope parameter versus the APA rutting of the gyratory and brick samples, respectively. A very good agreement can be seen between the m-Slope determined at 40°C versus the APA rutting. However, when comparing the m-Slope at 52°C, the results are highly scattered with no apparent correlation.
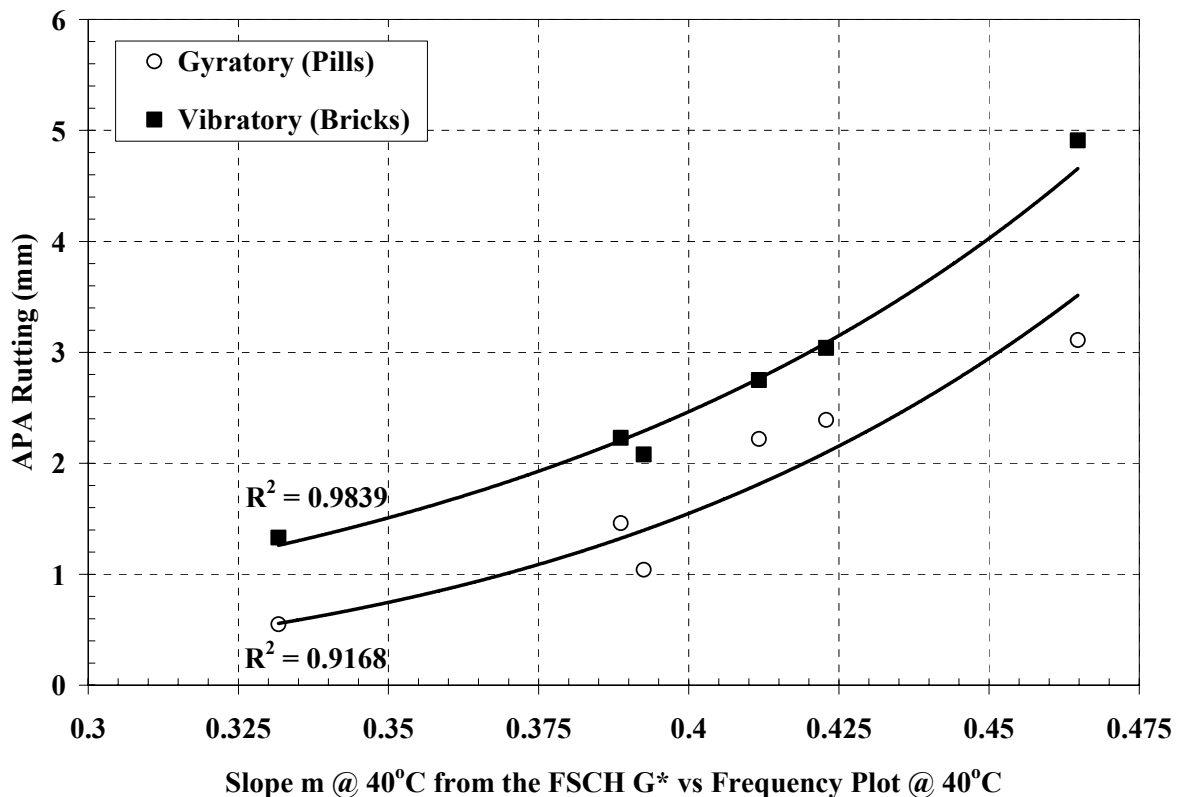
Figure 63 – FSCH m-Slope Parameters @ 40°C vs APA Rutting

Figures 65 and 66 show the FSCH m-Slope parameter versus the RSCH permanent shear strain. The results show a similar trend to the APA results, although the correlations were not as good. Again, when the m-Slope was determined at 40°C, the correlation to the RSCH was good, however, when determined at 52°C, the m-Slope showed no correlation to the rutting.
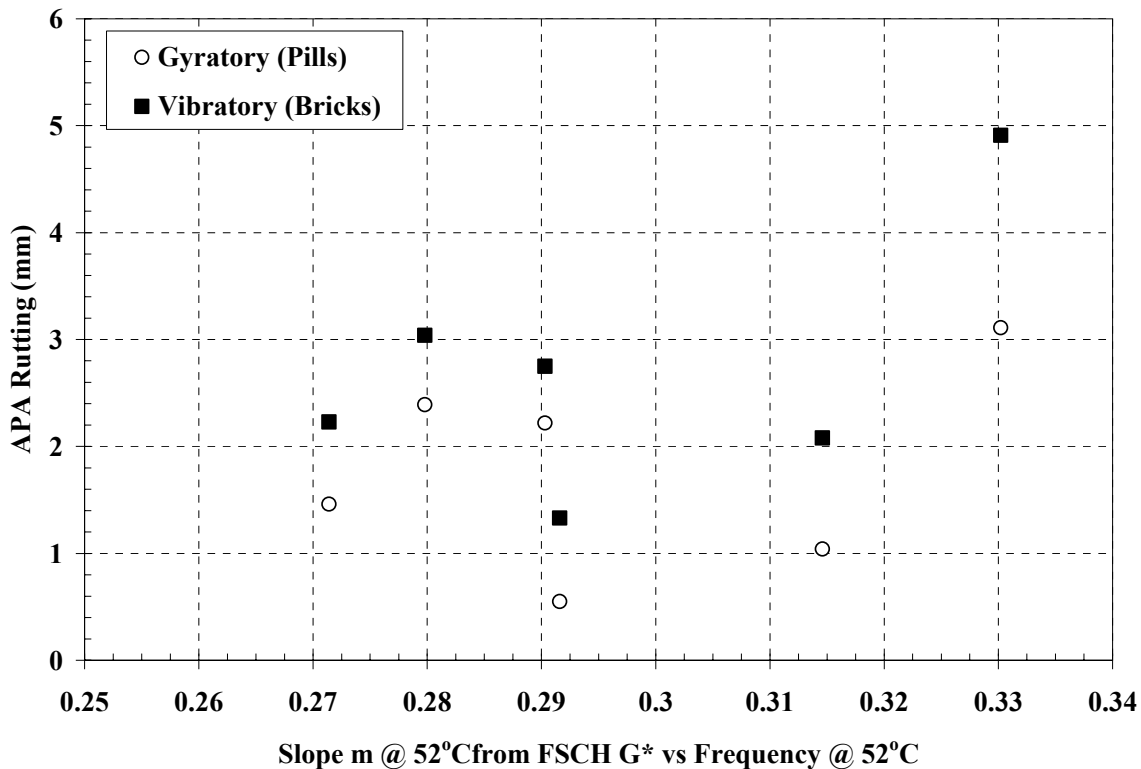
Figure 64 – FSCH m-Slope Parameters @ 52°C vs APA Rutting

One potential reason for the m slope parameter showing inconsistent correlations at 40 and 52°C is machine compliance. To move the shear table on the SST, a certain force is required. If the HMA sample is soft under the 52°C, the needed stress to develop a 0.01% shear strain may be similar, or even less, than the required shear table movement force. This may be especially true at low loading frequencies and high test temperatures where the HMA sample stiffness can be quite low.

Summary of FSCH Parameter Comparisons

The FSCH test parameters (rutting parameter and m-slope) were compared to the APA and RSCH results. Both the APA and RSCH have been shown to be able to accurately rank HMA materials based on their rutting susceptibility. Based on the comparisons made between the tests, the following conclusions can be made:

1. The rutting parameter (G*/sinϕ) had a good correlation with the APA testing when using the gyratory samples and a good to fair correlation with the vibratory brick samples. The differences may be explained by the slight variation in sample stiffness obtained by the different compaction methods. Better correlations were found when using a test temperature of 52°C for the FSCH tests.

78
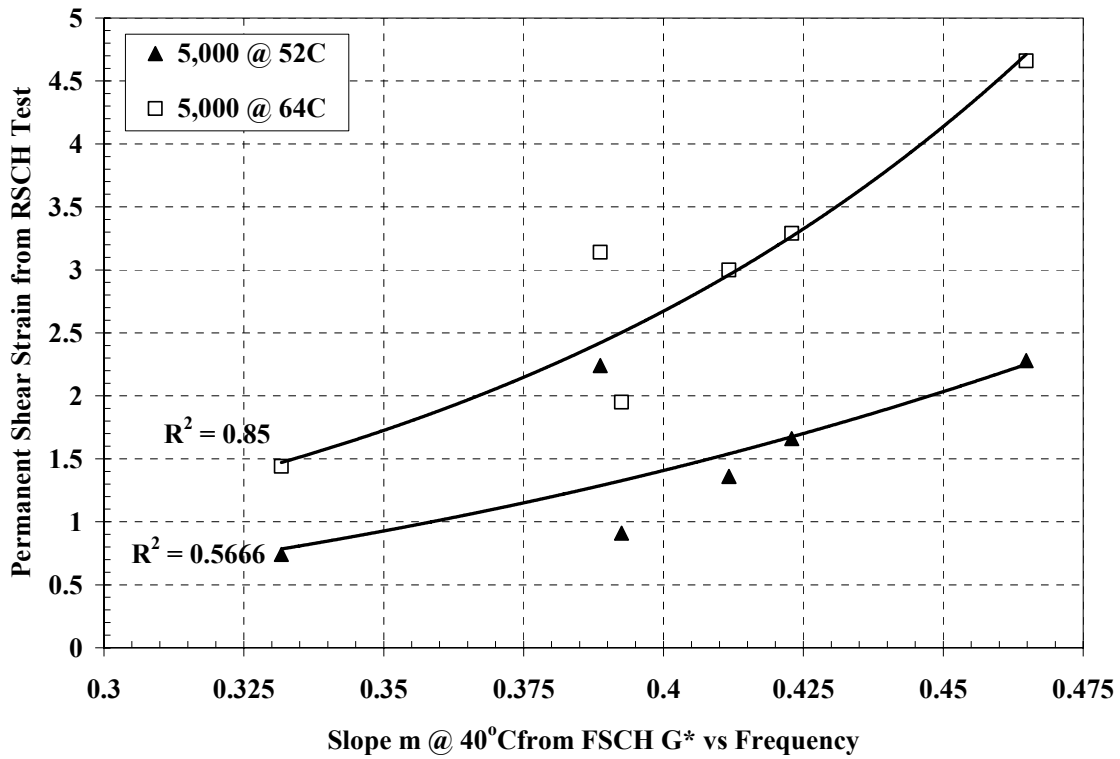
Figure 65 – FSCH m-Slope Parameters @ 40°C vs RSCH Permanent Shear Strain
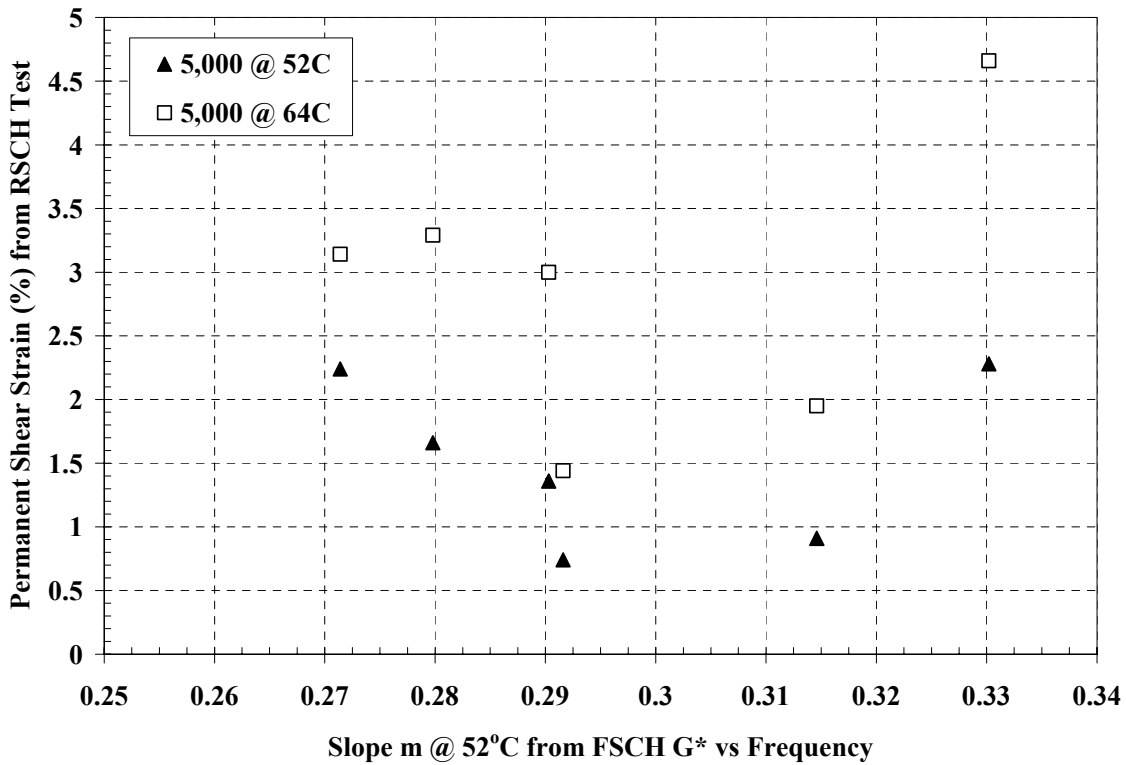
Figure 66 – FSCH m-Slope Parameters @ 52°C vs RSCH Permanent Shear Strain

2. The m-slope (slope of G* vs load frequency) had an excellent correlation to the APA tests when the m-slope was determined at 40°C. However, when the m-slope was determined at 52°C, a poor correlation existed. A similar trend existed when comparing the RSCH results to the m-slope. A good correlation existed between the RSCH tests conducted at 64°C and only a fair correlation existed when the RSCH was conducted at 52°C. Poor correlations existed for both RSCH test temperatures and the m-slope determined at 52°C.
3. The FSCH test can be used to aid in ranking materials for rutting susceptibility if conducted in the following manner.
   a. Based on the RSCH conducted at 64°C and APA tests conducted at 60°C, the FSCH rutting parameter determined at 52°C can be used to rank HMA materials.
   b. Based on the RSCH conducted at 64°C and APA tests conducted at 60°C, the FSCH m-slope determined at 40°C can be used to rank HMA materials.
4. The advantage of using the FSCH test is the time; approximately 30 minutes faster than the RSCH and 2 hours faster than the APA. The FSCH test also provides supplementary data, such as the dynamic shear modulus.

Simple Shear at Constant Height (SSCH) Correlations to Rutting Potential

The test parameters from the Simple Shear at Constant Height test were compared with the APA rutting and the Repeated Shear at Constant Height (RSCH) permanent shear strain at 5,000 cycles. The parameters evaluated from the SSCH were the maximum shear strain, the permanent shear strain, and the SSCH creep slope, all tested at 40°C. The SSCH parameters from 20°C were not evaluated due to the lower test temperature.

SSCH Permanent Shear Strain

The maximum shear strain was compared to the APA rutting results are shown in Figure 67. The results show that the SSCH maximum shear strain is in fair to good agreement with the APA rutting results. The same analysis was conducted using the RSCH permanent shear strain results at both 52 and 64°C. However, in this case, the RSCH results correlated much better than the APA results. This is most likely do to differences in testing mechanisms between the APA and the SST. In the APA, both volumetric and shear distortions are allowed. The volumetric distortion is the rutting from the initial compaction of the HMA due to the applied load, and the shear distortion is the rutting due to the shear failure of the material. However, unlike the APA, the volumetric distortion is not allowed during in the SST because the height of the sample remains constant. Therefore, the permanent deformation associated with the RSCH test is only due to the shear failure and not compaction-type deformations. It would then be assumed that the SSCH test conducted in the SST would compare better with the RSCH than the APA. The results of the comparisons between the RSCH and the SSCH are shown in Figure 68. A better correlation was found for the RSCH conducted at 64°C than at 52°C.
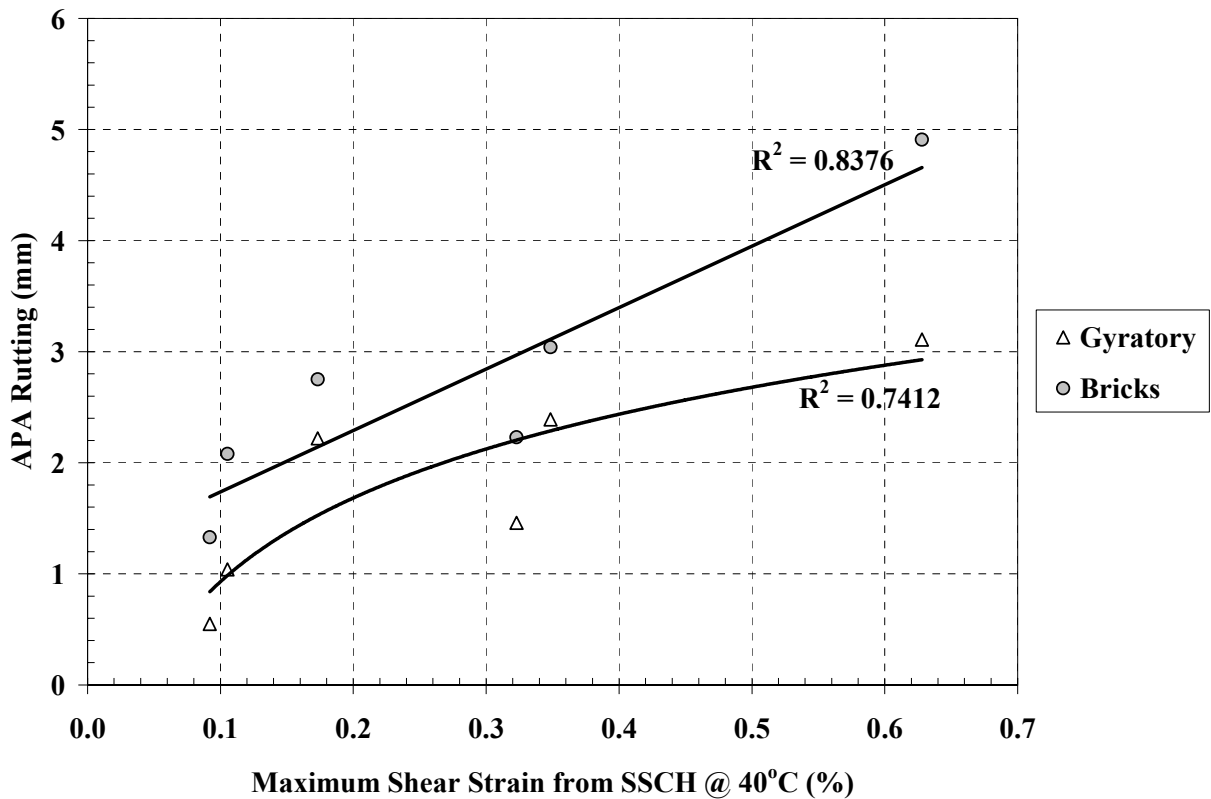
Figure 67 – APA Rutting Results vs SSCH Maximum Shear Strain at 40°C

SSCH Permanent Shear Strain

The permanent shear strain from the SSCH test conducted at 40°C was compared with the RSCH permanent shear strain at both 52 and 64°C, as well as with the APA rutting. The permanent shear strain is defined as the shear strain that remains on the sample after the test has been completed. This allows for the resilient properties of the material to be evaluated. Figure 69 shows the APA rutting results to the permanent shear strain of the SSCH at 40°C. The results show a good correlation, with the vibratory bricks having a better correlation than the gyratory samples. The RSCH results were also compared to the SSCH permanent shear strain. Again, the RSCH permanent shear strain correlated better with the SSCH permanent shear strain. The correlations are shown in Figure 70. A better correlation was obtained with the RSCH test conducted at 64°C.
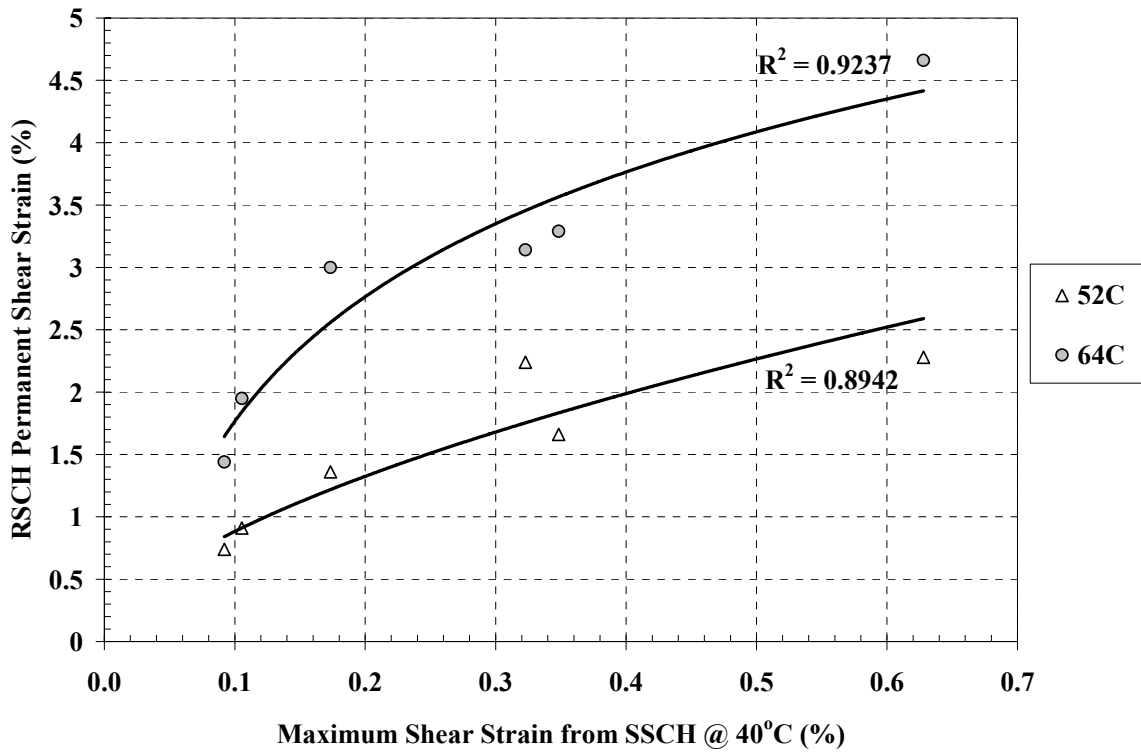
Figure 68 – RSCH Permanent Shear Strain vs Maximum Shear Strain from the SSCH at 40°C
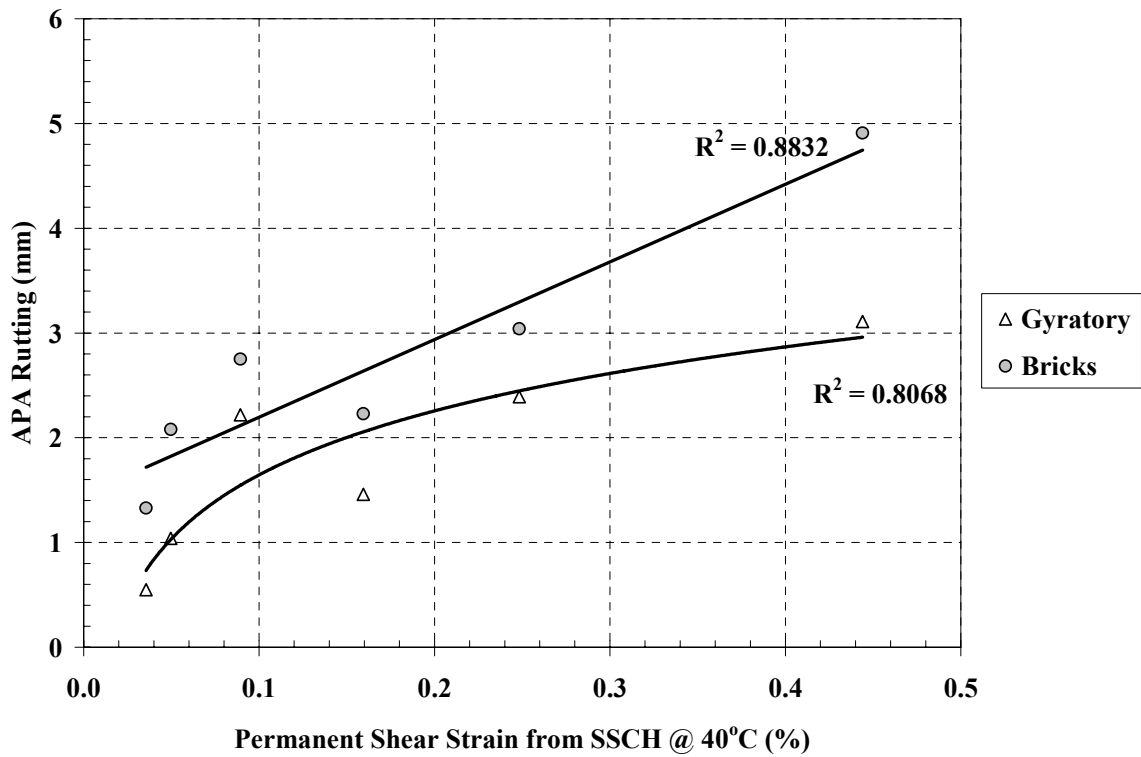
Figure 69 – APA Rutting vs SSCH Permanent Shear Strain at 40°C
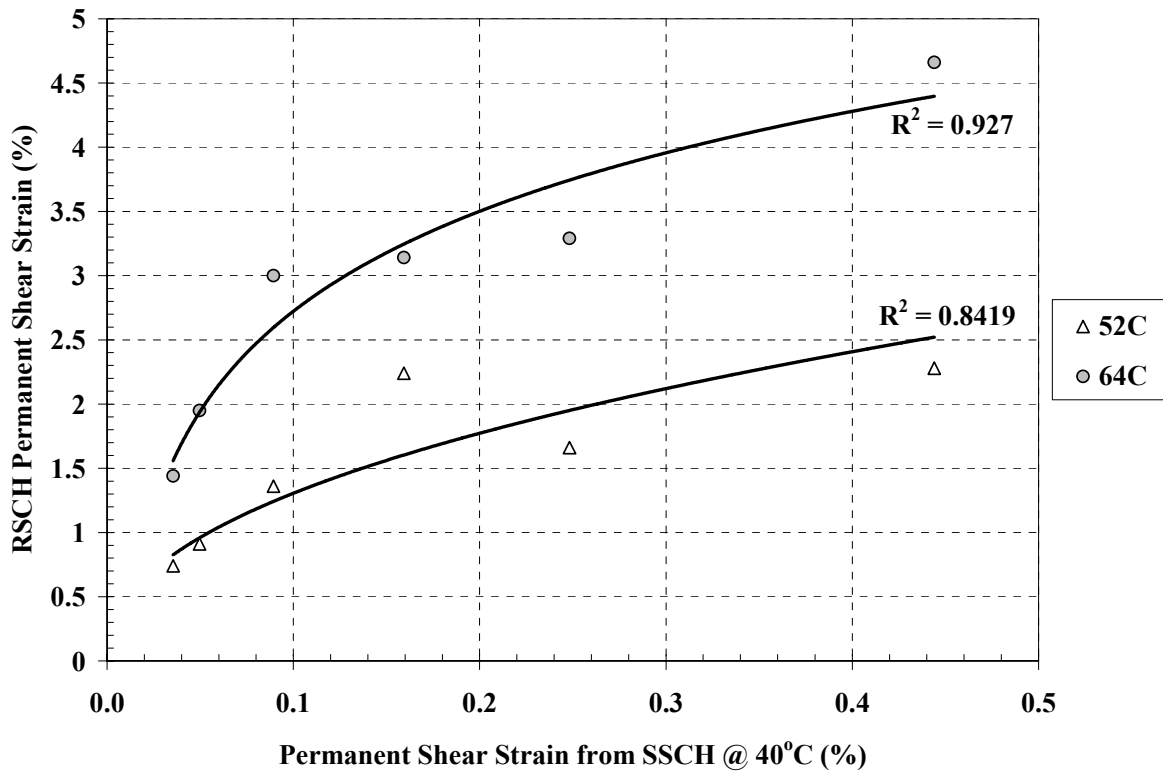
Figure 70 – RSCH Permanent Shear Strain vs SSCH Permanent Shear Strain at 40°C

SSCH Creep Slope

The creep slope from the SSCH was compared with the APA rutting and the RSCH permanent shear strain. The creep slope from the SSCH is defined as the slope of the shear strain and the time of constant creep loading (i.e. shear strain per second). The creep slope was determined by fixing the slope to zero and using a linear trendline. This allows only a single number to represent the creep slope, without the need for an intercept parameter.

The comparisons between the APA rutting and the SSCH creep slope are shown in Figure 71. As shown in the figure, an average correlation exists between the APA rutting results and the SSCH creep slope determined at 40°C. This is most likely due to a percentage of the APA rutting being caused by volumetric distortion, which is mechanism that the creep properties of the binder have only a small influence on.
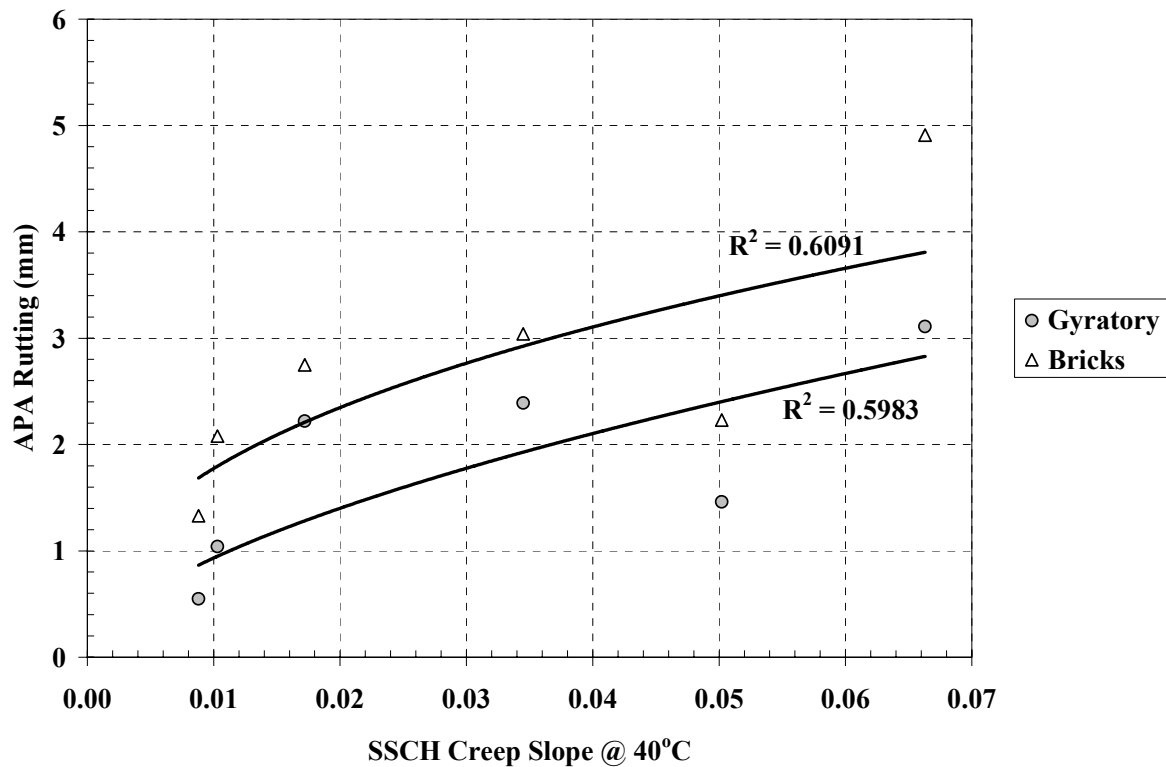
Figure 71 – APA Rutting vs SSCH Creep Slope at 40°C

The comparisons were also developed for the RSCH permanent shear strain. The results of the comparisons are shown in Figure 72. Excellent correlations were obtained for the RSCH conducted at 52°C, with a good correlation being found for the RSCH tested at 64°C.

The creep slope was also compared to the RSCH S-slope, which represents the rate of accumulation of permanent deformation in the RSCH test. The S-slope from the RSCH test is the part of the permanent deformation curve that relies heavily on the binder properties. A stiffer binder at higher temperatures will have a lower S-slope, as shown earlier. This is illustrated earlier with the permanent strain curves of the RSCH testing. The S-slope was lowest for the binders with the highest "true" high temperature performance grade. The same relationship exists for the SSCH creep slope. The stiffer the binder at high temperatures, the lower the creep slope. The results are shown in Figure 73. From the figure, it can be seen that an excellent correlation exists between the SSCH creep slope and the RSCH S-slope at 52°C. A good correlation exists with the RSCH S-slope at 64°C.
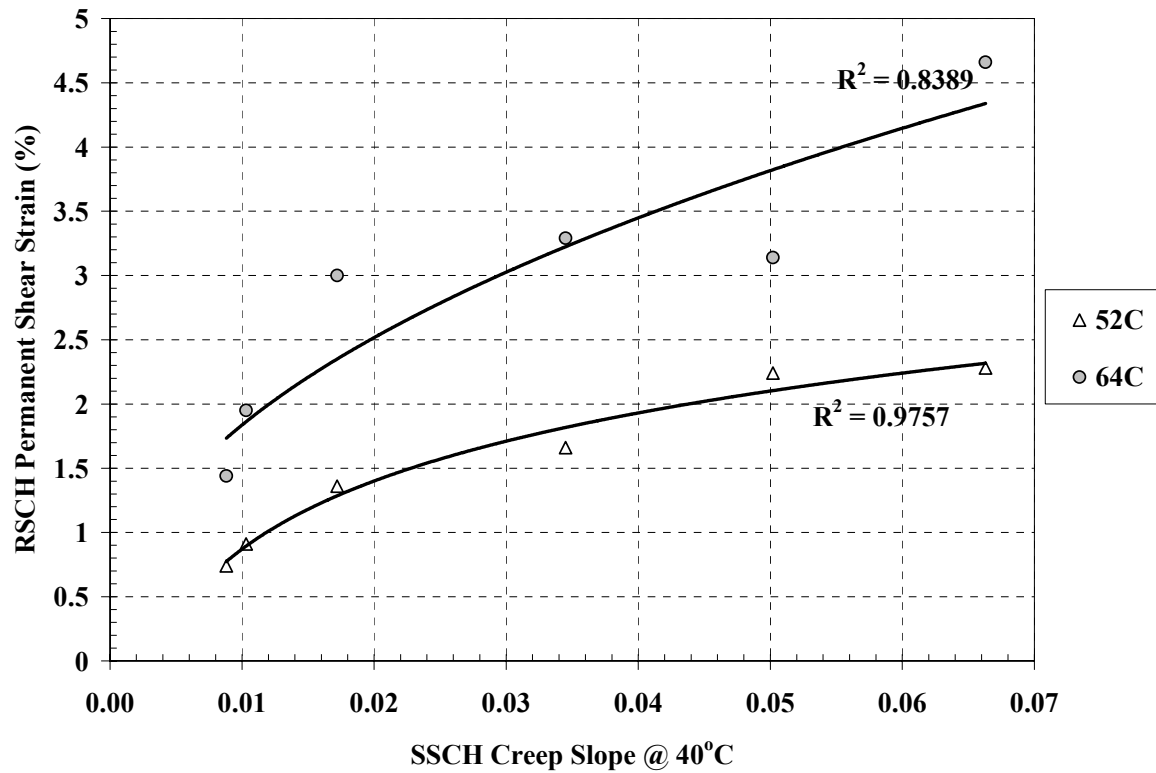
Figure 72 – RSCH Permanent Shear Strain vs SSCH Creep Slope at 40°C
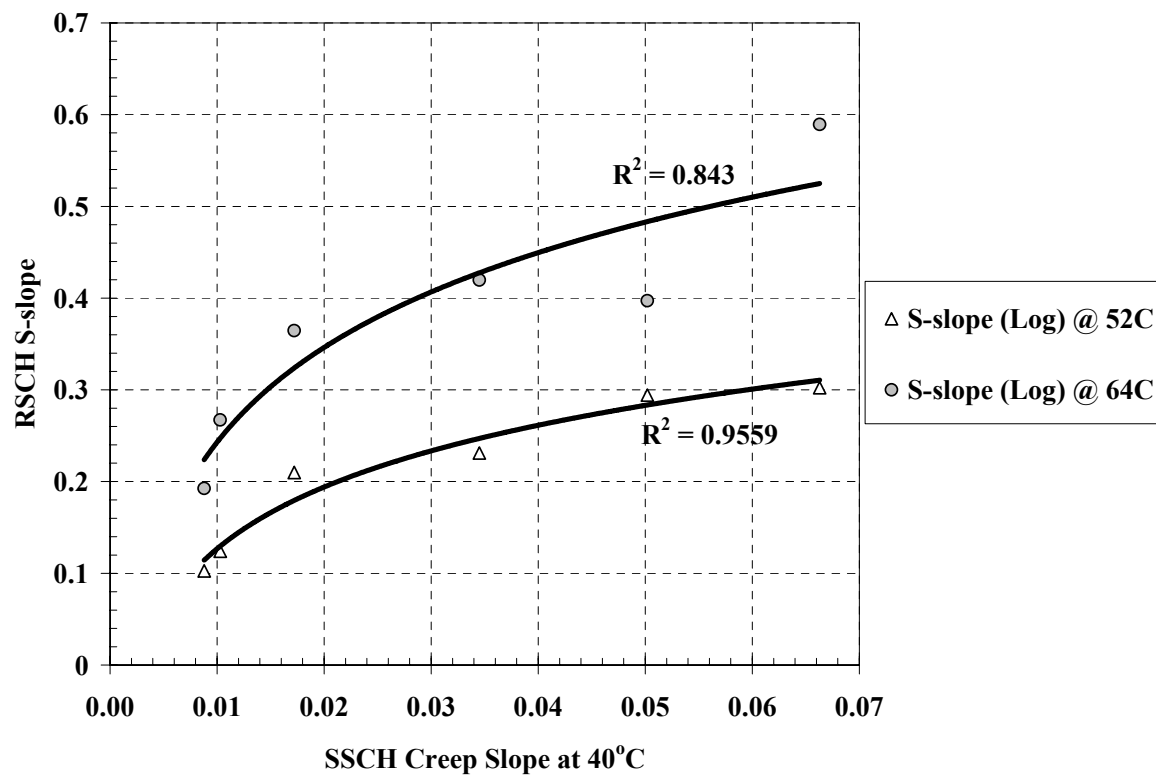
Figure 73 – RSCH S-Slope vs SSCH Creep Slope at 40°C

Summary of SSCH Parameter Correlations

The SSCH test parameters (maximum shear strain, permanent shear strain, and creep slope) were compared to the APA and RSCH results. Both the APA and RSCH have been shown to be able to accurately rank HMA materials based on their rutting susceptibility. Based on the comparisons made between the tests, the following conclusions can be made:

1. The SSCH maximum shear strain had a good correlation to the APA rutting results, and an excellent correlation to the RSCH test results. The same trend exists when comparing the permanent shear strain from the SSCH and the results of the RSCH and APA tests. The correlations improved when the RSCH tests were conducted at 64°C.
2. The SSCH creep slope had only a fair correlation to the APA, however, a good to excellent correlation was found to exist between the RSCH and the SSCH creep slope. However, the 52°C RSCH test found to correlate better, instead the 64°C RSCH test indicated earlier.
3. The mode of asphalt loading appears to have an impact on the correlations to the SSCH test results. The APA rutting is controlled by both a volumetric and shear distortion due to the loading. The volumetric due to the compaction of the air voids, while the shear is the moving of HMA material without the air voids changing. Meanwhile, the RSCH is only controlled by shear distortion since the height of the sample remains constant (no volume change).
4. The SSCH test can be used to aid in ranking materials for rutting susceptibility if conducted in the following manner.
    a. Based on the RSCH conducted at 64°C and the APA conducted at 60°C, the maximum and permanent shear strain can be used, with more emphasis placed on the permanent shear strain. The permanent shear strain is preferred since it also incorporates an elastic component to the analysis.
    b. The creep slope from the SSCH could also be used for rutting susceptibility, however, a better correlation was found to occur at a lower temperature of 52°C, instead of the typically used 64°C. A test temperature of 52°C is not recommended since it does not reflect the high temperature asphalt performance grade in New Jersey. Therefore, if the creep slope is used, the "good" correlation found at 64°C is recommended.

STATISTICAL ANALYSIS (SHORT TERM OVEN AGING – STOA)

The main goal of the statistical analysis is to determine if the asphalt modifiers performed in a similar manner to that of the baseline binders (Citgo PG64-22, Citgo PG76-22, and Koch PG76-22). A result of Equal means that the asphalt modifier performed in a statistically similar manner to the baseline binders. A result of Not Equal

only means that the material did not perform in a manner statistically, significantly equal. This could be either better or worse, but not equal.

A statistical analysis was conducted using a Student's t-test analysis (two sample assuming equal variances). The analysis was utilized to determine if the samples were statistically equal or statistically not equal among the common test results and parameters. A 95 percent confidence interval was chosen for the analysis. A similar type of statistical analysis was conducted by Jones et al. (1998) to evaluate the performance of modified asphalts from mixture testing and therefore was thought to be suitable to be used for this research.

The formula for the independent samples t-test employing a pooled variance is (Dretzke, 2001)

$$t = \frac{\left(\overline{X_1} - \overline{X_2}\right) - \left(\mu_1 - \mu_2\right)}{S_{(\overline{X_1} - \overline{X_2})}}$$

(5)

where,

$\left(\overline{X_1} - \overline{X_2}\right)$ - difference between the two sample means

$\left(\mu_1 - \mu_2\right)$ - the hypothesized difference between the population means

$S_{(\overline{X_1} - \overline{X_2})}$ - the standard error of the difference

The standard error is calculated using a pooled variance estimate. The formula for the pooled variance is

$$S^2_{pooled} = \frac{(n_1 - 1)S_1^2 + (n_2 - 1)S_2^2}{(n_1 - 1) + (n_2 - 1)}$$

(6)

where,

S_1^2 - the variance in sample 1

S_2^2 - the variance in sample 2

n_1 – the number of observations in sample 1

n_2 – the number of observations in sample 2

The pooled variance estimate is the weighted average of the sample variances where each variance is weighted by its respective degrees of freedom. The formula for the standard error of the difference is given by

$$S_{(\overline{X_1} - \overline{X_2})} = \sqrt{\left(\frac{S^2_{pooled}}{n_1} + \frac{S^2_{pooled}}{n_2}\right)}$$

(7)

The assumptions underlying the independent samples of the t-test are:
1. Observations are randomly sample from population 1 and population 2.
2. The sample of observations from population 1 is independent of the sample observations from population 2.
3. Observations are normally distributed in both population 1 and population 2.
4. The variances of population 1 and population 2 are unknown but are equal.

Statistical Results of the Repeated Shear at Constant Height Tests

The Student t-test was used to determine if the results from the Repeated Shear at Constant Height (RSCH) tests were significantly equal (Equal) or significantly not equal (Not Equal). The test parameters evaluated in the statistical analysis were the S-slope from the RSCH permanent deformation plot, and the RSCH maximum shear strain at 3,000 and 5,000 loading cycles. The analysis results are shown as Tables 23 to 28.

Table 23 – Results of Student t-Test for S-slope Determined from RSCH Test @ 52°C

	Citgo PG64-22	Citgo PG76-22	Koch PG76-22	Vestoplast	Eastman	HTI
Citgo PG64-22		Not Equal	Not Equal	Equal	Equal	Equal
Citgo PG76-22	Not Equal		Equal	Not Equal	Not Equal	Not Equal
Koch PG76-22	Not Equal	Equal		Not Equal	Not Equal	Not Equal
Vestoplast	Equal	Not Equal	Not Equal		Not Equal	Not Equal
Eastman	Equal	Not Equal	Not Equal	Not Equal		Equal
HTI	Equal	Not Equal	Not Equal	Not Equal	Equal	

Table 24 – Results of Student t-Test for S-slope Determined from RSCH Test @ 64°C

	Citgo PG64-22	Citgo PG76-22	Koch PG76-22	Vestoplast	Eastman	HTI
Citgo PG64-22		Not Equal	Not Equal	Equal	Equal	Not Equal
Citgo PG76-22	Not Equal		Equal	Equal	Not Equal	Not Equal
Koch PG76-22	Not Equal	Equal		Not Equal	Not Equal	Not Equal
Vestoplast	Equal	Equal	Not Equal		Equal	Not Equal
Eastman	Equal	Not Equal	Not Equal	Equal		Not Equal
HTI	Not Equal	Not Equal	Not Equal	Not Equal	Not Equal	

Table 25 – Results of Student t-Test for Maximum Shear Strain (3,000 Cycles) Determined from RSCH @ 52°C

	Citgo PG64-22	Citgo PG76-22	Koch PG76-22	Vestoplast	Eastman	HTI
Citgo PG64-22		Not Equal	Not Equal	Equal	Not Equal	Equal
Citgo PG76-22	Not Equal		Equal	Not Equal	Not Equal	Not Equal
Koch PG76-22	Not Equal	Equal		Not Equal	Not Equal	Not Equal
Vestoplast	Equal	Not Equal	Not Equal		Not Equal	Not Equal
Eastman	Not Equal	Not Equal	Not Equal	Not Equal		Equal
HTI	Equal	Not Equal	Not Equal	Not Equal	Equal	

Table 26 - Results of Student t-Test for Maximum Shear Strain (5,000 Cycles) Determined from RSCH @ 52°C

	Citgo PG64-22	Citgo PG76-22	Koch PG76-22	Vestoplast	Eastman	HTI
Citgo PG64-22		Not Equal	Not Equal	Equal	Not Equal	Equal
Citgo PG76-22	Not Equal		Equal	Not Equal	Not Equal	Not Equal
Koch PG76-22	Not Equal	Equal		Not Equal	Not Equal	Not Equal
Vestoplast	Equal	Not Equal	Not Equal		Not Equal	Not Equal
Eastman	Not Equal	Not Equal	Not Equal	Not Equal		Equal
HTI	Equal	Not Equal	Not Equal	Not Equal	Equal	

Table 27 - Results of Student t-Test for Maximum Shear Strain (3,000 Cycles) Determined from RSCH @ 64°C

	Citgo PG64-22	Citgo PG76-22	Koch PG76-22	Vestoplast	Eastman	HTI
Citgo PG64-22		Not Equal	Not Equal	Equal	Equal	Not Equal
Citgo PG76-22	Not Equal		Equal	Not Equal	Not Equal	Not Equal
Koch PG76-22	Not Equal	Equal		Not Equal	Not Equal	Not Equal
Vestoplast	Equal	Not Equal	Not Equal		Equal	Not Equal
Eastman	Equal	Not Equal	Not Equal	Equal		Not Equal
HTI	Not Equal	Not Equal	Not Equal	Not Equal	Not Equal	

Table 28 - Results of Student t-Test for Maximum Shear Strain (5,000 Cycles) Determined from RSCH @ 64°C

	Citgo PG64-22	Citgo PG76-22	Koch PG76-22	Vestoplast	Eastman	HTI
Citgo PG64-22		Not Equal	Not Equal	Equal	Equal	Not Equal
Citgo PG76-22	Not Equal		Equal	Not Equal	Not Equal	Not Equal
Koch PG76-22	Not Equal	Equal		Not Equal	Not Equal	Not Equal
Vestoplast	Equal	Not Equal	Not Equal		Equal	Not Equal
Eastman	Equal	Not Equal	Not Equal	Equal		Not Equal
HTI	Not Equal	Not Equal	Not Equal	Not Equal	Not Equal	

The following conclusions from the statistical analysis of the RSCH test data are as follows:

1. The S-slope, the slope of the permanent shear strain vs loading cycles, was statistically determined to be significantly equal between the PG64-22 baseline binder and all of the asphalt modifiers (Creanova's Vestoplast, Eastman EE-2, and Hydrocarbon Technology's Carbon Black). This means that the accumulation of permanent shear strain during the RSCH test was the same (i.e no improvement in performance).
2. The permanent shear strain from 5,000 loading cycles conducted at 52^oC indicates that Creanova's Vestoplast and Hydrocarbon Technology's carbon black performed in a similar manner to the PG64-22 (i.e. no improvement). Meanwhile the statistical analysis of the Eastman EE-2 showed that its performance was not statistically equal to the PG64-22. However, this is due to the fact that the Eastman EE-2 performed much worse than the PG64-22.
3. The permanent shear strain from 5,000 loading cycles conducted at 64^oC indicates that Creanova's Vestoplast and Eastman EE-2 material performed statistically equal to the PG64-22 (i.e. no improvement). The Hydrocarbon Technology's carbon black was statistically classified as being Not Equal. However, this was due to the material performing much poorer than the PG64-22.
4. The two PG76-22 polymer-modified binders were shown to be significantly equal, indicating that both of the PG76-22 performs in a similar manner. However, none of the other mixes were classified to be statistically equal to the two PG76-22 mixes.
5. The statistical results from the 3,000 loading cycles and the 5,000 loading cycles from both test temperatures are identical indicating that the test could be shortened to 3,000 cycles and still provide accurate rankings.

Statistical Results of the Frequency Sweep at Constant Height Tests

The Student t-test was used to determine if the results from the Frequency Sweep at Constant Height (FSCH) tests were significantly equal (Equal) or significantly not equal (Not Equal). The analysis results are shown as tables 29 to 31. The comparisons only consisted of evaluating the fatigue factor ($G^*sin\phi$) at 20^oC, and the rutting parameter ($G^*/sin\phi$) at 40 and 52^oC. As stated earlier, the m-slope was not chosen because it was not a true measure of rutting susceptibility. The m-slope is more of an indication of the material's sensitivity to load frequency (i.e. the lower the m-slope, the lower the dependency on load frequency). Therefore, it is recommended that the m-slope be used to decide between two materials that have similar rutting parameters.

Table 29 – Results of Student t-Test for Fatigue Factor (G*sinϕ) Determined at 20°C

	Citgo PG64-22	Citgo PG76-22	Koch PG76-22	Vestoplast	Eastman	HTI
Citgo PG64-22		Not Equal	Not Equal	Not Equal	Not Equal	Not Equal
Citgo PG76-22	Not Equal		Not Equal	Equal	Not Equal	Not Equal
Koch PG76-22	Not Equal	Not Equal		Not Equal	Equal	Not Equal
Vestoplast	Not Equal	Equal	Not Equal		Not Equal	Not Equal
Eastman	Not Equal	Not Equal	Equal	Not Equal		Equal
HTI	Not Equal	Not Equal	Not Equal	Not Equal	Equal	

Table 30 – Results of Student t-Test for Rutting Parameter (G*/sinϕ) Determined at 40°C

	Citgo PG64-22	Citgo PG76-22	Koch PG76-22	Vestoplast	Eastman	HTI
Citgo PG64-22		Not Equal	Not Equal	Not Equal	Not Equal	Equal
Citgo PG76-22	Not Equal		Equal	Equal	Not Equal	Not Equal
Koch PG76-22	Not Equal	Equal		Not Equal	Not Equal	Not Equal
Vestoplast	Not Equal	Equal	Not Equal		Not Equal	Not Equal
Eastman	Not Equal	Not Equal	Not Equal	Not Equal		Not Equal
HTI	Equal	Not Equal	Not Equal	Not Equal	Not Equal	

Table 31 – Results of Student t-Test for Rutting Parameter (G*/sinϕ) Determined at 52°C

	Citgo PG64-22	Citgo PG76-22	Koch PG76-22	Vestoplast	Eastman	HTI
Citgo PG64-22		Equal	Not Equal	Equal	Equal	Equal
Citgo PG76-22	Equal		Equal	Equal	Equal	Not Equal
Koch PG76-22	Not Equal	Equal		Not Equal	Not Equal	Not Equal
Vestoplast	Equal	Equal	Not Equal		Equal	Not Equal
Eastman	Equal	Equal	Not Equal	Equal		Not Equal
HTI	Equal	Not Equal	Not Equal	Not Equal	Not Equal	

The following conclusions from the statistical analysis of the FSCH test data are as follows:

1. All of the asphalt modifiers where found to be statistically Not Equal to the PG64-22. Based on the actual data, the Not Equal was due to the fact that all three modifiers increased the fatigue properties of the HMA.
2. The Citgo PG76-22 was found to be statistically Equal to Creanova's Vestoplast when comparing the fatigue factor, with the Koch Material's PG76-22 being found to be statistically Not Equal to the other PG76-22 (Citgo). Therefore, the addition of the Creanova's Vestoplast to the baseline binder increases the fatigue properties of the HMA to that of the Citgo PG76-22.
3. The best performing material was the Citgo PG76-22, with the Koch Materials PG76-22 found to be statistically Not Equal to the Citgo PG76-22. This is due to the Koch Materials not performing as well as the Citgo PG76-22. The

importance of this finding is that even though the performance grades of the two PG76-22 binders are the same, the fatigue performance was not equal.

4. The Eastman EE-2 polymer was found to be statistically Equal to the Koch Material's PG76-22. However, as stated earlier, the Koch PG76-22 did not perform as well as the Citgo PG76-22.

5. The Creanova Vestoplast was found to be statistically Equal to both PG76-22 binders, which were also found to be statistically Equal, for the rutting parameter determined at 40oC. Therefore, the Creanova's Vestoplast performed equally as well as two PG76-22 polymer modified binders.

6. The Eastman EE-2 was found to be statistically Not Equal to any of the other materials. It performed better than the HTI Carbon Black and the PG64-22, but not as well as the PG76-22 materials.

7. The HTI Carbon Black was found to be statistically Equal to the PG64-22. Therefore, the addition of the Carbon Black did not increase nor decrease the rutting properties of the baseline PG64-22.

8. The rutting parameter of the Koch Material's PG76-22 was found to be statistically Equal to the Citgo PG76-22, but not statistically Equal to any of ther other materials. Meanwhile, the Citgo PG76-22 was found to be statistically Equal to all of the materials except the HTI Carbon Black when comparing the rutting parameter determined at 52°C.

9. The larger scatter at 52°C is most likely due to increased variance among the test data. The larger the scatter in the test data, the more statistically similar the materials will be.

Statistical Results of the Simple Shear at Constant Height Tests

The Student t-test was used to determine if the results from the Simple Shear at Constant Height SSCH) tests were significantly equal (Equal) or significantly not equal (Not Equal). The analysis results are shown as tables 32 to 34. The comparisons consisted of evaluating the maximum shear strain, permanent shear strain, and the creep slope determined at 40°C. Only the 40°C temperature was chosen since the goal of the project was to evaluate the materials for rut mitigation.

Table 32 – Results of Student t-Test for Maximum Shear Strain Determined at 40°C

	Citgo PG64-22	Citgo PG76-22	Koch PG76-22	Vestoplast	Eastman	HTI
Citgo PG64-22		Not Equal	Not Equal	Not Equal	Equal	Not Equal
Citgo PG76-22	Not Equal		Equal	Not Equal	Not Equal	Not Equal
Koch PG76-22	Not Equal	Equal		Not Equal	Not Equal	Not Equal
Vestoplast	Not Equal	Not Equal	Not Equal		Not Equal	Not Equal
Eastman	Equal	Not Equal	Not Equal	Not Equal		Not Equal
HTI	Not Equal	Not Equal	Not Equal	Not Equal	Not Equal	

Table 33 – Results of the Student t-Test for Permanent Shear Strain Determined at 40°C

	Citgo PG64-22	Citgo PG76-22	Koch PG76-22	Vestoplast	Eastman	HTI
Citgo PG64-22		Not Equal	Not Equal	Not Equal	Equal	Not Equal
Citgo PG76-22	Not Equal		Equal	Not Equal	Not Equal	Not Equal
Koch PG76-22	Not Equal	Equal		Not Equal	Not Equal	Not Equal
Vestoplast	Not Equal	Not Equal	Not Equal		Equal	Not Equal
Eastman	Equal	Not Equal	Not Equal	Equal		Not Equal
HTI	Not Equal	Not Equal	Not Equal	Not Equal	Not Equal	

Table 34 – Results of the Student t-Test for Creep Slope Determined at 40°C

	Citgo PG64-22	Citgo PG76-22	Koch PG76-22	Vestoplast	Eastman	HTI
Citgo PG64-22		Not Equal	Not Equal	Not Equal	Equal	Not Equal
Citgo PG76-22	Not Equal		Equal	Not Equal	Not Equal	Not Equal
Koch PG76-22	Not Equal	Equal		Not Equal	Not Equal	Not Equal
Vestoplast	Not Equal	Not Equal	Not Equal		Not Equal	Not Equal
Eastman	Equal	Not Equal	Not Equal	Not Equal		Not Equal
HTI	Not Equal	Not Equal	Not Equal	Not Equal	Not Equal	

The following conclusions from the statistical analysis of the SSCH test data are as follows:

1. The two PG76-22 polymer modified binders were determined to be statistically Equal when evaluating the maximum shear strain. The Creanova's Vestoplast and HTI Carbon Black was found to be statistically Not Equal to the PG64-22. This was due to the Creanova's Vestoplast performing better than the PG64-22 and the HTI Carbon Black performing worse. The Eastman EE-2 was found to be statistically Equal to the PG64-22. None of the admixtures were found to be statistically Equal to the PG76-22 materials.

2. The two PG76-22 polymer modified binders were determined to be statistically Equal when evaluating the permanent shear strain. The Eastman EE-2 and Creanova's Vestoplast were found to be statistically Equal, however, neither material was found to be Equal to the PG76-22 materials. Therefore, both the Eastman EE-2 and Creanova's Vestoplast increased the shear strain creep performance from the baseline PG64-22, however, the increase was not enough to be comparable to the PG76-22 materials. The HTI Carbon Black was found to be Not Equal to the PG64-22 as the performance of the material was worse than the PG64-22.

3. The statistical results of the creep slope were identical to the statistical results of the maximum shear strain.

Statistical Analysis of Asphalt Pavement Analyzer (APA) Results

The Student t-test was used to determine if the results from the Asphalt Pavement Analyzer (APA) tests were significantly equal (Equal) or significantly not equal (Not Equal). The analysis results are shown as tables 35 and 36. The comparisons consisted of evaluating the measured rutting in the APA for both the gyratory samples and the brick samples.

Table 35 – Results of Student t-Test for APA Rutting of Gyratory Compacted Samples

	Citgo PG64-22	Citgo PG76-22	Koch PG76-22	Vestoplast	Eastman	HTI
Citgo PG64-22		Not Equal	Not Equal	Equal	Not Equal	Not Equal
Citgo PG76-22	Not Equal		Not Equal	Not Equal	Not Equal	Not Equal
Koch PG76-22	Not Equal	Not Equal		Not Equal	Not Equal	Not Equal
Vestoplast	Equal	Not Equal	Not Equal		Not Equal	Not Equal
Eastman	Not Equal	Not Equal	Not Equal	Not Equal		Not Equal
HTI	Not Equal	Not Equal	Not Equal	Not Equal	Not Equal	

Table 36 – Results of Student t-Test for APA Rutting of Vibratory Brick Samples

	Citgo PG64-22	Citgo PG76-22	Koch PG76-22	Vestoplast	Eastman	HTI
Citgo PG64-22		Not Equal	Not Equal	Equal	Equal	Not Equal
Citgo PG76-22	Not Equal		Equal	Equal	Equal	Not Equal
Koch PG76-22	Not Equal	Equal		Equal	Equal	Not Equal
Vestoplast	Equal	Equal	Equal		Equal	Not Equal
Eastman	Equal	Equal	Equal	Equal		Not Equal
HTI	Not Equal	Not Equal	Not Equal	Not Equal	Not Equal	

The following conclusions from the statistical analysis of the APA rutting test data are as follows:

1. The rutting trend between the gyratory samples and the vibratory brick samples are different. The majority of the APA rutting results for the gyratory samples are determined to be statistically Not Equal, meaning that all of the gyratory samples generally performed differently. However, the majority of the vibratory brick samples were found to be statistically Equal, meaning that the materials all had similar rutting properties. This disagrees with most of the findings in this study. Therefore, it can be concluded that the use of vibratory brick samples should not be used to evaluate the performance of different HMA mixes.
2. The Vestoplast Creanova material was found to be statistical Equal to the PG64-22. This means that the Creanova Vestoplast did not increase the rut resistance properties of the baseline PG64-22 material. The Hydrocarbon Technologies Carbon Black material was found to be statistically Not Equal; mainly due to the material performing poorer than the baseline PG64-22. Meanwhile, the Eastman

EE-2 material was also statistically determined to be Not Equal to the PG64-22, however, this was due to the material performing better than baseline PG64-22.
3. None of the additive materials tested in the APA (gyratory samples) had an equal performance to the polymer-modified binders.

Final Conclusions from the Statistical Analysis of STOA Testing

The Student t-Test analysis was used to compare the measured test parameters of the samples from the various performance tests. For proper use in ranking HMA materials, the test method/test parameter must be able to differentiate between the different materials tested. This would result in a Student t-Test matrix that obtained <u>the least amount</u> of statistically "Equal" responses. The following is the top five test methods/test parameters that obtained the least amount of statistically "Equal" responses.

1. APA rutting depth using the gyratory pill samples
2. Permanent shear strain and creep slope from the SSCH test @ 40°C
3. Permanent shear strain from RSCH @ 64°C, the maximum shear strain from the SSCH @ 40°C, and the FSCH Rutting Parameter @ 40°C.

As shown above, the test procedure that provided the best differentiation between the different asphalt modifiers was the APA rutting depth using the gyratory pill samples.

LONG TERM OVEN AGING – LTOA

Although the main focus of this study was to determine the effects of asphalt modifiers on the permanent deformation response of hot mix asphalt, it is also important to evaluate how the additive effects the long-term performance of the asphalt. Through mainly oxidation, asphaltic materials tend to undergo age hardening. This is natural stiffening of the asphalt due to environmental conditions. SHRP researchers Bell et al. (1994) evaluated the laboratory modeling of HMA and found that the age hardening effect can be simulated using a method called Long Term Oven Aging (LTOA). The procedure for the LTOA requires that the HMA sample, after it has been compacted, is placed in an oven for 5 to 7 days at 85°C. Depending on the climatic region, this simulates between 7 to 15 years of weather cycling. Many researchers have found that it is very difficult to actually "pin-point" the true amount of aging time, therefore the procedure is simply used as an aging mechanism to evaluate the effect of age hardening on the characteristics of HMA. For this study, all samples were LTOA for 5 days at 85°C.

The concern for age hardening is mainly in the increase in material stiffness and the decrease in creep properties. If the material becomes too stiff due to aging, it will be prone to low temperature fatigue cracking. The same can be said with the creep properties. If the HMA is not allowed to undergo some creep movement from traffic loading, it would be prone to low temperature fatigue cracking.

To provide guidance to the NJDOT on the selection of asphalt modifiers, criteria was established based on the aging characteristics of the baseline HMA materials. These were the Citgo PG64-22, Citgo PG76-22, and the Koch PG76-22. Both the shear stiffness properties from the frequency sweep at constant height (FSCH) and the creep properties from the simple shear at constant height (SSCH) were used to evaluated the effect of age hardening. The tests were conducted at the identical test temperatures performed earlier so a direct comparison could be established between the initial and age samples.

LTOA Testing – Frequency Sweep at Constant Height (FSCH)

Frequency Sweep at Constant Height (FSCH) tests were conducted with the Superpave Shear Tester (SST) at 20, 40, and 52°C test temperature to correspond to the initial testing. Although the main concern was the lower testing temperature of 20°C, all temperatures are shown for comparative purposes. Figures 74, 75, and 76 show the results for the baseline materials at 20, 40, and 52°C, respectively. The increase in stiffness is greatest at the lower test temperature (20°C), which would be in the typical range of fatigue failure. In contrast, the largest stiffness increase occurred at loading frequencies that are typical of rutting failure (less than 0.1 hertz), not fatigue failure.
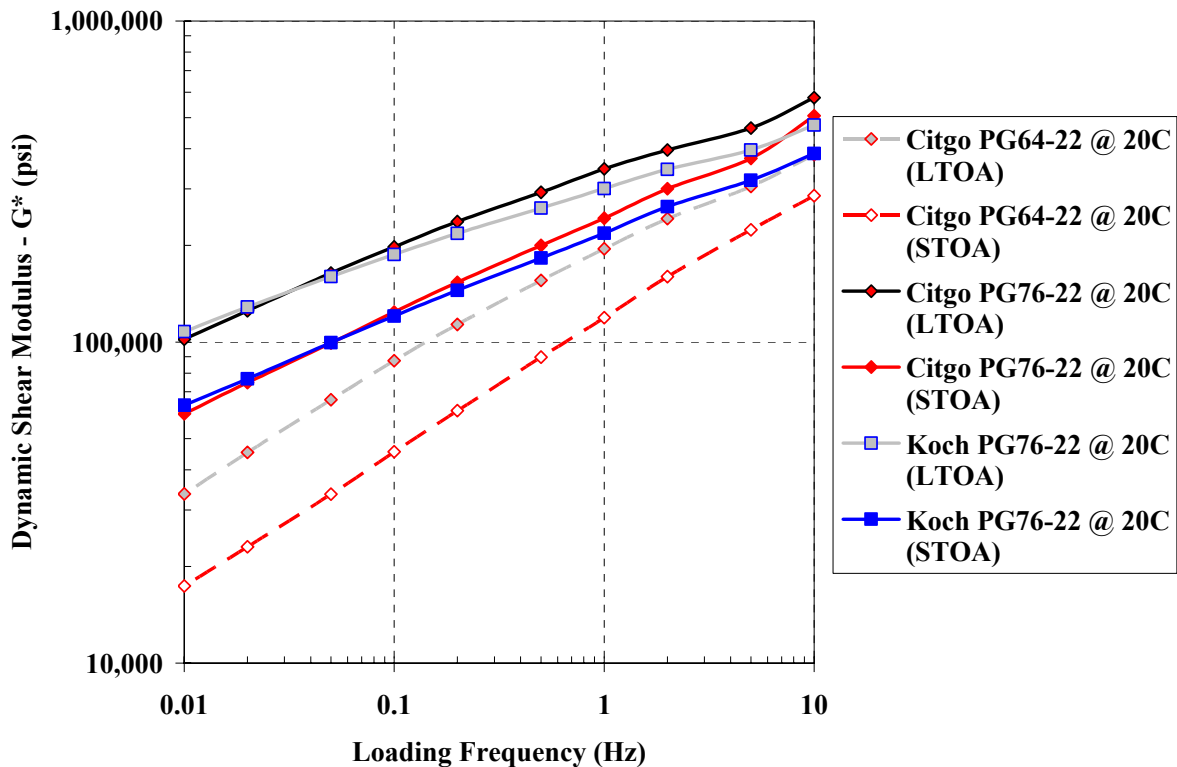

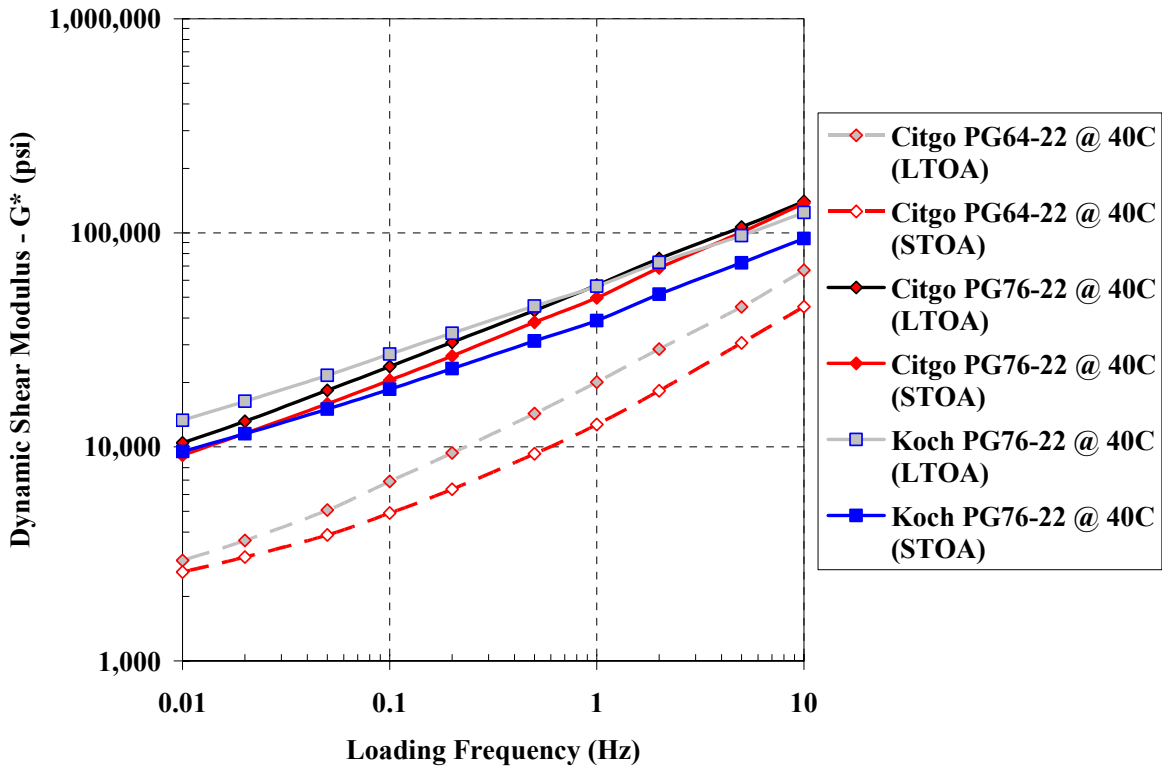Figure 74 – FSCH Results Tested @ 20C for Initial and Aged Samples

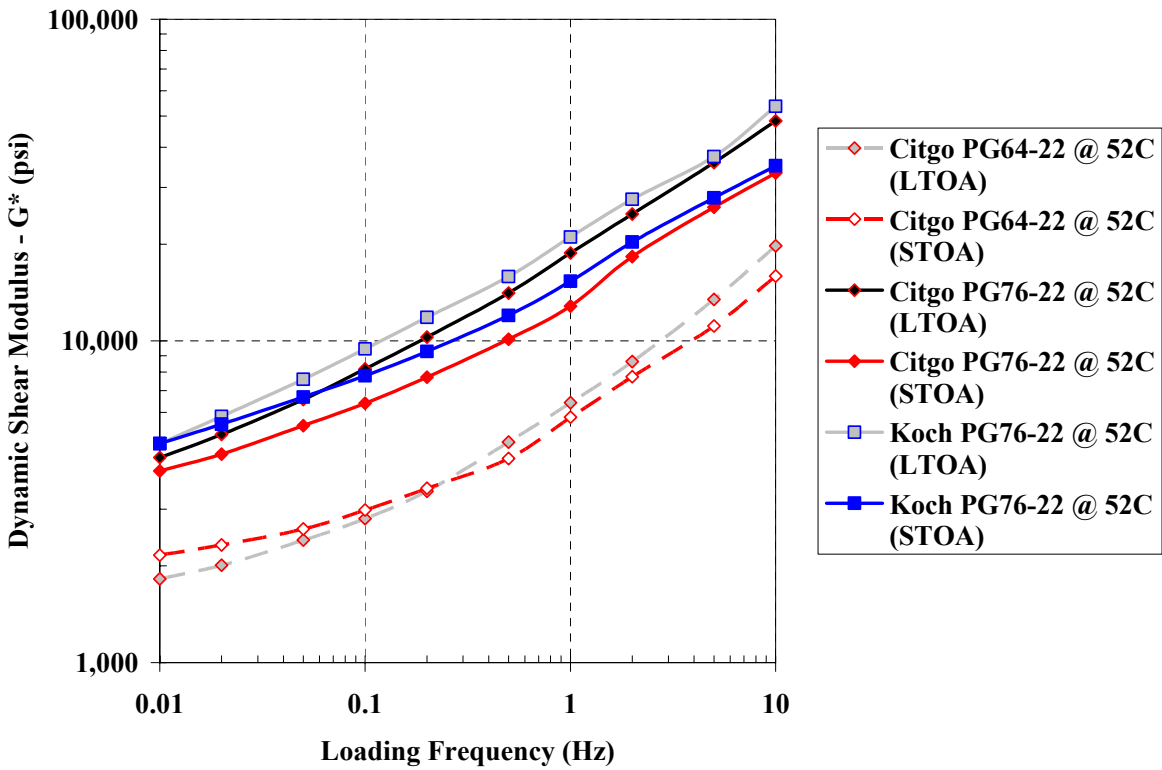Figure 75 – FSCH Results Tested @ 40C for Initial and Aged Samples

Figure 76 – FSCH Results Tested @ 52C for Initial and Aged Samples

97

Table 37 provides the ratios between the initial and aged stiffness values for all three baseline samples tested. It was found that the ratios between the aged and initial samples did not go above 2 for any of the test temperatures. Also, the 52°C test temperature tested at a loading frequency of 0.01 Hz was almost identical to the initial values. In fact, the Citgo PG64-22 aged samples actually achieve a shear modulus less than the initial (unaged) samples. The age softening at high temperature/low loading did not occur in the polymer-modified samples, although the Koch Materials achieved an aged to unaged ratio of 1.0. If the values for all loading frequencies were averaged, each material, regardless of test temperature, had an increase in stiffness due to aging.

Table 37 – Ratio of LTOA to STOA from FSCH Dynamic Modulus (G*) – Baseline

| Loading Frequency | Ratio of (G* LTOA):(G* STOA) | | | | | | | | |
| | Citgo PG64-22 | | | Citgo PG76-22 | | | Koch Materials PG76-22 | | |
(Hz)	20°C	40°C	52°C	20°C	40°C	52°C	20°C	40°C	52°C
10	1.34	1.48	1.24	1.14	1.02	1.45	1.23	1.33	1.53
5	1.37	1.47	1.21	1.24	1.06	1.38	1.24	1.34	1.34
2	1.52	1.57	1.11	1.32	1.11	1.36	1.31	1.41	1.36
1	1.64	1.58	1.11	1.43	1.15	1.46	1.38	1.45	1.37
0.5	1.73	1.54	1.12	1.46	1.13	1.39	1.43	1.46	1.32
0.2	1.86	1.48	0.98	1.55	1.16	1.33	1.50	1.46	1.28
0.1	1.92	1.40	0.94	1.59	1.16	1.28	1.55	1.46	1.21
0.05	1.97	1.31	0.92	1.65	1.16	1.21	1.61	1.44	1.14
0.02	1.97	1.19	0.86	1.68	1.14	1.15	1.67	1.42	1.06
0.01	1.94	1.13	0.84	1.71	1.14	1.10	1.70	1.40	1.00
AVERAGE	**1.72**	**1.42**	**1.03**	**1.48**	**1.12**	**1.31**	**1.46**	**1.42**	**1.26**

The phase angle was also evaluated to see how the material behaves after it has aged. The phase angle can provide information on the material's deformation characteristics. As an example, the closer the phase angle is to zero degrees, the more elastic the behavior of the visco-elastic material. However, the closer the phase angle is to 90 degrees, the more viscous the behavior.   Therefore, by comparing the general trend of the phase angle of the unaged and aged samples, one can determine if a material is hardening (closer to zero) or softening (closer to 90 degrees). Figure 77 shows the phase angle versus load frequency for the Citgo PG64-22 at 20°C. As can be seen in the figure, the LTOA (aged) phase angle is lower than the STOA (unaged) phase angle. This means that the material has hardened due to the aging. However, when the same analysis is done at 52°C, as shown in Figure 78, the opposite occurs. In this case, the LTOA phase angle is greater than the STOA phase angle, thereby showing that the material has actually softened due to the aging process.
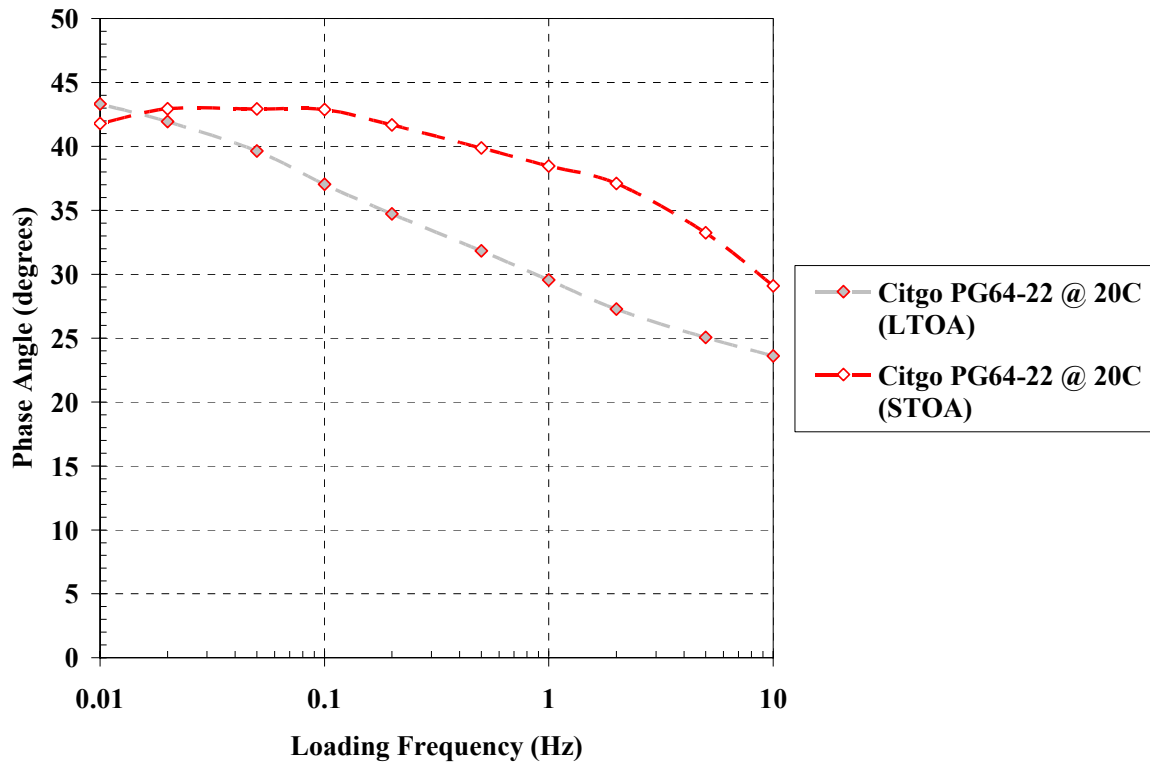
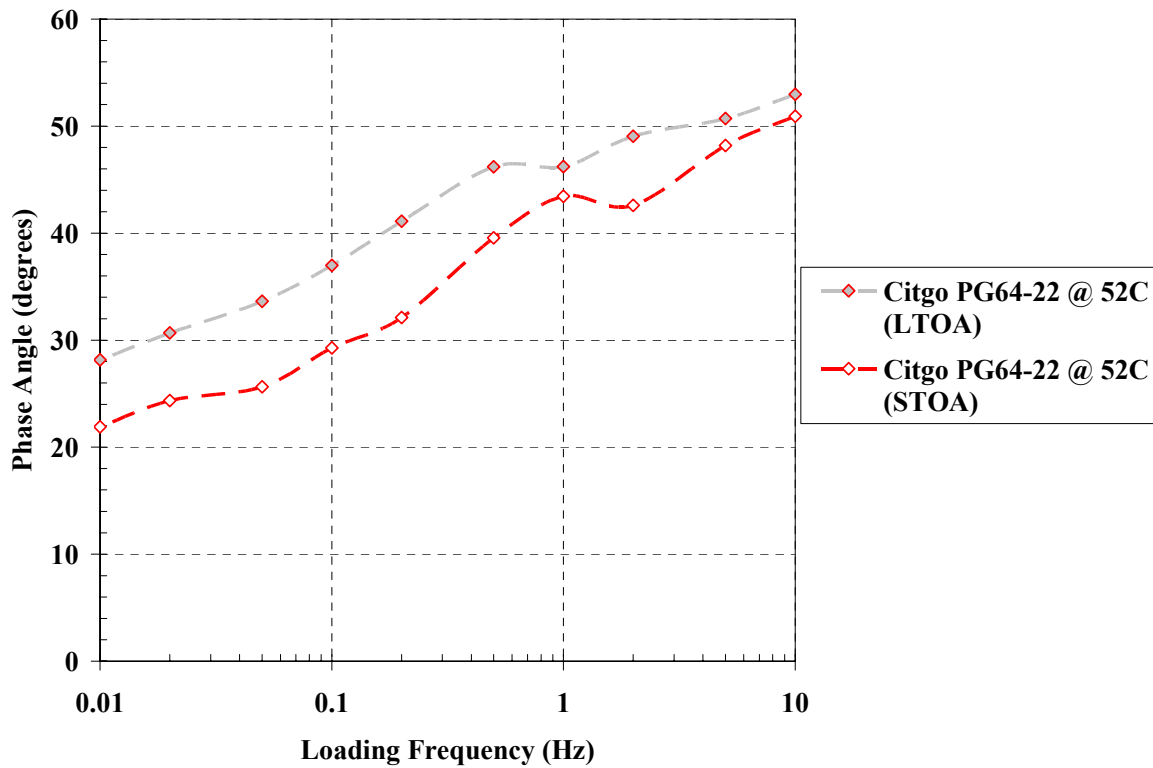Figure 77 – Phase Angle versus Loading Frequency for Citgo PG64-22 at 20°C

Figure 78 – Phase Angle versus Loading Frequency for Citgo PG64-22 at 52°C

The same general trend occurred for the both the Citgo PG76-22 and the Koch Materials PG76-22, although not as severe. Table 38 shows the ratios between the LTOA (aged) and STOA (unaged). In the table, if the ratio is below 1.0, then the material has stiffened based on the viscosity elasticity properties. If above 1.0, then the material has softened.

Table 38 – Ratio of LTOA to STOA for FSCH Phase Angle (ϕ)- Baseline

| Loading Frequency | Ratio of (ϕ LTOA):(ϕ STOA) | | | | | | | | |
| | Citgo PG64-22 | | | Citgo PG76-22 | | | Koch Materials PG76-22 | | |
(Hz)	20°C	40°C	52°C	20°C	40°C	52°C	20°C	40°C	52°C
10	0.70	0.88	1.04	0.72	0.91	0.93	0.72	0.87	0.89
5	0.75	0.93	1.05	0.72	0.92	0.96	0.75	0.89	0.97
2	0.74	0.95	1.15	0.68	0.90	1.01	0.72	0.89	1.03
1	0.77	0.97	1.06	0.69	0.95	0.95	0.72	0.93	1.01
0.5	0.80	1.02	1.17	0.75	0.97	0.99	0.76	0.93	1.03
0.2	0.83	1.08	1.28	0.76	0.99	1.05	0.76	0.97	1.07
0.1	0.86	1.12	1.26	0.77	1.00	1.07	0.79	0.99	1.09
0.05	0.92	1.18	1.31	0.79	1.02	1.08	0.80	1.03	1.13
0.02	0.98	1.24	1.26	0.85	1.01	1.12	0.83	1.06	1.15
0.01	1.04	1.25	1.29	0.85	1.03	1.11	0.83	1.09	1.12
AVERAGE	0.84	1.06	1.19	0.76	0.97	1.03	0.77	0.97	1.05

The phase angle ratio comparisons for the baseline samples generally showed that the aged materials were stiffer at the lower test temperature and softer at the higher test temperature than the unaged samples.

As mentioned earlier, it is generally accepted that the aging that occurs during the life of the asphalt increases the stiffness and typically warrants concern for fatigue cracking. However, the occurrence of age softening was not expected. The age softening was also found to be greatest at low loading frequencies, typical of slow moving traffic where the rutting potential is greatest. Therefore, based on the comparisons between the aged and unaged samples, when aged, the asphalt material will generally be stiffer at low temperatures and softer at warmer temperatures than it would be when recently placed. If the laboratory aging is truly representative to field aging, then the potential for fatigue cracking or rutting would increase with the life of the asphalt pavement.

The same aging ratio analysis was conducted for the three admixtures evaluated in the study (Hydrocarbon Technology's Carbon Black, Eastman EE-2, and Creanova's Vestoplast). The aging ratio results for the dynamic modulus (G*) are shown in Table 39 and the aging ratio results for the phase angle are shown in Table 40. The dynamic modulus analysis showed that the addition of the Eastman EE2 and the Creanova Vestoplast lowered the ratio between the LTOA and STOA dynamic shear modulus at 20°C when compared to the Citgo PG64-22 and the two PG76-22 samples. Therefore, the addition of either material would aid in reducing the potential for fatigue cracking. The addition of the Carbon Black helped to keep the aging ratio less than that obtained from the PG64-22, but not less than the two PG76-22 samples.

Table 39 - Ratio of LTOA to STOA from FSCH Dynamic Modulus (G*) – Admixtures

| Loading Frequency | Ratio of (G* LTOA):(G* STOA) | | | | | | | | |
| | Creanova Vestoplast | | | Eastman EE-2 | | | HTI Carbon Black | | |
(Hz)	20°C	40°C	52°C	20°C	40°C	52°C	20°C	40°C	52°C
10	1.04	0.94	1.06	1.41	1.38	1.06	1.27	0.94	1.11
5	1.06	0.97	1.16	1.12	1.17	0.98	1.37	0.94	1.08
2	1.12	1.02	0.97	1.31	1.23	0.94	1.41	1.02	0.95
1	1.17	1.01	0.98	1.37	1.26	0.92	1.47	1.01	1.00
0.5	1.19	0.97	0.88	1.32	1.14	0.91	1.52	0.98	1.01
0.2	1.23	0.93	0.78	1.34	1.10	0.73	1.63	0.93	0.87
0.1	1.26	0.89	0.72	1.35	1.07	0.72	1.69	0.92	0.84
0.05	1.27	0.85	0.64	1.39	1.04	0.68	1.75	0.90	0.81
0.02	1.28	0.78	0.63	1.37	0.97	0.66	1.80	0.86	0.78
0.01	1.25	0.76	0.62	1.36	0.94	0.64	1.80	0.89	0.75
AVERAGE	**1.19**	**0.91**	**0.84**	**1.33**	**1.13**	**0.82**	**1.57**	**0.94**	**0.92**

When comparing the 52°C aging ratios, the admixtures showed that they were more prone to increased age softening than the baseline values. Especially the Vestoplast and the EE2 where at a loading frequency of 0.01 Hz, the G* ratio between the aged and unaged samples were approximately 0.6 (or 60%). This means that there was a 40% loss in stiffness due to the material being aged. The Carbon Black material was only 0.75. However, when compared to the baseline values, especially the PG64-22, this drop in stiffness is below the baseline obtained values.

The phase angle ratios between the aged and unaged admixture samples were also analyzed. This is shown in Table 40. Again, if the ratio between the LTOA and STOA phase angles are less than 1.0, then the material has hardened or become stiffer. If the ratio is greater than 1.0, the material has softened.

Table 40 - Ratio of LTOA to STOA for FSCH Phase Angle (φ) - Admixtures

| Loading Frequency | Ratio of (φ LTOA):(φ STOA) | | | | | | | | |
| | Creanova Vestoplast | | | Eastman EE-2 | | | HTI Carbon Black | | |
(Hz)	20°C	40°C	52°C	20°C	40°C	52°C	20°C	40°C	52°C
10	0.88	1.02	1.10	0.71	0.93	1.04	0.80	0.96	1.03
5	0.84	1.01	1.13	0.84	0.96	1.09	0.82	0.98	1.06
2	0.81	0.98	1.21	0.79	0.96	1.06	0.80	1.00	1.09
1	0.83	1.00	1.08	0.83	0.96	1.05	0.83	0.98	1.06
0.5	0.84	1.03	1.26	0.87	1.05	1.04	0.83	1.02	1.14
0.2	0.89	1.07	1.28	0.91	1.03	1.23	0.85	1.06	1.32
0.1	0.91	1.09	1.26	0.92	1.06	1.22	0.86	1.07	1.31
0.05	0.92	1.09	1.24	0.94	1.09	1.17	0.87	1.12	1.39
0.02	0.96	1.13	1.27	0.99	1.09	1.24	0.89	1.15	1.37
0.01	1.01	1.13	1.20	1.02	1.15	1.23	0.93	1.19	1.34
AVERAGE	**0.89**	**1.06**	**1.20**	**0.88**	**1.03**	**1.14**	**0.85**	**1.05**	**1.21**

The results of the admixtures are similar to the baseline materials. At the low test temperature (20°C), the phase angle shows that the material stiffened. However, at the higher test temperature (52°C), the results indicate that the asphalt material softened.

LTOA Testing – FSCH Parameters (Fatigue Factor – G*sinϕ)

The fatigue factor is a measure of the stiffness at intermediate effective pavement temperatures for fatigue cracking or Teff(FC). G*sinϕ was measured at 1.0 hertz to represent fast moving traffic. A Teff(FC) of 20°C was used. High values of G*sinϕ at 1.0 hertz indicate high stiffness at intermediate temperatures and, therefore, low resistance to fatigue cracking according to Superpave.

The results for the STOA (unaged) and the LTOA (aged) samples were compared and are shown in Figure 79. The results show that the fatigue resistance properties remain relatively unchanged for the two PG76-22 samples, as well as for the Creanova Vestoplast, although slight increases are evident. However, a much larger increase in the fatigue factor was found for the PG64-22, Eastman EE2, and the Hydrocarbon Technologies Carbon Black, with the PG64-22 having the largest increase (30%).

LTOA Testing – FSCH Parameters (Rutting Parameter – G*/sinϕ)

The rutting parameter is a measure of HMA stiffness at high pavement temperature (40 and 52°C) at a slow rate of loading (0.1 cycle/second). Higher values of G*/sinϕ indicate an increased stiffness of HMA mixtures and, therefore, increased resistance to rutting. G* is the complex modulus and ϕ is the phase angle when HMA is tested under dynamic loading.

The rutting parameter showed the largest increase in the two PG76-22 samples, with minimal change in the remaining samples (Figure 80). The aging process seemed to have only increased the rutting resistance (stiffness) of the PG76-22 samples when evaluated at 40°C.

When evaluated at 52°C, the rutting parameter showed a very similar trend to the 40°C test data, however, this time there was a dramatic decrease in rutting resistance for the remaining four mixes (PG64-22, Vestoplast, EE2 and Carbon Black). The rutting parameter decreased by approximately 40% for each of the four mixes, while the rutting parameter increased 42% and 13%, respectively, for the Citgo PG76-22 and the Koch PG76-22 (Figure 81).
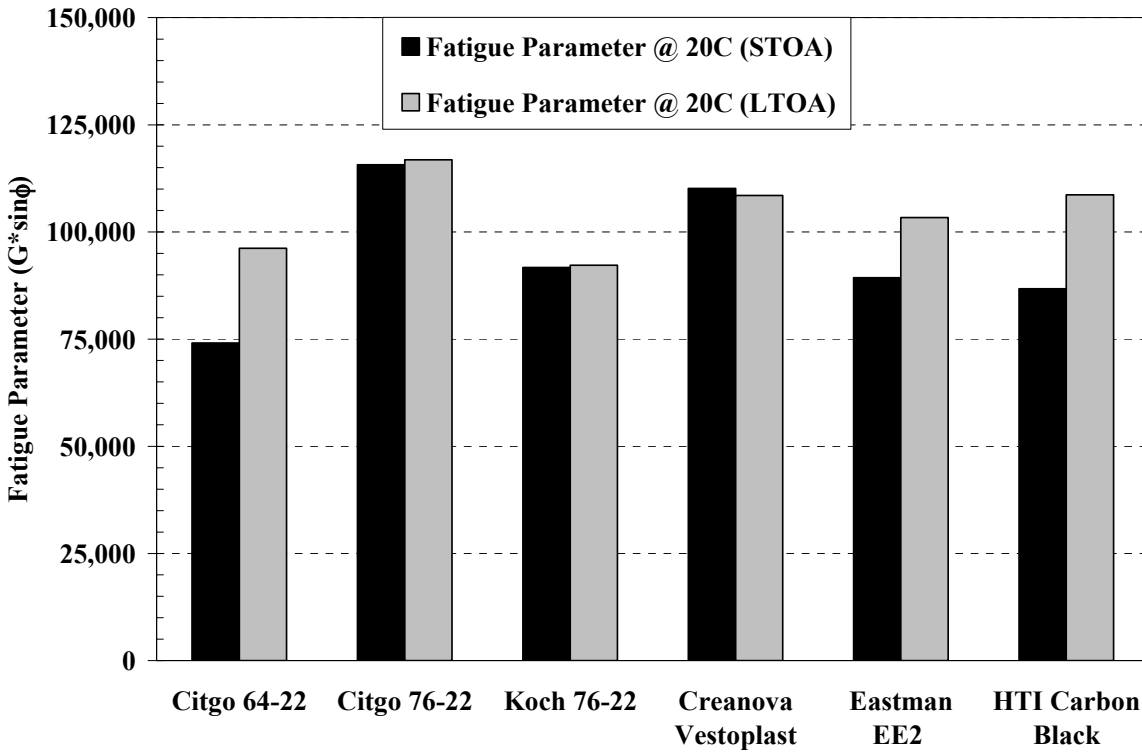
Figure 79 – Comparison of Aging Effects on the Fatigue Factor from the Superpave Shear Tester Frequency Sweep at Constant Height (FSCH) @ 20°C
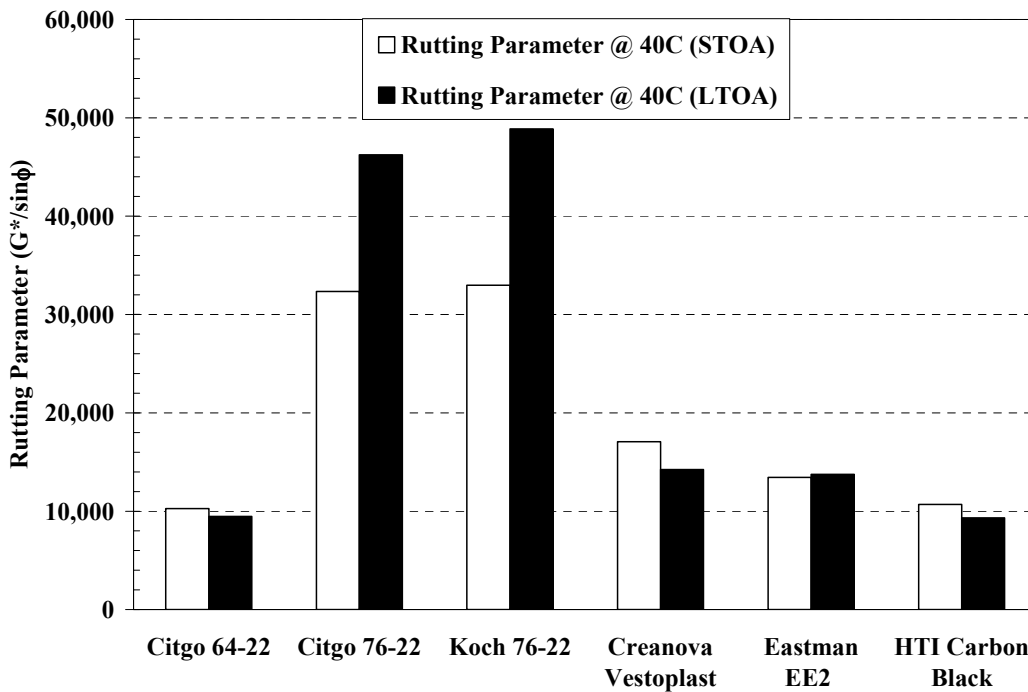

Figure 80 – Comparison of Aging Effects on the Rutting Parameter from the Superpave Shear Tester Repeated Shear at Constant Height (RSCH) @ 40°C
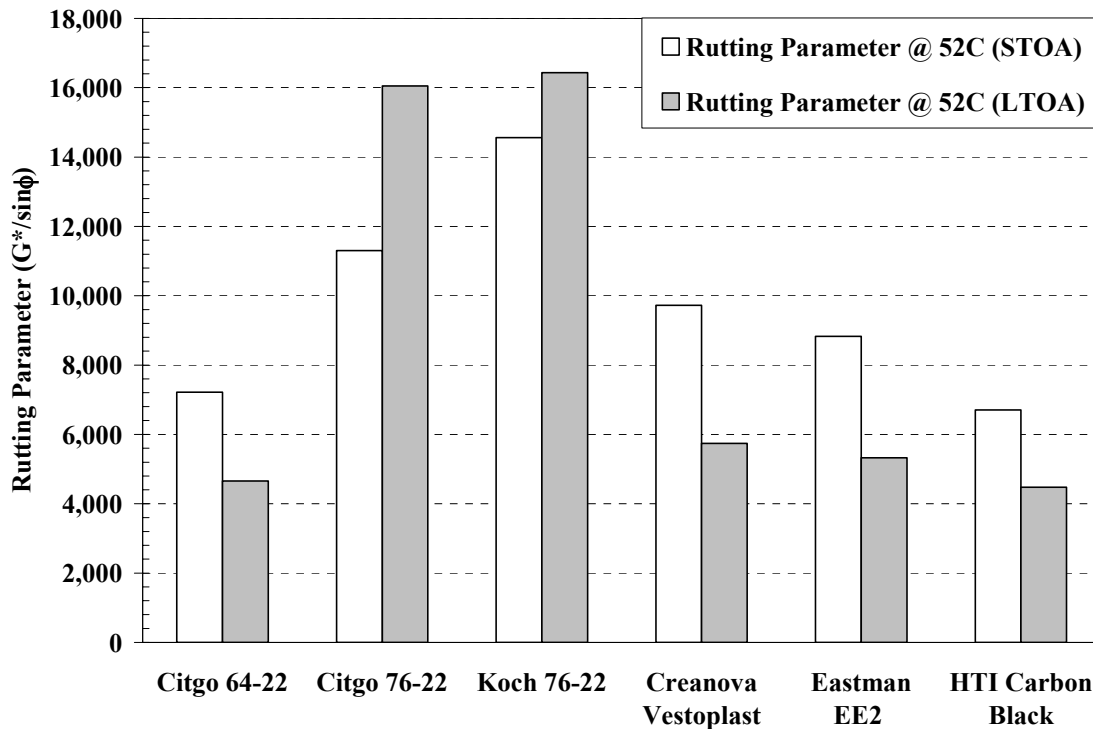
Figure 81 - Comparison of Aging Effects on the Rutting Parameter from the Superpave Shear Tester Repeated Shear at Constant Height (RSCH) @ 52°C

Summary of the Affect of Aging on Frequency Sweep at Constant Height Results

The Frequency Sweep at Constant Height (FSCH) measures shear stiffness of the material, as well as providing a measurement of the visco-elastic response of the material via the phase angle (ϕ). Compacted samples were aged through a process called Long Term Oven Aging (LTOA), where the samples are placed in an oven for 5 days at 85°C. SHRP research has shown that this represents the aging that would occur after a service life of approximately nine years. Both unaged and aged samples were tested under identical temperature and loading conditions using the FSCH test. The following is a summary of the results.

- At the low test temperatures (20°C), there is an increase in the measured dynamic shear modulus (G*). This represents age hardening. Both of the PG76-22 samples showed an average increase of approximately 1.5 times, with the PG64-22 having an average increase of 1.7 times. The average was taken by averaging the ratio between the aged and unaged samples at each test frequency. The admixtures showed an increase of 1.2, 1.33, and 1.6, respectively, for the Creanova Vestoplast, Eastman EE2, and Hydrocarbon Technology's Carbon Black.

104

- At high test temperature (52°C), there was a general decrease in the measured dynamic shear modulus (G*). This represents age softening. The decrease in G* occurred only for the admixtures used in the study, when averaging the data from all of the loading frequencies. The average decrease in G* was 0.84, 0.82, and 0.92 for the Creanova Vestoplast, Eastman EE2, and Hydrocarbon Technology's Carbon Black, respectively. The baseline samples did not exhibit age softening when averaging all of the loading frequencies. However, if evaluating the loading frequencies individually, as the loading frequency decreased, the ratio between the aged and unaged stiffness decreased. Only the PG76-22 samples did not have aged to unaged ratio less than 1.0 when the loading frequency was less than 0.2 Hz.

- The phase angle was used to evaluate the visco-elastic response of the material at the different test temperatures and loading frequencies. The phase angle is the delay that occurs between the applied load and the deformation response. In purely elastic material, there is minimal to no delay and the phase angle is zero degrees. However, in purely viscous materials, there is a much longer delay in the deformation response, with a phase angle theoretically being ninety degrees. Therefore, a material that has stiffening will show a decrease in the phase angle or the ratio between the aged and unaged phase angle will be less than 1.0. Meanwhile, if the material softened, the phase angle will increase, resulting in an aged to unaged phase angle ratio greater than 1.0. At the low test temperature, the average phase angle for all samples tested resulted in an aged to unaged ratio less than 1.0, illustrating age hardening had occurred for this test temperature. Meanwhile, for the high test temperature, the average aged to unaged phase angle ration was greater than 1.0, indicating that the material had undergone age softening at this test temperature.

- Further evaluation of the rutting parameter (G*/sinϕ), which showed an excellent correlation to the Repeated Shear at Constant Height test, indicated that the baseline PG64-22 and the three admixture samples will be more rut susceptible due to the aging process. Both of the PG76-22 samples had an increase in the rutting parameter (i.e. increase in rut resistance). This essentially shows that as the service life of the asphalt pavement increases, so does the potential for rutting due to aging effects.

- Evaluation of the fatigue factor (G*sinϕ) at the low test temperature, showed that the aged samples had an increase in the fatigue factor. According to the Superpave models, this would provide an increase in fatigue resistance.

- The 40°C test temperature showed to be the general area where the age hardening turned over to age softening. This occurred for all samples tested, although at different loading frequencies. The baseline samples did not show this in the G* comparisons, although it was evident in the phase angle comparisons.

- In summary, the aging of the asphalt samples causes both a stiffness increase at low temperatures and a stiffness decrease at high temperatures. This trend was not found in the two PG76-22 samples, which showed an increase in the stiffness at the high temperature.

LTOA Testing – Simple Shear at Constant Height (SSCH)

Simple Shear at Constant Height (SSCH) tests were conducted at 4, 20, and 40°C with the Superpave Shear Tester (SST). The testing was again conducted on samples that had be aged using the Long Term Oven Aging (LTOA) procedure. The parameters used for comparing to the unaged samples were the maximum shear strain, permanent shear strain, and the creep slope.

The results of the SSCH testing of the samples at the different test temperatures are shown as Figures 82, 83, and 84. The basic trend in the aged sample curves is similar to the SSCH curves for the unaged samples.

LTOA Testing – SSCH Parameters (Maximum Shear Strain)

The maximum shear strain is defined as the largest amount of shear strain that was obtained during the entire test time at that particular test temperature. The maximum shear strain was determined for the test temperatures of 4, 20, and 40°C. If age hardening exists, then it would be expected that the maximum shear strain obtained in the aged samples would be less than that obtained for the unaged samples. If age softening exists, then the opposite would hold true.

Figure 85, 86, and 87 shows the comparison of the maximum shear strain for the aged (LTOA) and unaged (STOA) samples. At 4°C, it is obvious that all samples had undergone age hardening since the maximum shear strains of the LTOA samples were less than those of the STOA samples. At the 20°C test temperature, the results of the aged and unaged samples are closer, with a majority of the samples still showing some type age hardening. The Creanova Vestoplast did show age softening at this test temperature. This might be somewhat expected since the Creanova Vestoplast showed the earliest signs of age softening in the FSCH test results. At 40°C, again only the Creanova Vestoplast showed age softening. The most probable reason for the lack of age softening evidence from the SSCH test is that the test temperature may not have been high enough. The FSCH test results at 20°C showed an age hardening with the 40°C test results indicating that a change from hardening to softening was taking place. Eventually the results at 52°C did show that age softening existed. Therefore, the test temperatures associated with the SSCH may not be high enough to determine if age softening occurs when comparing the SSCH maximum shear strain.
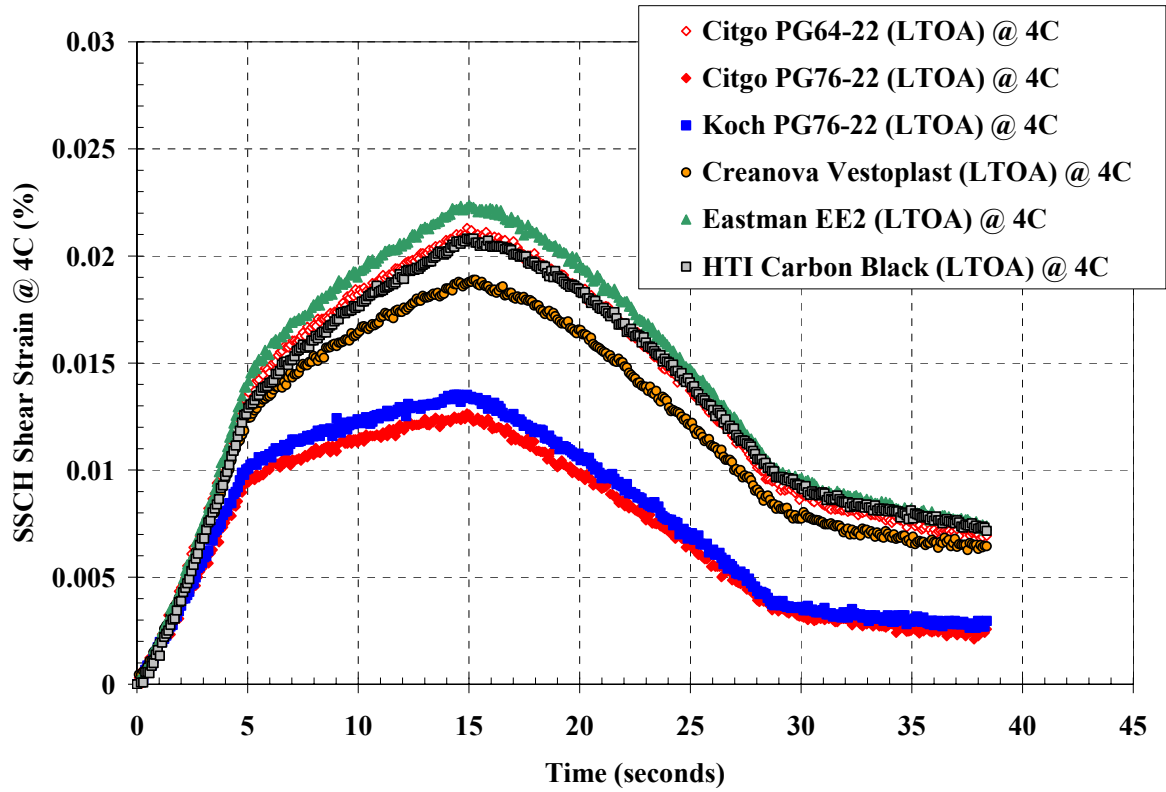
Figure 82 – SSCH Test Curves for the Aged Samples Tested at 4°C
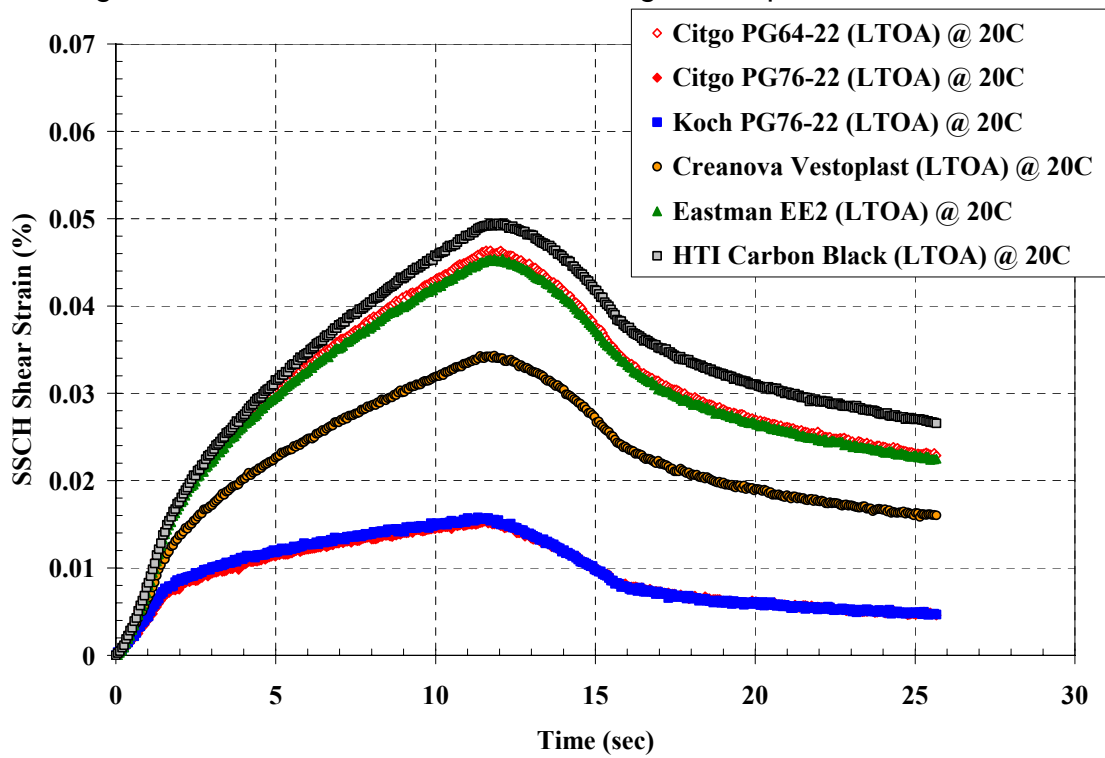
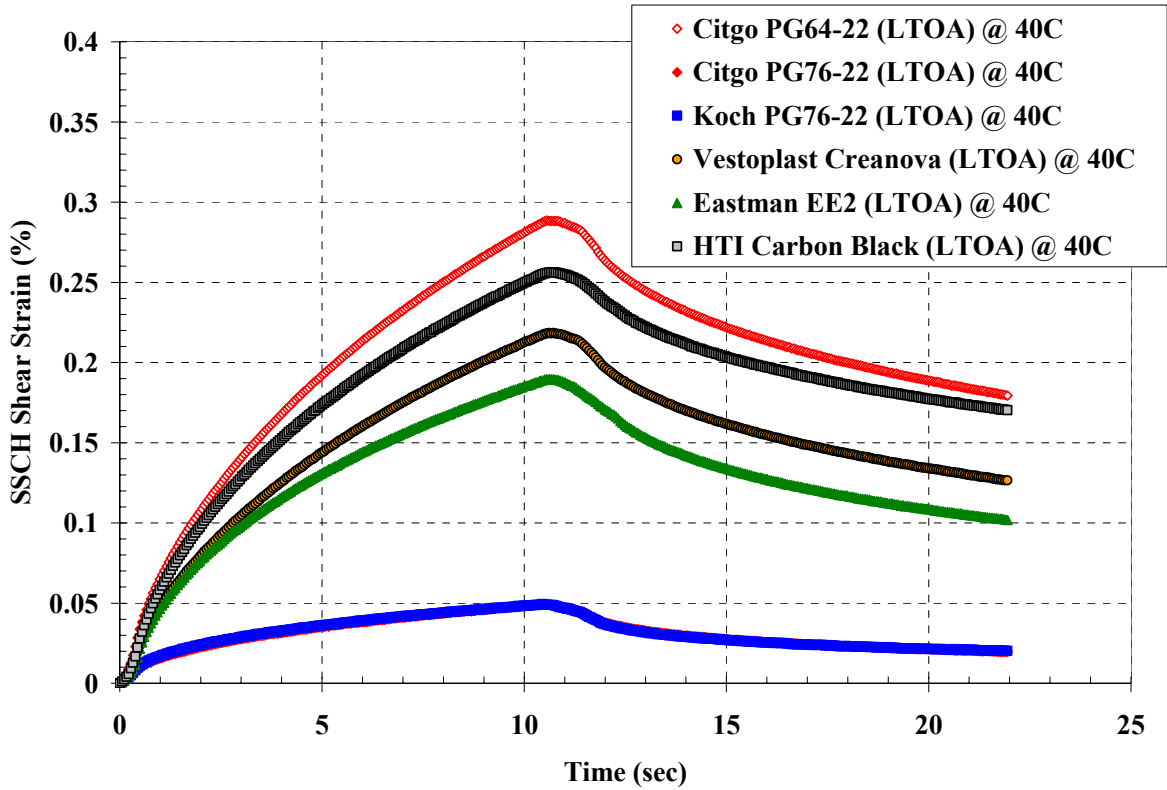Figure 83 – SSCH Test Curves for the Aged Samples Tested at 20°C

107

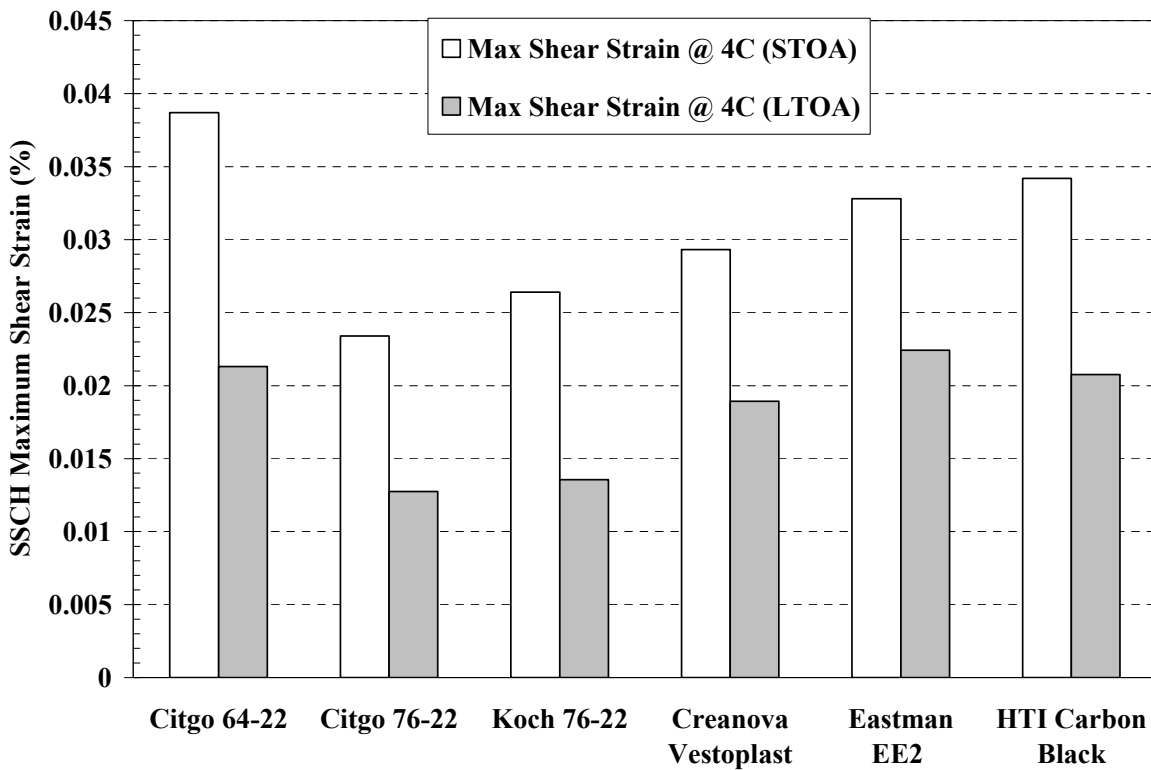Figure 84 – SSCH Test Curves for the Aged Samples Tested at 40°C

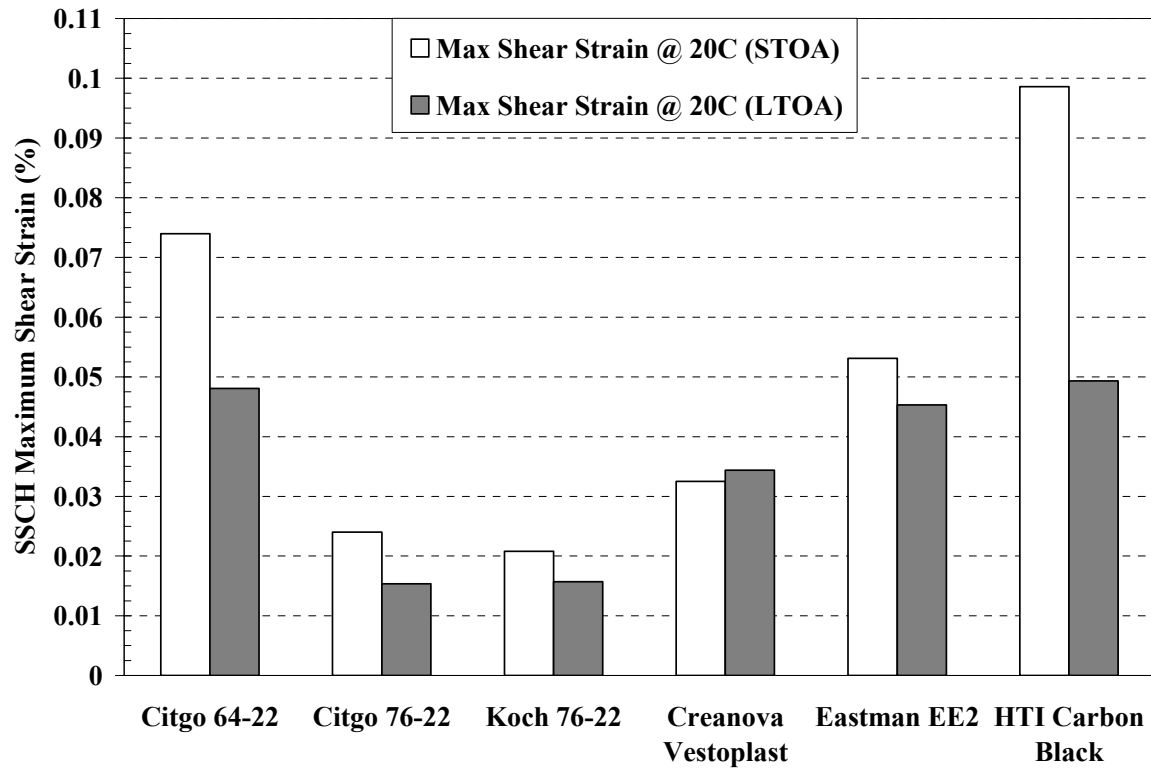Figure 85 – Maximum Shear Strain of Aged and Unaged Samples from SSCH @ 4C

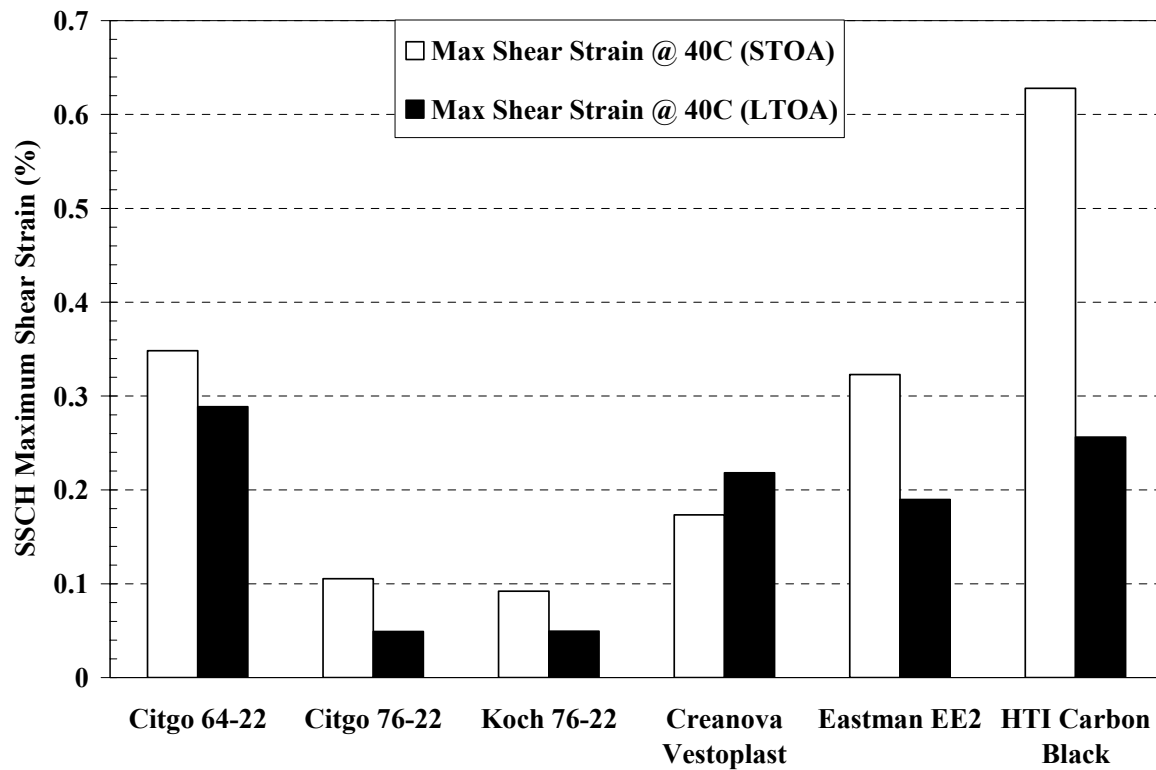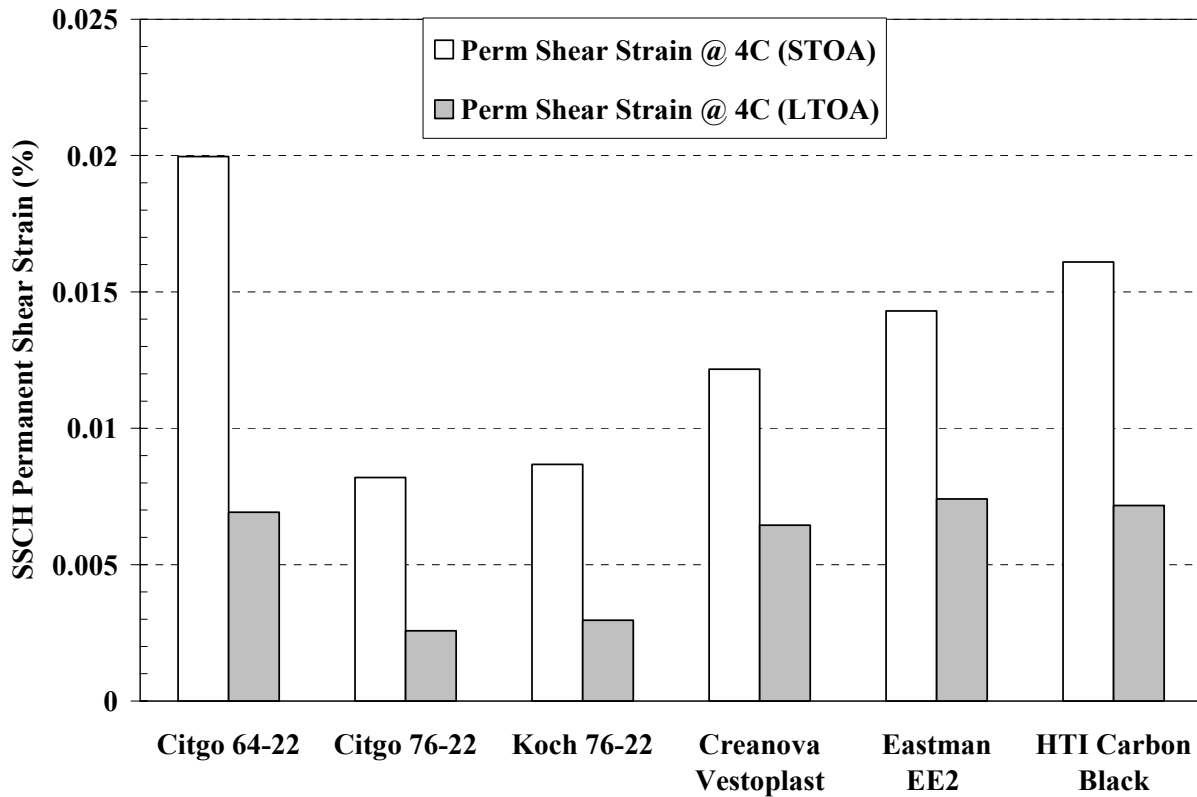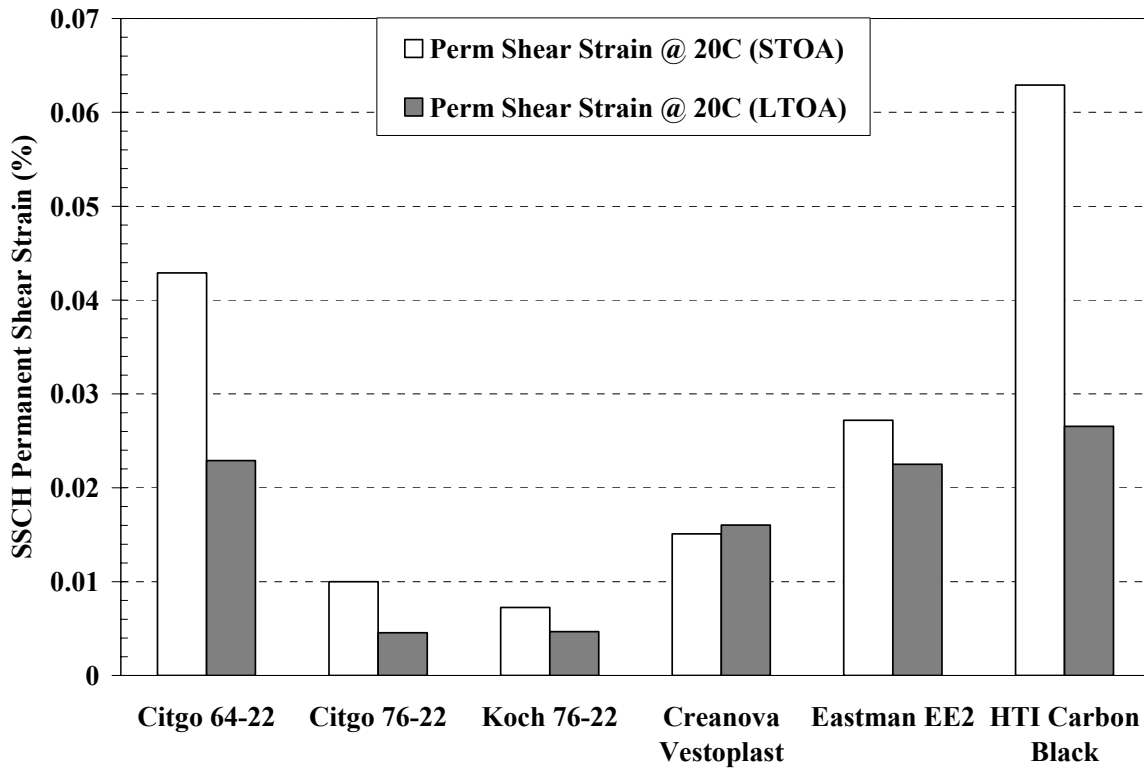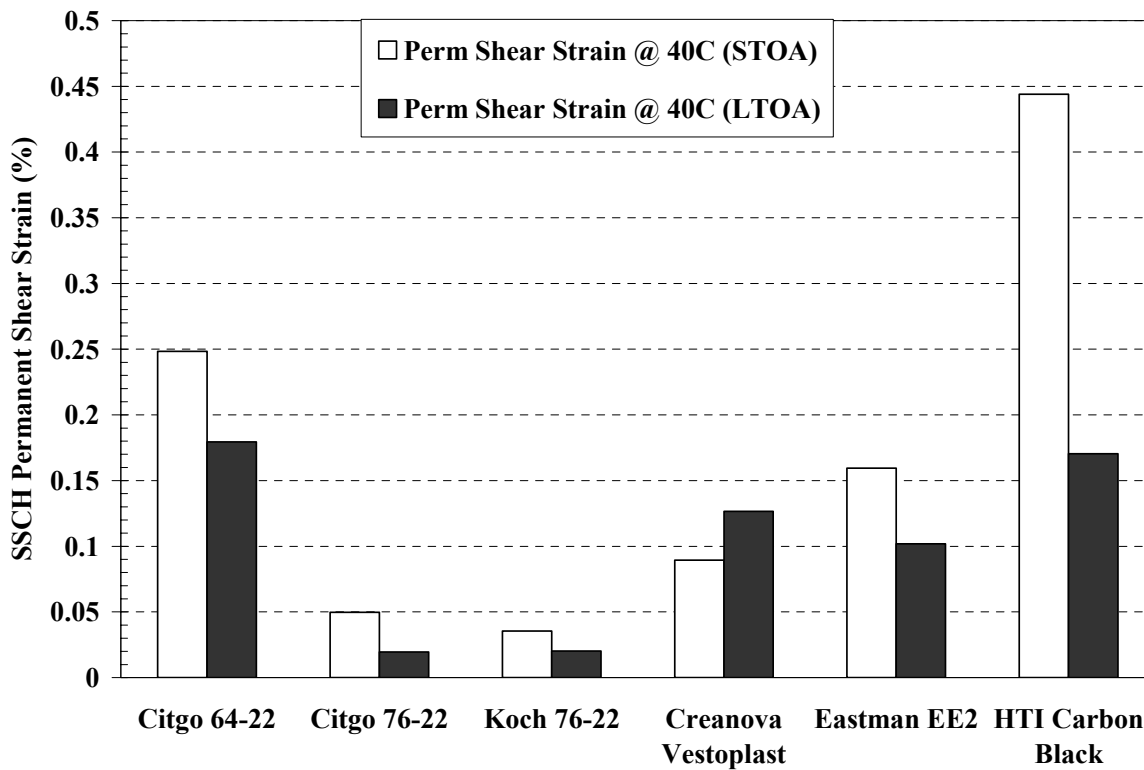Figure 86 – Maximum Shear Strain of Aged and Unaged Samples from SSCH @ 20C

Figure 87 – Maximum Shear Strain of Aged and Unaged Samples from SSCH @ 40C

109

LTOA Testing – SSCH Parameters (Permanent Shear Strain)

The permanent shear strain is defined as the amount of shear strain remaining after the load has been released and the material is allowed to rebound for ten seconds. This parameter provides a means of evaluating the resiliency of the asphalt material. Again, as stated earlier, a lower permanent shear strain is indicative of a stiffer material, and therefore one that has aged. The results each of the test temperatures are shown as Figure 88, 89, and 90.

Figure 88 – Permanent Shear Strain of Aged and Unaged Samples from SSCH @ 4C

Figure 89 – Permanent Shear Strain of Aged and Unaged Samples from SSCH @ 20C

Figure 90 – Permanent Shear Strain of Aged and Unaged Samples from SSCH @ 40C

111

The results from the SSCH testing show that age hardening seems to exist for most of the samples tested. Again, the Creanova Vestoplast material showed to have age softening, with it being more problematic at the higher test temperature (40°C).

LTOA Testing – SSCH Parameters (Creep Slope)

The creep slope is defined as the slope of the shear strain versus time of creep load application, with the creep load being a constant applied load. This parameter is a creep rate parameter that is similar to the creep compliance test used in the Indirect Tensile device. The creep slope was found to have good correlations with the RSCH permanent shear strain, which has been proven to indicate rut potential of HMA. The results of the creep slope determined for both aged and unaged samples are shown in Figures 91, 92, and 93.
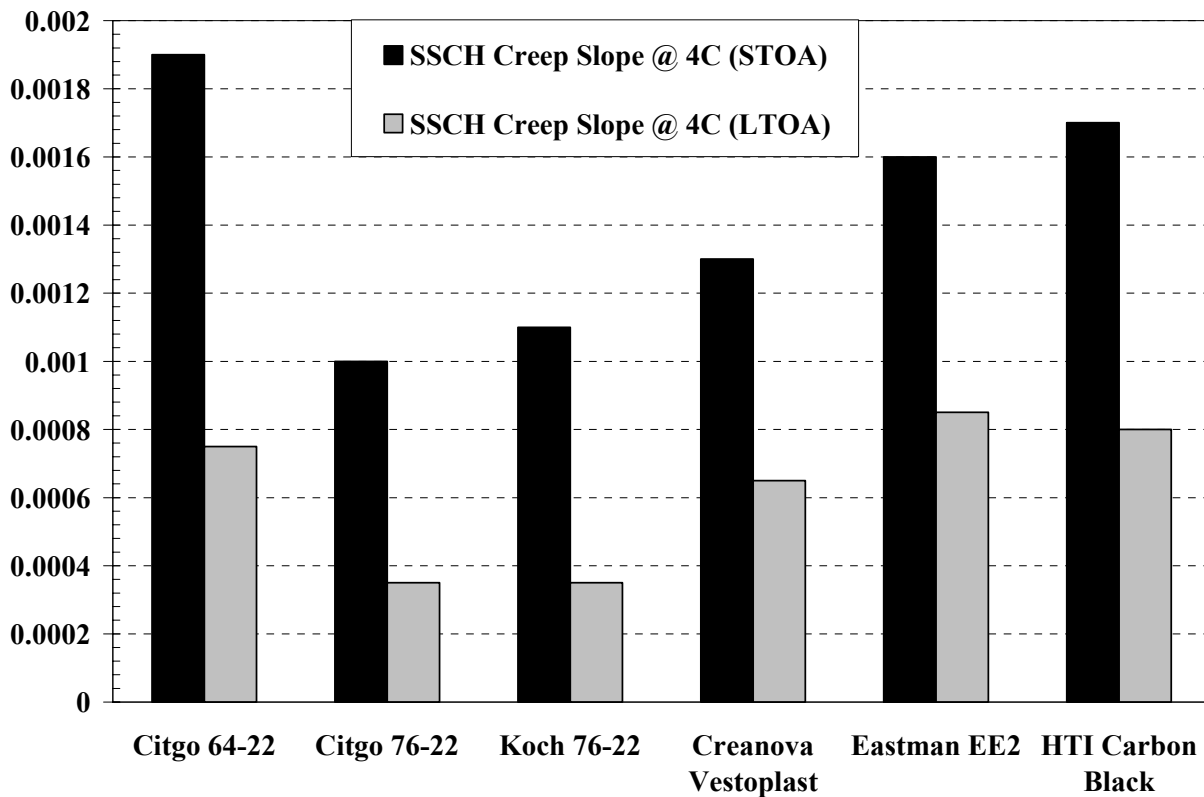
Figure 91 – Creep Slope of Aged and Unaged Samples from SSCH @ 4C

Again, as the other SSCH parameters, the age hardening is evident for all samples at all temperature, except for the Creanova Vestoplast sample. For each of the SSCH parameters, only the Creanova Vestoplast sample showed any signs of age softening.
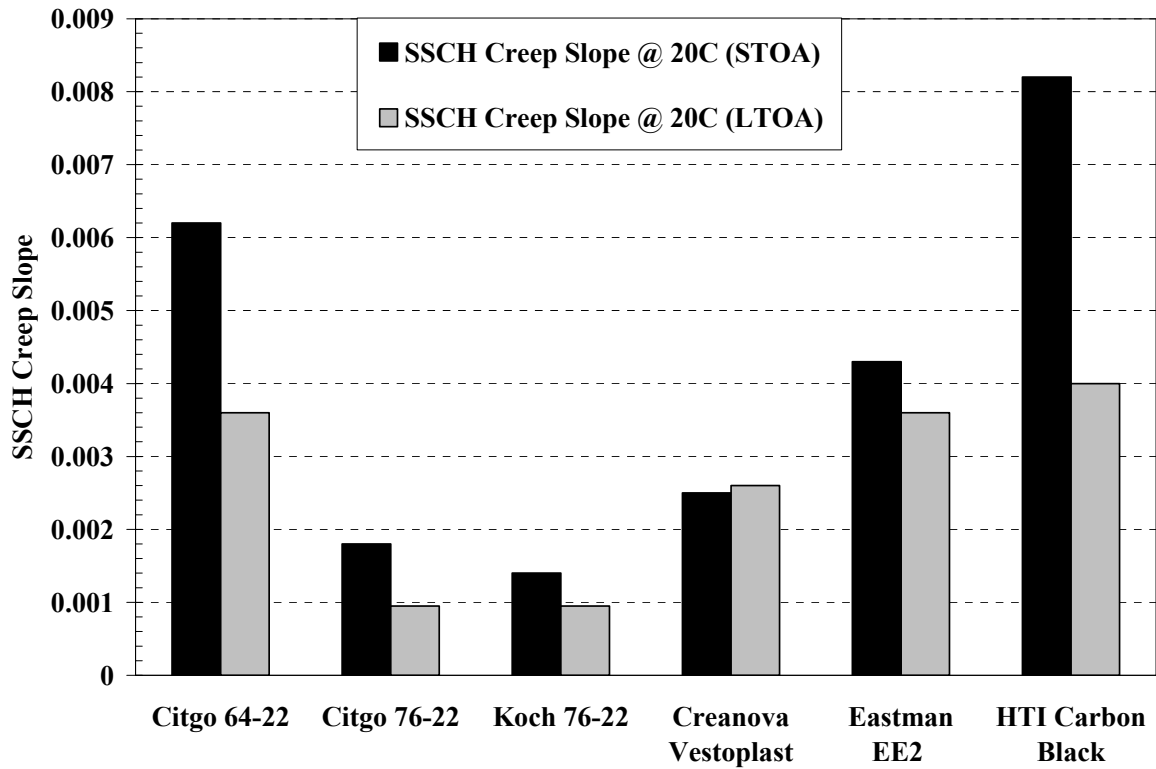
Figure 92 – Creep Slope of Aged and Unaged Samples from SSCH @ 20C
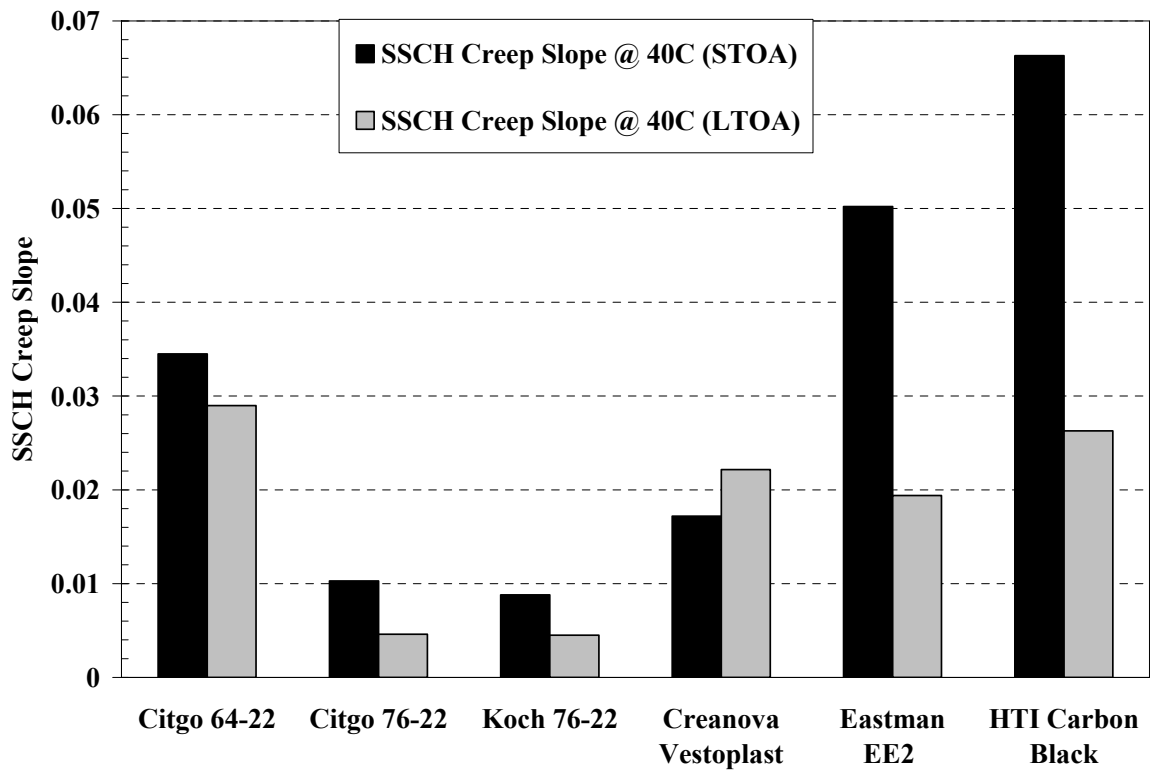
Figure 93 – Creep Slope of Aged and Unaged Samples from SSCH @ 40C

113

Summary of the Affect of Aging on Simple Shear at Constant Height Results

Simple Shear at Constant Height tests were conducted on samples that were aged using the Long Term Oven Aging (LTOA). The SSCH results of the aged samples were compared to the unaged samples. The SSCH parameters used for comparison were the Maximum Shear Strain, Permanent Shear Strain, and the SSCH Creep Slope. A summary of the test results and comparisons are as follows:

- For all test temperatures, the comparisons suggest that the materials underwent an age hardening. This means that the material's creep properties stiffened, which may be problematic for fatigue-type loading applications.
- Only the Creanova Vestoplast sample showed signs of age softening. This occurred at test temperatures of 20 and 40°C.
- The asphalt binder modifier samples stiffened under creep loading at similar, if not less, magnitudes when compared to the currently used PG64-22 and two PG76-22 asphalt binder samples. This suggests that the addition of the modifiers evaluated in the study do not contribute to additional age hardening at low temperatures. The age hardening at low temperatures is more critical than intermediate or high temperatures due to the HMA potential for low temperature fatigue cracking.

LTOA Testing – Repeated Shear at Constant Height (RSCH)

The premise of using the LTOA on the samples was to evaluate how the performance of the various materials could potentially change after years of in-service aging. Traditionally, when asphalt materials undergo aging, the materials stiffen. This was clearly evident in the SSCH creep response of the materials. However, when evaluating the FSCH data, especially at the higher test temperature of 52°C, the materials did not exhibit stiffening when compared to the STOA samples. In fact, the material response could be categorized as age softening. This is highly contradictive to the SSCH response. The age softening would also indicate that as the materials aged, they would be more prone to permanent deformation (rutting). Therefore, it was imperative to evaluate the rutting potential of the LTOA HMA materials at higher test temperatures.

RSCH tests were conducted at 64°C on the LTOA test samples to provide verification of the age softening phenomena that was experienced in the FSCH testing. Unfortunately, the PG64-22 samples were not able to be tested since there were no longer any samples of this type left for testing. All of the test samples were mixed and compacted within the same time frame and it was felt that if this new batch of samples were to be prepared long after the initial samples, natural variability would occur.

The results from the RSCH at 64°C on LTOA samples are shown as Figure 94. The figure clearly indicates that no appreciable increase or decrease in permanent strain was observed when comparing the STOA and the LTOA samples. Statistical analysis also showed no statistical difference between the STOA and LTOA samples.
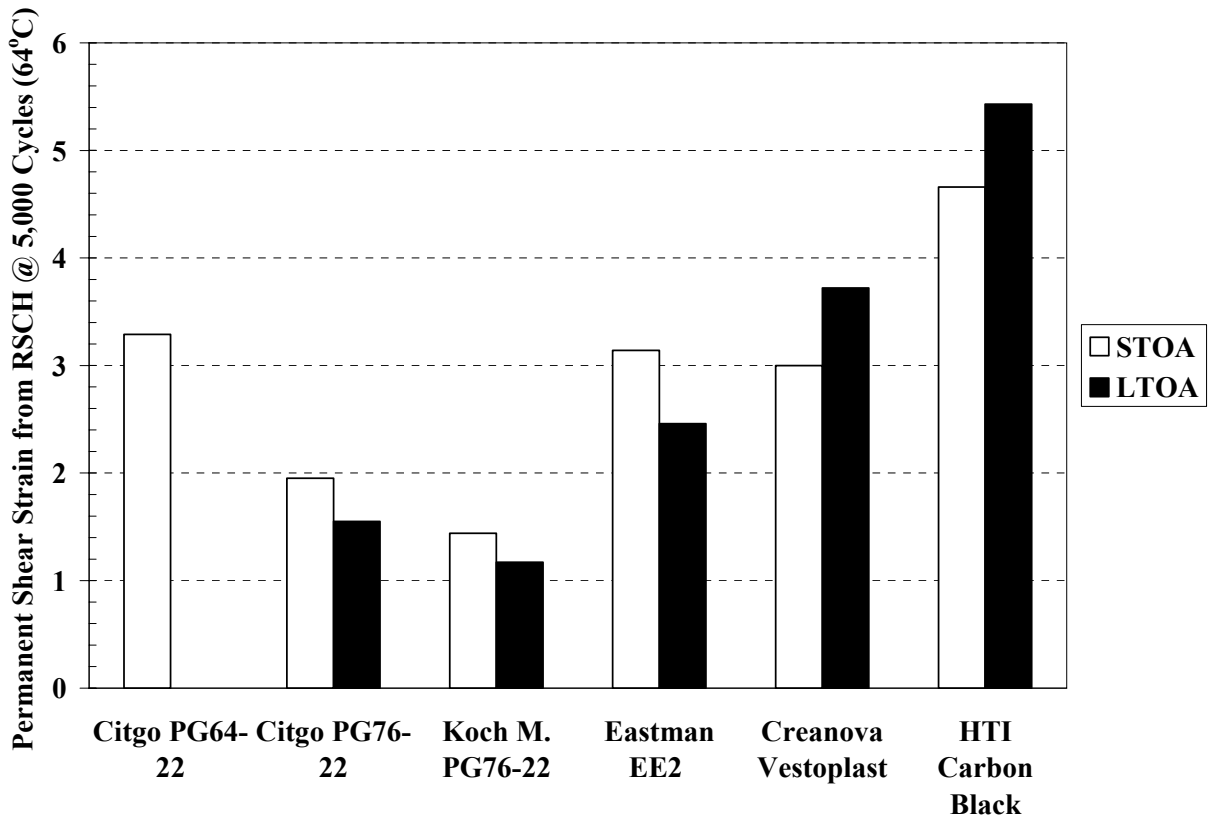
Figure 94 – RSCH Test Results from STOA and LTOA Test Samples

Discussion of LTOA Testing

The test results from the FSCH conducted at 52°C indicated that the material may undergo age softening due to the LTOA procedures. However, this contradicted the SSCH creep results, and eventually the RSCH results. This raised the question of whether or not the results from the FSCH at the 52°C were valid. Four asphalt researchers were contacted to help in this discussion. The researchers are researchers with a great deal of experience in the asphalt community and with the Superpave Shear Tester (SST). The researchers were either contacted via phone or email and their eventual conclusions are summarized below.

Ray Bonaquist (Chief Operating Officer and Lead Researcher at Advanced Asphalt Technologies) – Believed that errors due to FSCH testing at temperatures 52°C and above was the main cause. The FSCH requires 0.01% shear strain and at high test temperatures, this does not relate to large applied stresses. Since a certain amount of load is required to move the shear table, the actual stress measured from the load cell may just be the required movement load due the asphalt mix being soft at these temperatures.

Although this may have some general validity on the overall FSCH measurement at high temperatures, this type of error would have most likely occurred for both the STOA and the LTOA samples.

John Harvey (Professor and Researcher for the University of California at Berkley) – Believed that the decrease in small strain stiffness may be due to the some type of binder/additive separation during oven aging process. He suggested that there may be change in the phases of the binder/additive at the elevated temperatures at prolonged time periods.

Unfortunately, as we further discussed the problem, he also realized that all additives were added to the sample PG64-22 which also exhibited the decrease in stiffness when tested neat. A slight decrease in the stiffness also occurred in the two PG76-22 binder samples, providing additional evidence against the separation theory.

Rebecca McDaniel (Researcher at the Northeast Superpave Center) – Unfortunately Dr. McDaniel had little experience on FSCH testing of aged samples, especially at elevated temperatures. She graciously arranged further discussions with Terhi Pellinen. Dr. McDaniel did suggest to try to extract the binder from the samples and conduct binder testing to evaluate it characteristics.

Terhi Pellinen (Assistant Professor at Purdue University) – After reviewing a summary of the data, Dr. Pellinen was convinced that the material stiffness does soften due to the aging. However, she believes that it is more due to the development of micro-cracks within the HMA, than actual softening. The FSCH is conducted at low shear strains (0.01%), which for a 50 mm thick sample correlates to 0.005 mm of shear deformation. What may be occurring is that a portion of the 0.005 mm is actually taken up by the closing of the micro-cracks. Therefore, less stress is needed to deform the sample 0.01% which results in a lower G*. As opposed to the SSCH and RSCH, which when compared to the FSCH, are larger strain tests, although both are conducted in a stress-controlled environment. The SSCH, when tested at 40°C, may achieve maximum shear strains of 0.1 to 0.6%, which relates to 0.05 to 0.3 mm in deformation, over 10 times larger than the FSCH. This larger strain may overcome the influence of the micro-crack, and therefore, may not be witnessed during the SSCH creep testing. The strain levels are even higher for the RSCH test procedure.

Based on the discussions and further review of the data, the theory of Dr. Pellinen seems to provide a reasonable explanation for the difference in results. Further research may be warranted to examine whether the LTOA process properly models the field aging of the HMA.

FINAL CRITERIA/METHODOLOGY FOR MODIFIER EVALUATION

The final criteria/methodology for the evaluation of asphalt modifiers is based on testing the asphalt mix with the Superpave Shear Tester (SST). The SST provides a means of evaluating both the fundamental properties (creep and shear stiffness), as well as being used in more of a simulative mode (repetitive shear loading). Two types of testing procedures were developed for the future analysis of the addition of asphalt binder modifiers in HMA. The two procedures are termed the "Quick Procedure" and the "Standard Procedure".

The development of the test procedures is based on the statistical evaluation of the test data. The main criteria for selection was that the test method/test parameter must be able to statistically differentiate between the various materials.

"Quick Procedure"

The "Quick Procedure" would be used when concerns for age hardening of the HMA is not an issue. This would occur if the NJDOT would like to rank two or three asphalt modifiers that they have used in the past with some success. A more formal test procedure is located in the Appendix.

A total number of 6 samples are needed for the analysis. Three of the samples are used for a baseline comparison. The first set of three samples has the identical binder to be used with the additive. The remaining set of three samples contains the asphalt binder modifier for evaluation.

In the "Quick Procedure", only uses two test temperatures. At the first test temperature of $40^{o}C$, the samples are tested first under the FSCH test mode to determine the Rutting Parameter ($G^{*}/\sin\phi$). Immediately after the FSCH test, the same sample is tested under the SSCH test mode. In particular, the maximum shear strain and the creep slope, both at $40^{o}C$, are used for comparisons.

Once these two tests have finished at $40^{o}C$, the test chamber is increased to $64^{o}C$. Once the samples have reached equilibrium, a RSCH test is conducted to 5,000 loading cycles. The permanent shear strain at after 5,000 loading cycles is used for comparison.

This procedure provides two important modes of HMA testing; simulative loading and fundamental loading. The simulative loading is defined as a test that loads the HMA in a manner that is similar to field conditions. This is conducted using the RSCH mode. The fundamental loading is defined as a test that loads the HMA in a manner to determine fundamental properties of the HMA. This is conducted using the FSCH and SSCH test modes.

Once the samples have been compacted and cut, the testing procedure should take only two days to complete.

"Full Test Procedure"

The "Full Test Procedure" uses a total of 18 samples. Six of the samples are used for a baseline comparison. The first set of three samples has the identical binder to be used with the additive, while the second set of three samples contains the binder properties desired. The third set of three samples contains the asphalt binder modifier for evaluation. The testing protocols are similar to the identical to the "Quick Procedure", however, unlike the "Quick Procedure", this test procedure also evaluates the material for age hardening. Therefore, the remaining 9 samples are LTOA for 5 days at 85°C.

The first temperature of 4°C is used to conduct SSCH testing to determine the maximum shear strain and creep slope. It is not recommended to conduct FSCH testing at this test temperature due to problems associated with the equipment being able to reach the desired strain at high testing frequencies. Once the 4°C testing has been conducted, the chamber and samples are allowed to reach 40°C overnight.

After the chamber and samples has equalized at 40°C, again the samples are tested under the FSCH test mode to determine the Rutting Parameter. Immediately after the FSCH, the sample is tested under the SSCH test mode to evaluate the maximum shear strain and the creep slope. After all testing at 40°C has completed, the test chamber is allowed to heat up to 64°C.

Once the test chamber equalizes, the RSCH test mode is conducted on the samples at 64°C. The samples are tested until 5,000 loading cycles. The permanent shear strain recorded after 5,000 loading cycles is used for comparisons.

After the RSCH testing has completed, the SSCH at 4°C needs to be conducted to evaluate the age hardening potential at low temperatures. The maximum shear strain and the creep slope are used for this comparison.

Once the samples have been compacted and cut, this testing procedure should take approximately six to seven days to complete.

CONCLUSIONS

The main goal of the research project was to develop a testing procedure to evaluate the performance of HMA when an asphalt modifier has been added. In doing so, a number of different performance tests, testing configurations, and test parameters were evaluated. Based on this, the following conclusions can be made:

- The ranking of mixtures from the FSCH testing matches that of the "true" performance grading conducted on the asphalt binder additives added to the PG64-22 asphalt binder. This is a similar finding to those found in the literature (Williams et al., 1998; Harvey et al., 1998).
- APA testing should be conducted using gyratory pill samples, instead of the vibratory bricks. Based on the statistical analysis conducted on both sets of results, the APA can distinguish sample characteristics, in this case asphalt binder stiffness, better when using gyratory pills than vibratory bricks. This is most likely due to the higher variability associated with the vibratory brick samples versus the gyratory pills. The vibratory bricks had an average standard deviation of 0.68, while the gyratory pills had an average standard deviation of 0.25.
- It is extremely important to evaluate both fundamental and simulative property responses of HMA. The fundamental properties, such as creep and small strain stiffness, more closely represent the binder properties, while the simulative properties, such as the resistance to repeated shear loading, is more representative of the entire asphalt mix. An example of the value of using both simulative and fundamental is the carbon black material. The small strain stiffness measured from the FSCH testing showed the carbon black to have a slightly greater shear modulus than the baseline PG64-22 samples. This corresponds exactly to the binder testing. Meanwhile, when the RSCH testing was conducted, the carbon black material accumulated the largest amount of permanent deformation, even larger than the PG64-22. The contradiction can be explained by the addition of the carbon black "over asphalting" the HMA mix. Since the main idea behind the study was to evaluate binder additives that can be directly added to any pre-determined mix design, separate HMA designs were not conducted. It is most likely the case that the addition of the carbon black created an over-asphalted condition. Therefore, this particular material would need to have a separate mix design conducted for eventual use. However, by simply conducting binder testing, this would never have been discovered.
- Based on the Student t-Test analysis conducted on all of the test data, the APA provided the best method to differentiate between the various binders used. However, as stated earlier, for a proper evaluation, an understanding of both the simulative, such as the APA, and the fundamental material response is essential. The next best test method/test parameter to differentiate the different binders was the maximum shear strain and creep slope from the SSCH test.

- The Long Term Oven Aging (LTOA) procedure developed by the SHRP researchers may cause pre-mature micro-cracking in HMA compacted samples. Based on the comparison of data from the FSCH, SSCH, and RSCH test results, along with the recommendation provided by Dr. Terhi Pellinen, the LTOA may induce micro-cracking that only affects the small strain stiffness performance at high test temperatures. Further verification of this phenomena needs to be considered if the LTOA is to be used to simulate field aging of laboratory compacted samples.
- The test response parameters evaluated in the study were compared to one another to evaluate how well each test correlated to one another. In particular, how well the test parameters correlated to the APA rutting and the RSCH permanent strain. This is important for two reasons; 1) Both the RSCH and the APA have been shown to be reliable test methods to rank rut susceptible materials, and 2) Both the RSCH and APA are somewhat time consuming tests (approximately 1.5 hours for the RSCH and the 3.5 hours for the APA). Therefore, if a quicker test can be conducted that correlated well with either the APA or RSCH, it has the potential for future use under time limited projects. The test parameters that correlated the best ($R^2 > 0.9$) were as follows:
  - FSCH m-slope @ 40°C to the APA Gyratory ($R^2 = 0.98$)
  - SSCH Creep Slope @ 40°C to the RSCH @ 52°C ($R^2 = 0.98$)
  - SSCH Permanent Shear Strain @ 40°C to the RSCH @ 64°C ($R^2 = 0.93$)
  - FSCH Rutting Parameter @ 52°C to the RSCH @ 64°C ($R^2 = 0.93$)
  - SSCH Maximum Shear Strain @ 40°C to the RSCH @ 64°C ($R^2 = 0.92$)

RECOMMENDATIONS

The following recommendations are made based on the work and analysis conducted within this study:

- To evaluate the true effects of an asphalt modifier, both simulative and fundamental testing needs to be conducted, especially if the modifier is to be used as a direct add-in to an existing mix design. This was clearly shown in the laboratory when comparing the FSCH and RSCH test results. Therefore, it is recommended that the NJDOT use either the "Quick Procedure" or the "Full Test Procedure" to evaluate HMA mixes that contain asphalt modifiers. For materials which the NJDOT has no prior experience with, it is recommended that the "Full Test Procedure" be used since it also incorporates a means of evaluating the detrimental effects of age hardening.
- The procedure developed from this study provides an excellent means of ranking HMA mixes based on rutting susceptibility. However, this was solely conducted under laboratory conditions. It is recommended that the NJDOT evaluate using some existing asphalt modifiers, especially the Creanova Vestoplast and the Eastman EE-2 in a trial field study. Laboratory testing can be conducted and correlated to the field performance of the placed mixes, providing the NJDOT with additional verification of the testing procedures developed within this study.

REFERENCES

American Association of State Highway and Transportation Officials (AASHTO), Test Method for Determining the Permanent Shear Strain and Stiffness of Asphalt Mixtures Using the Superpave Shear Tester (SST), AASHTO TP7-01, AASHTO Provisional Standards, pp. 146 – 156.

Anderson, R.M. and McGennis, R.B., 1998, *Ruggedness Evaluation of AASHTO TP7 and TP9, Phase I: Simple Shear Test at Constant Height (TP7) and Indirect Tensile Strength Test (TP9),* Federal Highway Administration National Asphalt Training Center II, Task J, 44 pp.

Anderson, R.M., Huber, G.A., Stegar, R.K., and Romero, P., 2003, "Precision of Shear Tests Used for Evaluating Asphalt Mixtures.", Presented at the 82nd Annual Meeting of the Transportation Research Board, Washington, D.C.

APA User's Group Meeting Minutes. Jackson, Mississippi. September 26-27, 2000.

Bell, C., Wieder, A., and Fellin, M., *Laboratory Aging of Asphalt-Aggregate Mixtures: Field Validation.* SHRP-A-390, Strategic Highway Research Program Report, National Research Council, Washington D.C., 1994.

Bennert, T., Maher, A., and Walker, L., 2001, "Evaluation of a Rutting/Fatigue Cracking Device.", FHWA-NJ-2001-031, New Jersey Department of Transportation, 81 pp.

Brown, E.R. and Cross, S.A., 1989, "A Study of In-Place Rutting of Asphalt Pavements.", Asphalt Paving Technology, Association of Asphalt Paving Technologists, Volume 58, pp. 1 – 39.

Brown, E., Kandhal, P., and Zhang, J., 2001, "Performance Testing for Hot Mix Asphalt.", NCAT Report No. 2001-05, 72 pp.

Buncher, M., Peterson, R., Walker, D., Turner, P., and Anderson, M., 2000, "Laboratory Process for Comprehensive Evaluation of Mixture Properties.", Paper Submitted for Presentation at the 2000 Transportation Research Board Annual Meeting.

Collins, R., Watson, D., and Campbell, B., 1995, "Development and Use of Georgia Loaded Wheel Tester.", Transportation Research Record 1492, Transportation Research Board, pp. 202 – 207.

Eisenmann, J. and Hilmer, A., 1987, Influence of Wheel Load and Inflation Pressure on the Rutting Effect at Asphalt-Pavements – Experiments and Theoretical Investigations.", Proceedings of the Sixth International Conference on the Structural Design of Asphalt Pavements, Volume I, pp. 392 – 403.

Hanson, D., Mallick, R., and Brown, R., 1994, "Five Year Evaluation of HMA Properties

at the AAMAS Tests.", National Center for Asphalt Technology, Paper No. 94-0360, Auburn University.

Harvey, J., Lee, T., Sousa, J.B., Pak, J., and Monismith, C.L., 1994, "Evaluation of Fatigue Stiffness and Permanent Deformation Properties of Several Modified and Conventional Field Mixes Using SHRP-A-003A Equipment.", Paper Accepted and Presented at the TRB 1994 Annual Meeting.

Harvey, J., I. Guada, and F. Long, 1999, "Effect of Material Properties, Specimen Geometry, and Specimen Preparation Variables on Asphalt Concrete Tests for Rutting.", A Final Report for the Federal Highway Administration, Office of Technology Applications, Washington, D.C., 84 pp.

Hofstra, A., and Klomp, A.J., 1972, "Permanent Deformation of Flexible Pavements Under Simulated Road Traffic Conditions.", Proceedings of the Third International Conference on the Structural Design of Asphalt Pavements, Volume I, pp. 613 – 621.

Kandhal, P. and Cooley, L., 2002, "Evaluation of Permanent Deformation of Asphalt Mixtures Using Loaded Wheel Tester.", NCAT Report No. 2002-08, 13 pp.

Monismith, C.L., Harvey, J.T., Long, F., and Weissman, S., 2000, "Tests to Evaluate the Stiffness Permanent Deformation Characteristics of Asphalt/Binder-Aggregate Mixes.", Technical Memorandum: TM-UCB PRC-2000-1, 86 pp.

Nazarian, 2002, Personal Communication.

Nazarian, S. and Feliberti, M., 1993, "Methodology for Resilient Modulus Testing of Cohesionless Subgrades.", In *Transportation Research Record 1406,* TRB, National Research Council, Washington, D.C., pp. 108 – 115.

Pellinen, T., 2001, Investigation on the Use of Dynamic Modulus as an Indicator of Hot-Mix Asphalt Performance", A Dissertation Presented in Partial Fulfillment of the Requirements for the Degree Doctor of Philosophy, Arizona State University, 804 pp.

Sousa, J.B., Soliamanian, M., and Weissman, S.L., 1994, "Development and Use of the Repeated Shear Test (Constant Height): An Optional Superpave Mix Design Tool.", SHRP-A-698, Strategic Highway Research Program, National Research Council.

Stokoe, K.H., Kim, D.S., and Andres, R., 1990, "Development of Synthetic Specimens for Calibration and Evaluation of MR Equipment.", Presented at the 69th Annual Meeting of the Transportation Research Board, Washington, D.C.

Wambura, J., Maina, J., and Smith, H., 1999, "Kenya Asphaltic Materials Study.",

Submitted for Presentation at the 78th Annual Transportation Research Board, Washington D.C.

Williams, C. and Prowell, B., 1999, "Comparison of Laboratory Wheel-Tracking Test Results to WesTrack Performance.", Presented at the 78th Annual Meeting of the Transportation Research Board, Washington, D.C.

Williams, R.C., P. Romero, and K.D. Stuart, 1998, "Comparison of Superpave Shear Test Results to WesTrack Performance.", Submitted to the ASTM Journal of Materials Testing.

Witzcak, M.W., Bonaquist, R., Von Quintus, H., and Kaloush, K., 2000, "Specimen Geometry and Aggregate Size Effects in Uniaxial Compression and Constant Height Shear Tests.", Asphalt Paving Technology, Association of Asphalt Paving Technologists, Volume 69.

APPENDIX A – SUPERPAVE DESIGN

		Max. Theoretical Specific Gravity (Gmm) Worksheet		

	5.0 % AC	4.7 % AC	4.5 % AC	Blend 4
User-Supplied Average Gmm:	2.683	2.720	2.720	
Gmm Used in Calculations:	2.683	2.720	2.720	0.000

Methods:
AASHTO: T 209-90
ASTM: D2041-91

		Bulk Specific Gravity (Gmb) Worksheet		

	5.0 % AC			4.7 % AC			4.5 % AC			Blend 4	
	Specimen 1	Specimen 2	Specimen 3	Specimen 1	Specimen 2	Specimen 3	Specimen 1	Specimen 2	Specimen 3	Specimen 1	Specimen 2
Specimen Weight in Air:	5050.3	5089.5	5080.5	5104.5	5156.0	5134.0	5106.8	5148.9	5161.1		
Specimen Weight in Water:	3132.7	3171.5	3161.3	3169.5	3189.7	3171.3	3172.1	3187.7	3189.9		
SSD Weight in Air:	5053.8	5093.1	5086.2	5112.8	5167.5	5141.0	5119.6	5158.8	5177.9		
Gmb @ Nmax (from mass):	2.629	2.649	2.639	2.627	2.607	2.606	2.622	2.612	2.596		
Gmm (average):	2.683	2.683	2.683	2.720	2.720	2.720	2.720	2.720	2.720	0.000	0.000
%Gmm @ Nmax (corrected):	97.98%	98.72%	98.37%	96.57%	95.84%	95.83%	96.41%	96.04%	95.45%	#VALUE!	#VALUE!
%Air Voids @ Nmax (corrected):	2.018	1.283	1.627	3.430	4.157	4.173	3.594	3.963	4.554	#VALUE!	#VALUE!
Gmb @ Nmax (from Height):	2.577	2.595	2.581	2.570	2.553	2.560	2.566	2.565	2.549	#VALUE!	#VALUE!

Methods:
AASHTO: T 166-88
ASTM: D2726-93

		Trial Asphalt Binder Content (%AC) Worksheet		

	5.0 % AC	4.7 % AC	4.5 % AC	Blend 4
Aggregate Bulk Specific Gravity (Gsb):	2.927	2.927	2.927	
Percent Binder by wt. of mix (Pbi):	5.0	4.7	4.5	
Percent Aggregate (Ps):	95.0	95.3	95.5	

124

Dust Proportion (Fines/Pbe) Worksheet

	Inputs			
	5.0 % AC	4.7 % AC	4.5 % AC	Blend 4
Specific Gravity of Binder(Gb):	**1.030**	**1.030**	**1.030**	
Fines (% Passing .075mm Sieve)	**5.1**	**5.1**	**5.1**	

	Outputs			
Absorbed binder: % by wt. of aggregate (Pba)	**0.042**	**0.386**	**0.250**	#N/A
Absorbed binder: % by total wt. of mixture (Pba')	**0.040**	**0.368**	**0.238**	#N/A
Percent AC (Pbi)	**5.0**	**4.7**	**4.5**	#N/A
Effective Specific Gravity (Gse)	**2.931**	**2.959**	**2.948**	#N/A
Effective % Binder (Pbe)	**4.960**	**4.332**	**4.262**	#N/A

Dust Proportion (Fines/Pbe)	**1.0**	**1.2**	**1.2**	

Project Name: Sample Project with Data		**N Initial:** 7	
Workbook Name: Sample Mix Design - AC%.xls		**N Design:** 75	
Technician: EJK		**N Max:** 115	
Date: 7/25/00		**Nom. Sieve Size:** 12.5mm	
Asphalt Grade: PG64-22		**Design Temperature:** 200°C	
Compaction Temp: 180°C		**Design ESAL's (millions):** .3	

Blend	%AC	%Gmm @ N = 7 (corrected)	%Gmm @ N = 75 (corrected)	%Gmm @ N = 115 (corrected)	%Air Voids @ NDesign	%VMA @ NDesign
5.0 % AC	5.0	87.7	97.1	98.4	2.9	15.5
4.7 % AC	4.7	85.7	94.7	96.1	5.3	16.1
4.5 % AC	4.5	85.6	94.6	96.0	5.4	16.0
Blend 4						

Blend	Estimated %AC @ 4% Va	%Gmm @ N = 7 (90.5% Max)	Estimated %Gmm @ N = 75 (96% Max)	Estimated %Gmm @ N = 115 (98% Max)	Estimated %VMA @ NDesign (14 % Min)	%VFA @ NDesign (65% - 78%)
5.0 % AC	4.6	86.6	96.0	97.3	15.6	74.3
4.7 % AC	5.2	87.1	96.0	97.4	15.9	74.8
4.5 % AC	5.0	87.0	96.0	97.3	15.7	74.6
Blend 4						

	5.0 % AC	4.7 % AC	4.5 % AC	Blend 4
Ag. Bulk Specific Gravity (Gsb):	2.927	2.927	2.927	
Percent Binder by wt. of mix (Pbi):	5.0	4.7	4.5	
Percent Aggregate (Ps):	95.0	95.3	95.5	
Specific Gravity of Binder (Gb):	1.030	1.030	1.030	
Fines (%Passing 0.075mm Sieve):	5.1	5.1	5.1	
Effective Specific Gravity (Gse):	2.931	2.959	2.948	
Effective % Binder (Pbe):	5.0	4.3	4.3	
Dust Proportion (0.6-1.2%):	1.0	1.2	1.2	

Project Name:	Sample Project with Data	N Initial:	7
Workbook Name:	Sample Mix Design - AC%.xls	N Design:	75
Technician:	EJK	N Max:	115
Date:	7/25/00	Nom. Sieve Size:	12.5mm
Asphalt Grade:	PG64-22	Design Temperature:	200°C
Compaction Temp:	180°C	Design ESAL's (millions):	.3

%Gmm vs. Gyrations

%Air Voids vs. %Binder

%VMA vs. %Binder @NDes

%VFA vs. %Binder @NDes

Blend	Y %AC	Air Voids @ NMax	X Air Voids @ NDesign	%VMA NDesign	%VFA @ NDesign
5.0 % AC	5.0	1.6	2.9	15.5	81.1
4.7 % AC	4.7	3.9	5.3	16.1	67.1
4.5 % AC	4.5	4.0	5.4	16.0	66.5
Blend 4	#N/A				

126

Project Name:	Sample Project with Data		N Initial:	7
Workbook Name:	Sample Mix Design - AC%.xls		N Design:	75
Technician:	EJK		N Max:	115
Date:	7/25/00			
Asphalt Grade:	PG64-22		Design Temperature:	200°C
Compaction Temp:	180°C		Design ESAL's (millions):	.3

%Gmm @ Nini

%Gmm @ Nmax

Density

Dust/Asphalt Ratio

Blend	%AC	%Gmm @ NInitial	%Gmm @ Nmax	Unit Wt. (kg/m^3) NDesign	Dust/Asph Ratio
5.0 % AC	5.0	87.7	98.4	2605	1.0
4.7 % AC	4.7	85.7	96.1	2576	1.2
4.5 % AC	4.5	85.6	96.0	2574	1.2
Blend 4	#N/A				

Mixture Summary Report for Varying %AC Analysis

Project Name:	Sample Project with Data	**N Initial:**	7
Workbook Name:	Sample Mix Design - AC%.xls	**N Design:**	75
Technician:	EJK	**N Max:**	115
Date:	7/25/00	**Nom. Sieve Size:**	12.5 mm
Asphalt Grade:	PG64-22	**Compaction Temperature:**	180 °C
		Mixture Temperature:	200°C
Design ESAL's (millions):	.3	**Depth from Surface (mm):**	30 mm
Design Temperature:	200°C	**Mold Size:**	150 mm

Property	Results				Criteria
	5.0 % AC	4.7 % AC	4.5 % AC	Blend 4	
%AC	5.0	4.7	4.5		
%Air Voids (V_a)	2.9	5.3	5.4		4.0 %
%VMA	15.5	16.1	16.0		14.0 % Min.
%VFA	81.1	67.1	66.5		65.0 % Min.
					78.0 % Max.
Dust/Asphalt Ratio	1.0	1.2	1.2		0.6 - 1.2 %
Max. Specific Gravity (G_{mm})	2.683	2.720	2.720	0.000	
Bulk Specific Gravity (G_{mb})	2.639	2.613	2.610		
%G_{mm} @ N_{ini}	87.7	85.7	85.6		90.5 % Max.
%G_{mm} @ N_{des}	97.1	94.7	94.6		96.0 % Max.
%G_{mm} @ N_{max}	98.4	96.1	96.0		98.0 % Max.
Effective Sp. Gravity of Blend (G_{se})	2.931	2.959	2.948		---
Sp. Gravity of Binder (G_b)	1.030	1.030	1.030		---
Sp. Gravity of Aggregate (Gs_b)	2.927	2.927	2.927		---

128

APPENDIX B – REPEATED SHEAR AT CONSTANT HEIGHT (RSCH) TEST RESULTS

Appendix B.1 – RSCH Results for Citgo PG64-22
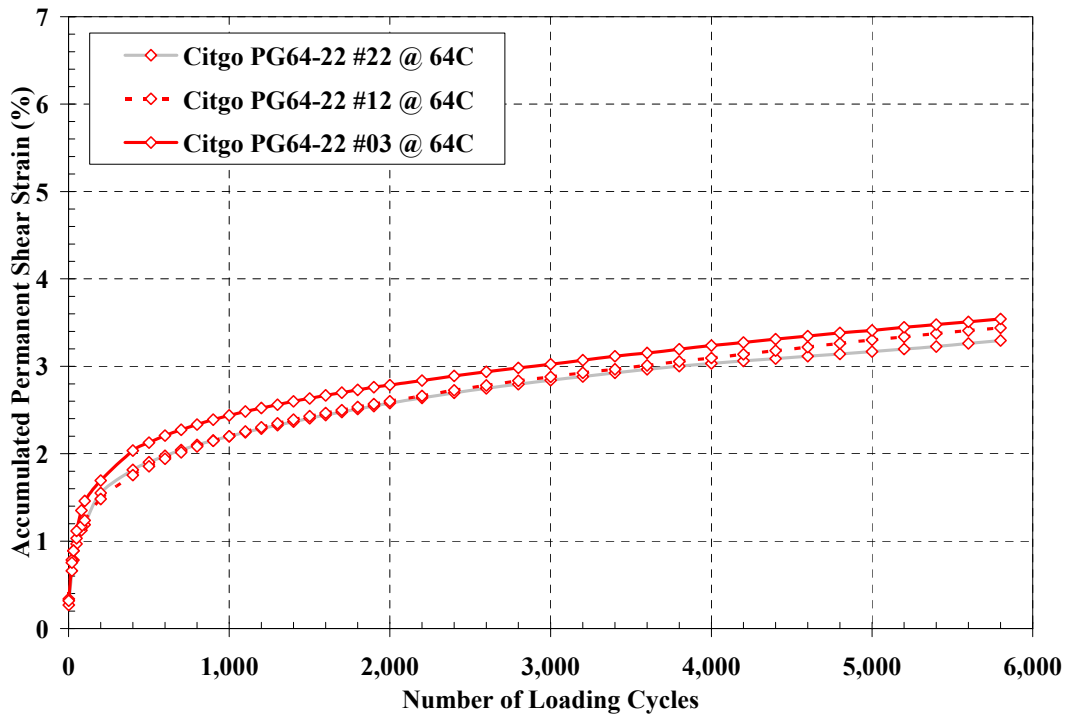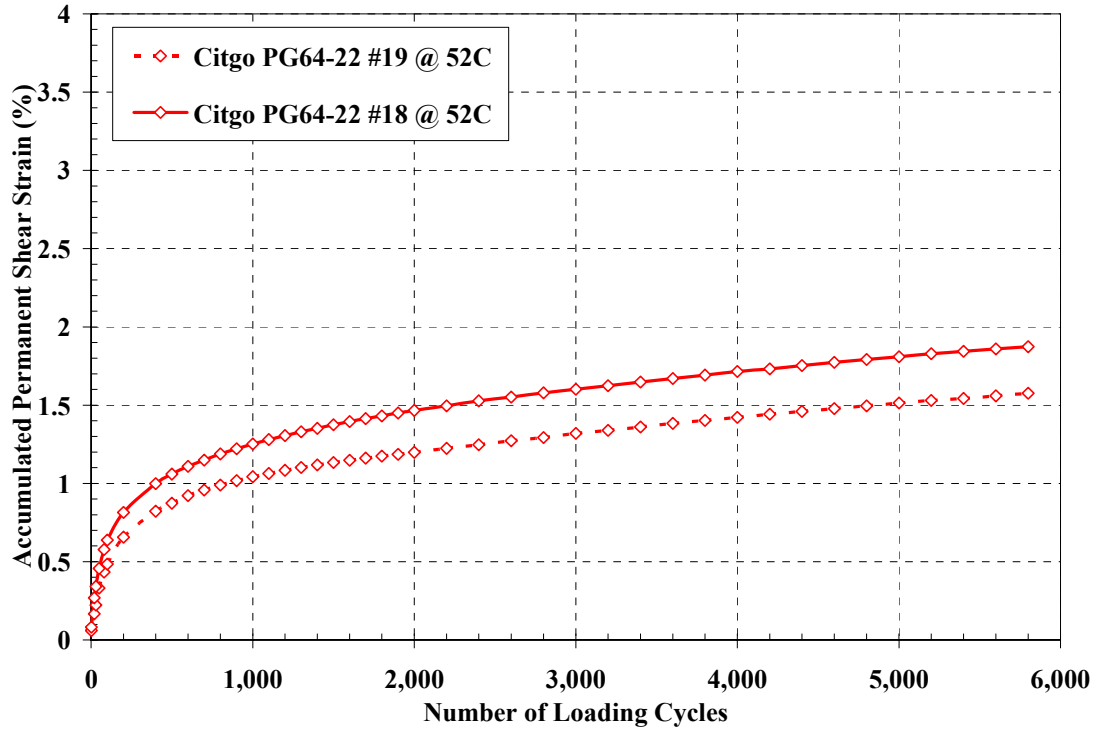
Appendix B.2 – RSCH Results for Citgo PG76-22
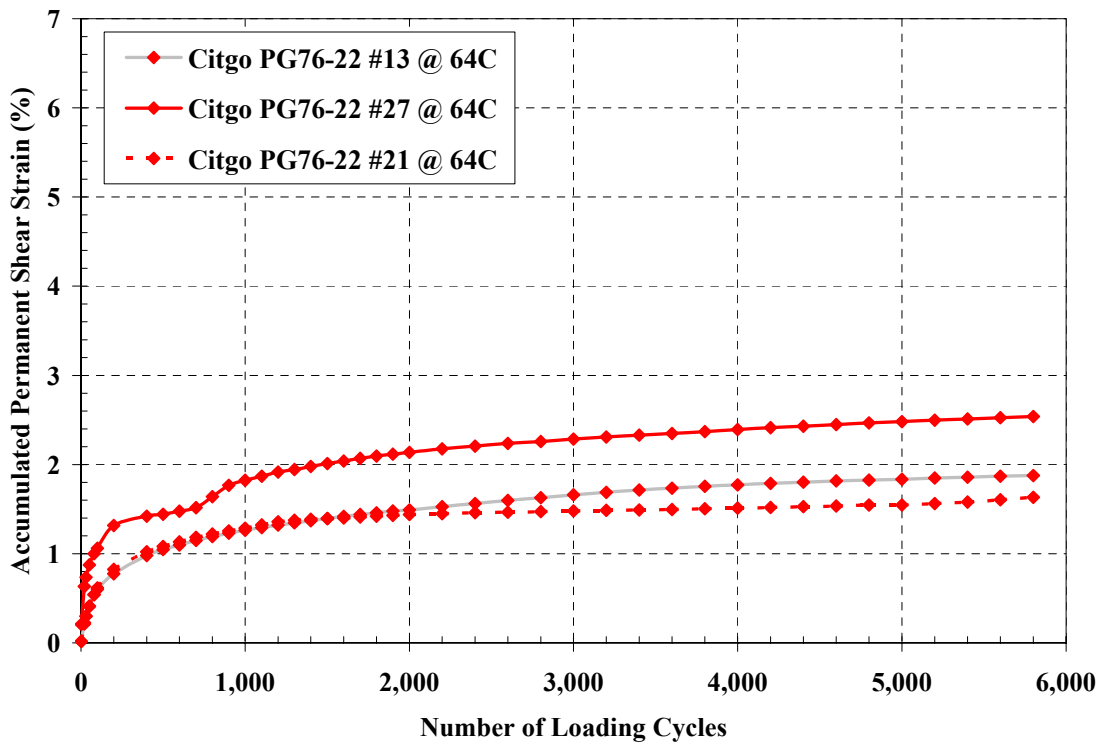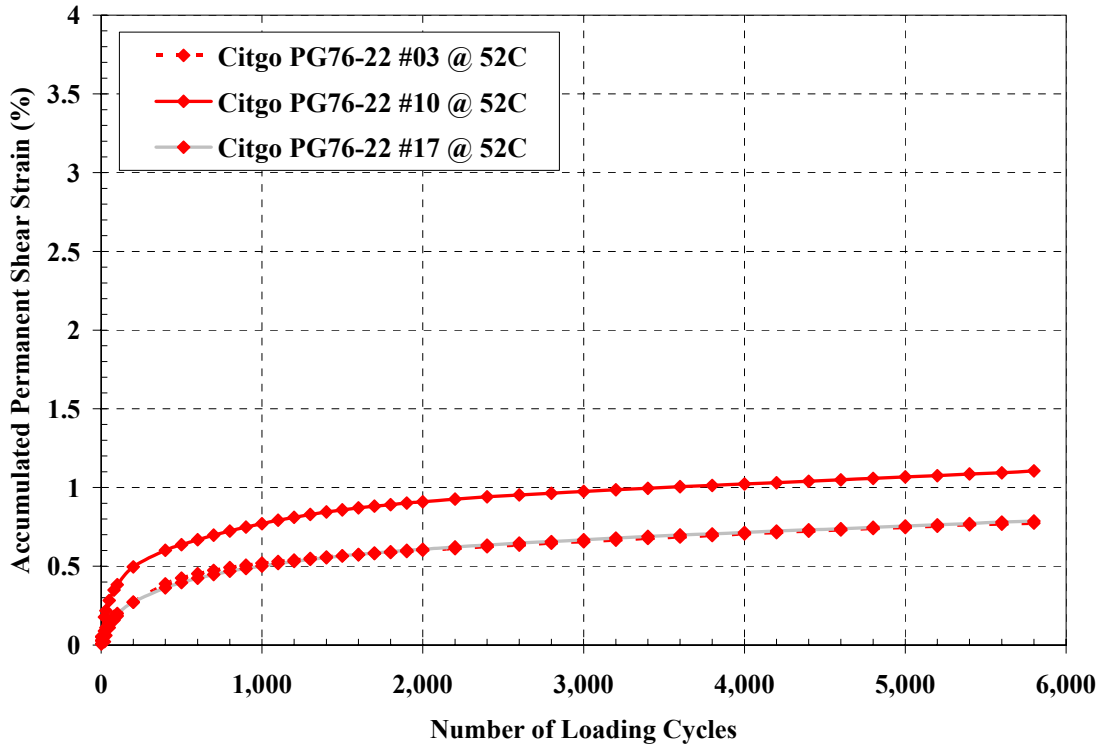
Appendix B.3 – RSCH Results for Koch Materials PG76-22
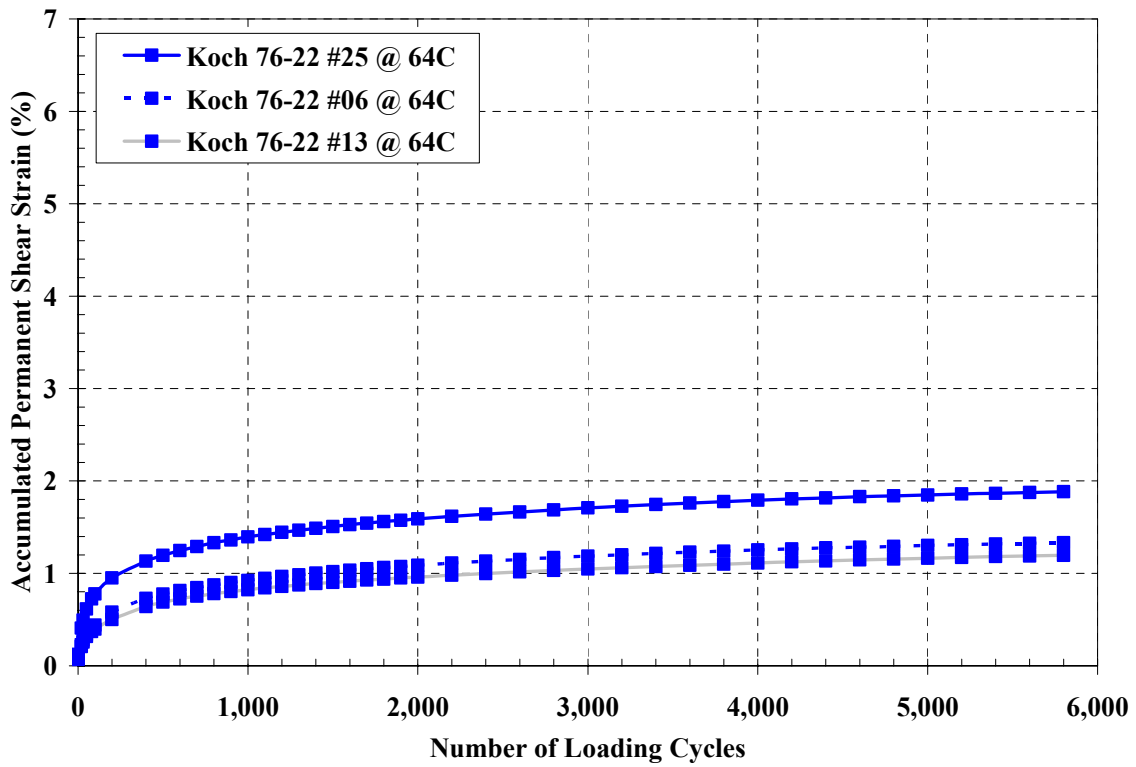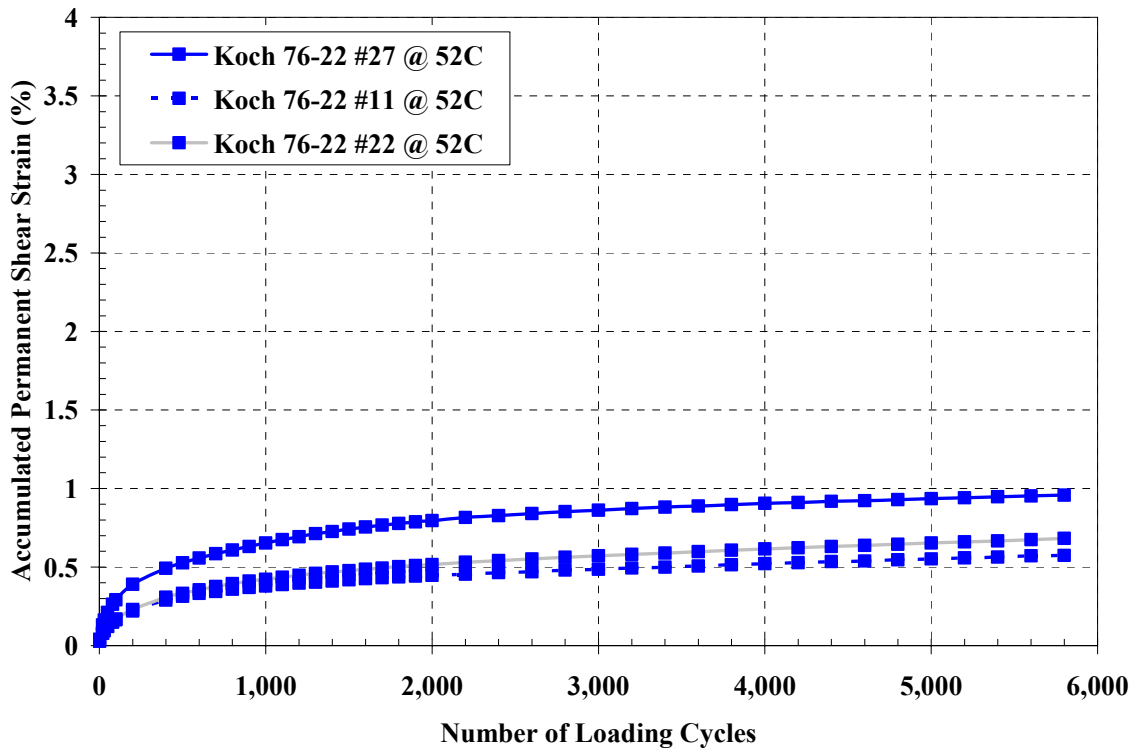
Appendix B.4 – RSCH Results for Creanova Vestoplast
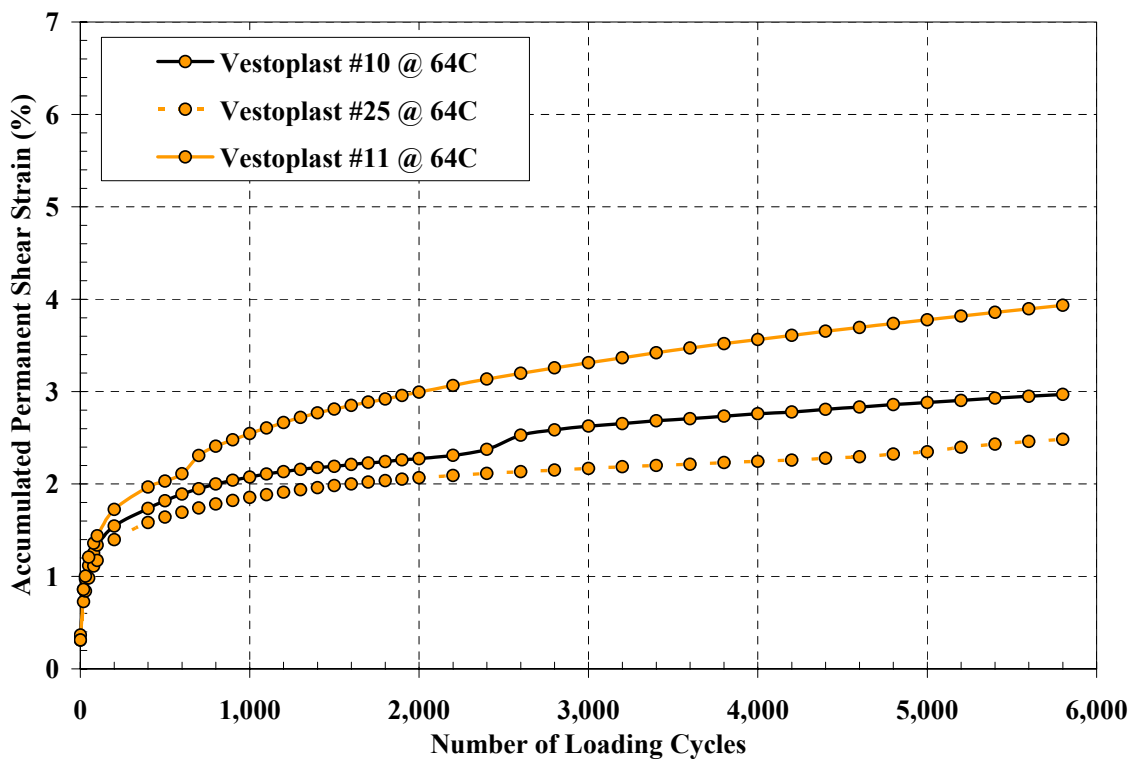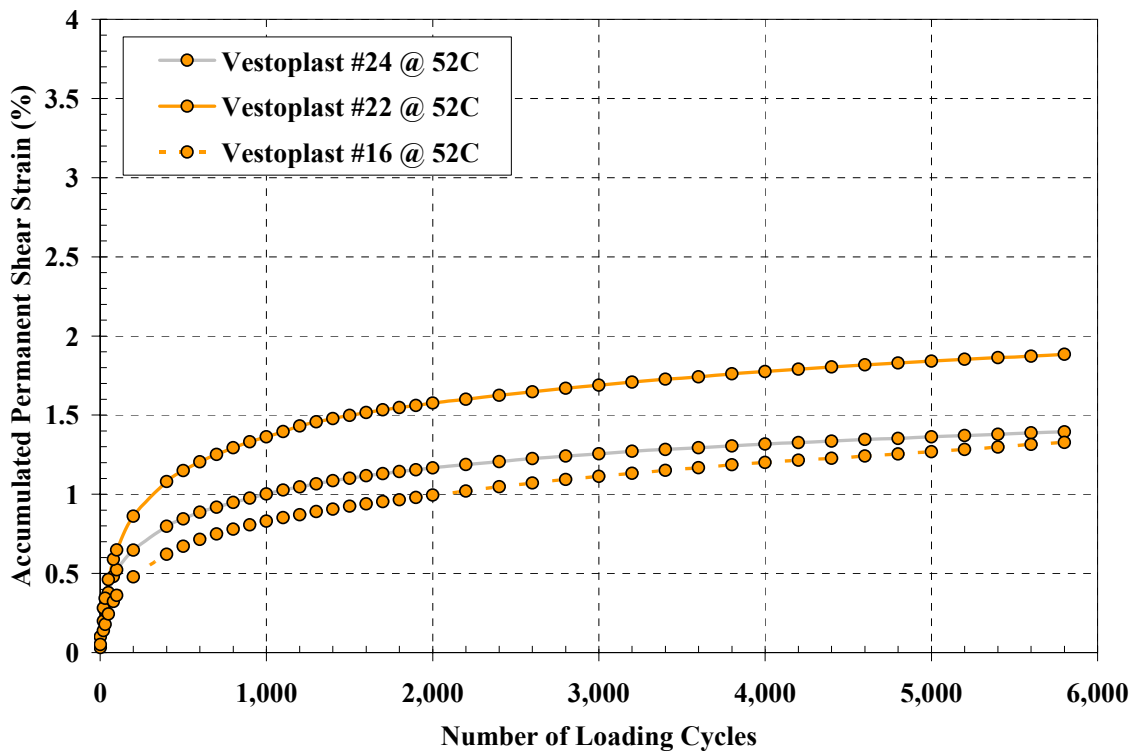
Appendix B.5 – RSCH Results for Eastman EE-2
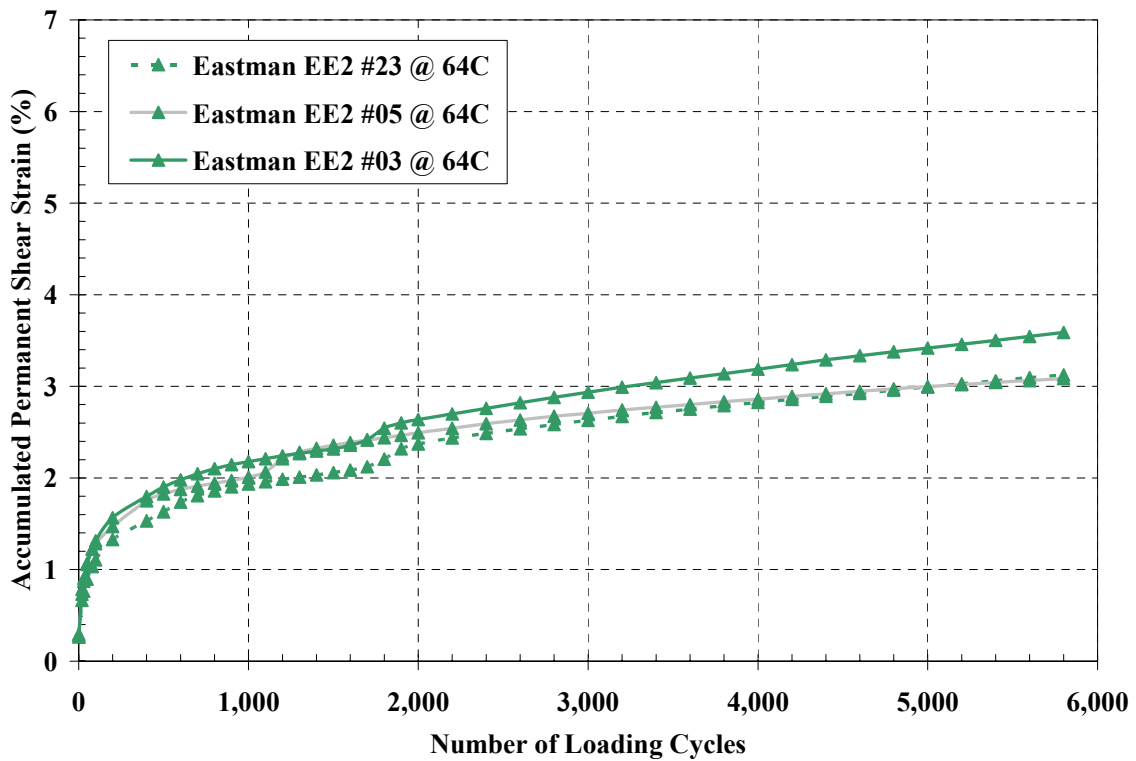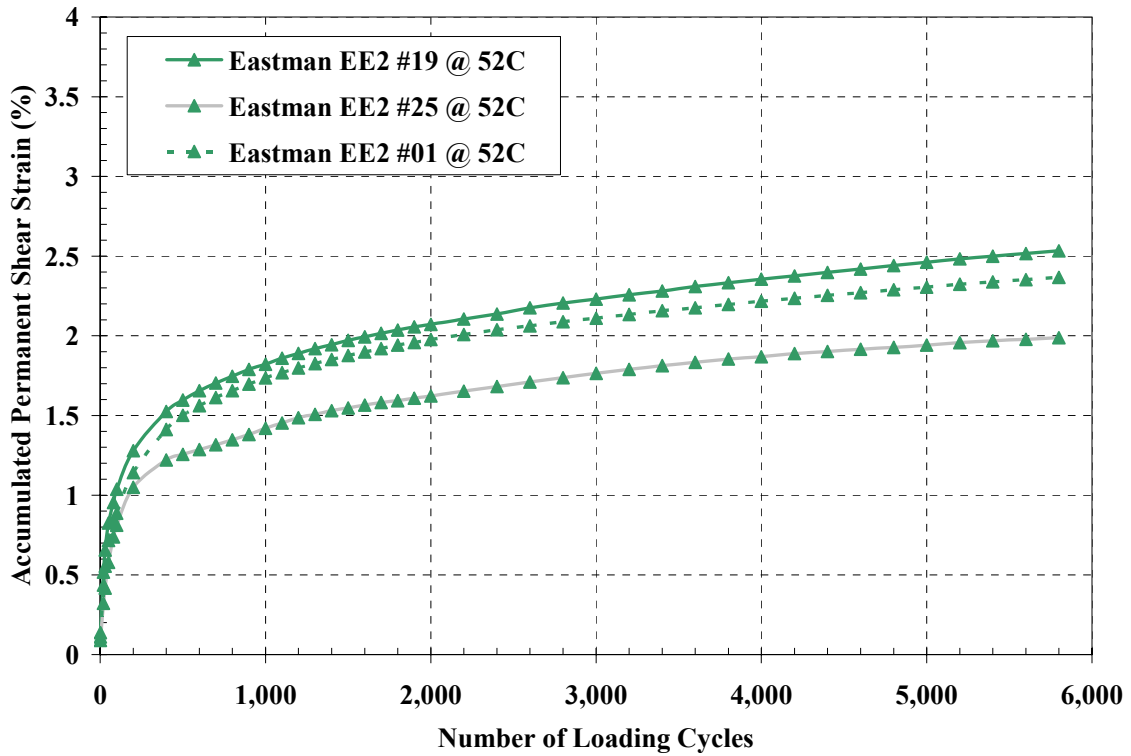
Appendix B.6 – RSCH Results for Hydrocarbon Technologies Carbon Black
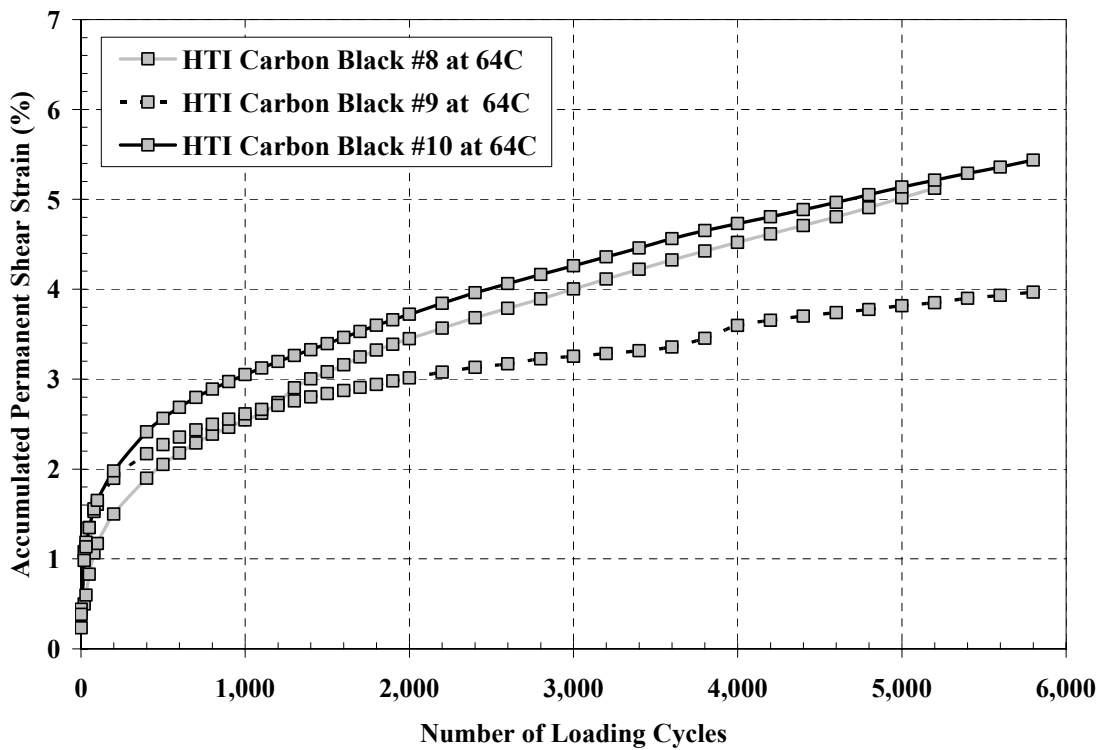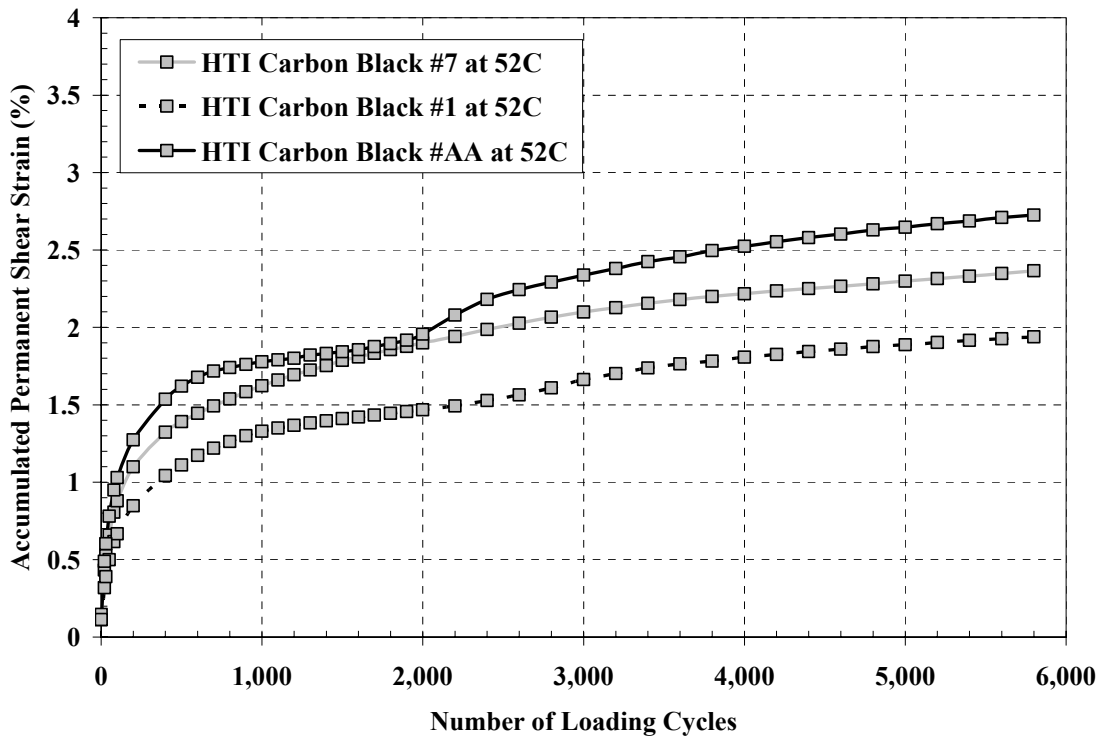
APPENDIX C – FREQUENCY SWEEP AT CONSTANT HEIGHT (FSCH) TEST RESULTS

Appendix C.1 – FSCH Results for Citgo PG64-22
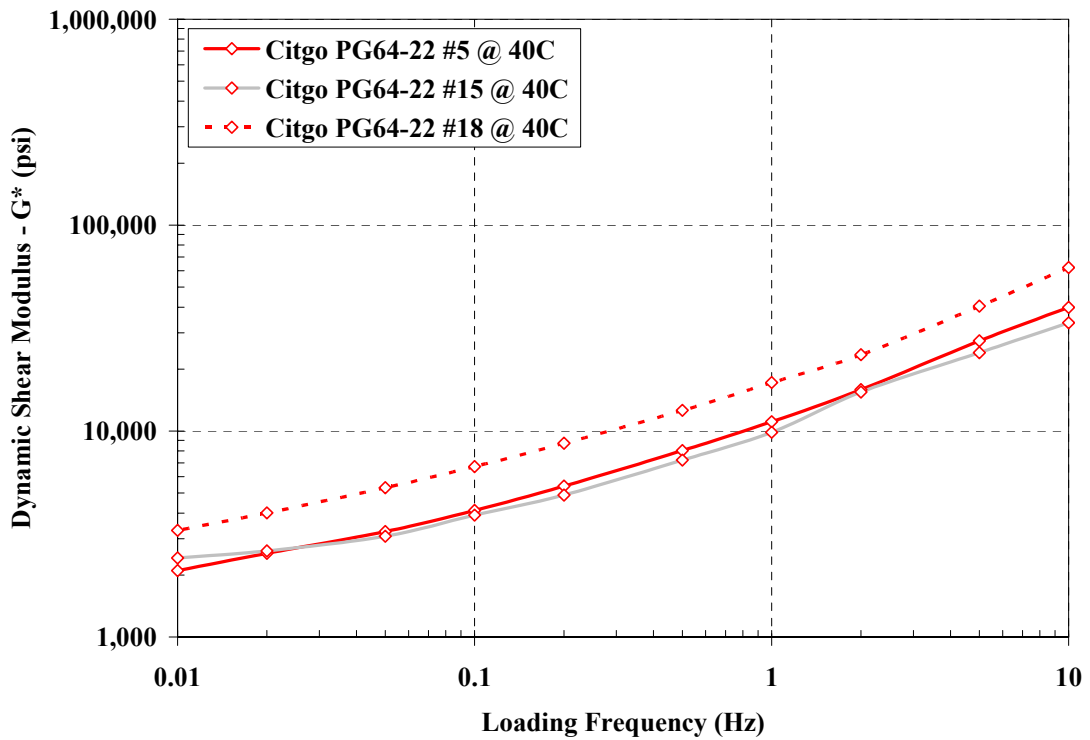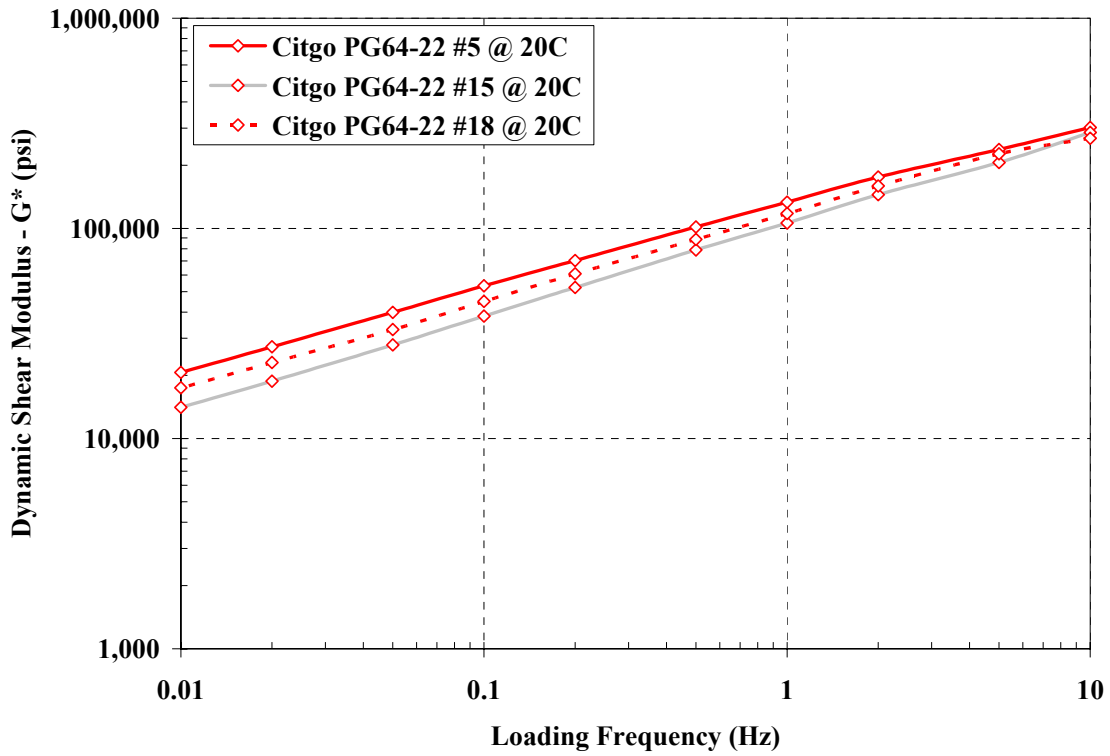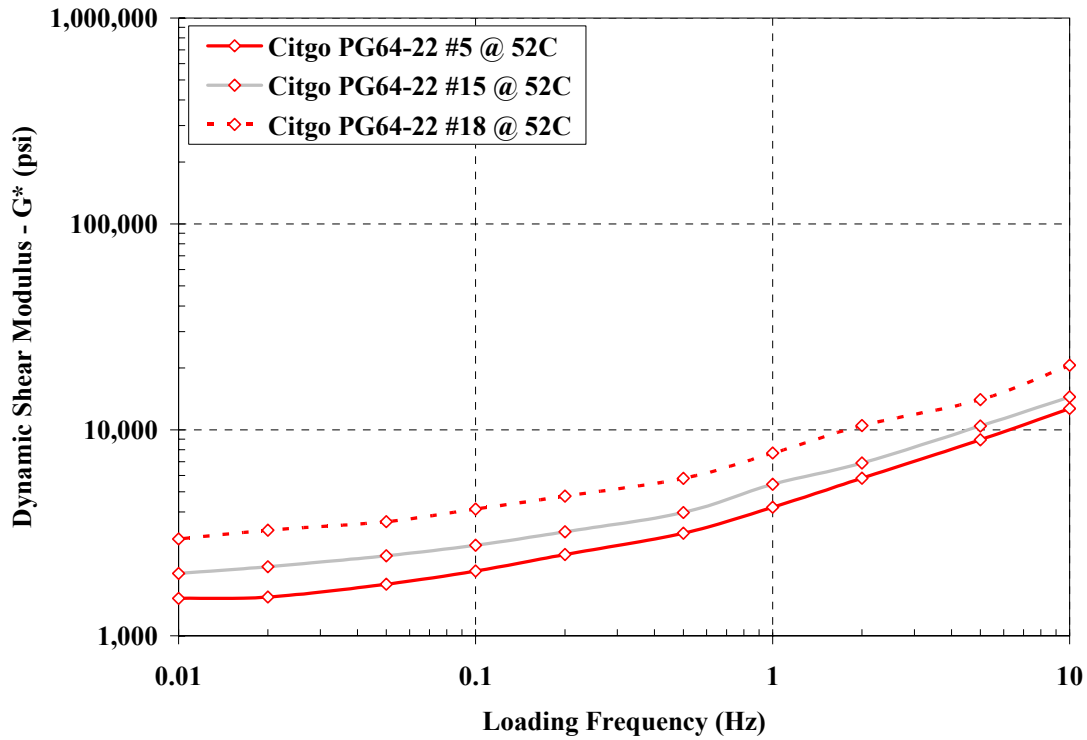
Dynamic Shear Modulus - G* (psi) vs **Loading Frequency (Hz)**

Legend:
- Citgo PG64-22 #5 @ 52C
- Citgo PG64-22 #15 @ 52C
- Citgo PG64-22 #18 @ 52C

Temperature = 20 C

Loading Frequency (Hz)	G* (psi) Citgo PG64-22 #5 @ 20C	Phase Angle (degrees) Citgo PG64-22 #5 @ 20C	G* (psi) Citgo PG64-22 #15 @ 20C	Phase Angle (degrees) Citgo PG64-22 #15 @ 20C	G* (psi) Citgo PG64-22 #18 @ 20C	Phase Angle (degrees) Citgo PG64-22 #18 @ 20C
10	302242	30.82	286148	32.91	268378	37.27
5	237794	30.88	205945	35.43	226652	33.43
2	175670	34	144768	40.06	159125	37.24
1	133551	35.72	106099	41.06	117656	38.62
0.5	101656	37.28	79054	42.18	88565	40.15
0.2	70336	39	52343	44.01	60858	42.03
0.1	53274	41.65	38254	44.58	44977	42.41
0.05	39856	41.63	27926	44.46	33025	42.69
0.02	27331	42.46	18747	43.34	23033	43.03
0.01	20624	42.01	14101	42.17	17460	41.19

Temperature = 40 C

Actual Frequency (Hz)	G* (psi) Citgo PG64-22 #5 @ 40C	Phase Angle (degrees) Citgo PG64-22 #5 @ 40C	G* (psi) Citgo PG64-22 #15 @ 40C	Phase Angle (degrees) Citgo PG64-22 #15 @ 40C	G* (psi) Citgo PG64-22 #18 @ 40C	Phase Angle (degrees) Citgo PG64-22 #18 @ 40C
10	39832	50.6	33559	55.25	62181	45.94
5	27405	51.34	24013	53.3	40420	48.6
2	15904	51.85	15466	51.54	23495	49.33
1	11112	50.64	9854	55.03	17195	48.06
0.5	8040	49.78	7232	49.23	12607	47.27
0.2	5408	45.26	4885	44.84	8735	43.98
0.1	4111	42.67	3906	41.1	6717	41.79
0.05	3252	38.4	3084	36.34	5307	39.46
0.02	2548	34.24	2622	32.8	4007	34.41
0.01	2103	32.46	2417	32.1	3292	33.05

Temperature = 52 C

Actual Frequency (Hz)	G* (psi) Citgo PG64-22 #5 @ 52C	Phase Angle (degrees) Citgo PG64-22 #5 @ 52C	G* (psi) Citgo PG64-22 #15 @ 52C	Phase Angle (degrees) Citgo PG64-22 #15 @ 52C	G* (psi) Citgo PG64-22 #18 @ 52C	Phase Angle (degrees) Citgo PG64-22 #18 @ 52C
10	12689	54.5	14433	51.8	20602	46.45
5	8948	50.79	10440	48.94	14015	44.8
2	5827	44.28	6913	42.96	10489	40.51
1	4208	45.55	5447	43.78	7718	40.99
0.5	3150	40.76	3970	41.13	5814	36.82
0.2	2480	33.73	3199	33.41	4771	29.22
0.1	2065	30.96	2754	30.69	4123	26.22
0.05	1780	25.71	2449	27.88	3585	23.3
0.02	1544	25.63	2166	24.61	3256	22.85
0.01	1518	22.85	2008	22.59	2952	20.27

136

Appendix C.2 – FSCH Results for Citgo PG76-22
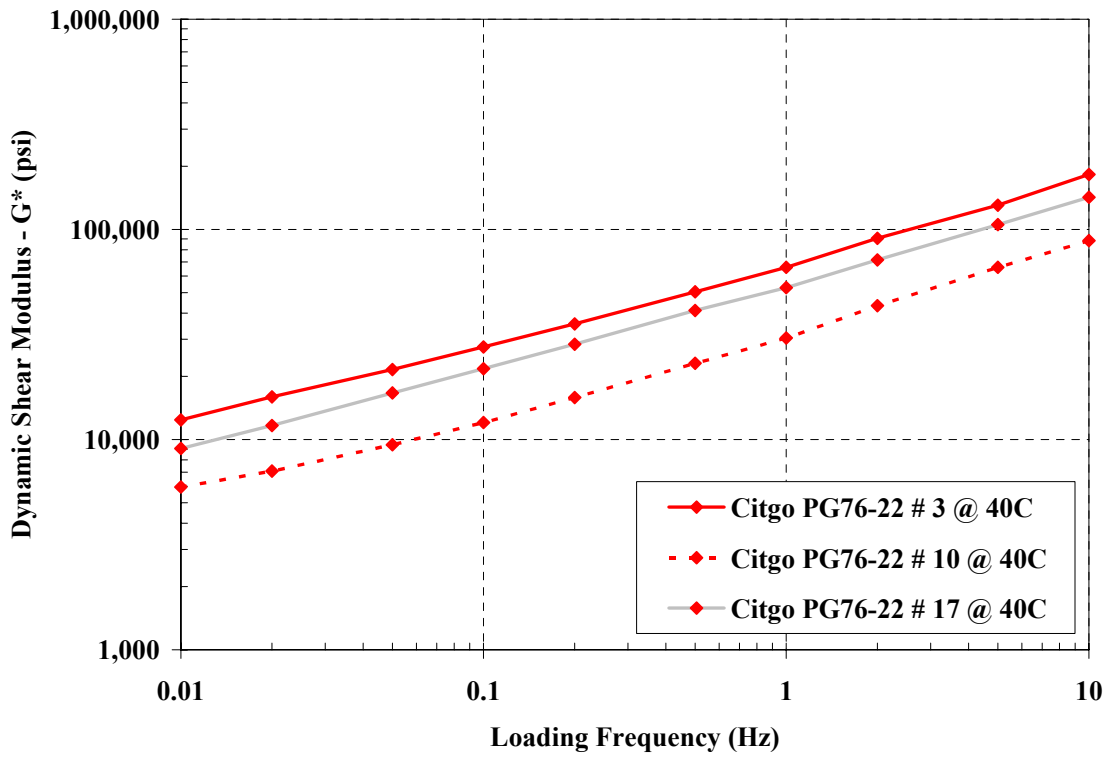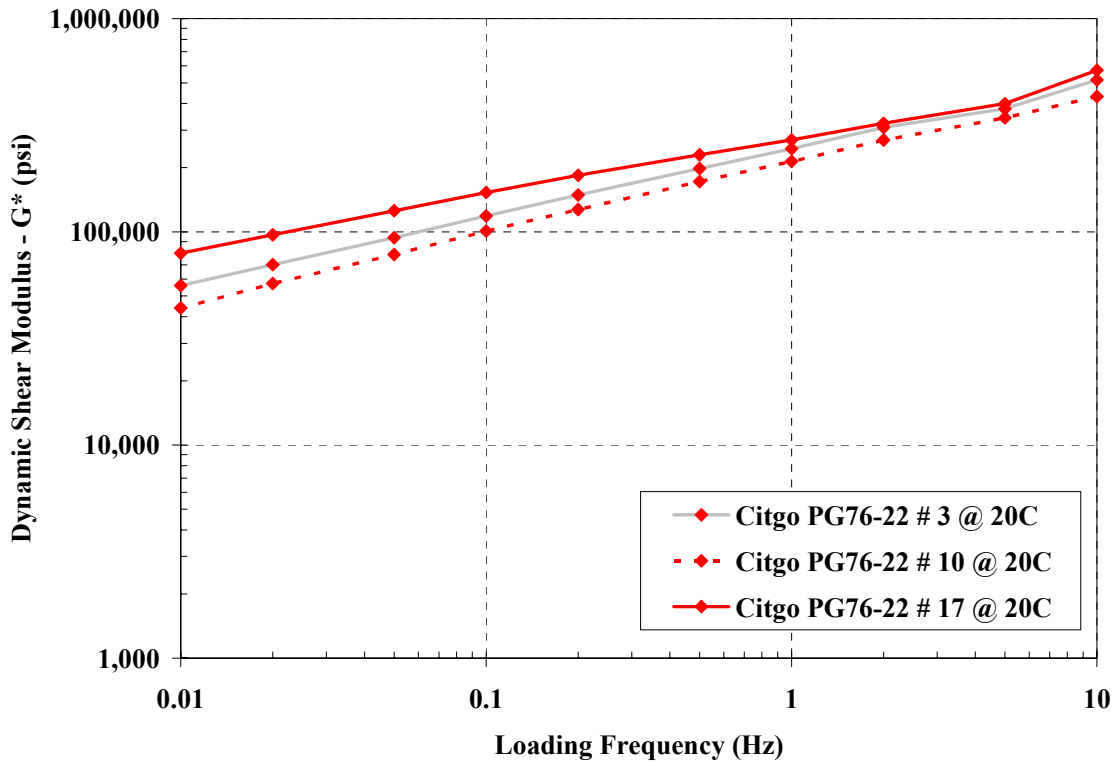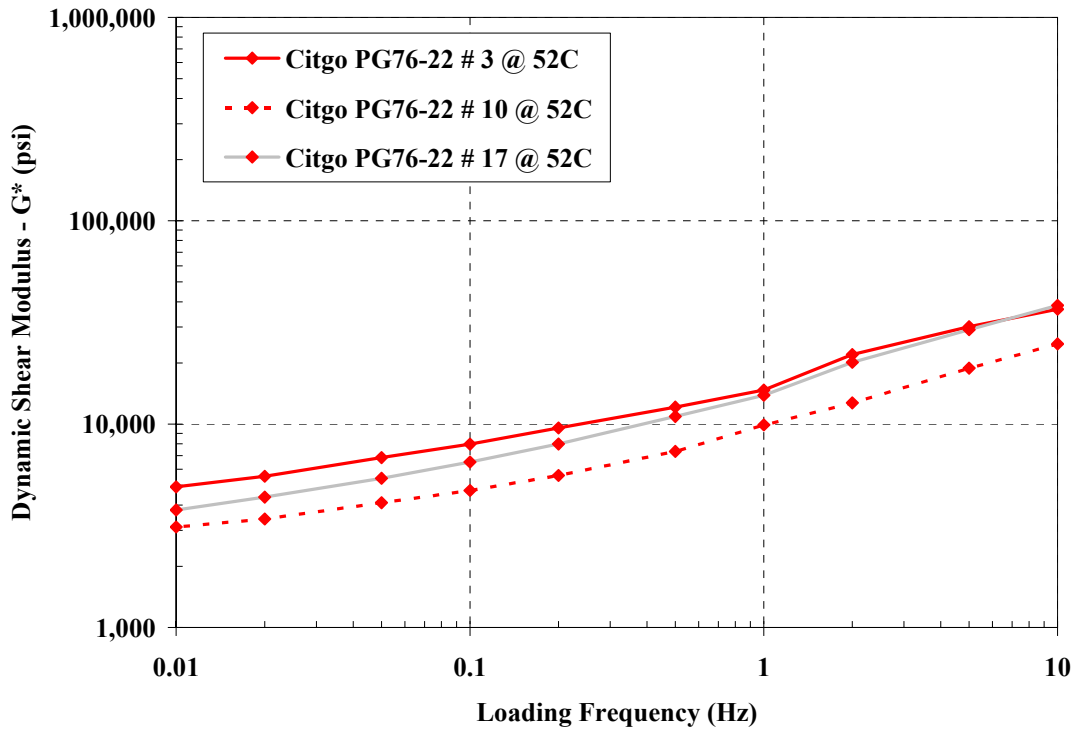
Temperature = 20 C

Loading Frequency (Hz)	G* (psi) Citgo PG76-22 # 3 @ 20C	Phase Angle (degrees) Citgo PG76-22 # 3 @ 20C	G* (psi) Citgo PG76-22 # 10 @ 20C	Phase Angle (degrees) Citgo PG76-22 # 10 @ 20C	G* (psi) Citgo PG76-22 # 17 @ 20C	Phase Angle (degrees) Citgo PG76-22 # 17 @ 20C
10	515177	28	431172	26.68	572568	26.65
5	377974	24.77	342219	26.25	399748	22.51
2	309024	27.25	269355	28.94	322776	25.55
1	245356	28.89	213695	30.6	269886	25.8
0.5	198232	30.3	172109	31.51	229609	26.79
0.2	148959	32.03	127187	33.19	184140	29.19
0.1	118682	33.6	100844	34.43	152815	30
0.05	93859	34.02	78263	35.93	125653	31.56
0.02	70120	34.65	57169	35.67	96832	32.89
0.01	55947	35.59	43992	36.84	79328	35.07

Temperature = 40 C

Actual Frequency (Hz)	G* (psi) Citgo PG76-22 # 3 @ 40C	Phase Angle (degrees) Citgo PG76-22 # 3 @ 40C	G* (psi) Citgo PG76-22 # 10 @ 40C	Phase Angle (degrees) Citgo PG76-22 # 10 @ 40C	G* (psi) Citgo PG76-22 # 17 @ 40C	Phase Angle (degrees) Citgo PG76-22 # 17 @ 40C
10	182472	33.76	88477	43.65	142101	37.92
5	130419	36.41	65985	43.82	105319	39.34
2	90619	39.37	43320	45.55	71695	40.9
1	65933	38.76	30434	44.67	52842	40.51
0.5	50479	38.11	23049	43.1	41122	39.67
0.2	35470	38.32	15861	41.67	28392	40.71
0.1	27599	37.88	12059	40.13	21763	39.86
0.05	21563	36.85	9449	38.3	16665	39.46
0.02	15958	36.39	7086	37.29	11670	39.03
0.01	12404	35.82	5948	35.73	9072	38.53

Temperature = 52 C

Actual Frequency (Hz)	G* (psi) Citgo PG76-22 # 3 @ 52C	Phase Angle (degrees) Citgo PG76-22 # 3 @ 52C	G* (psi) Citgo PG76-22 # 10 @ 52C	Phase Angle (degrees) Citgo PG76-22 # 10 @ 52C	G* (psi) Citgo PG76-22 # 17 @ 52C	Phase Angle (degrees) Citgo PG76-22 # 17 @ 52C
10	36735	45.96	24797	50.73	38395	47.51
5	30121	41.61	18839	48.02	29123	45.42
2	21968	38.57	12716	44.02	20142	42.11
1	14700	43.87	9905	43.78	13860	45.05
0.5	12130	39.41	7343	42.74	10899	42.18
0.2	9567	35.75	5590	37.59	7984	38.46
0.1	7962	33.24	4718	34.27	6509	35.9
0.05	6840	31.46	4105	32.73	5416	34.99
0.02	5544	29.9	3416	29.9	4380	30.97
0.01	4918	28.88	3119	29.49	3780	31.32

Appendix C.3 – FSCH Results for Koch Materials PG76-22
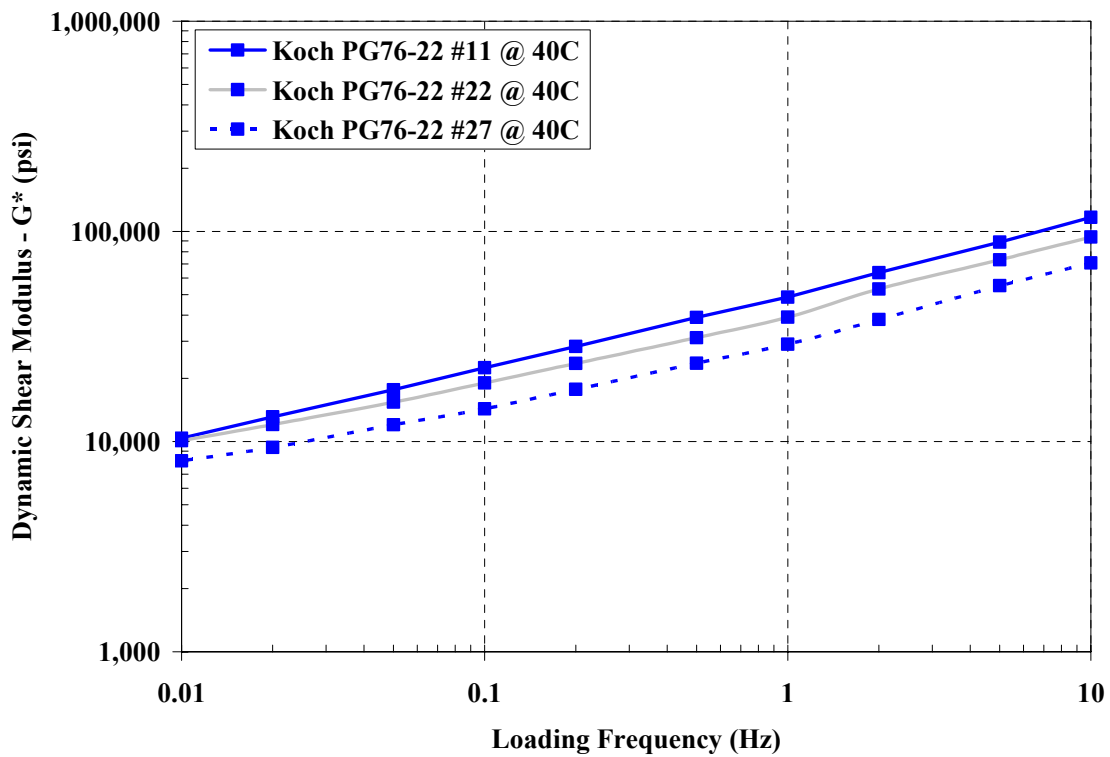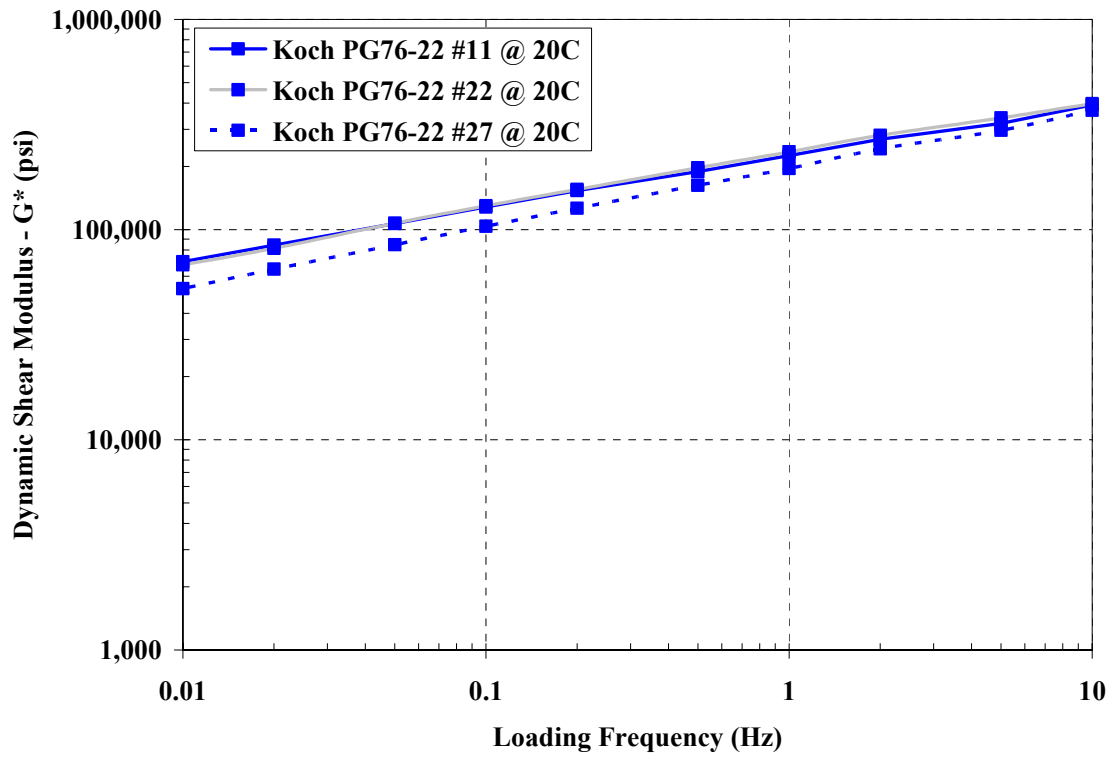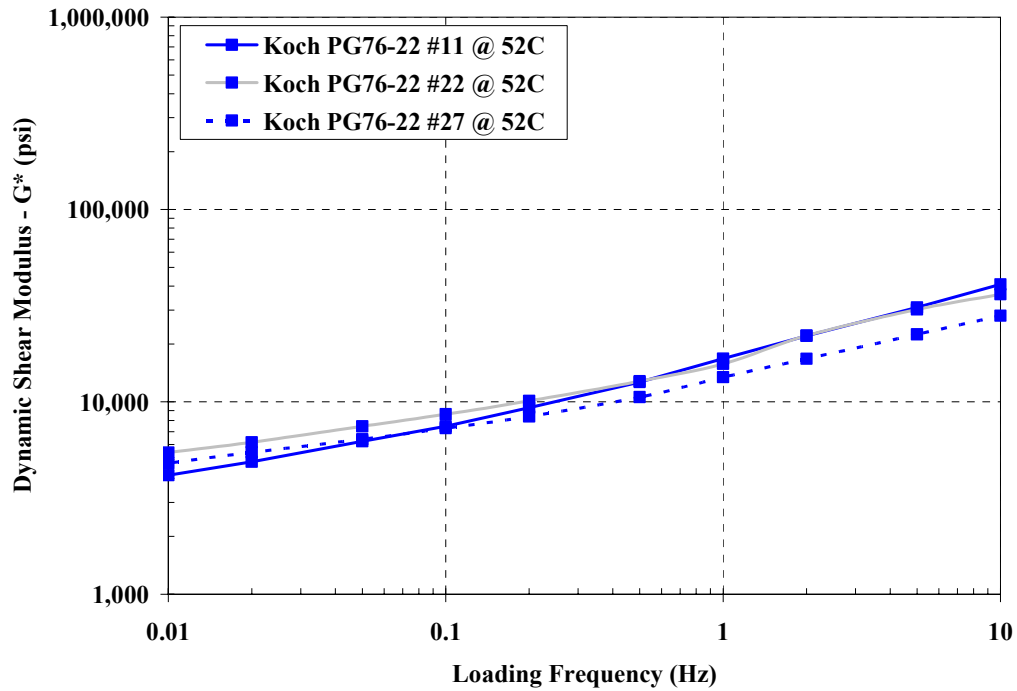
Temperature = 20 C

Loading Frequency (Hz)	G* (psi) Koch M. #11 @ 20C	Phase Angle (degrees) Koch M. #11 @ 20C	G* (psi) Koch M. #22 @ 20C	Phase Angle (degrees) Koch M. #22 @ 20C	G* (psi) Koch M. #27 @ 20C	Phase Angle (degrees) Koch M. #27 @ 20C
10	392029	20.56	397940	22.56	369465	21.13
5	320125	21.6	340394	22.58	296664	23.45
2	268904	22.45	281083	23.04	242488	24.45
1	225145	23.52	234330	24.33	195219	26.71
0.5	188773	23.33	196777	25.54	162481	26.66
0.2	153160	24.83	155317	26.14	126482	28.74
0.1	128155	25.71	129779	27.63	103809	29.39
0.05	106871	26.71	107243	28.53	84743	30.78
0.02	84313	27.63	81490	29.88	64821	31.21
0.01	70395	29.22	67918	31.44	52388	31.21

Temperature = 40 C

Actual Frequency (Hz)	G* (psi) Koch M. #11 @ 40C	Phase Angle (degrees) Koch M. #11 @ 40C	G* (psi) Koch M. #22 @ 40C	Phase Angle (degrees) Koch M. #22 @ 40C	G* (psi) Koch M. #27 @ 40C	Phase Angle (degrees) Koch M. #27 @ 40C
10	116796	33.19	94016	35.35	70845	38.54
5	88768	33.89	73327	34.66	55161	38.51
2	63703	34.74	53190	35.99	38069	39.8
1	48696	34.53	39065	34.98	29054	37.46
0.5	38928	34.46	31225	35.17	23592	36.58
0.2	28384	34.32	23555	35.1	17735	35.33
0.1	22445	35.04	18995	33.96	14316	33.9
0.05	17643	34.86	15404	33.46	12010	32.44
0.02	13117	35.28	12046	32.22	9394	31.17
0.01	10379	35.59	10085	31.44	8089	29.33

Temperature = 52 C

Actual Frequency (Hz)	G* (psi) Koch M. #11 @ 52C	Phase Angle (degrees) Koch M. #11 @ 52C	G* (psi) Koch M. #22 @ 52C	Phase Angle (degrees) Koch M. #22 @ 52C	G* (psi) Koch M. #27 @ 52C	Phase Angle (degrees) Koch M. #27 @ 52C
10	40751	40.26	36236	40.82	28054	42.01
5	30948	39.01	30237	37.89	22436	37.84
2	22062	37.7	22092	34.43	16743	35.67
1	16784	39.72	15756	38.9	13425	37.63
0.5	12656	37.66	12794	35.7	10584	36.64
0.2	9330	36.59	10114	32.81	8391	33.29
0.1	7461	35.55	8619	30.3	7297	31.25
0.05	6239	34.48	7457	29.5	6395	28.94
0.02	4882	32.49	6172	26.81	5465	28.58
0.01	4149	33.29	5449	26.3	4799	26.99

Appendix C.4 – FSCH Results for Creanova Vestoplast

Loading Frequency (Hz)

Temperature = 20 C

Loading Frequency (Hz)	G* (psi) Vestoplast # 16 @ 20C	Phase Angle (degrees) Vestoplast # 16 @ 20C	G* (psi) Vestoplast # 22 @ 20C	Phase Angle (degrees) Vestoplast # 22 @ 20C	G* (psi) Vestoplast # 24 @ 20C	Phase Angle (degrees) Vestoplast # 24 @ 20C
10	448413	26.4	423713	22.92	405939	23.59
5	332823	27.36	327589	26.09	362534	26.21
2	252990	31	250323	29.98	284568	29.27
1	197414	33.38	198884	31.69	226907	31.02
0.5	157205	34.72	158844	33.46	179093	33.07
0.2	111655	37.19	115091	35.35	130571	35.85
0.1	85203	38.69	89523	37.16	101936	36.15
0.05	64801	39.72	68809	38.12	77955	37.78
0.02	45074	41.04	48016	39.5	55295	38.96
0.01	34979	39.65	37039	39.77	42270	38.74

Temperature = 40 C

Actual Frequency (Hz)	G* (psi) Vestoplast # 16 @ 40C	Phase Angle (degrees) Vestoplast # 16 @ 40C	G* (psi) Vestoplast # 22 @ 40C	Phase Angle (degrees) Vestoplast # 22 @ 40C	G* (psi) Vestoplast # 24 @ 40C	Phase Angle (degrees) Vestoplast # 24 @ 40C
10	94425	44.24	105128	41.72	89524	39.91
5	66655	45.79	75203	42.76	56801	44.44
2	40166	47.49	45853	45.78	35608	47.32
1	28598	47.39	33557	45.98	24775	45.22
0.5	21055	46.31	24289	46.51	19577	42.55
0.2	14118	46.16	16473	44.42	14551	40.93
0.1	10478	44.43	12306	43.7	11756	39.08
0.05	8046	42.36	9437	42.95	9697	37.35
0.02	5930	39.13	6906	41.13	7518	36.02
0.01	4654	37.18	5492	37.78	6390	35.31

Temperature = 52 C

| Actual Frequency (Hz)	G* (psi) Vestoplast # 16 @ 52C	Phase Angle (degrees) Vestoplast # 16 @ 52C	G* (psi) Vestoplast # 22 @ 52C	Phase Angle (degrees) Vestoplast # 22 @ 52C	G* (psi) Vestoplast # 24 @ 52C	Phase Angle (degrees) Vestoplast # 24 @ 52C
10	24697	48.22	20648	50.33	38566	43.31
5	17036	44.16	14885	47.29	21993	45.11
2	12022	41.42	10679	41.83	17910	40.47
1	8733	43.06	7863	45.47	12181	44.26
0.5	7072	37.19	6218	39.54	9622	40.96
0.2	5511	34.14	4944	33.96	7480	34.23
0.1	4768	31.13	4176	31.65	6419	32.54
0.05	4117	29.49	3892	29.24	5845	30.83
0.02	3574	25.85	3228	25.77	4918	28.73
0.01	3181	25.34	2927	25.74	4364	27.07

Appendix C.5 – FSCH Results for Eastman EE-2
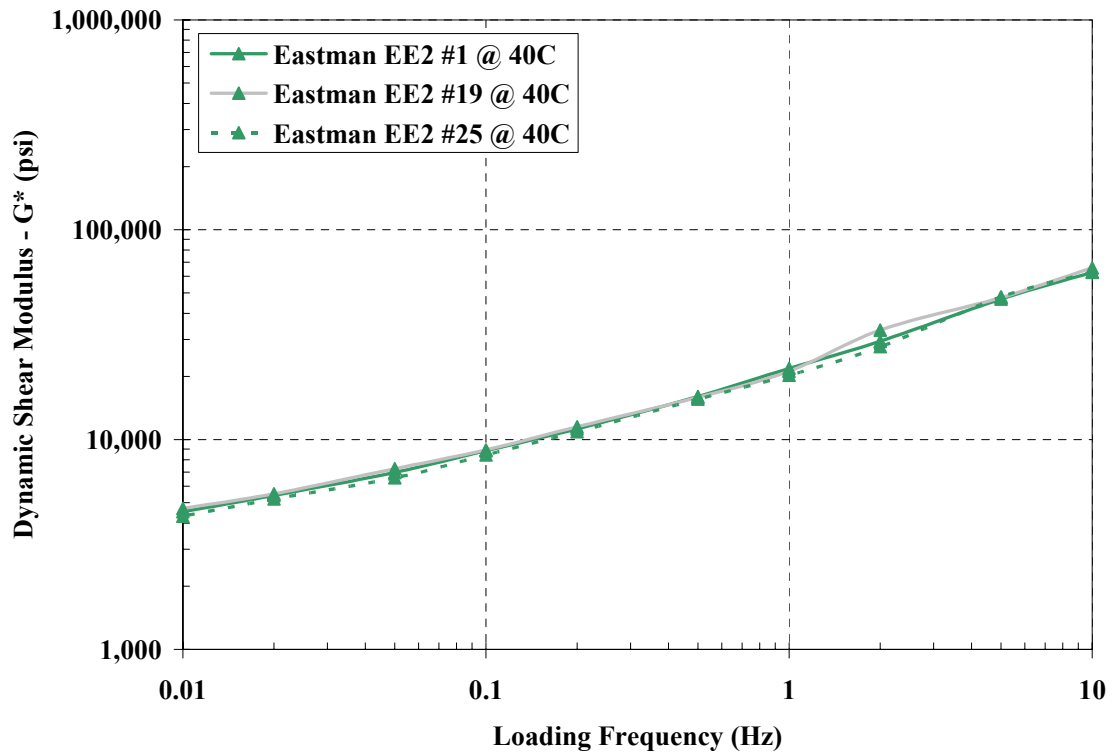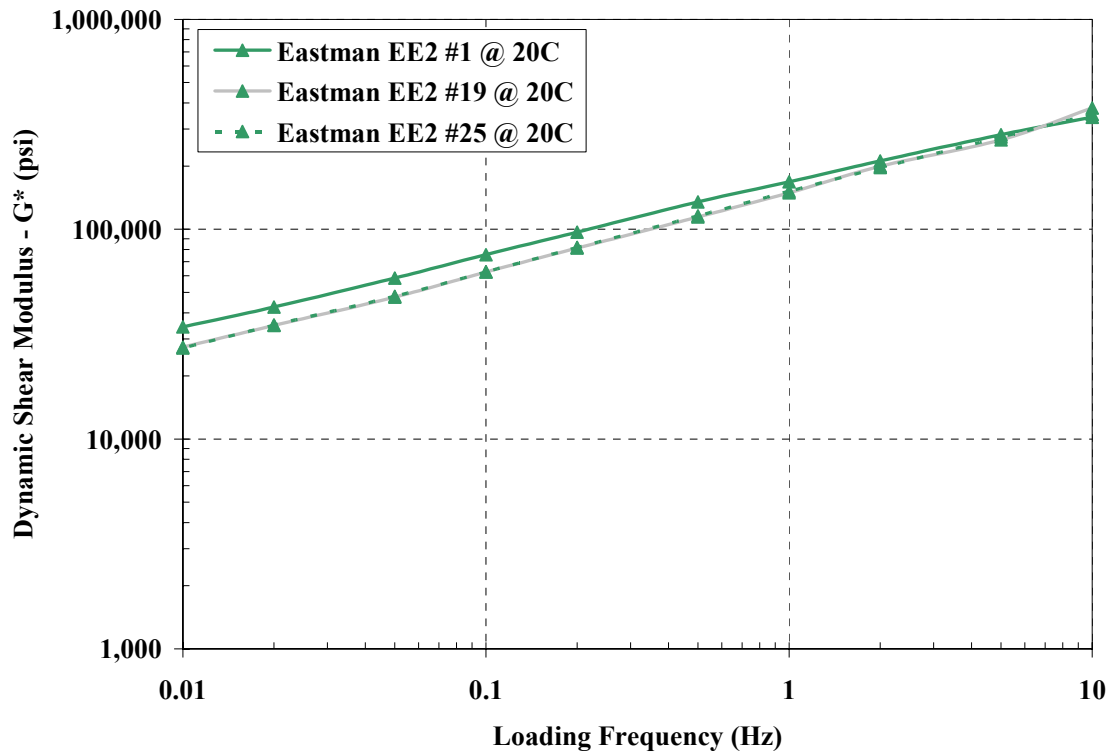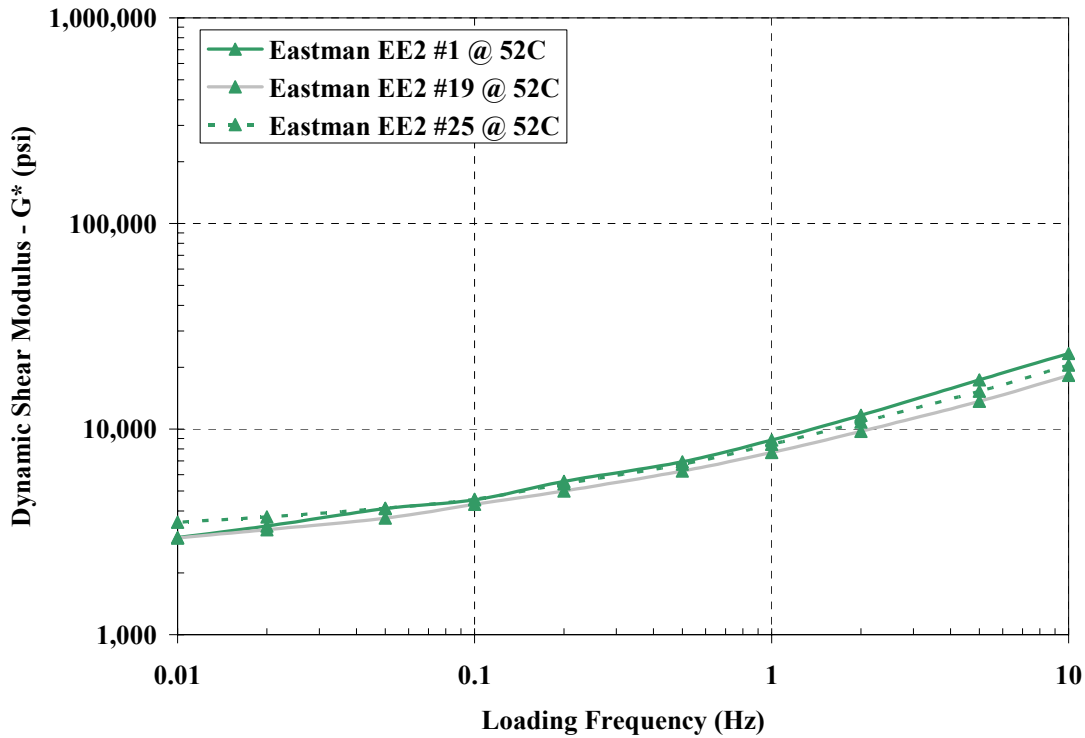
Dynamic Shear Modulus - G* (psi) vs Loading Frequency (Hz)

Legend:
- Eastman EE2 #1 @ 52C
- Eastman EE2 #19 @ 52C
- Eastman EE2 #25 @ 52C

Temperature = 20 C

| Loading Frequency (Hz)	G* (psi) Eastman EE2 #1 @ 20C	Phase Angle (degrees) Eastman EE2 #1 @ 20C	G* (psi) Eastman EE2 #19 @ 20C	Phase Angle (degrees) Eastman EE2 #19 @ 20C	G* (psi) Eastman EE2 #25 @ 20C	Phase Angle (degrees) Eastman EE2 #25 @ 20C
10	341476	27.63	378155	26.61	352876	28.89
5	282462	28.47	266570	30.75	275052	30.99
2	211398	31.62	199215	34.34	196569	35.75
1	168180	32.2	149101	36.01	151989	36.25
0.5	134904	33.7	114244	37.8	115964	37.52
0.2	96769	35.27	81311	39.21	81922	39.05
0.1	75649	35.84	62454	39.83	62689	39.32
0.05	58523	36.21	47466	39.97	47949	38.65
0.02	42620	36.13	34799	39.32	34948	37.57
0.01	34234	35.58	27430	38.52	27189	37.45

Temperature = 40 C

Actual Frequency (Hz)	G* (psi) Eastman EE2 #1 @ 40C	Phase Angle (degrees) Eastman EE2 #1 @ 40C	G* (psi) Eastman EE2 #19 @ 40C	Phase Angle (degrees) Eastman EE2 #19 @ 40C	G* (psi) Eastman EE2 #25 @ 40C	Phase Angle (degrees) Eastman EE2 #25 @ 40C
10	62691	46.5	65882	46.9	62916	48.56
5	46730	46.01	47468	46.48	47967	45.54
2	29401	46.57	33252	44.69	27741	48.29
1	21850	46.32	21164	46.43	20243	46.61
0.5	16046	44.96	15892	45.84	15613	45.13
0.2	11248	42.61	11499	43.74	10908	42.17
0.1	8849	40.26	8925	41.29	8448	40.17
0.05	6964	37.92	7266	39.36	6577	38.93
0.02	5414	36.53	5514	37.35	5206	35.64
0.01	4528	33.24	4695	34.76	4321	33.05

Temperature = 52 C

| Actual Frequency (Hz)	G* (psi) Eastman EE2 #1 @ 52C	Phase Angle (degrees) Eastman EE2 #1 @ 52C	G* (psi) Eastman EE2 #19 @ 52C	Phase Angle (degrees) Eastman EE2 #19 @ 52C	G* (psi) Eastman EE2 #25 @ 52C	Phase Angle (degrees) Eastman EE2 #25 @ 52C
10	23323	47.93	18233	48.82	20478	48.04
5	17356	45.56	13654	44.75	15297	43.76
2	11665	43.88	9764	43.34	10817	40.2
1	8855	43.06	7710	41.16	8428	38.87
0.5	6939	39.52	6244	38.68	6757	34.86
0.2	5561	35.85	5002	34.9	5420	30.09
0.1	4523	33.17	4306	31.89	4553	25.96
0.05	4102	31.1	3688	30.89	4124	24.85
0.02	3377	27.39	3242	27.04	3745	21.23
0.01	2967	24.96	2956	25.56	3523	21.22

Appendix C.6 – FSCH Results for HTI Carbon Black
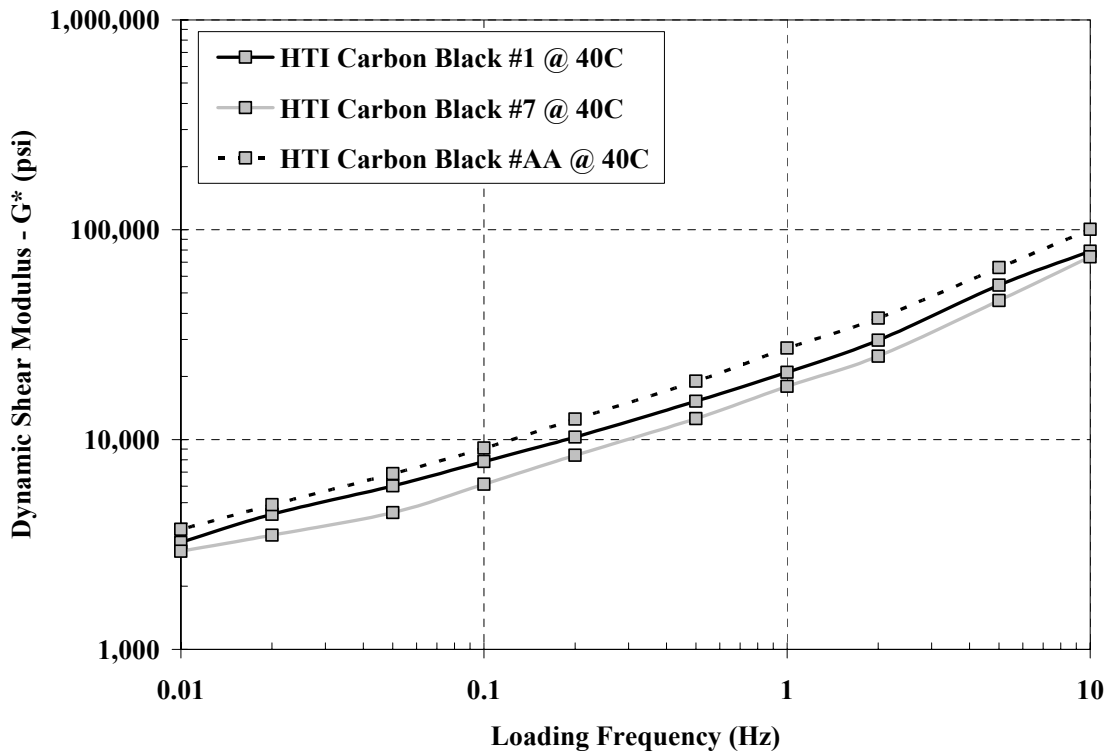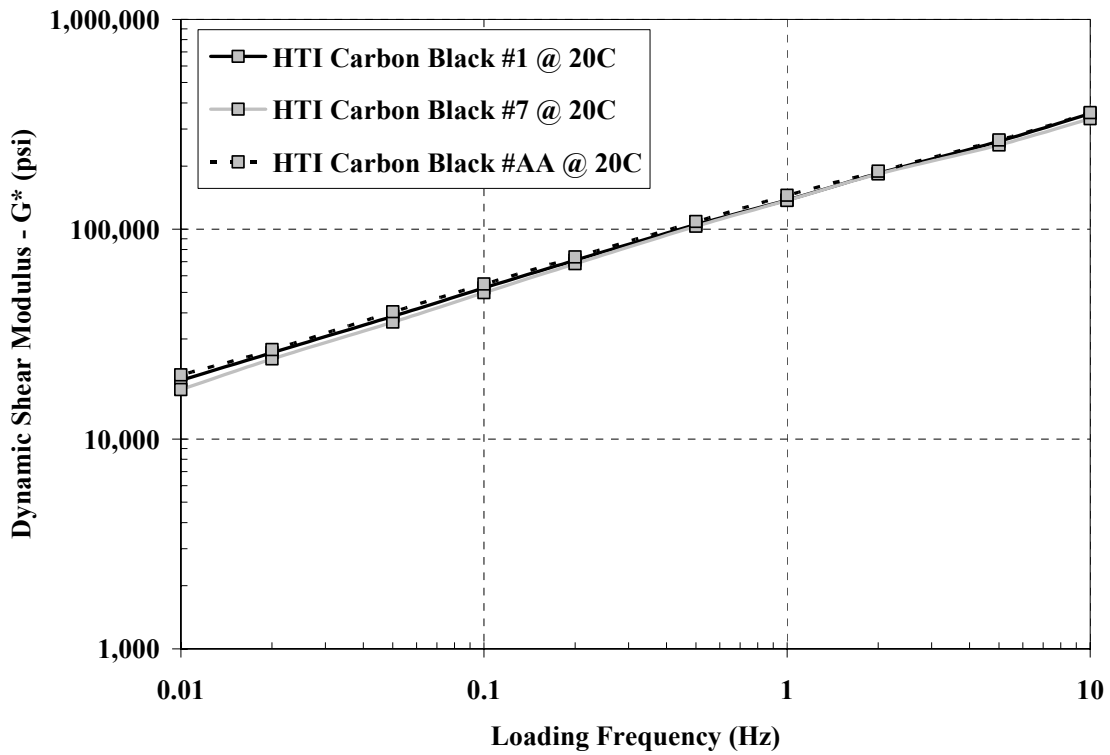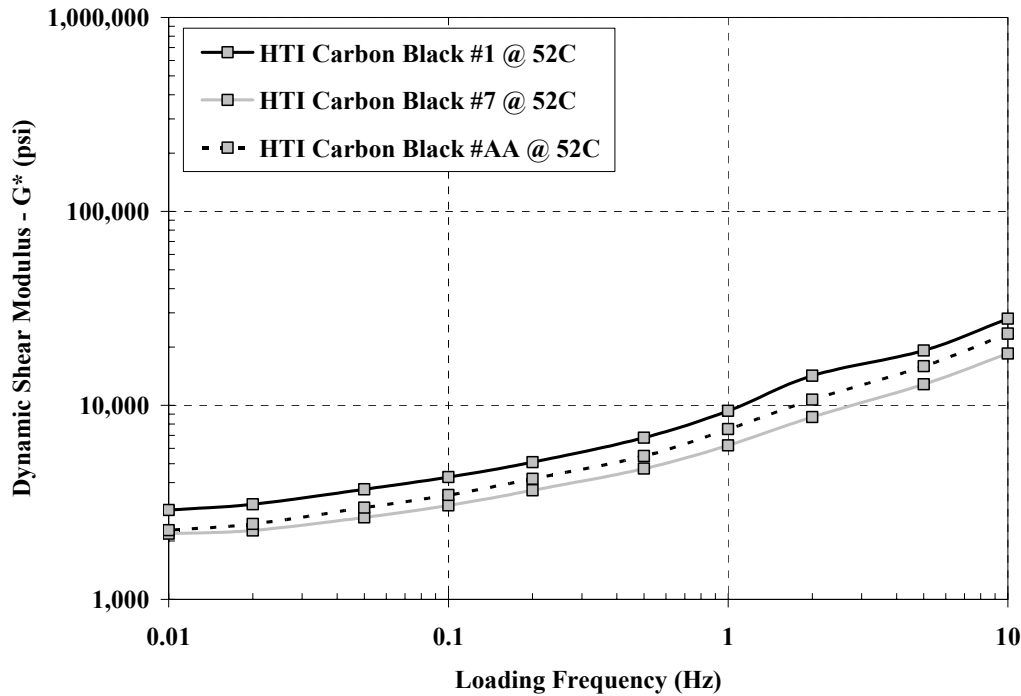
Temperature = 20 C

Loading Frequency (Hz)	G* (psi) Carbon Black #1 @ 20C	Phase Angle (degrees) Carbon Black #1 @ 20C	G* (psi) Carbon Black #7 @ 20C	Phase Angle (degrees) Carbon Black #7 @ 20C	G* (psi) Carbon Black #AA @ 20C	Phase Angle (degrees) Carbon Black #AA @ 20C
10	355804	44.71	336457	30.16	359510	27.06
5	262689	31.9	251981	31.33	265893	31.44
2	184599	35.4	183458	35.21	188720	35.5
1	137779	38.77	137244	38.29	145110	37.78
0.5	105179	41	103294	41.22	108663	40.16
0.2	71170	43.26	68478	43.67	73702	42.69
0.1	52485	45.39	49827	45.14	54826	44.75
0.05	38459	45.72	36058	46.72	40411	44.33
0.02	25763	46.16	24087	46.74	26681	45.68
0.01	19066	46.6	17195	47.18	20219	44.66

Temperature = 40 C

Actual Frequency (Hz)	G* (psi) Carbon Black #1 @ 40C	Phase Angle (degrees) Carbon Black #1 @ 40C	G* (psi) Carbon Black #7 @ 40C	Phase Angle (degrees) Carbon Black #7 @ 40C	G* (psi) Carbon Black #AA @ 40C	Phase Angle (degrees) Carbon Black #AA @ 40C
10	78945	46	74320	50.31	100430	44.55
5	54359	48.92	45985	52.07	65978	47.99
2	29714	50.76	24959	52.43	37933	49.18
1	20920	50.39	17929	52.38	27311	49.43
0.5	15205	49.54	12583	52.49	18958	49.54
0.2	10276	46.72	8412	49.37	12516	48.58
0.1	7858	43.96	6126	47.34	9112	47.04
0.05	6014	41.02	4488	42.16	6881	44.36
0.02	4409	37.33	3502	40.07	4888	40.94
0.01	3232	31.95	2933	37.68	3734	37.67

Temperature = 52 C

Actual Frequency (Hz)	G* (psi) Carbon Black #1 @ 52C	Phase Angle (degrees) Carbon Black #1 @ 52C	G* (psi) Carbon Black #7 @ 52C	Phase Angle (degrees) Carbon Black #7 @ 52C	G* (psi) Carbon Black #AA @ 52C	Phase Angle (degrees) Carbon Black #AA @ 52C
10	27961	52.86	18494	53.43	23451	53.05
5	19177	51.07	12831	49.18	15913	50.47
2	14205	45.92	8705	47.49	10704	47.32
1	9359	48.74	6219	44.64	7548	47.66
0.5	6820	42.79	4718	41	5483	43.9
0.2	5094	36.37	3651	35.19	4177	36.16
0.1	4270	32.6	3046	32.12	3446	32.28
0.05	3688	28.31	2643	27.06	2970	29.16
0.02	3090	26.32	2266	26.8	2447	22.6
0.01	2888	24.82	2181	23.74	2269	22.91

APPENDIX D – SIMPLE SHEAR AT CONSTANT HEIGHT (SSCH) TEST RESULTS
Appendix D.1 – SSCH Results for Citgo PG64-22
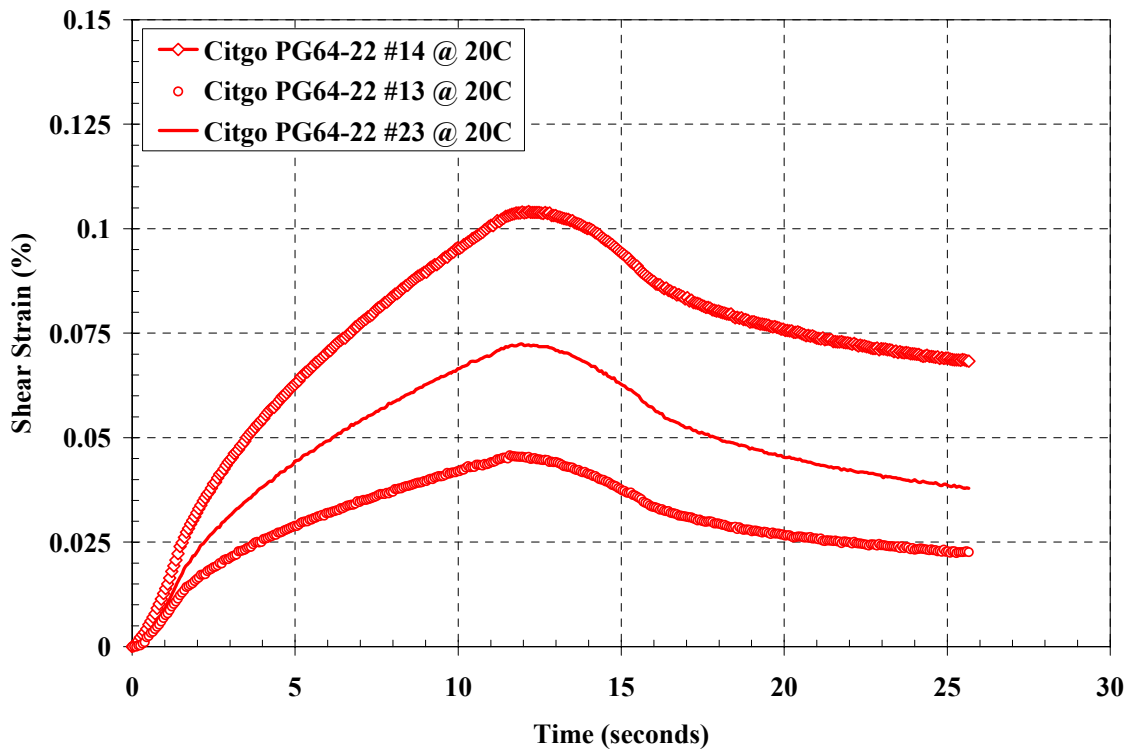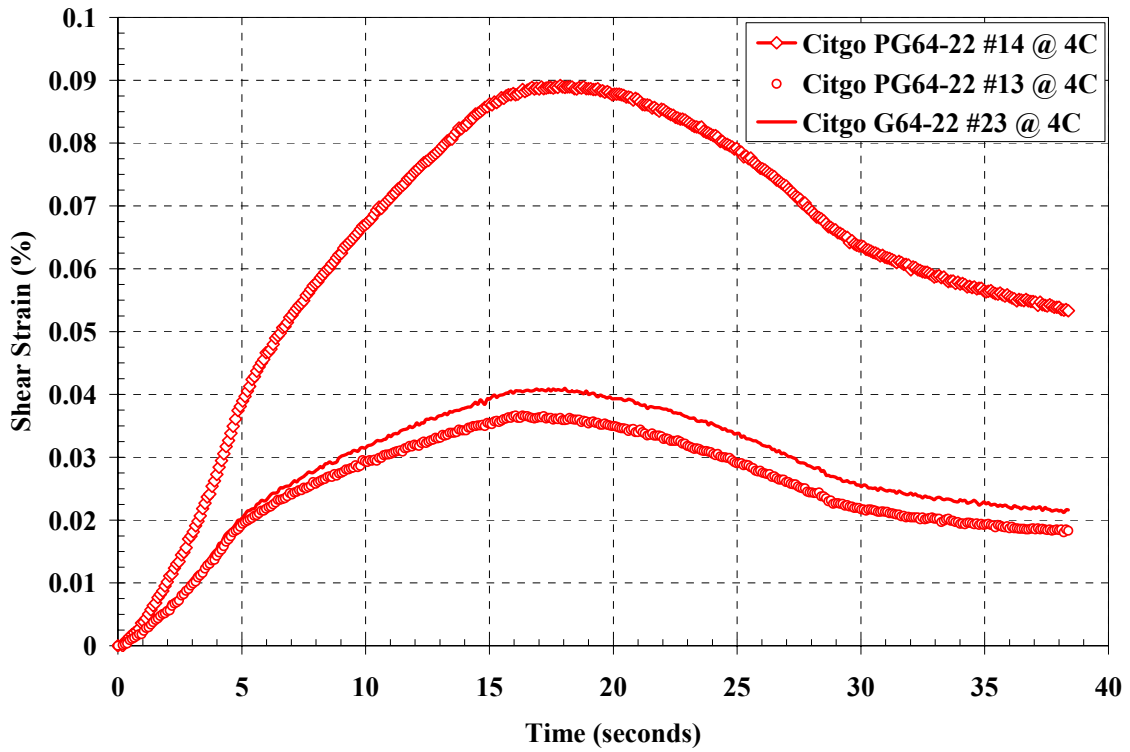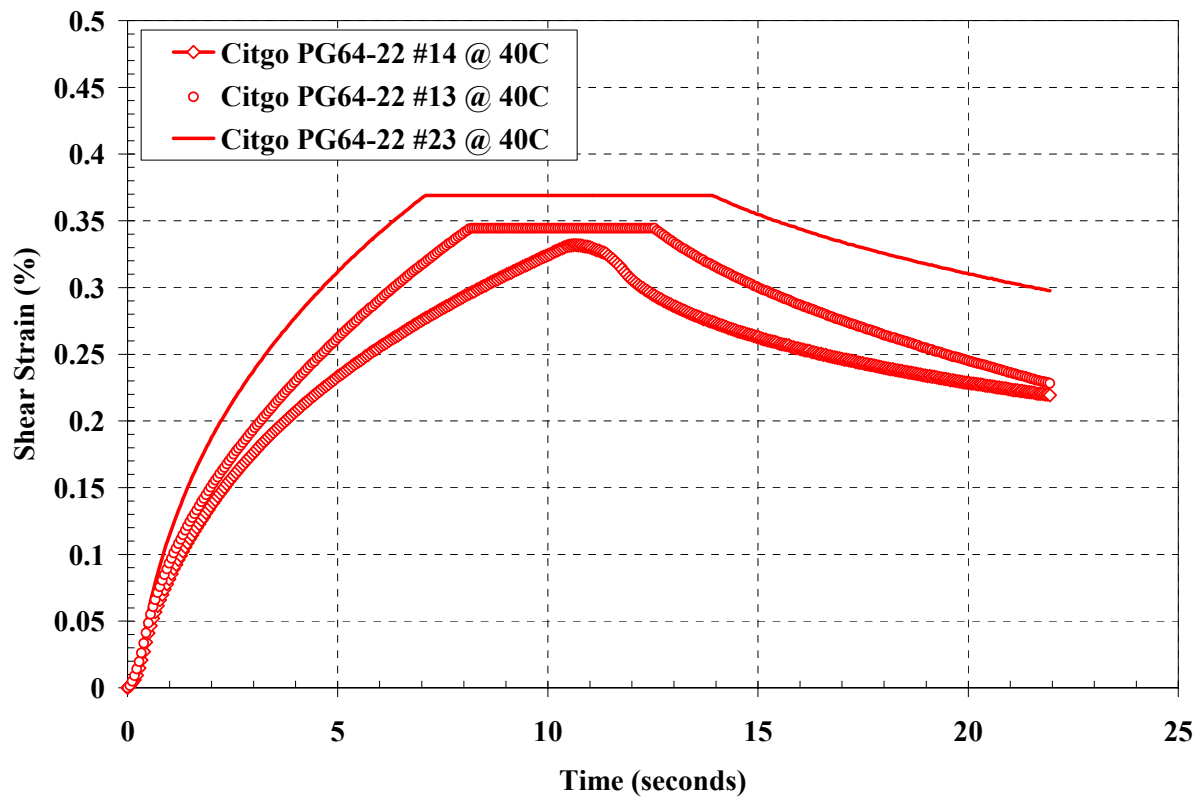
Appendix D.2 – SSCH Test Results for Citgo PG76-22
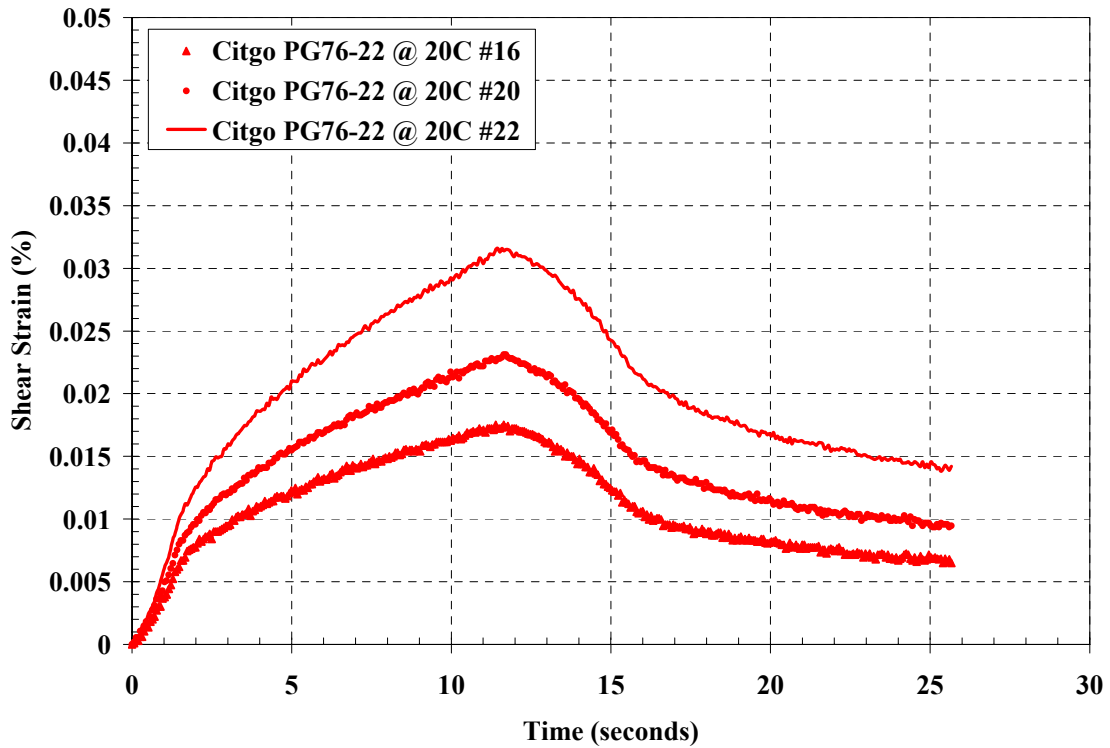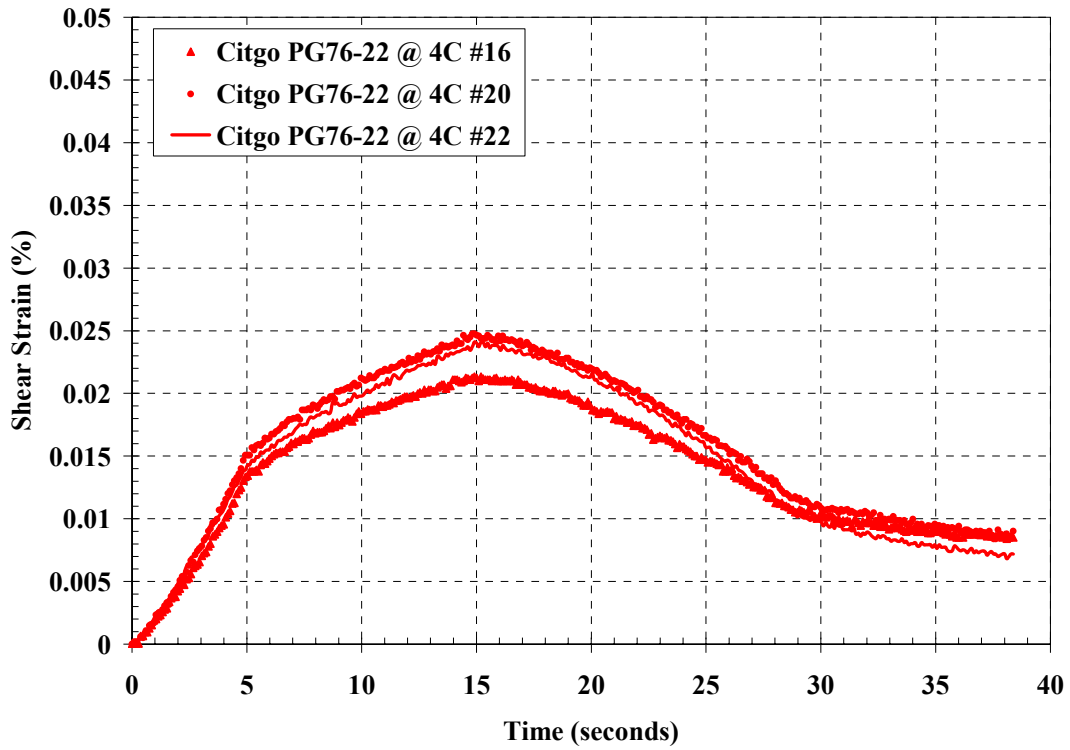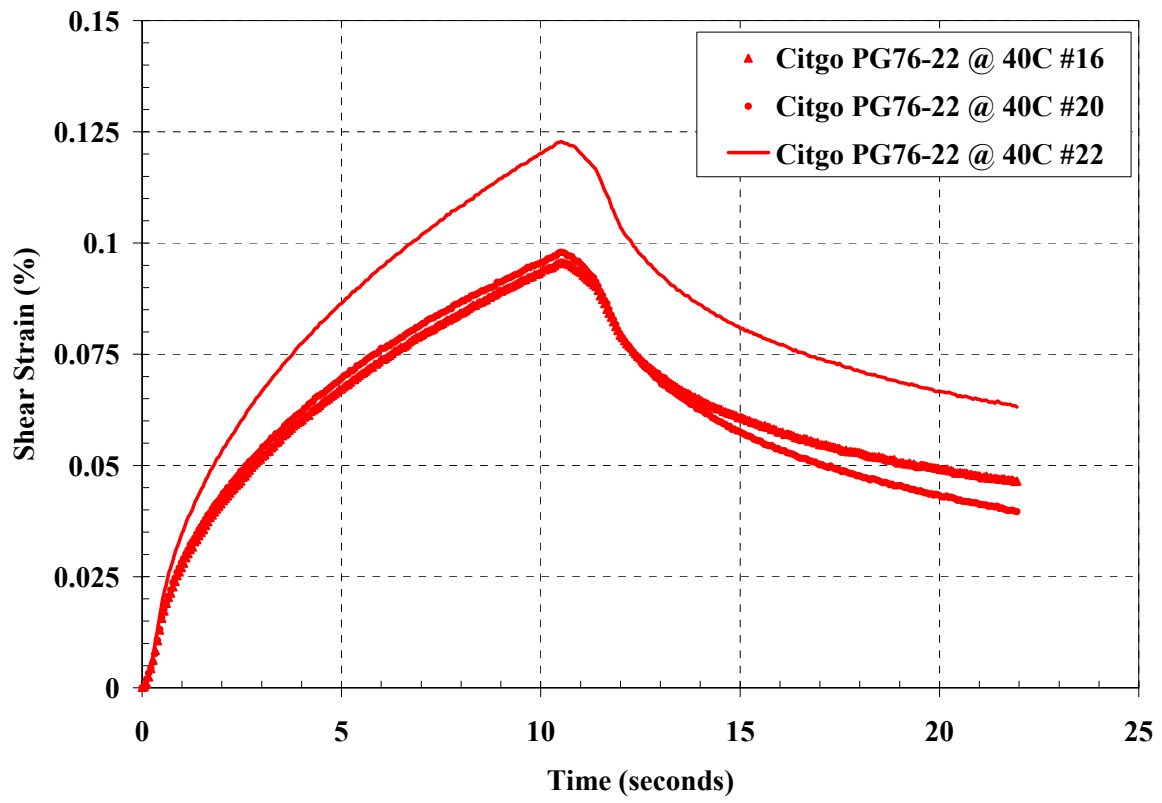
Appendix D.3 – SSCH Results for Koch Materials PG76-22
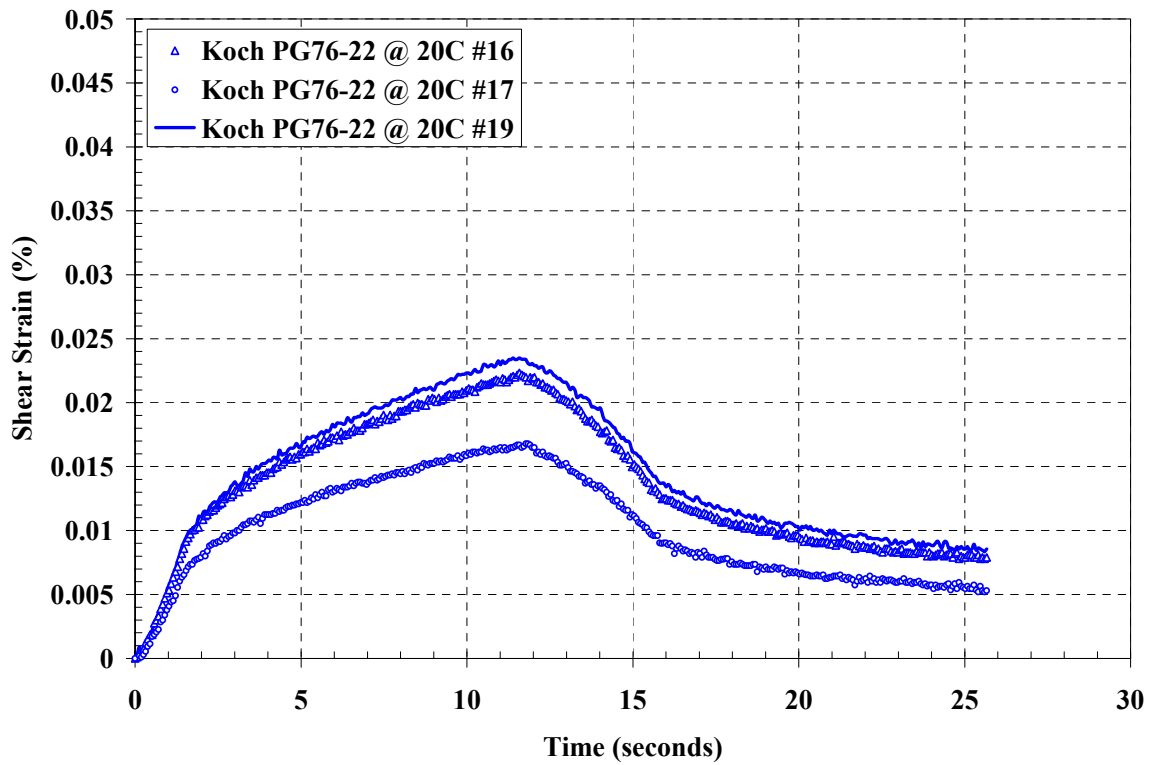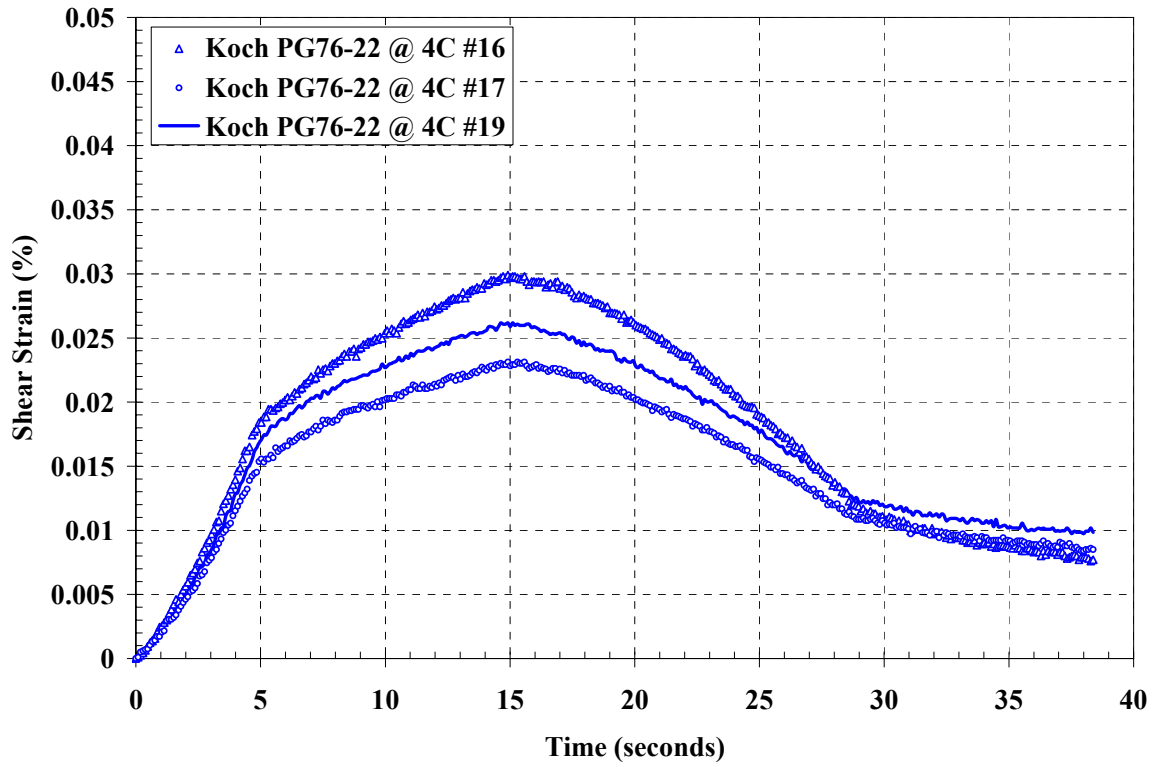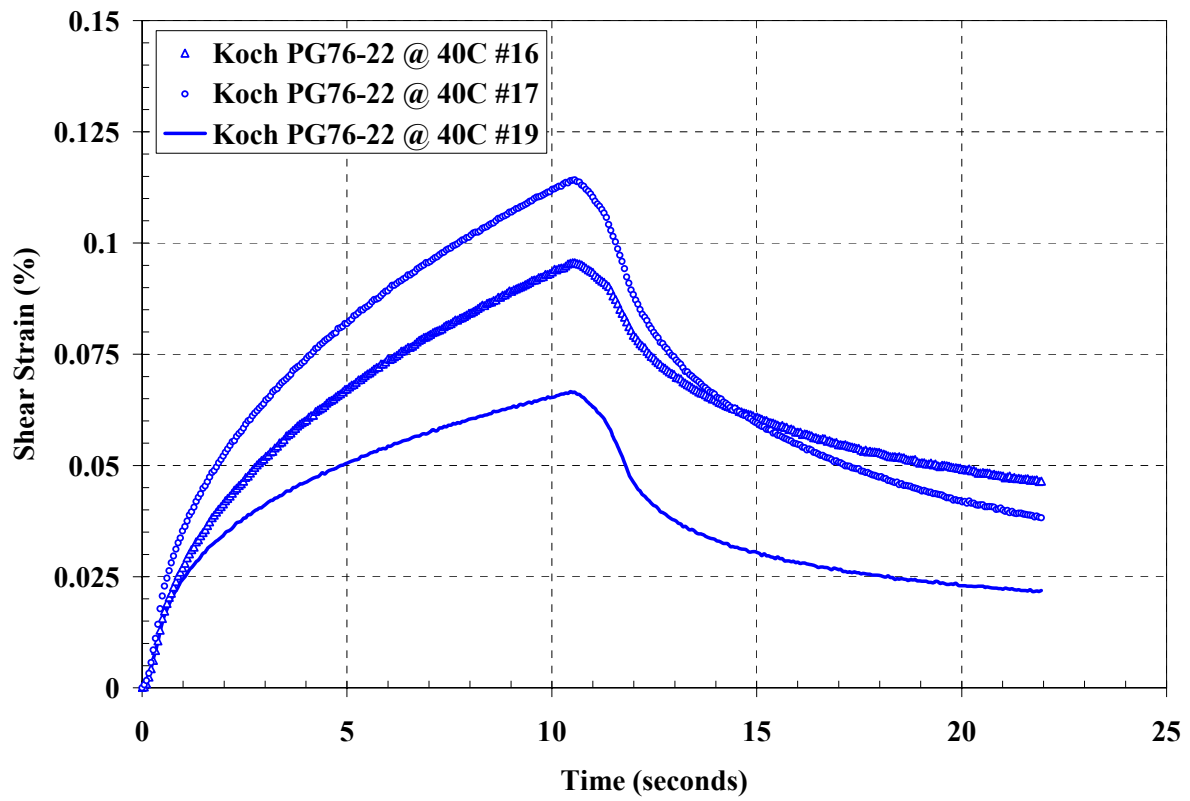
Appendix D.4 – SSCH Results for Creanova Vestoplast
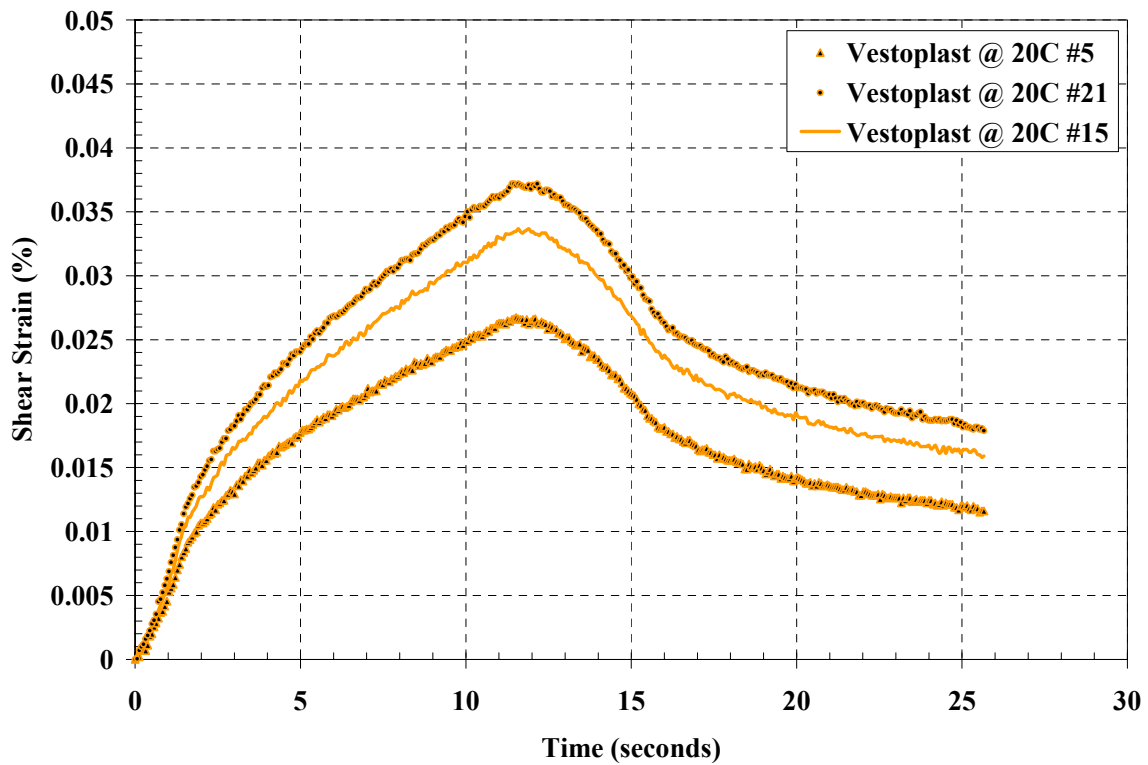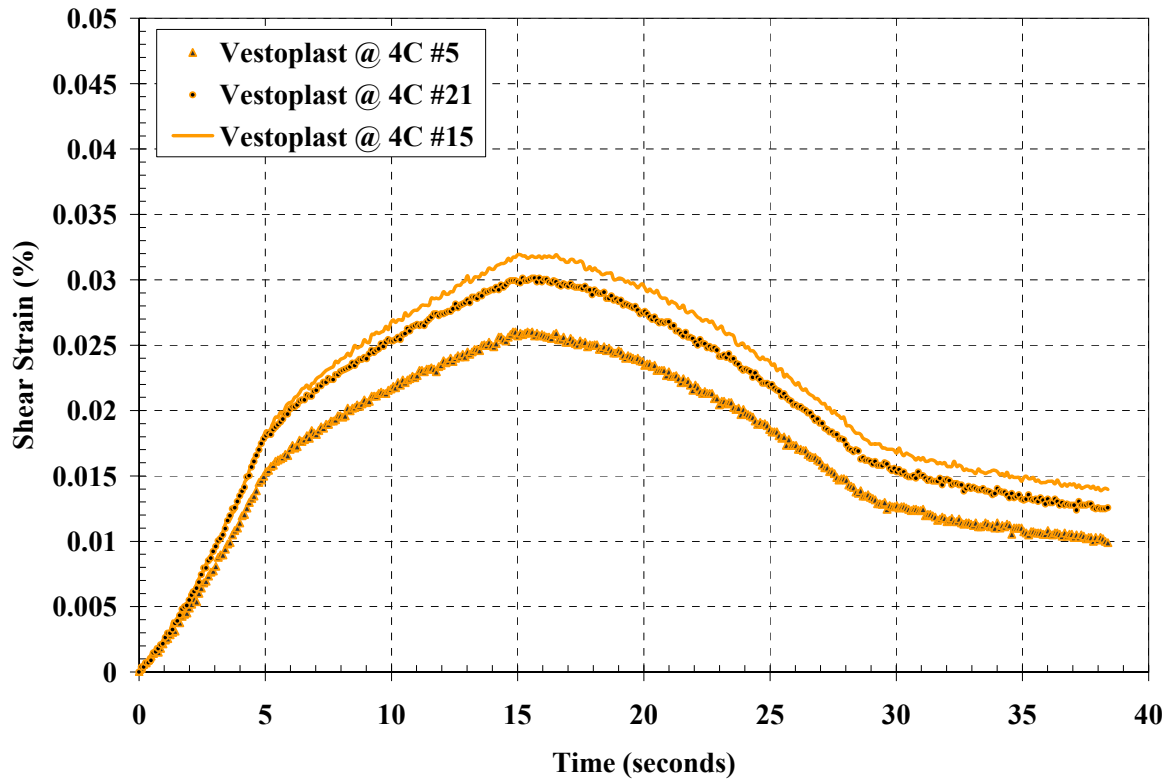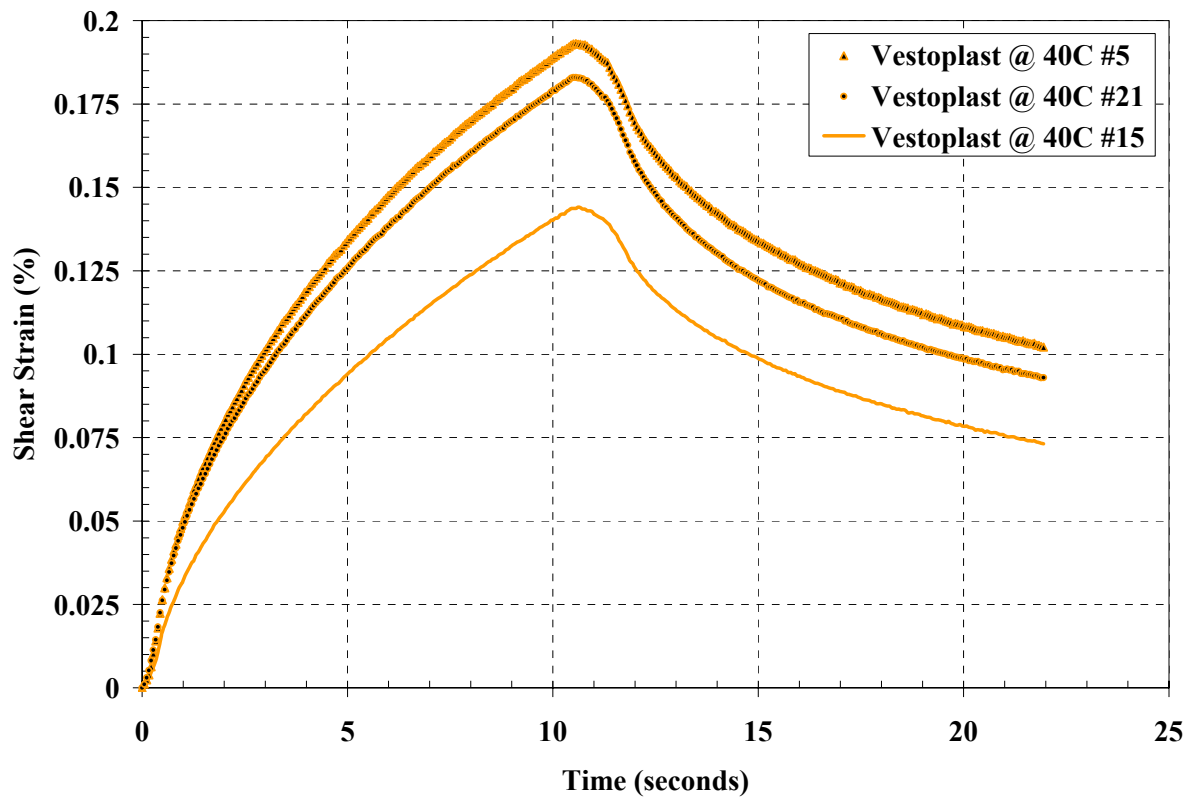
Appendix D.5 – SSCH Results of Eastman EE2
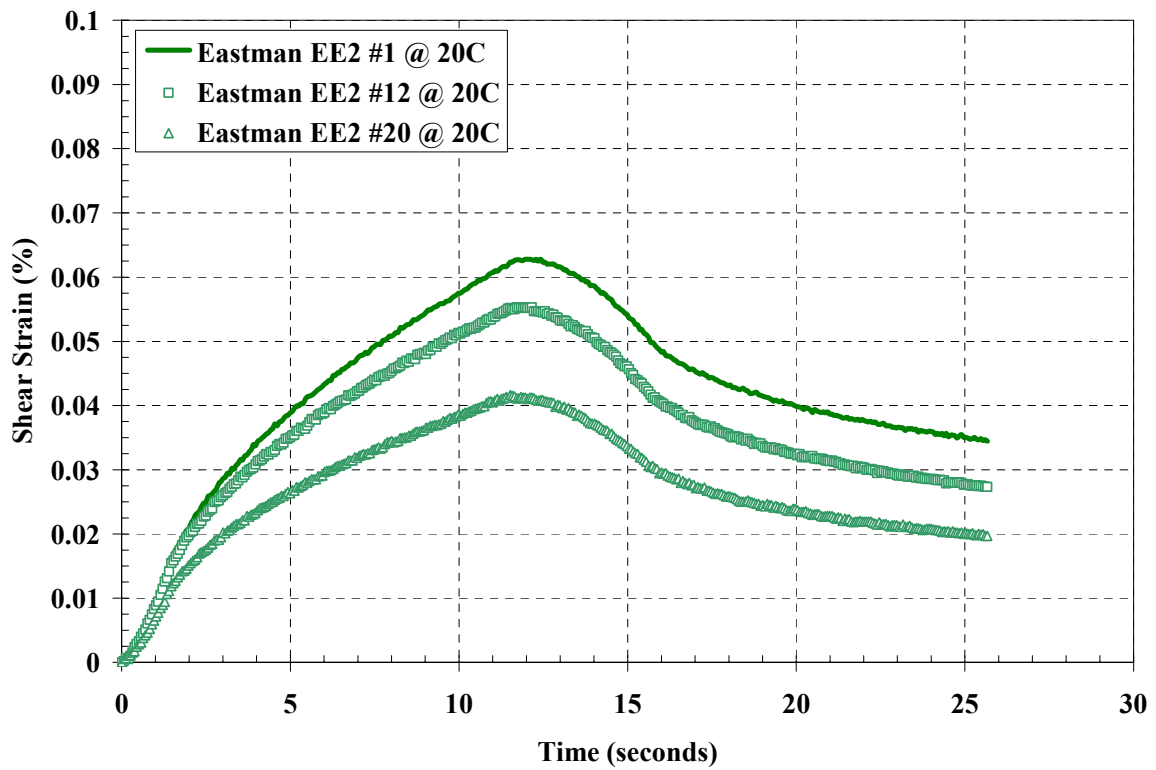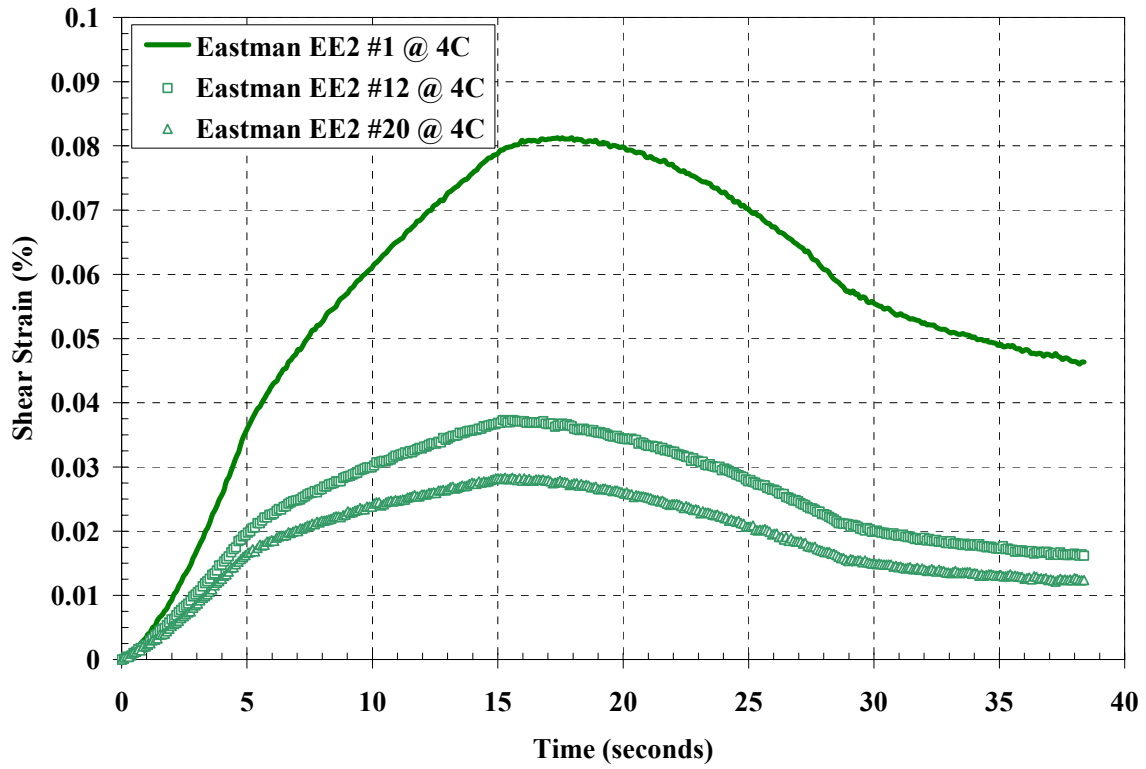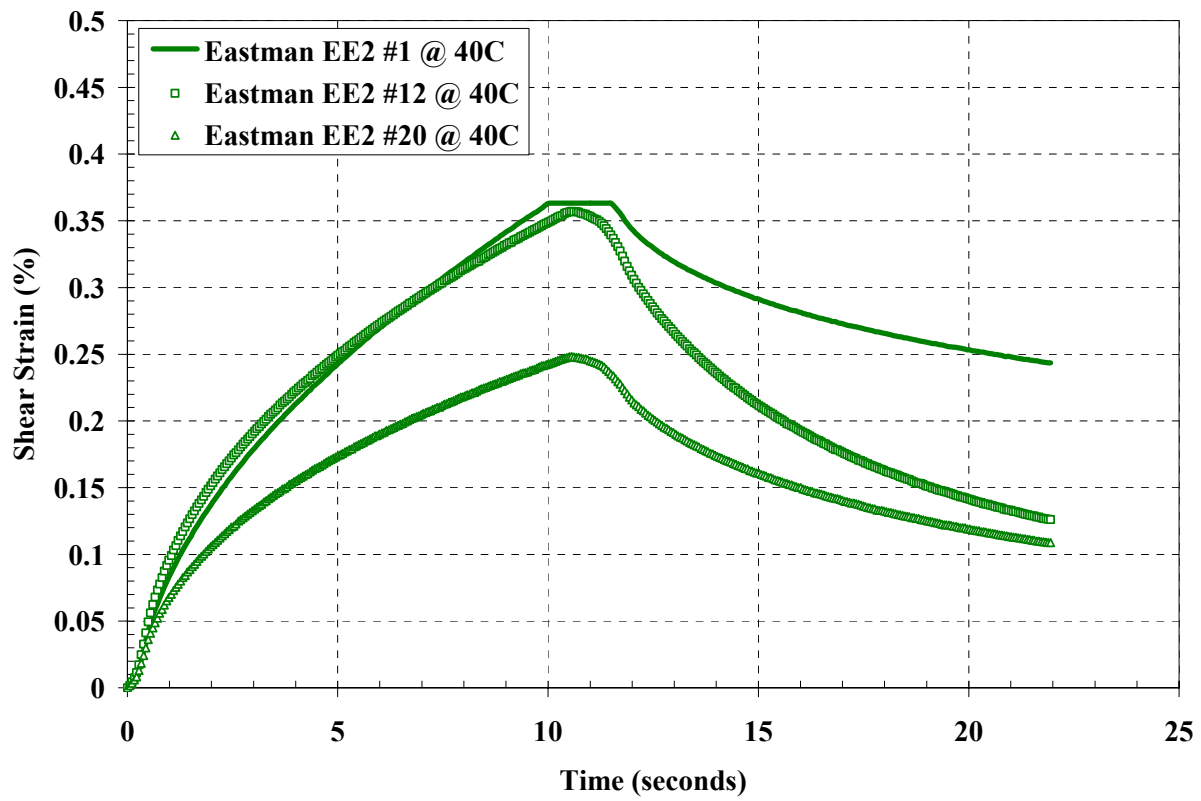
Appendix D.6 – SSCH Results for HTI Carbon Black
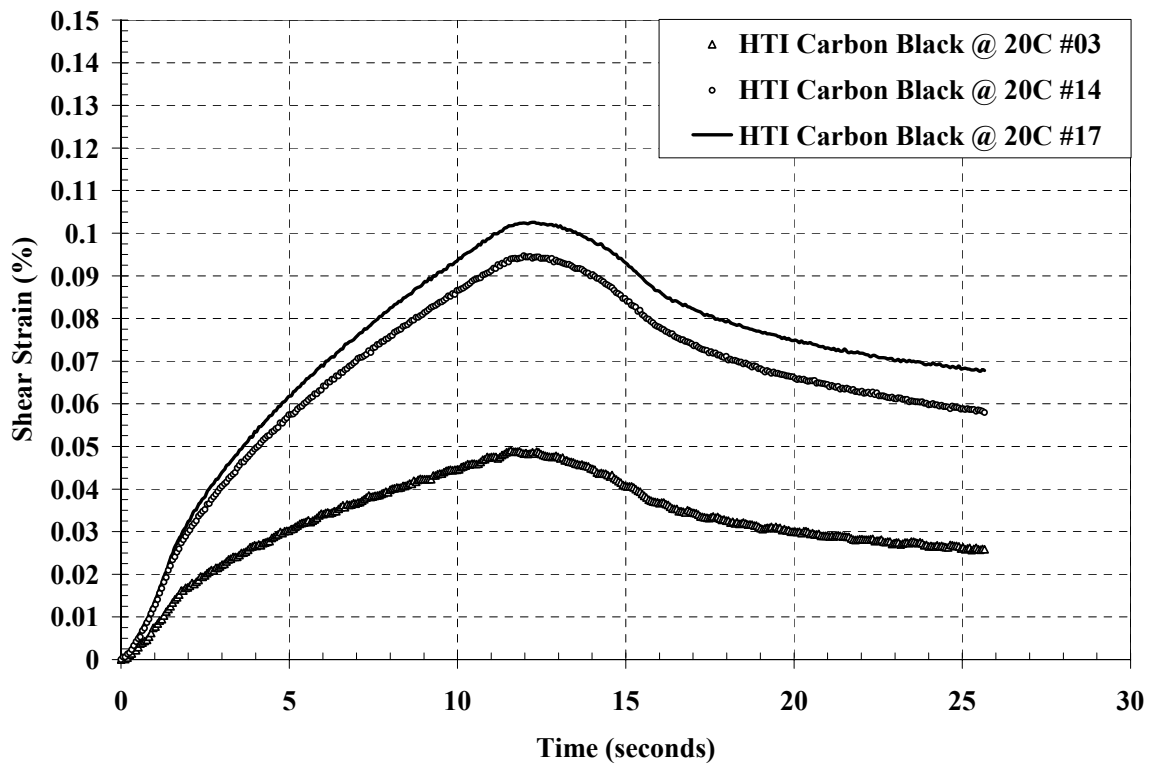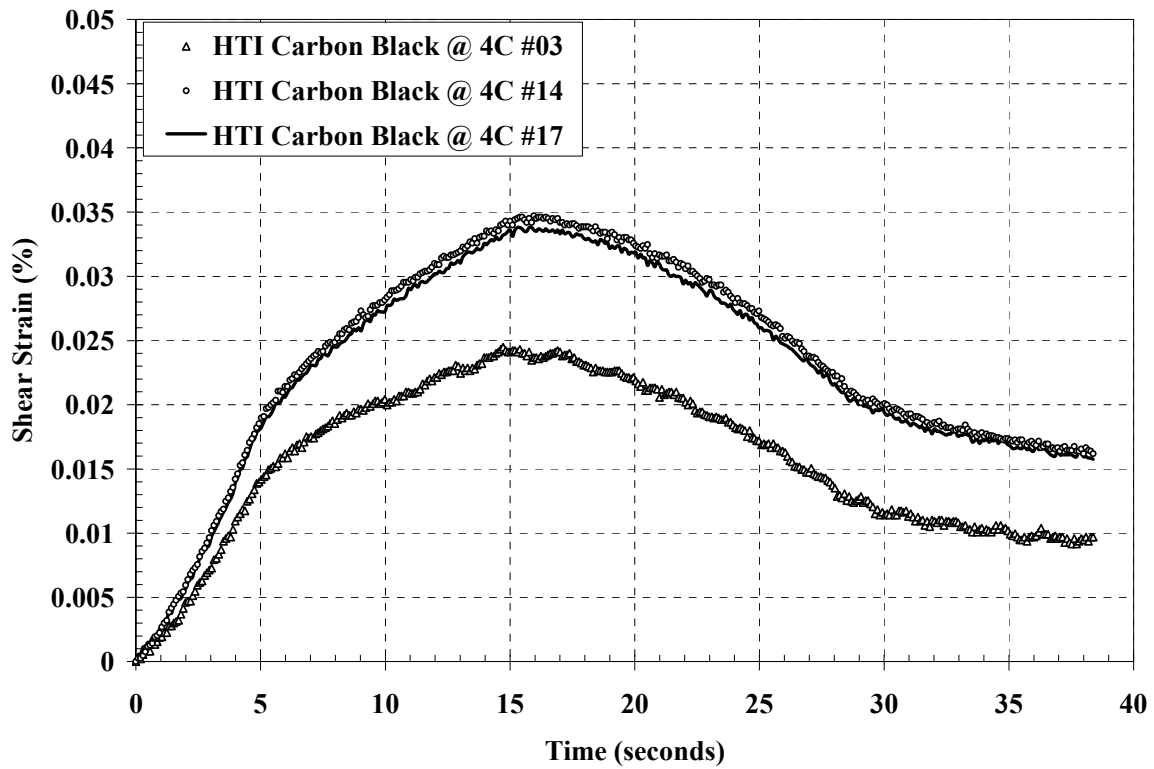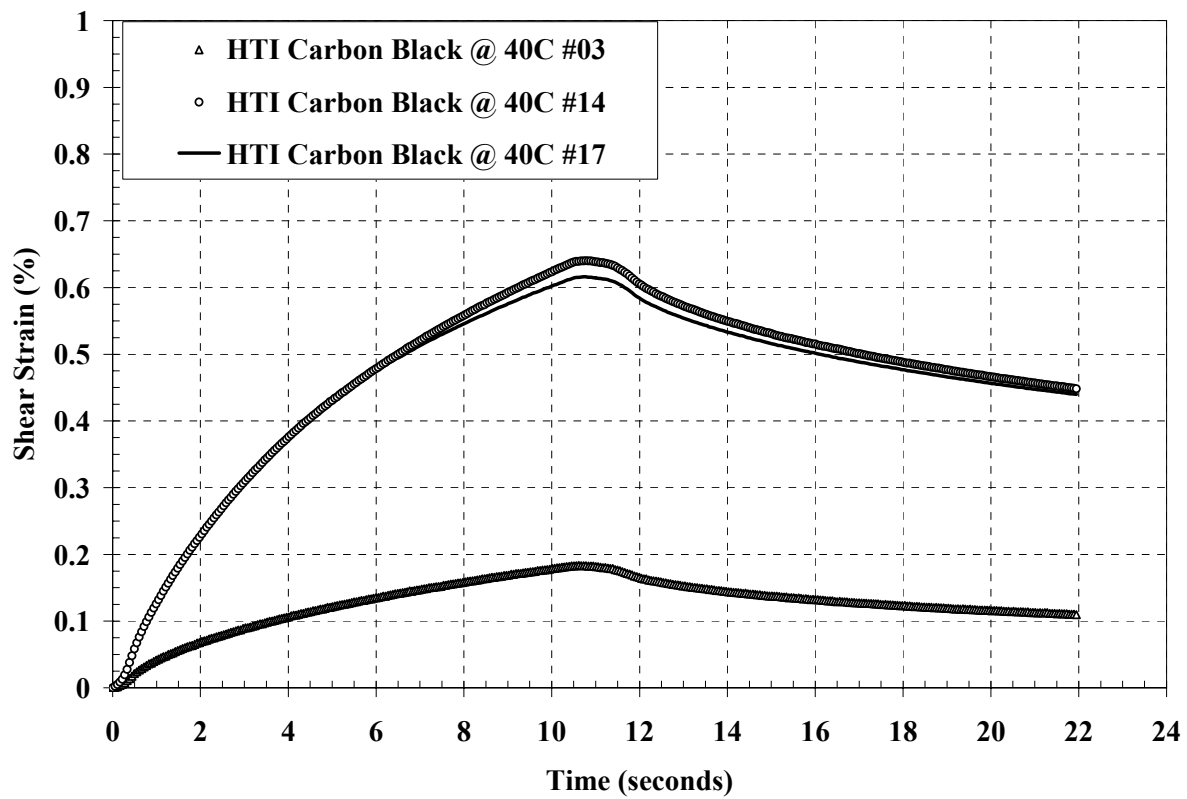
APPENDIX E – LTOA AND STOA COMPARISONS
Appendix E.1.2 – FSCH Results for LTOA and STOA Citgo PG64-22
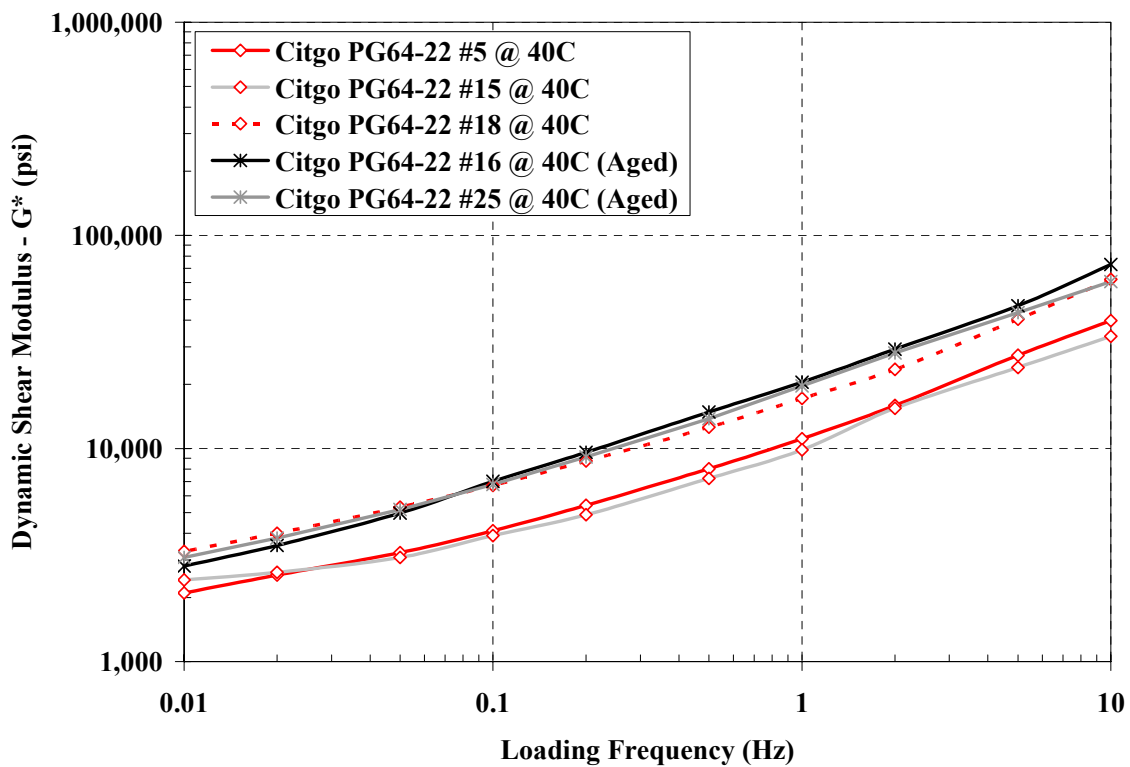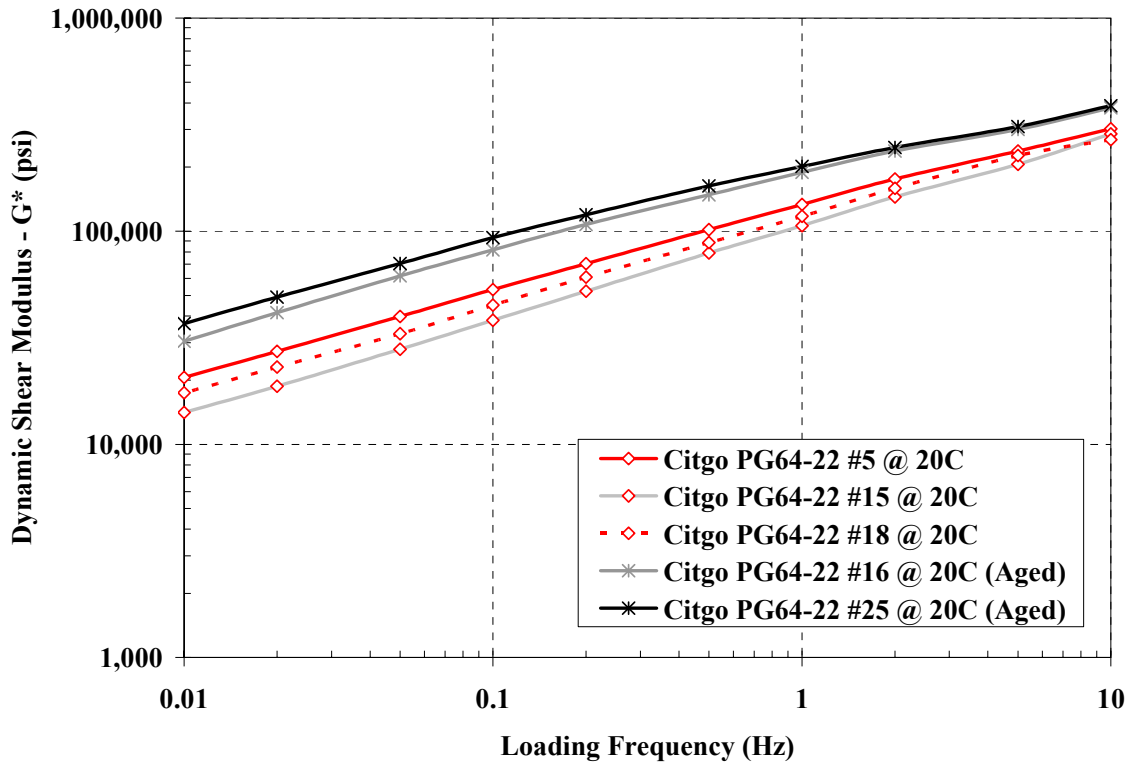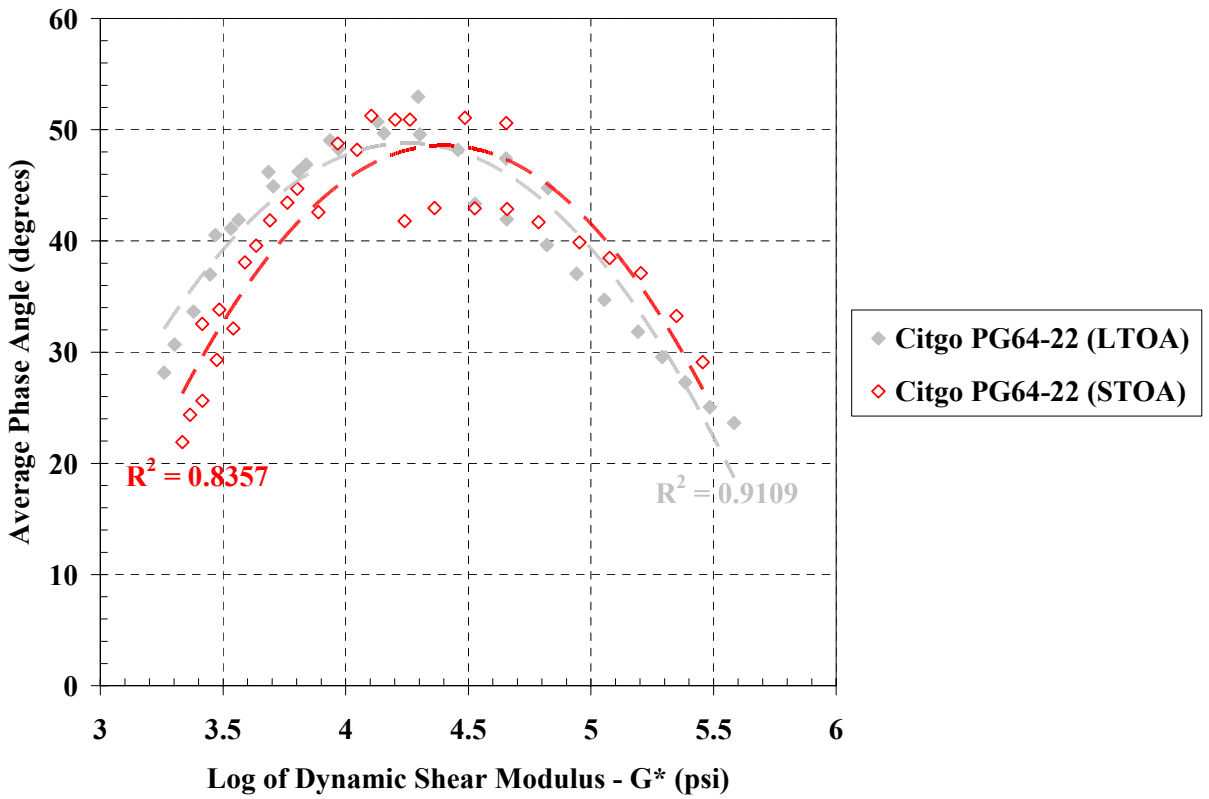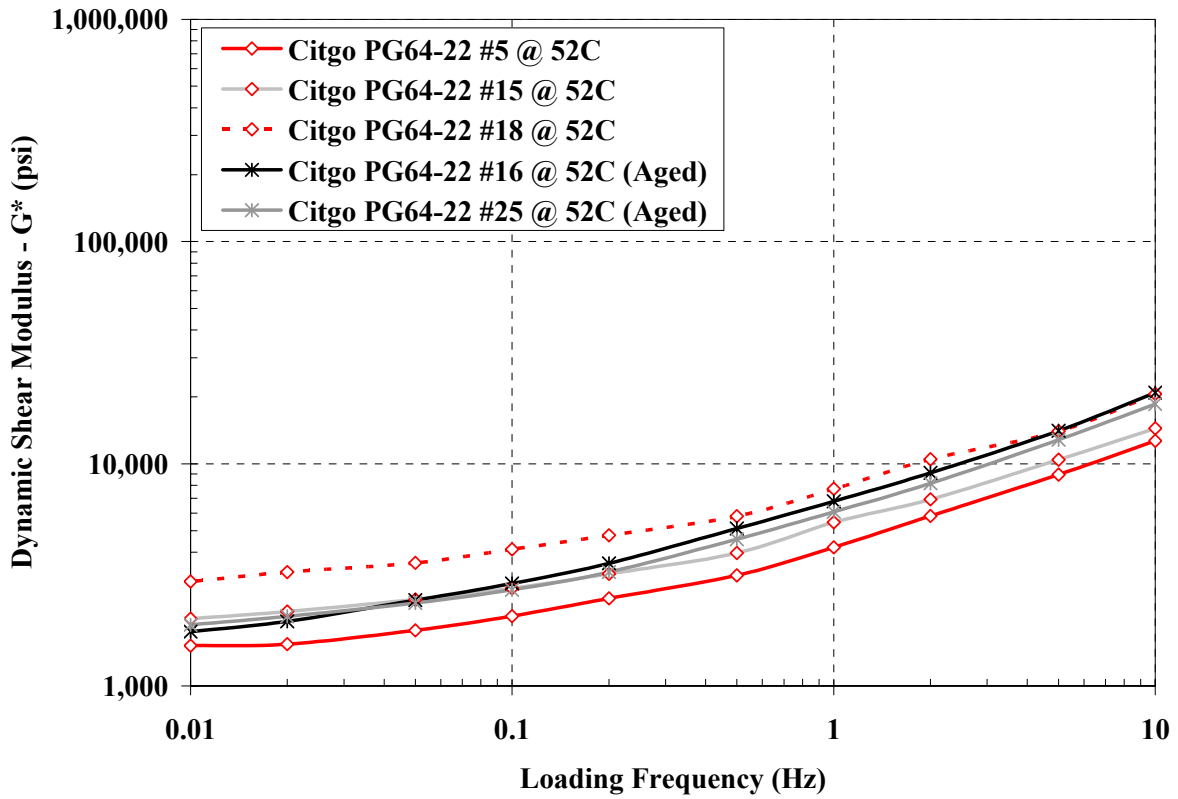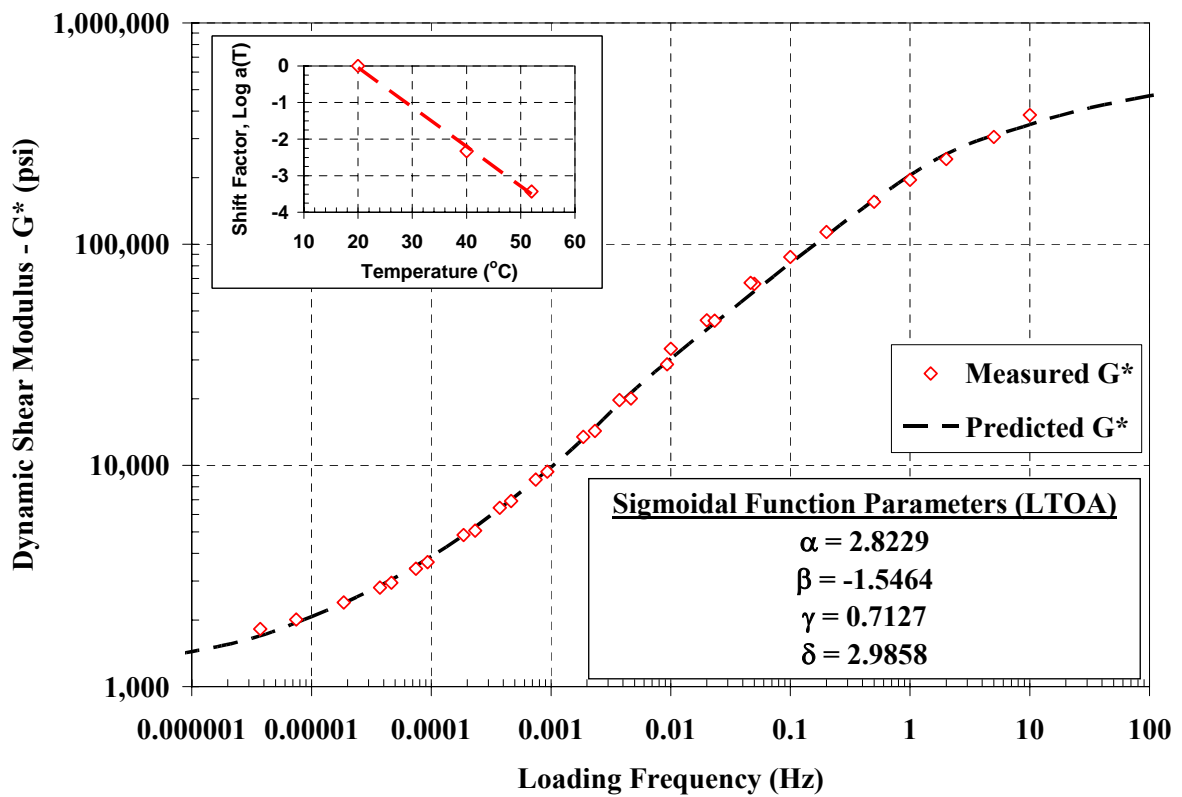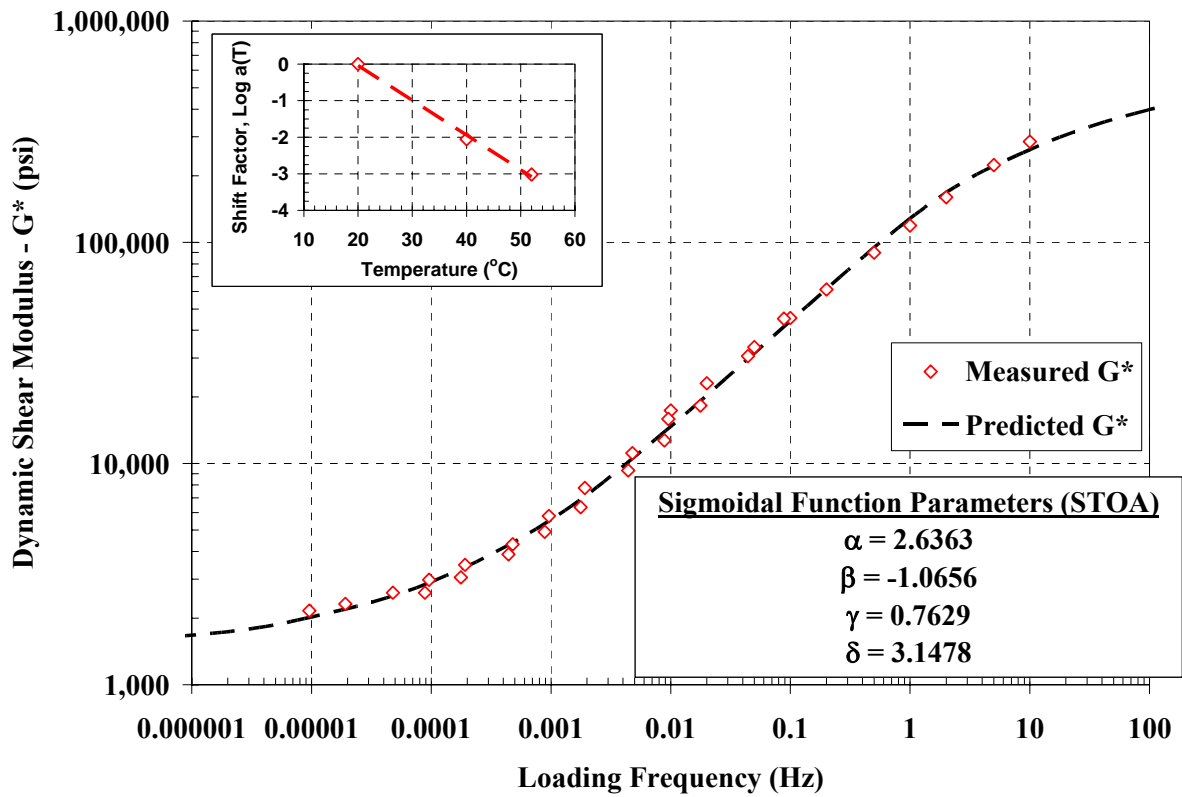
Appendix E.1.3 – SSCH Results for LTOA and STOA Citgo PG64-22
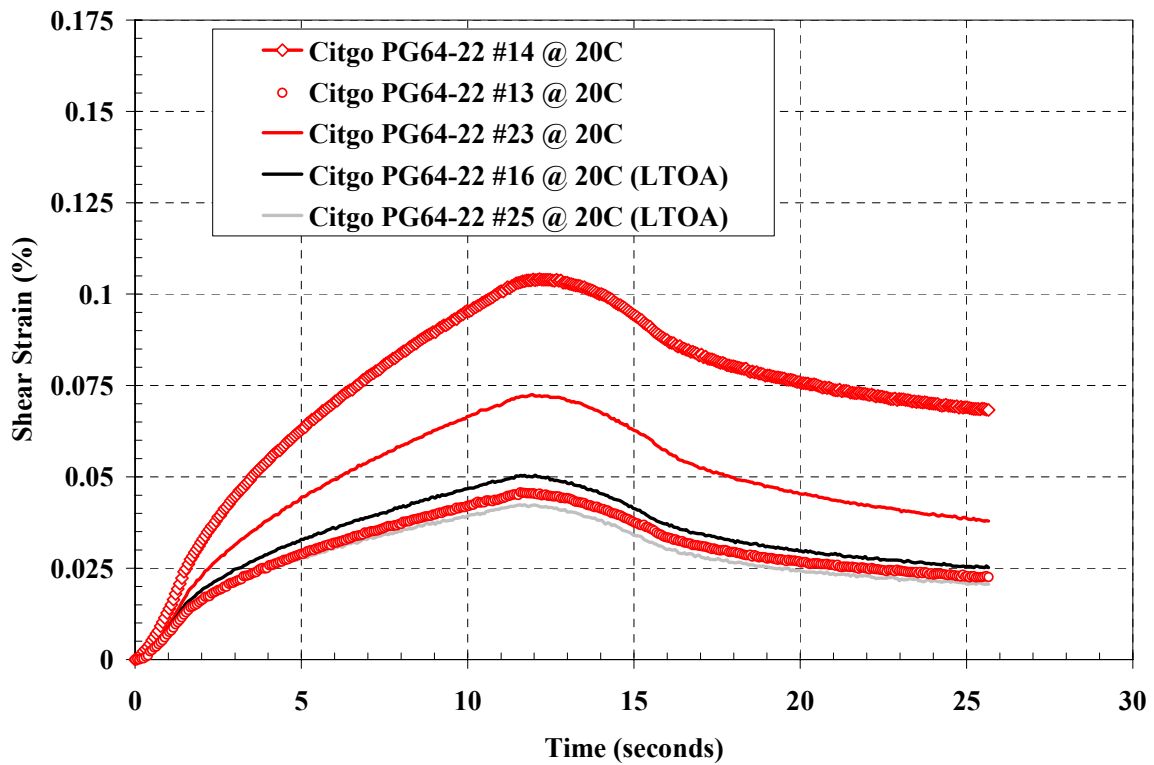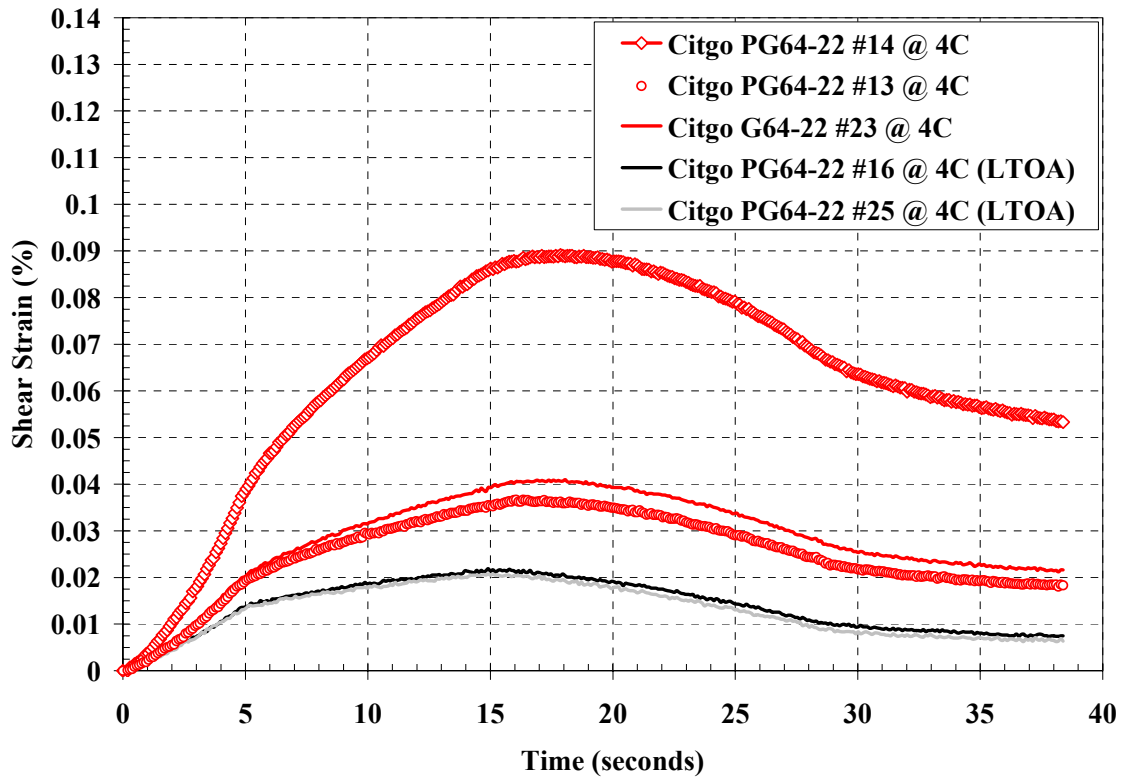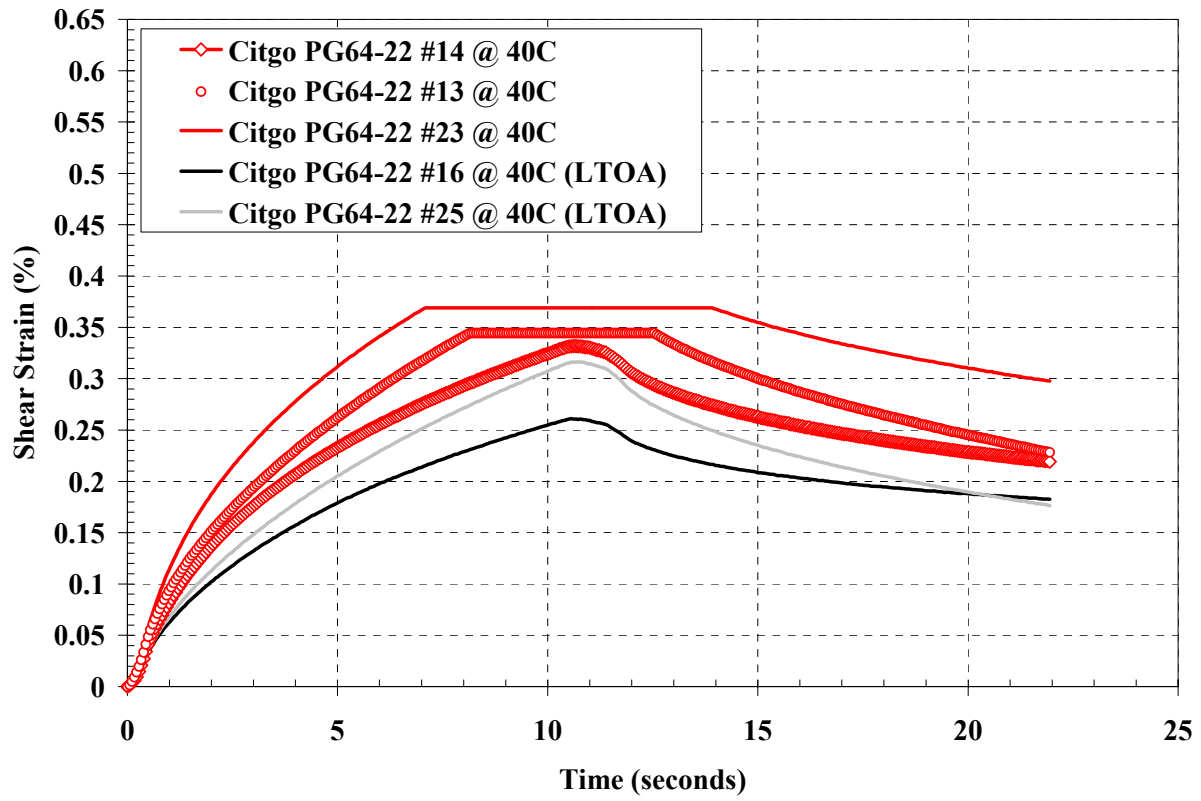
Appendix E.2.1 – RSCH Results for LTOA and STOA Citgo PG76-22
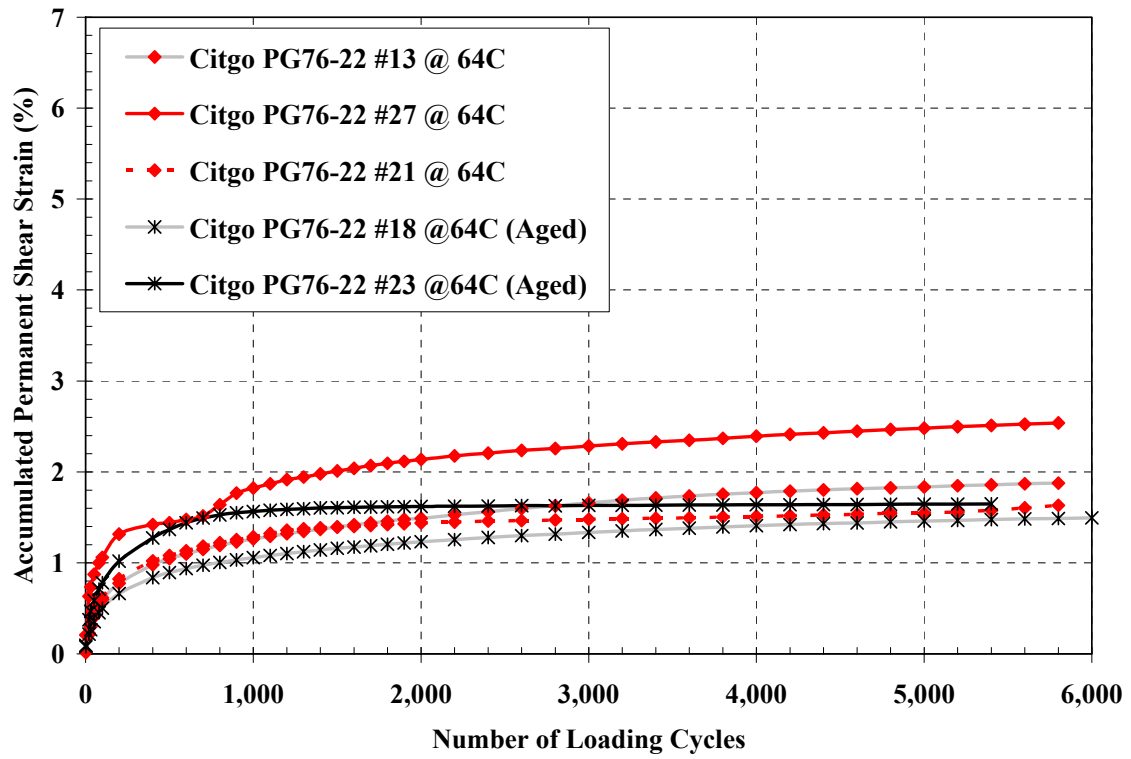
Appendix E.2.2 – FSCH Results for LTOA and STOA Citgo PG76-22
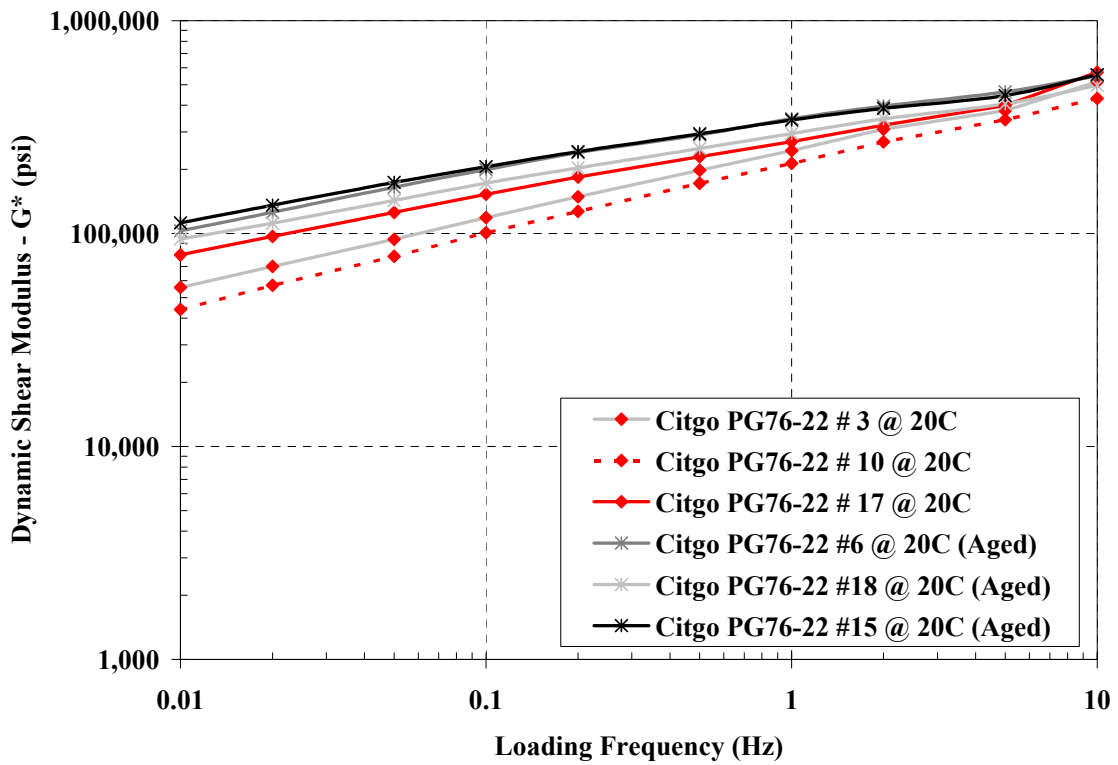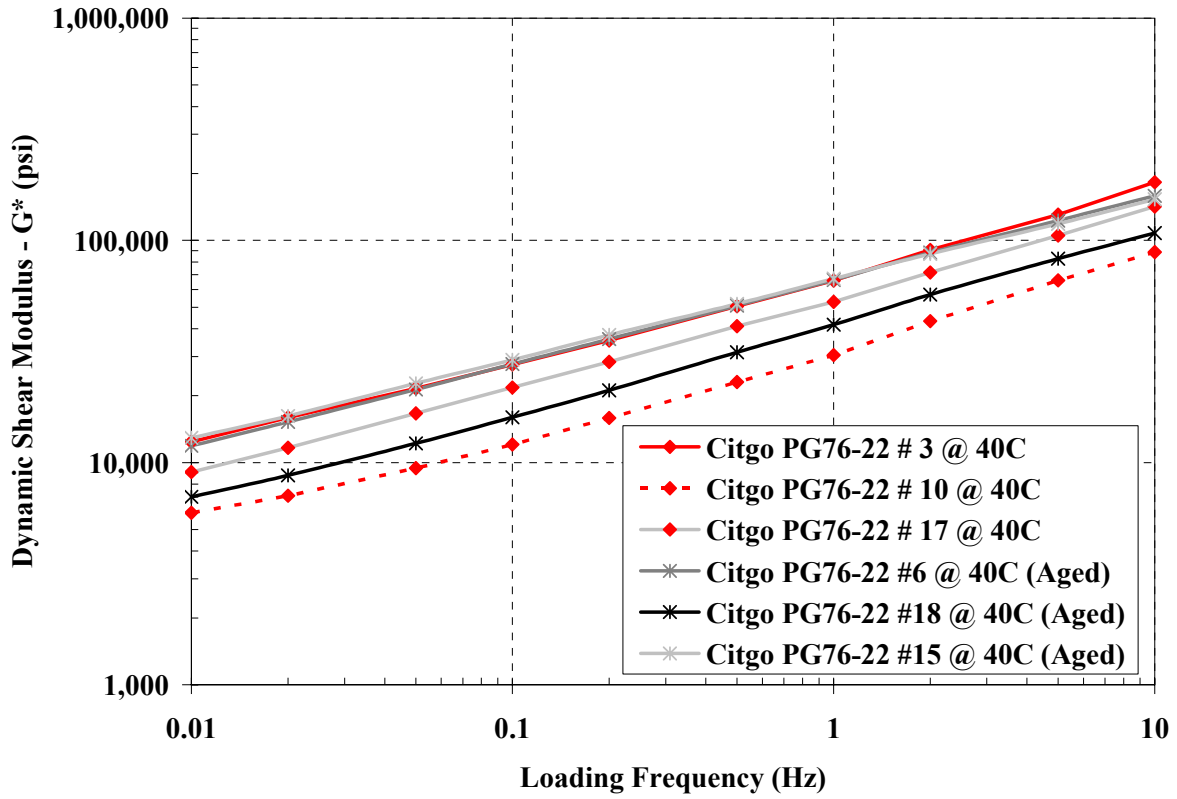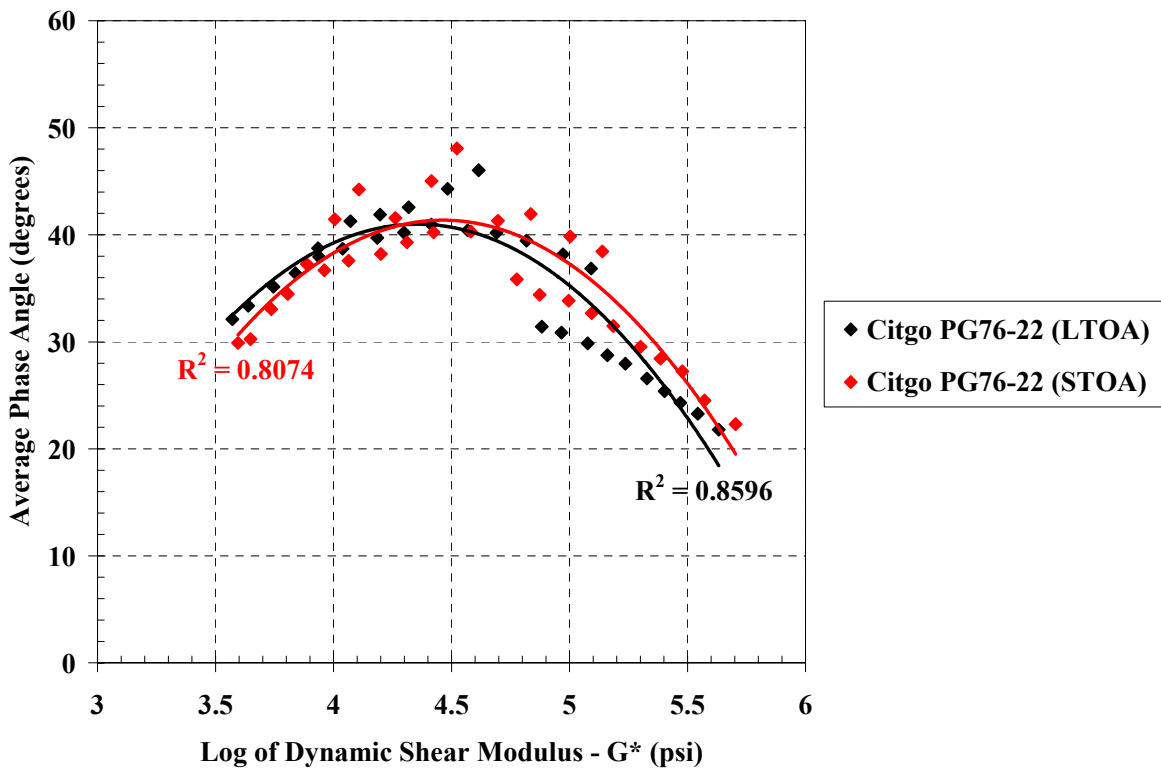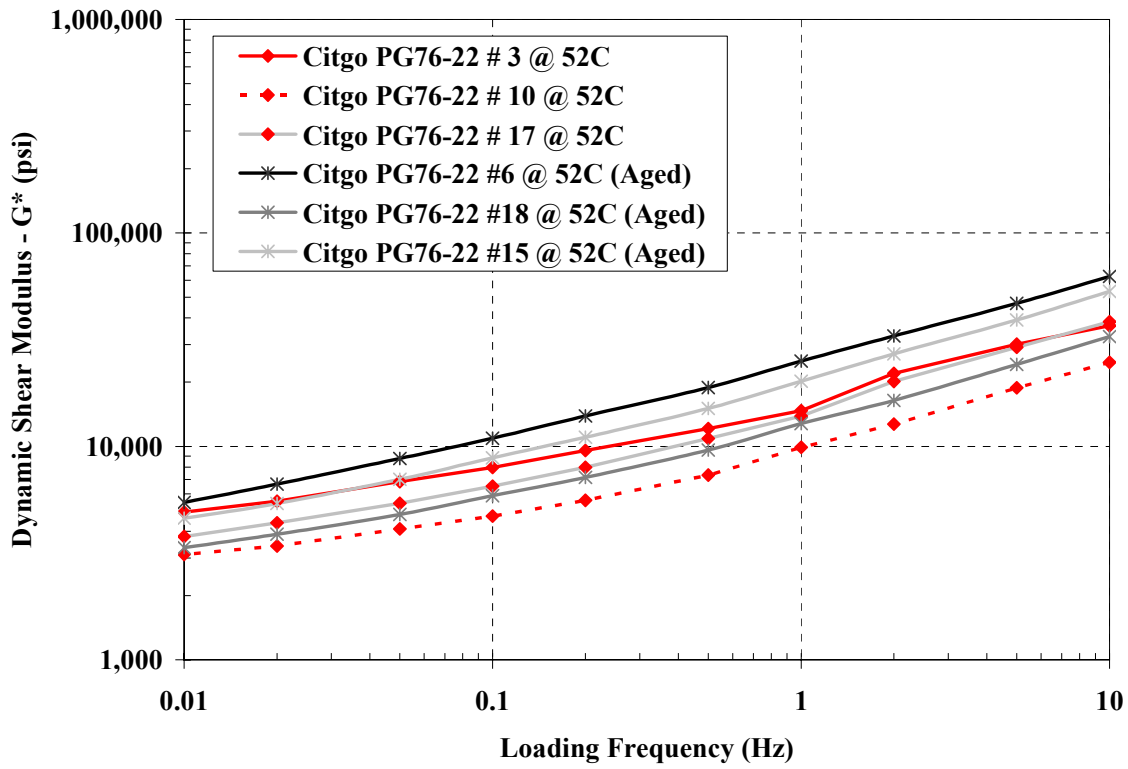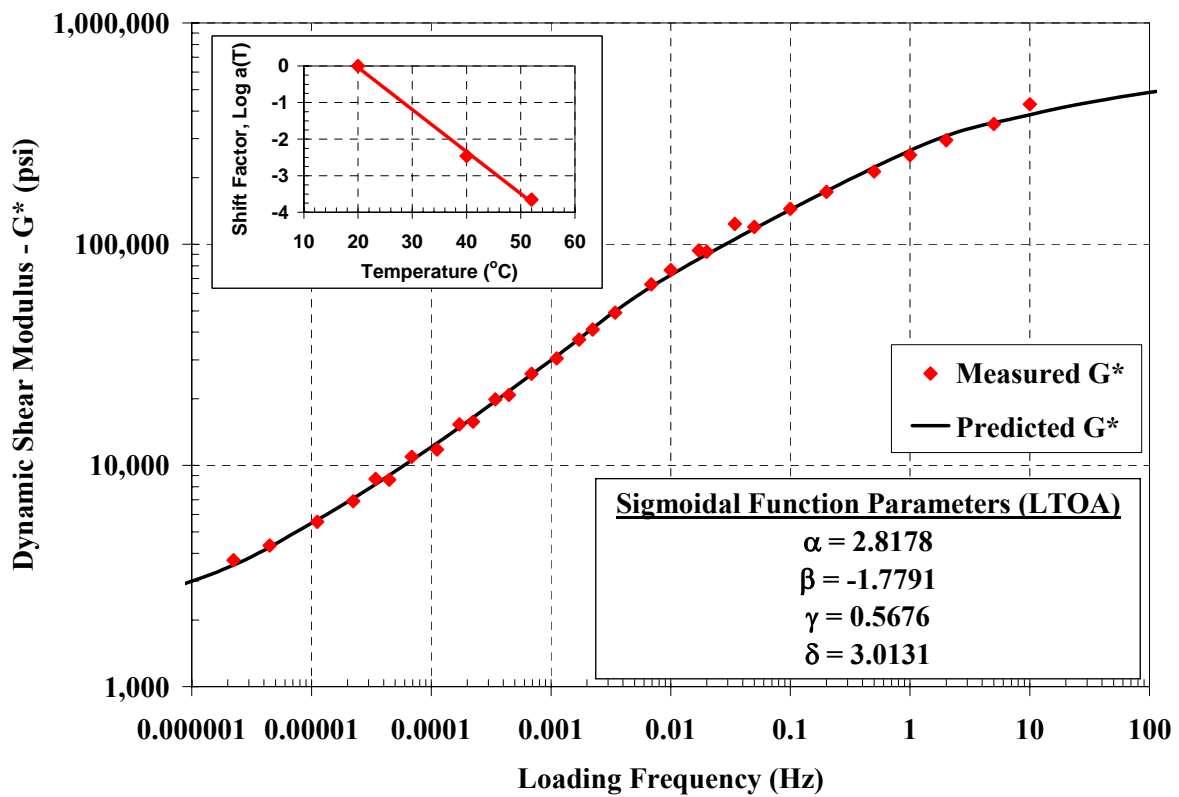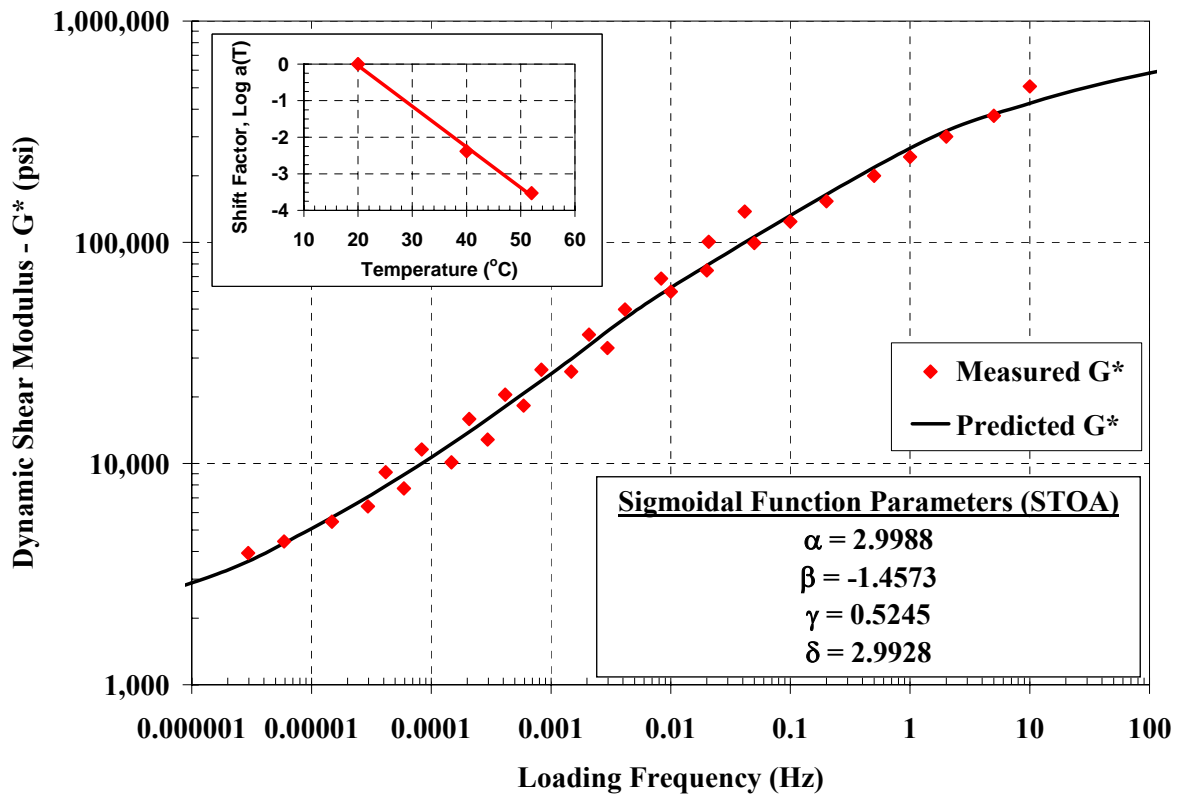
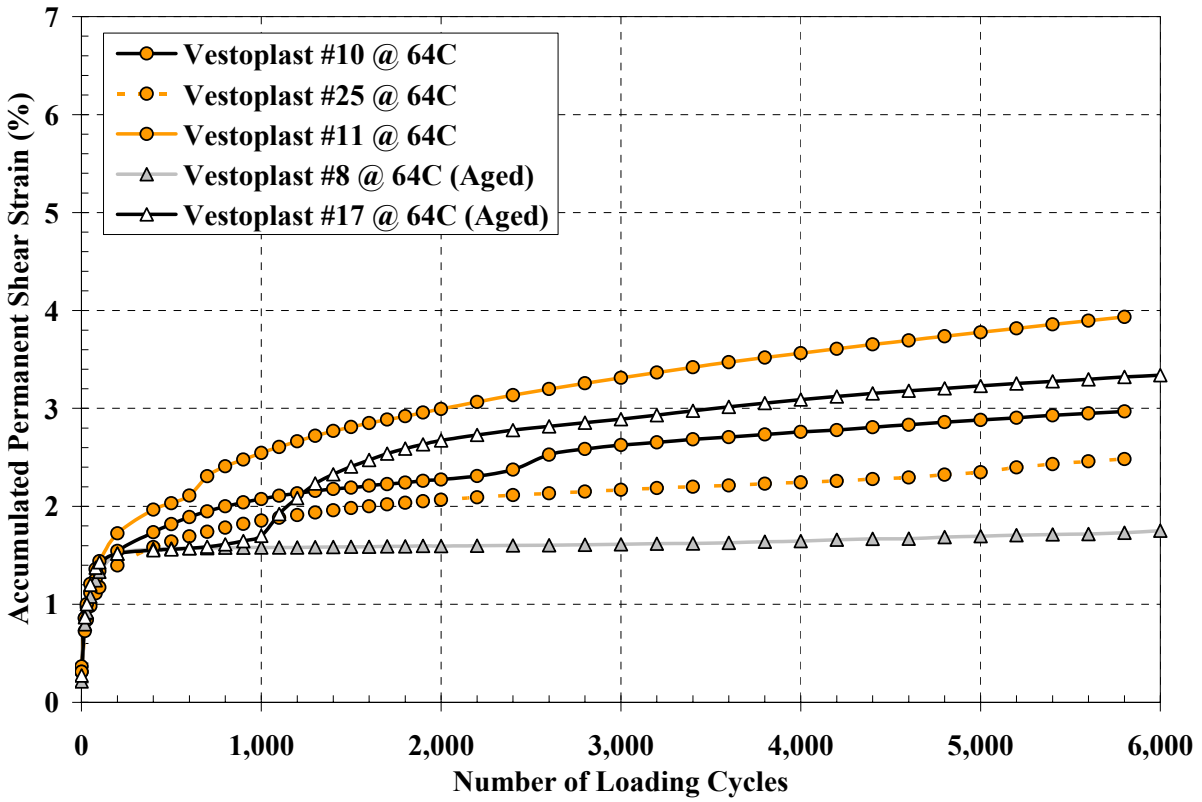Appendix E.2.3 – SSCH for LTOA and STOA Citgo PG76-22
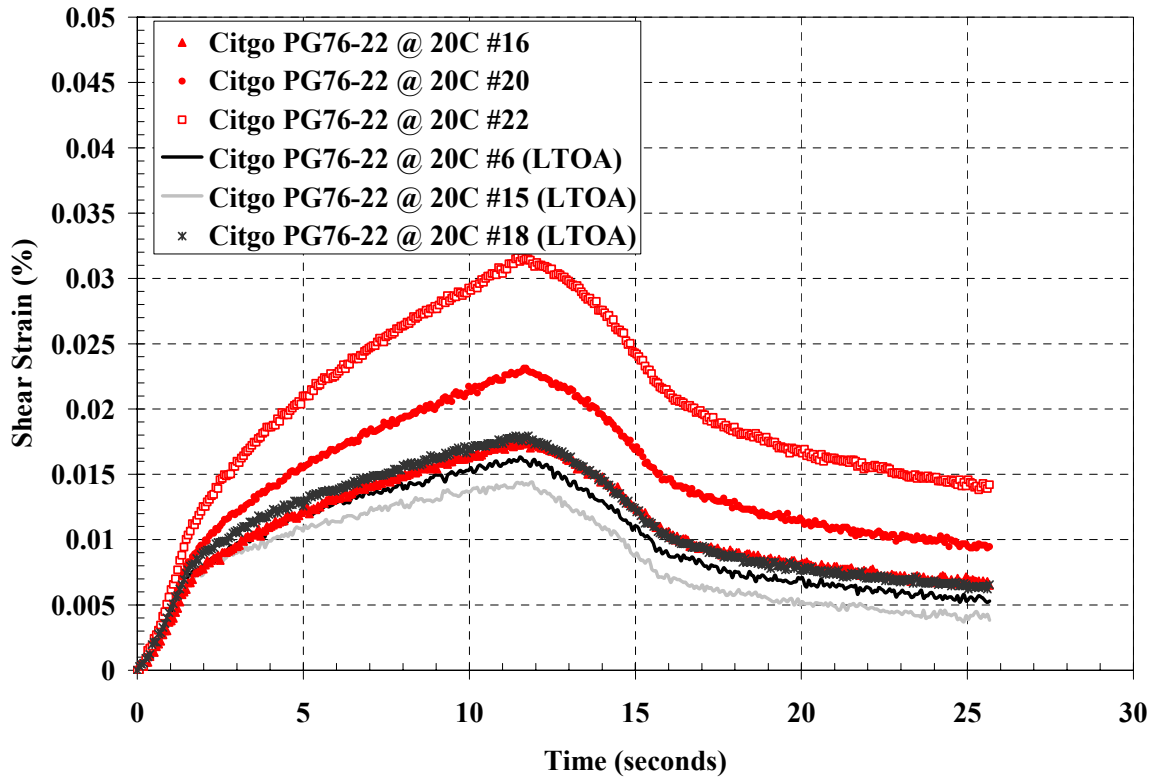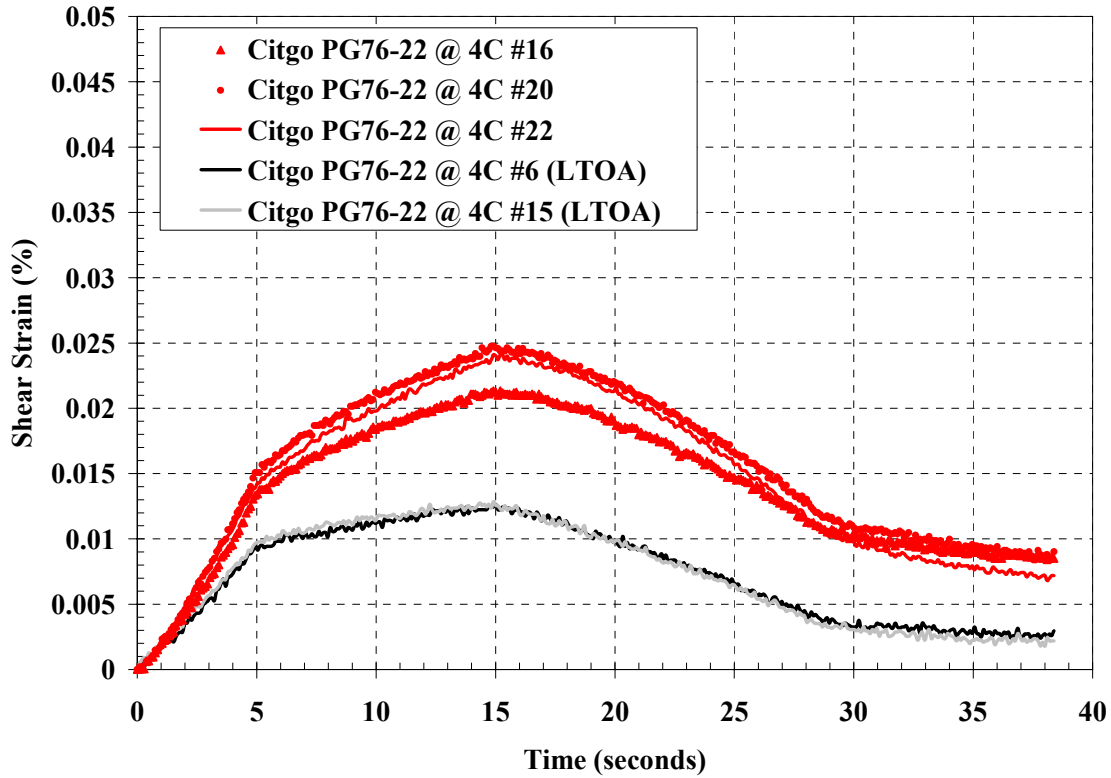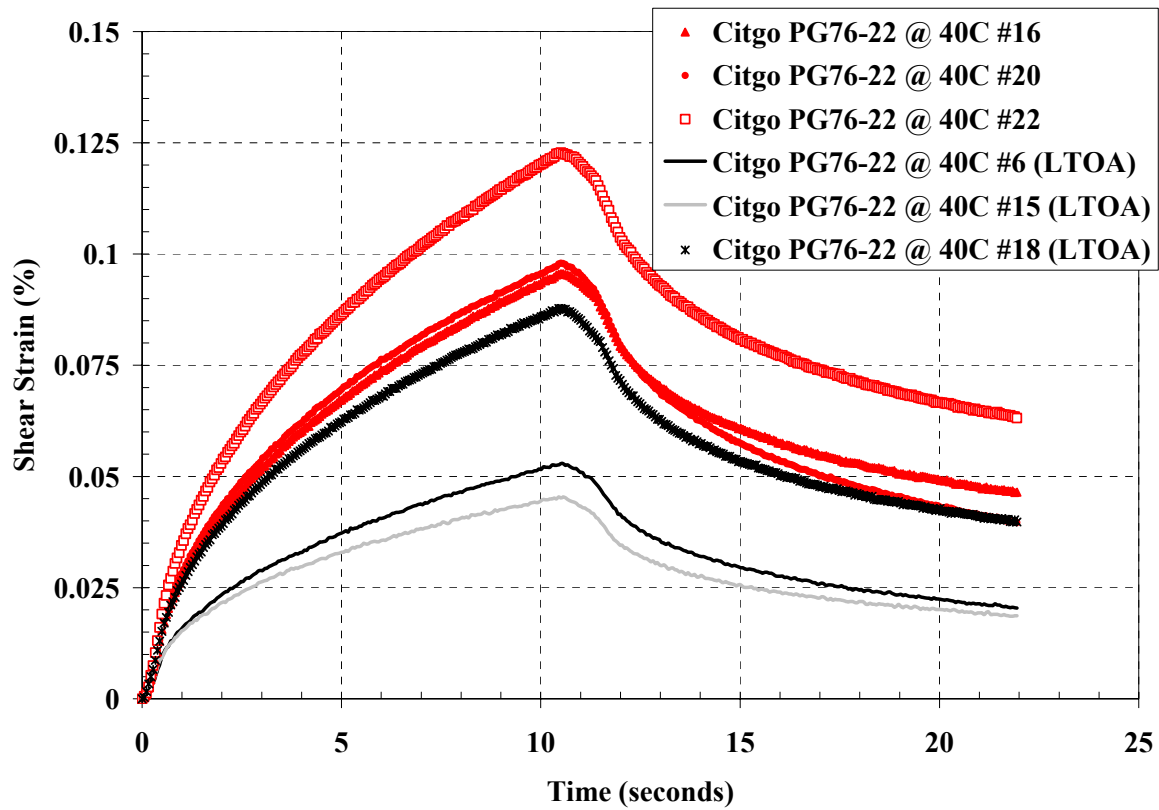
## Appendix E.3.1 – RSCH for LTOA and STOA Koch Materials PG76-22

Legend:
- Koch 76-22 #25 @ 64C
- Koch 76-22 #06 @ 64C
- Koch 76-22 #13 @ 64C
- Koch 76-22 #02 @ 64C (Aged)
- Koch 76-22 #23 @ 64C (Aged)

X-axis: Number of Loading Cycles
Y-axis: Accumulated Permanent Shear Strain (%)
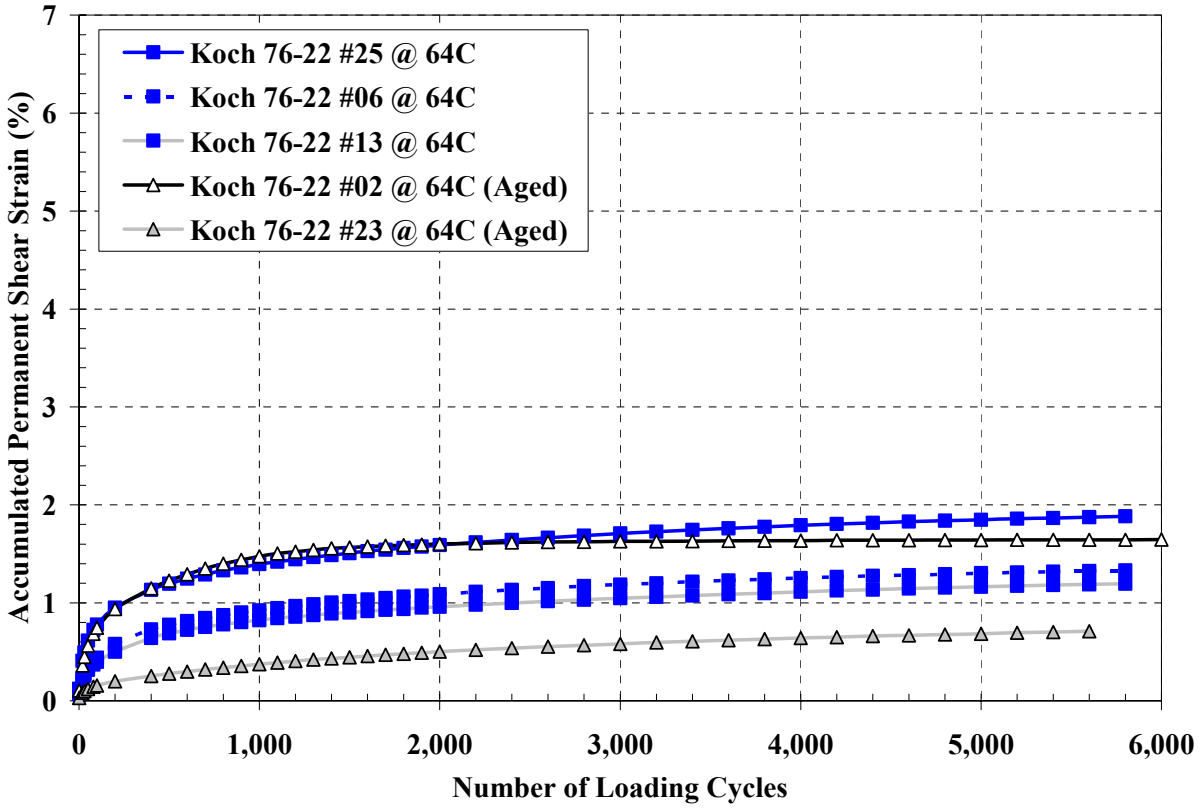
Appendix E.3.2 – FSCH for LTOA and STOA Koch Materials PG76-22

Top figure — Dynamic Shear Modulus vs Loading Frequency (STOA):

- Y-axis: Dynamic Shear Modulus – G* (psi)
- X-axis: Loading Frequency (Hz)
- Inset: Shift Factor, Log a(T) vs Temperature (°C)
- Legend: Measured G*, Predicted G*

Sigmoidal Function Parameters (STOA)
$\alpha = 2.7788$
$\beta = -1.3025$
$\gamma = 0.4957$
$\delta = 3.1734$

Bottom figure — Dynamic Shear Modulus vs Loading Frequency (LTOA):

- Y-axis: Dynamic Shear Modulus – G* (psi)
- X-axis: Loading Frequency (Hz)
- Inset: Shift Factor, Log a(T) vs Temperature (°C)
- Legend: Measured G*, Predicted G*

Sigmoidal Function Parameters (LTOA)
$\alpha = 3.575$
$\beta = -1.7773$
$\gamma = 0.3906$
$\delta = 2.2871$

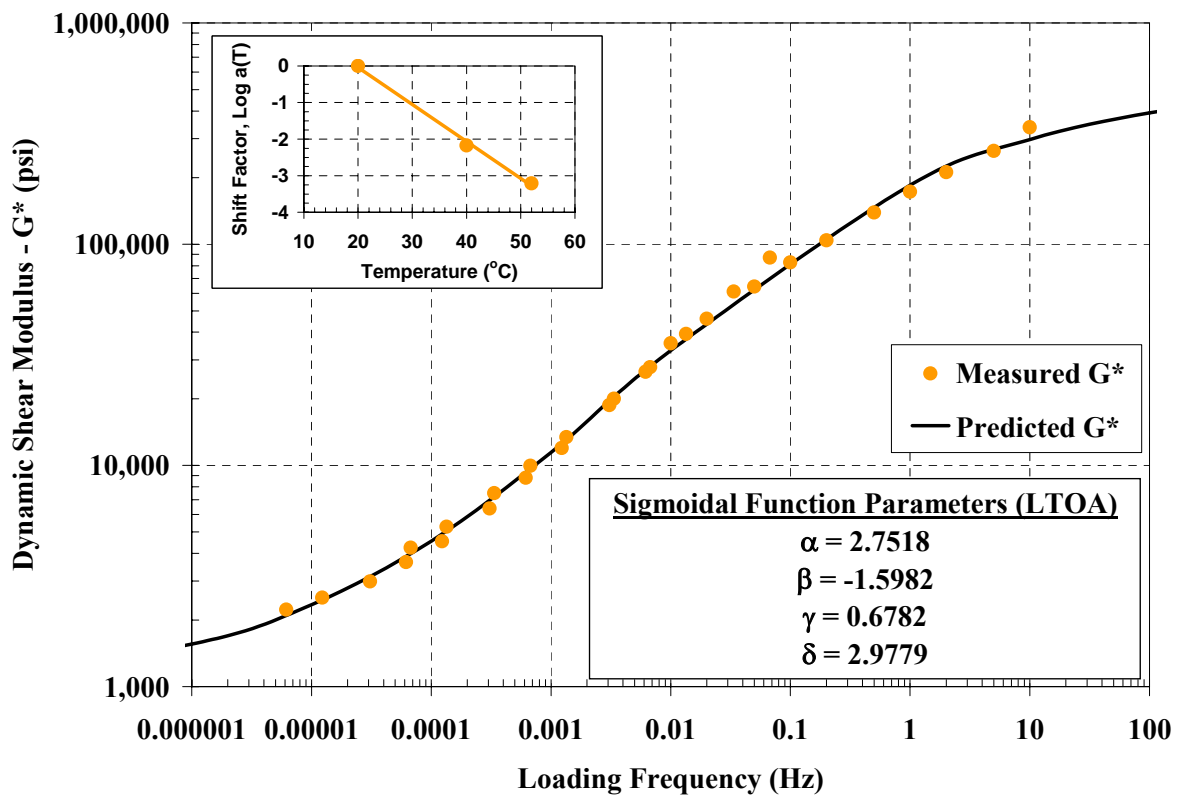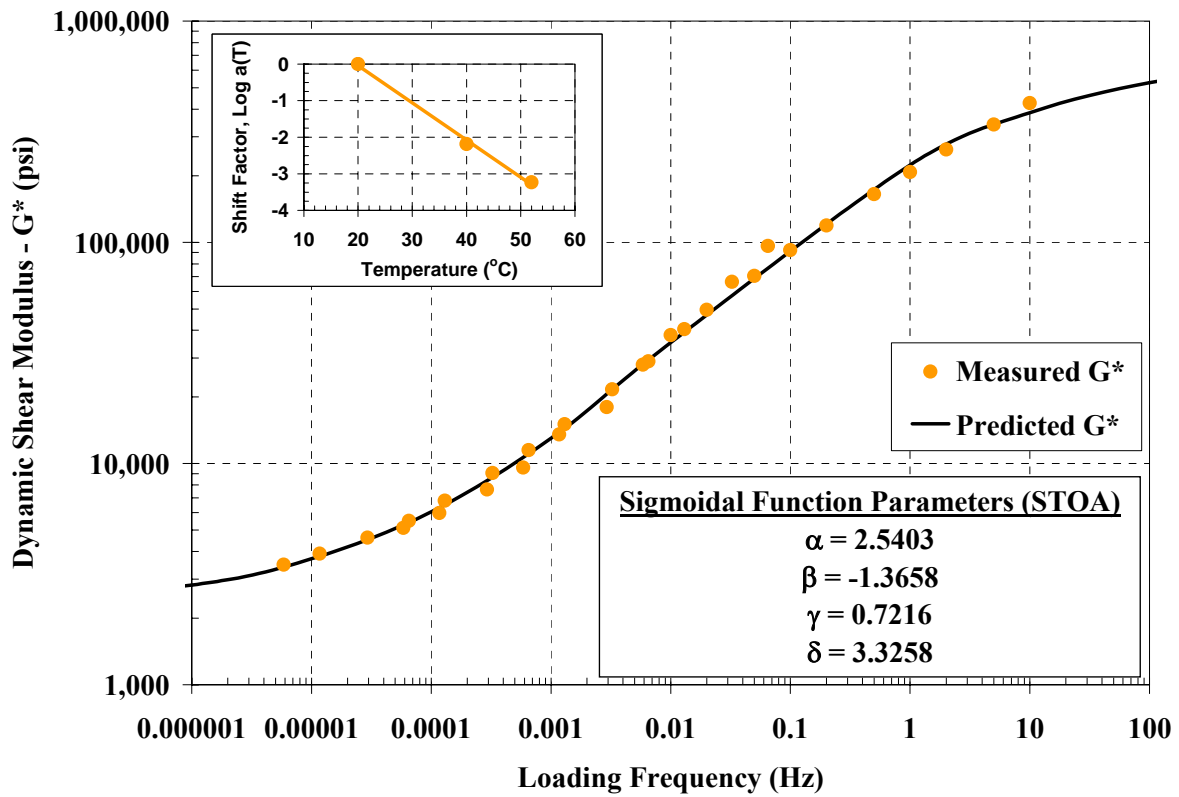Appendix E.3.3 – SSCH for LTOA and STOA Koch Materials PG76-22
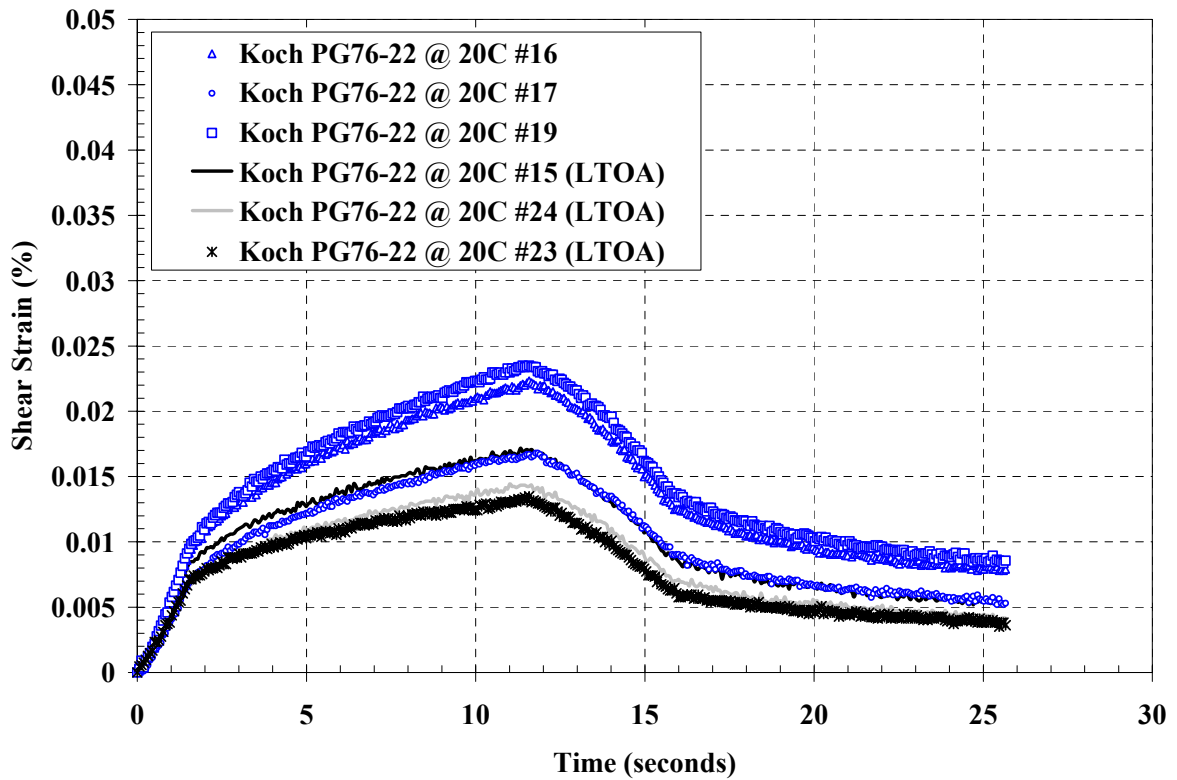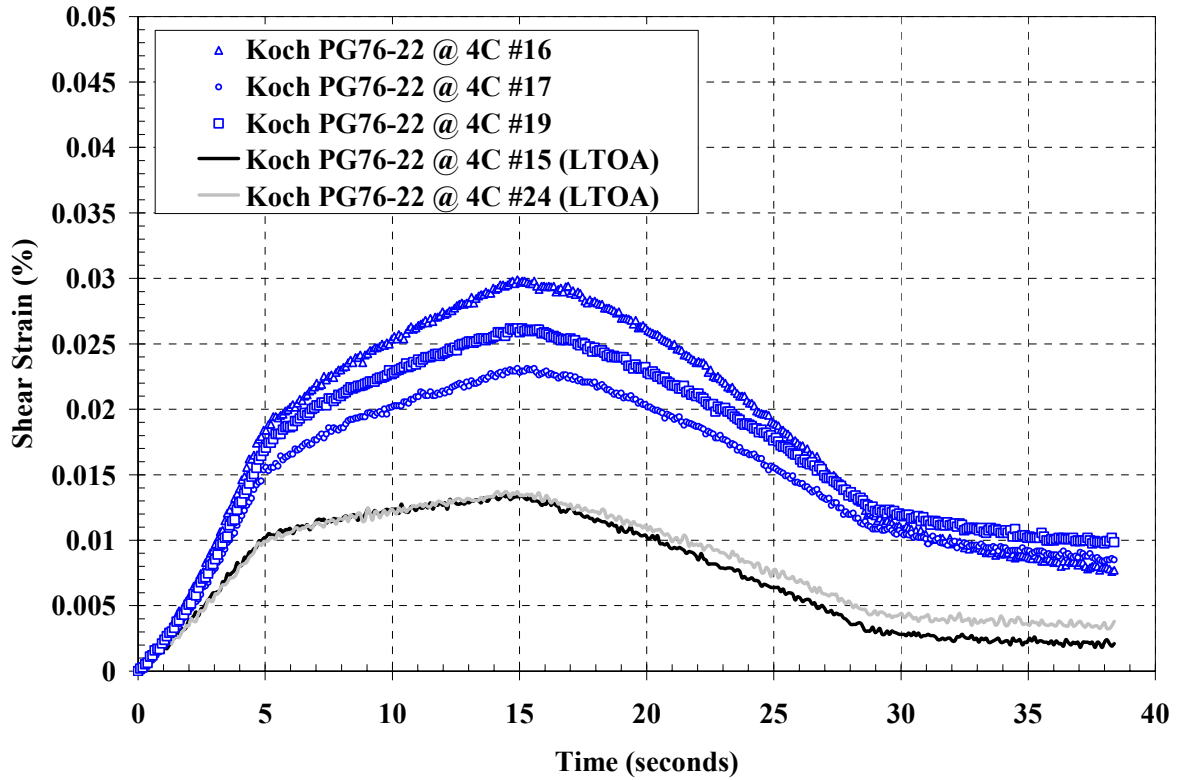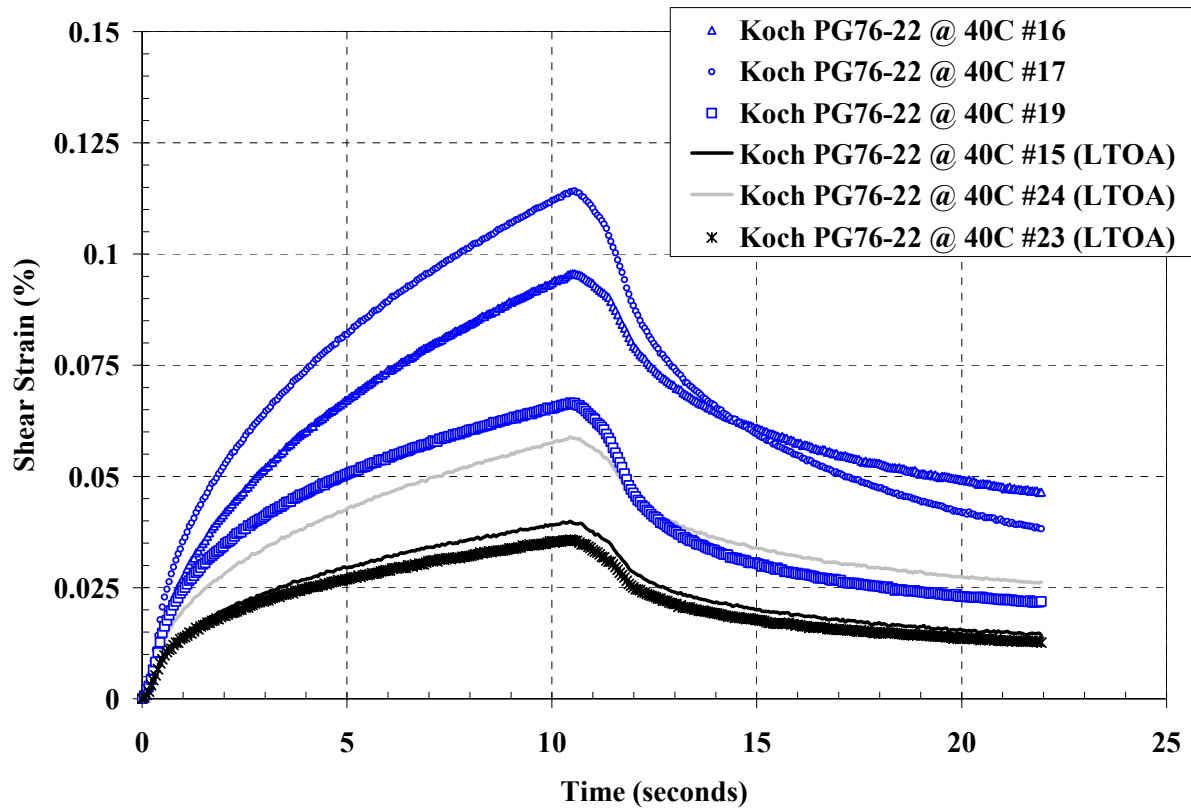
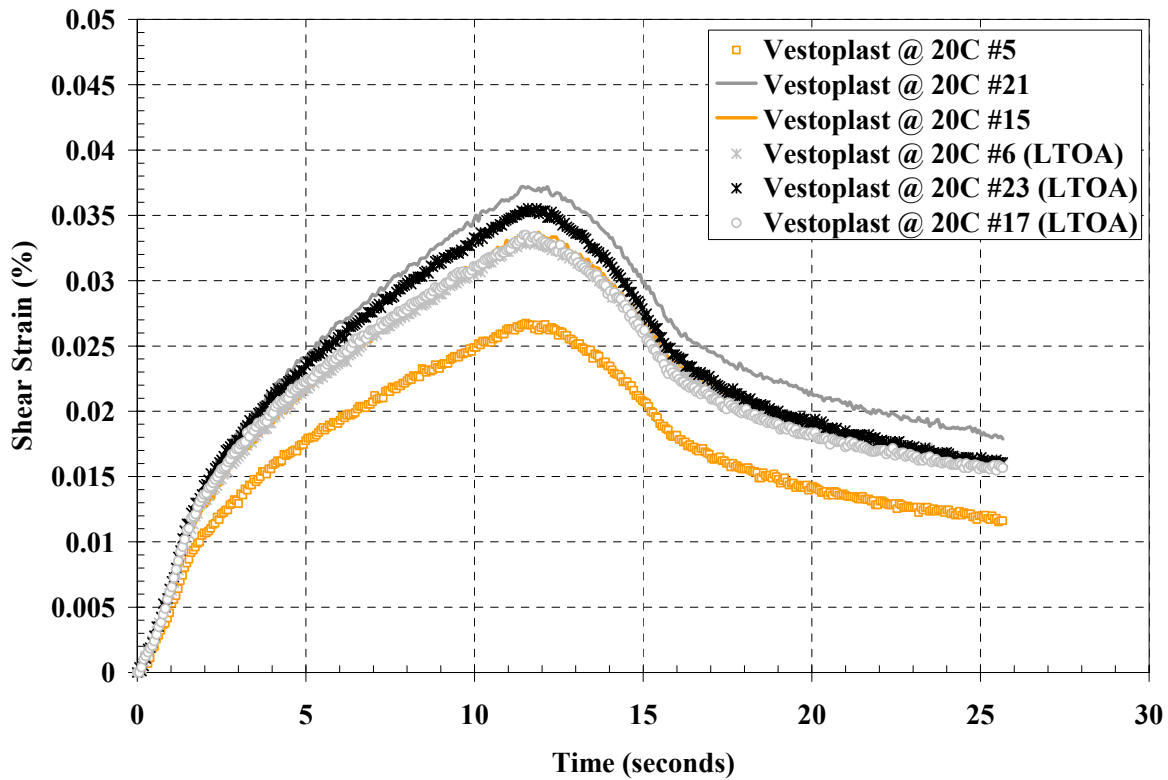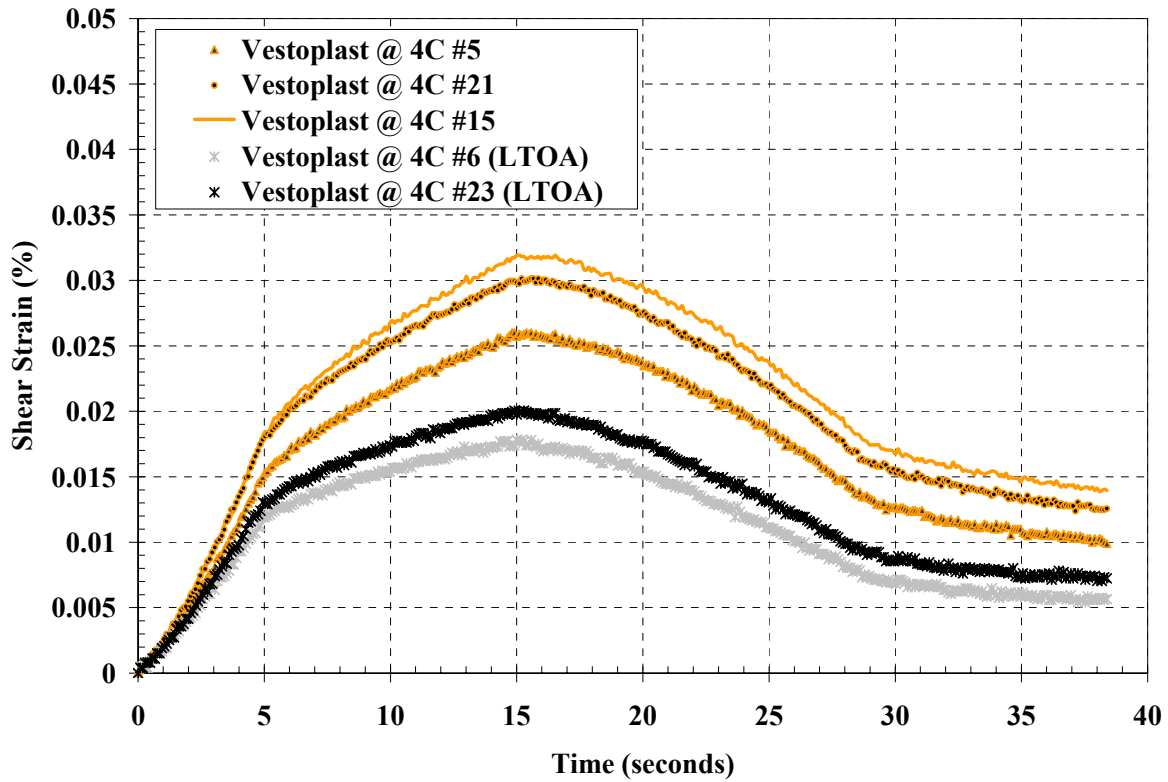## Appendix E.4.1 – RSCH for LTOA and STOA Creanova Vestoplast
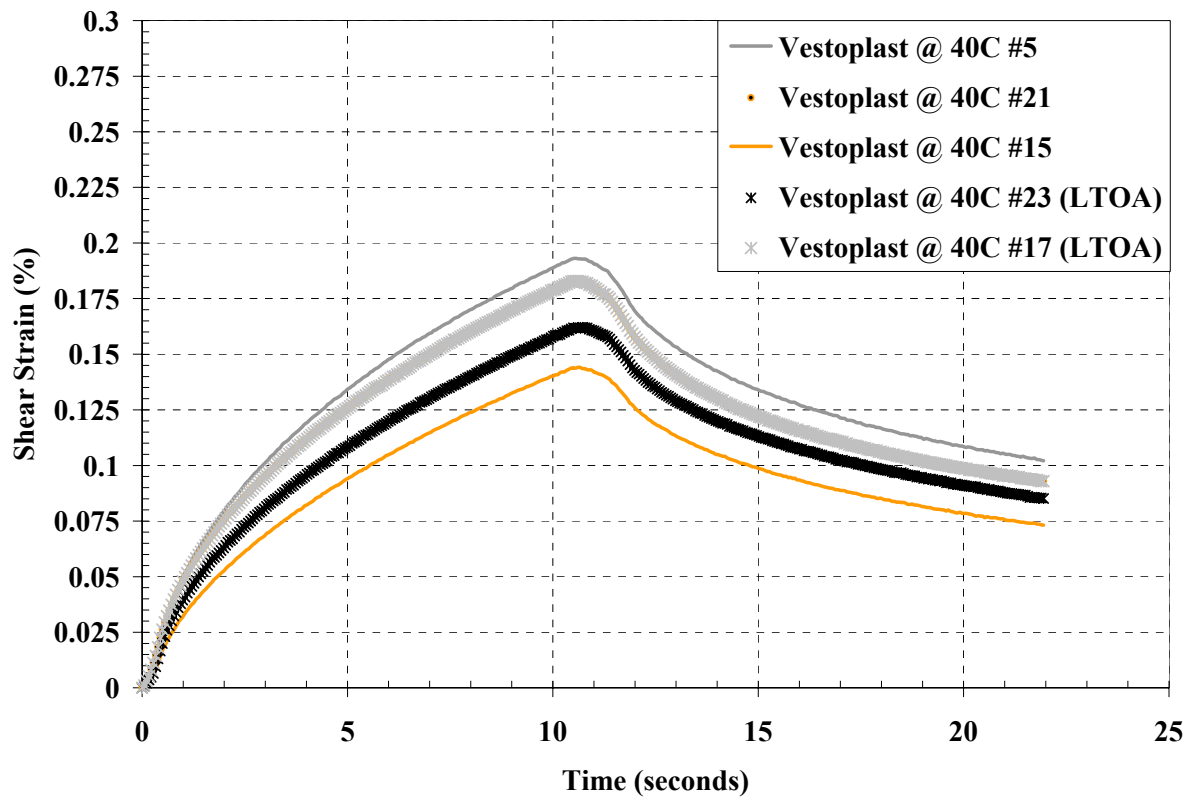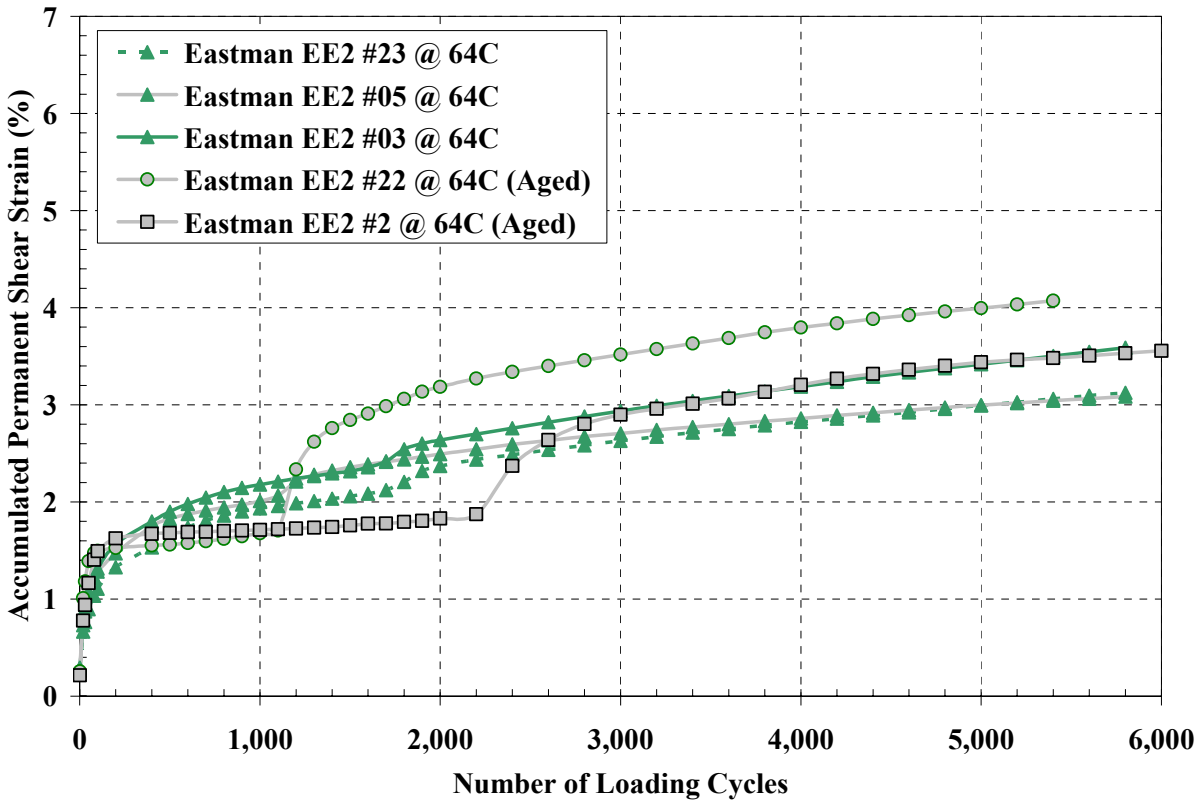
Appendix E.4.2 – FSCH for LTOA and STOA Creanova Vestoplast
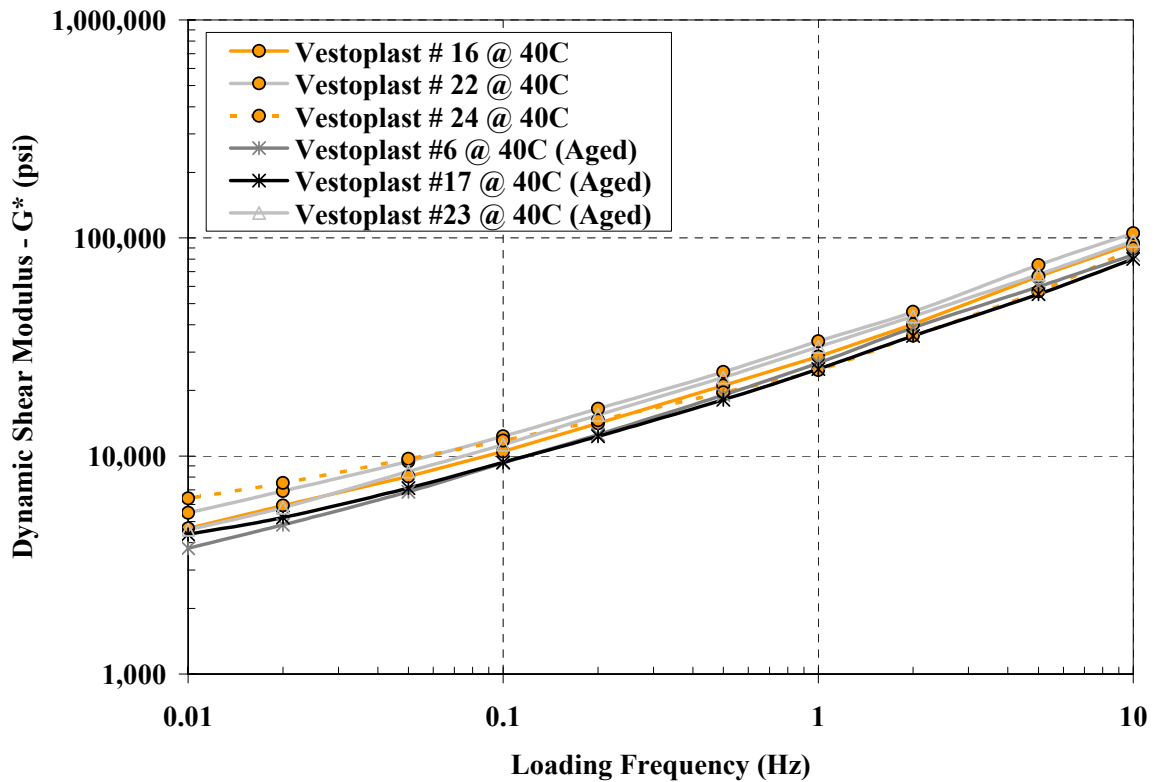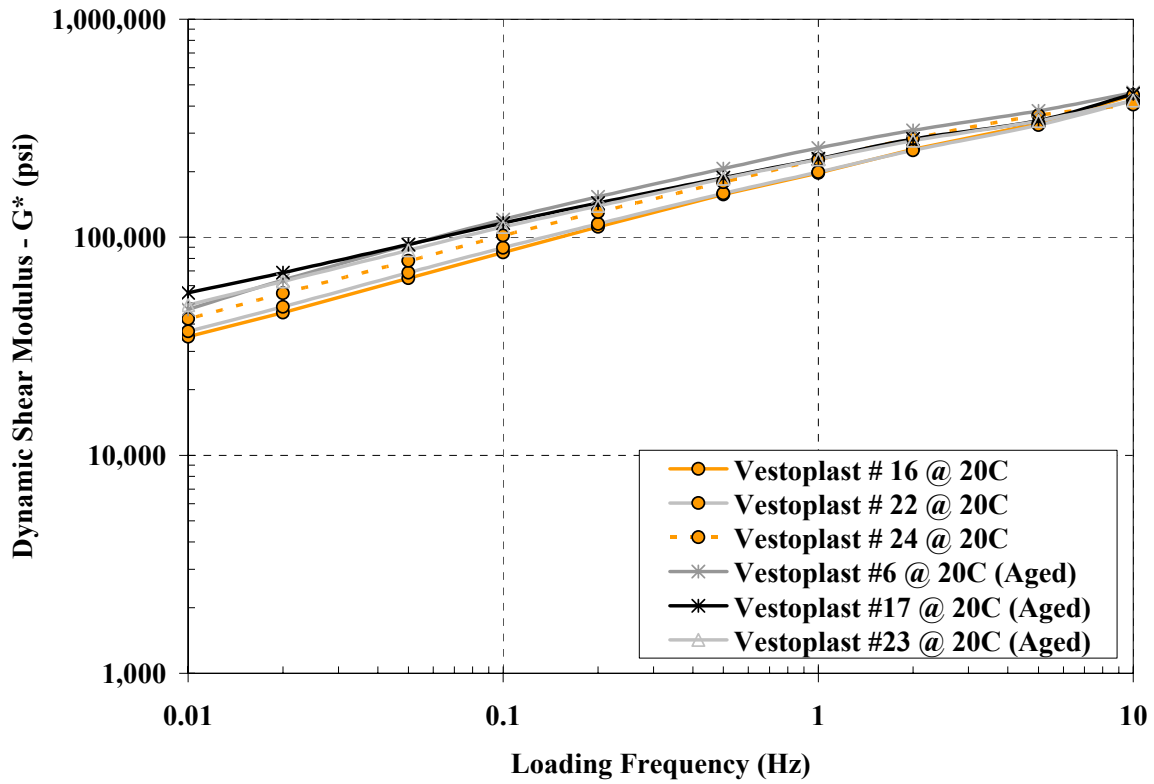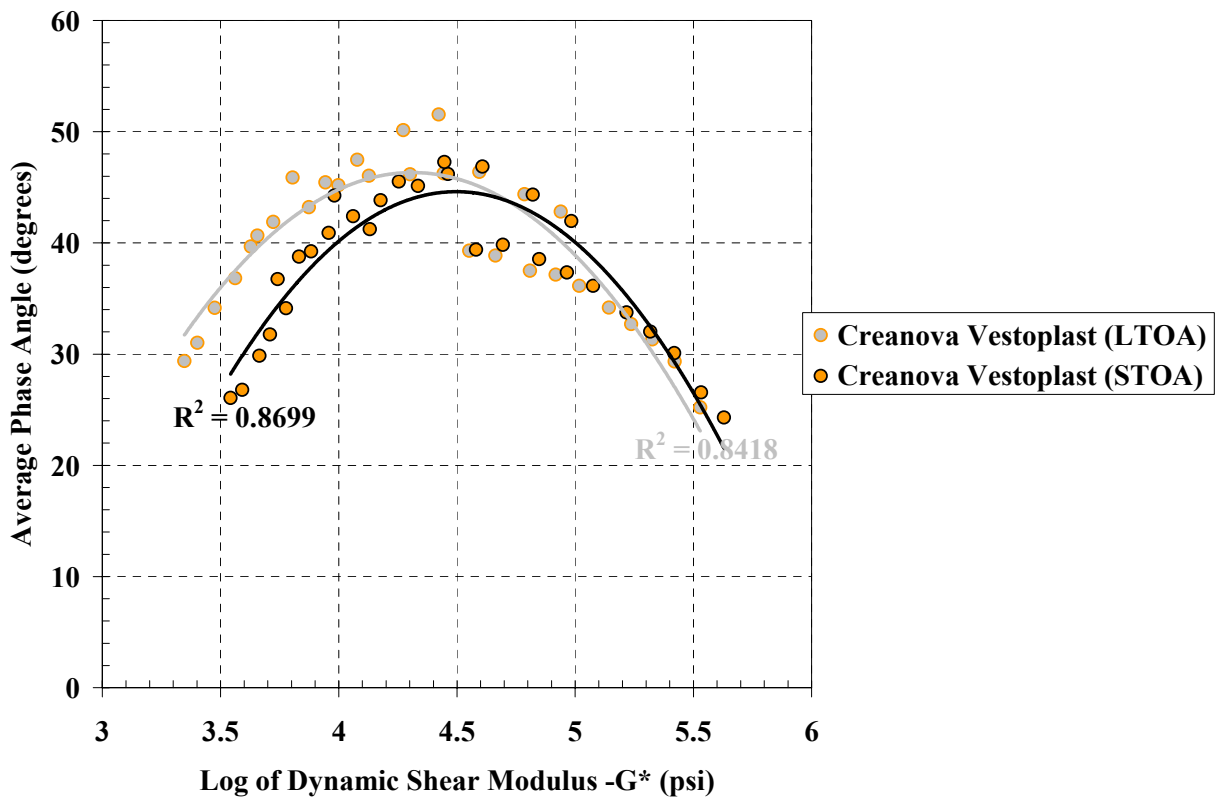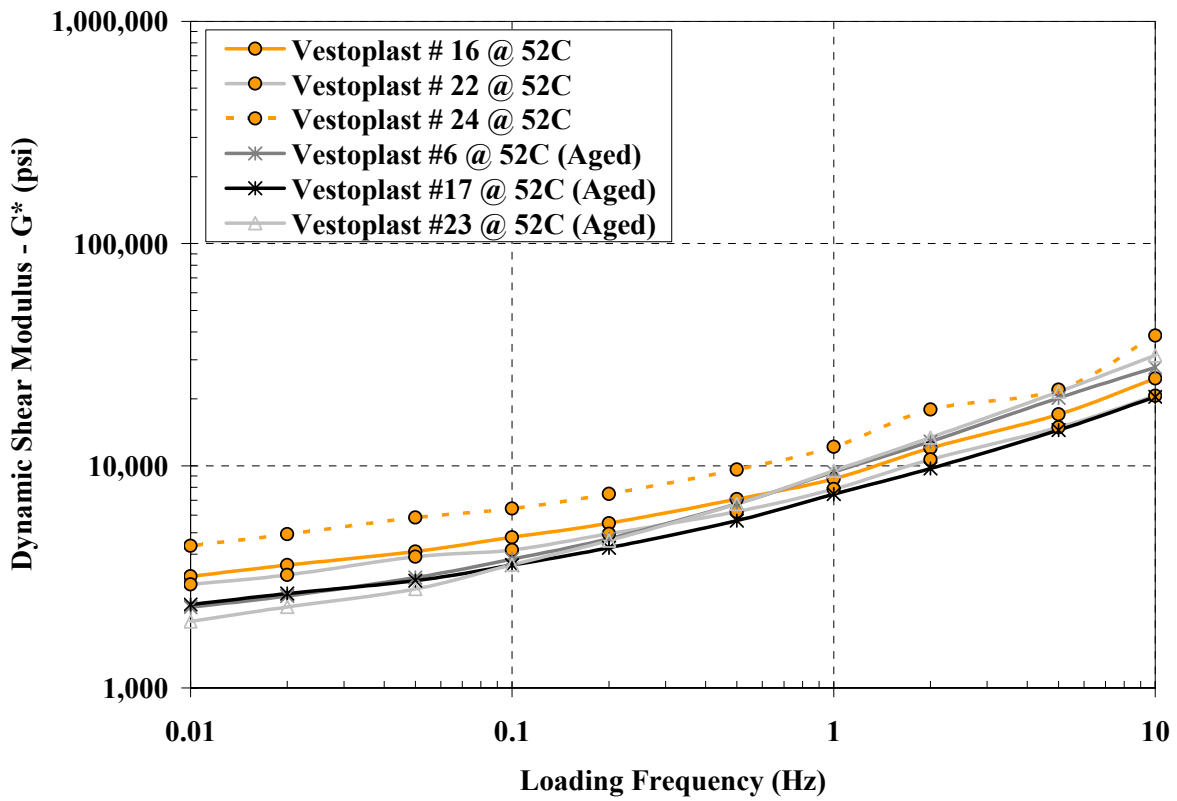
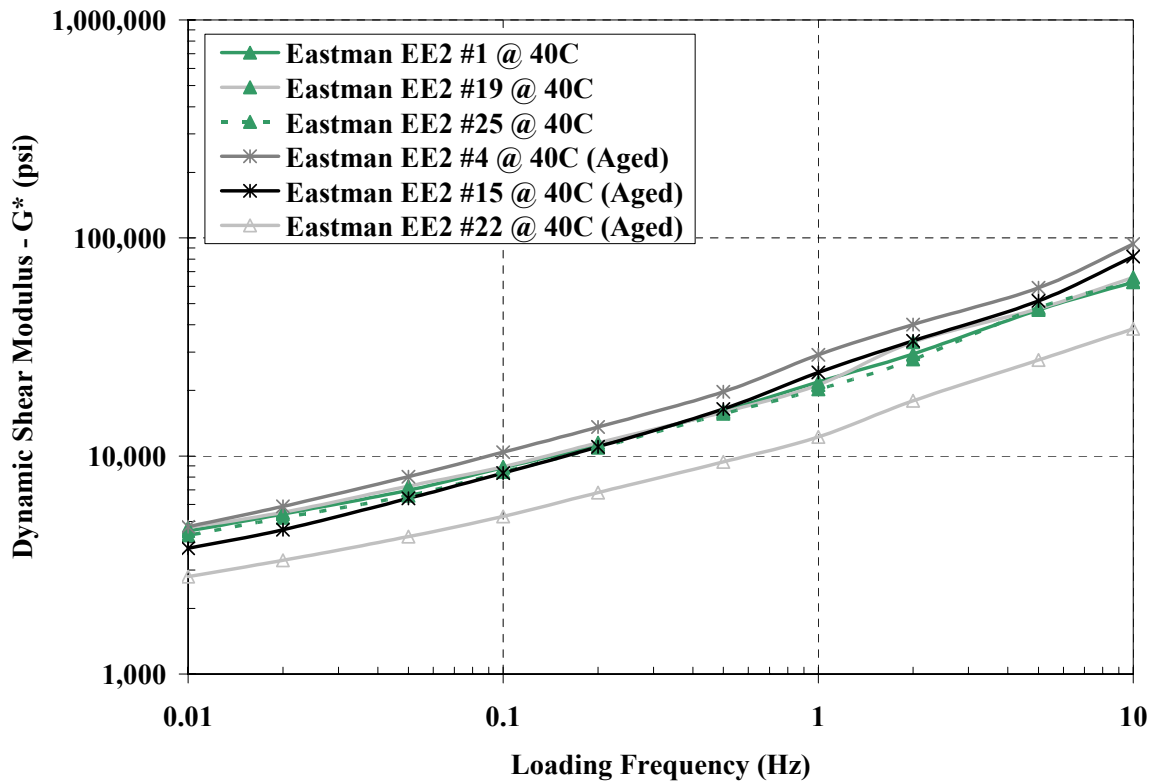# Appendix E.4.3 – SSCH for LTOA and STOA Creanova Vestoplast

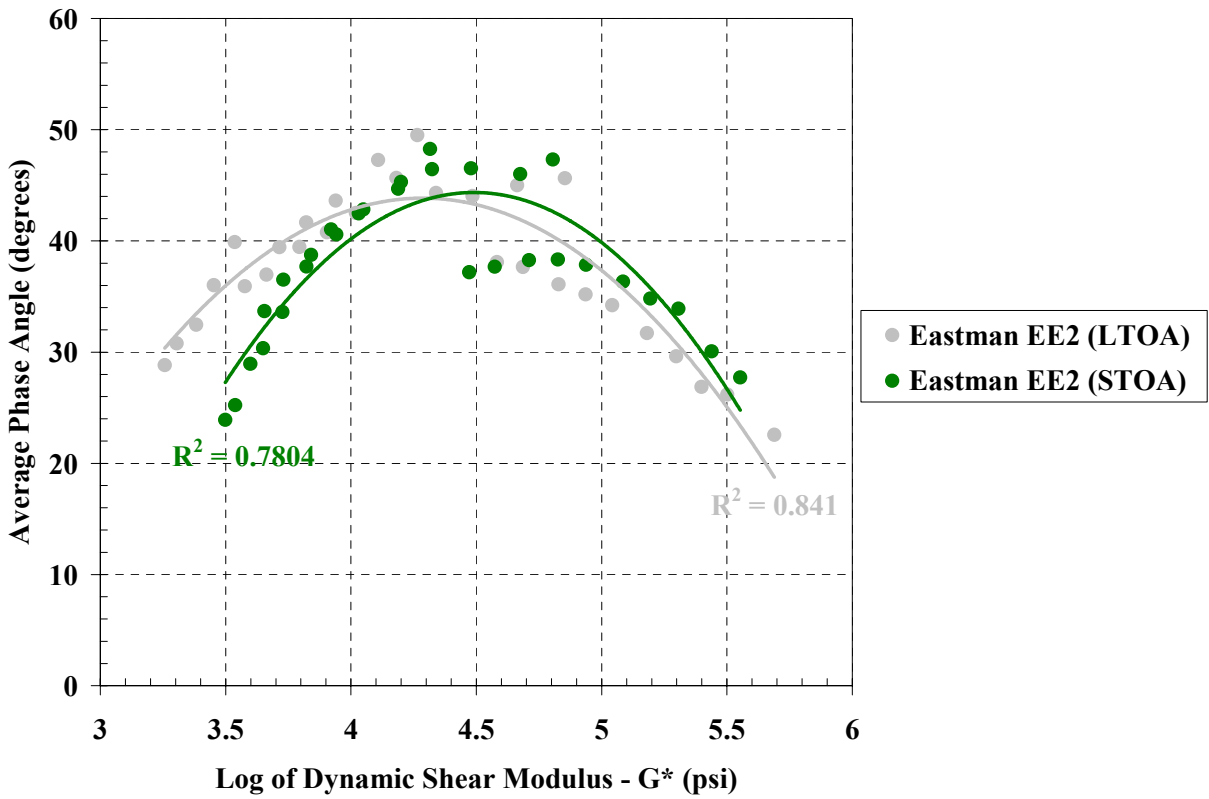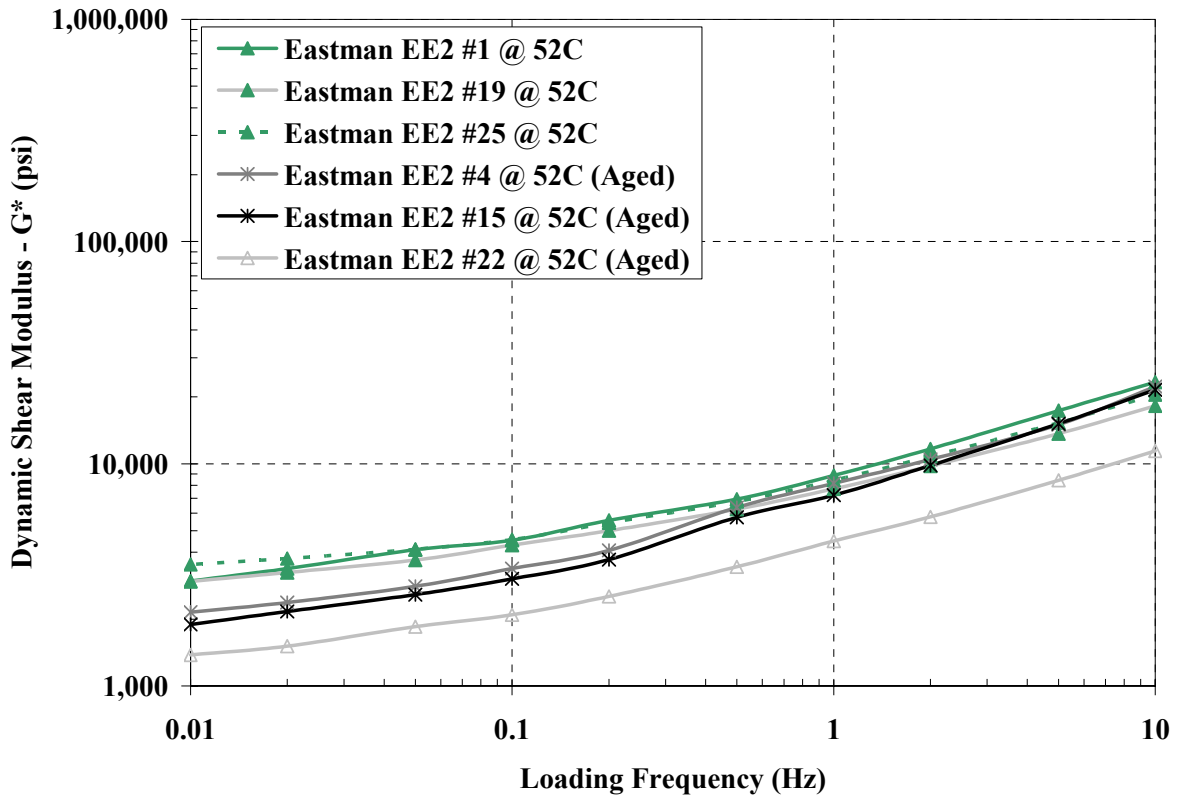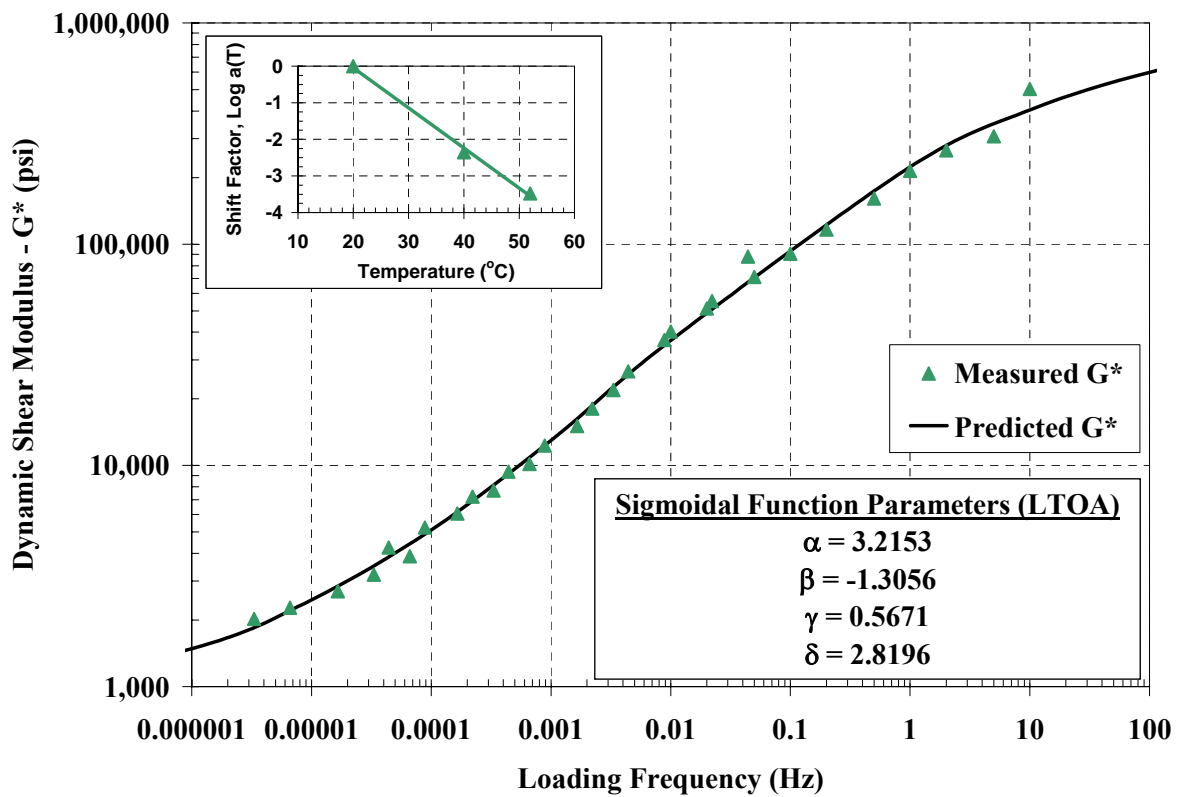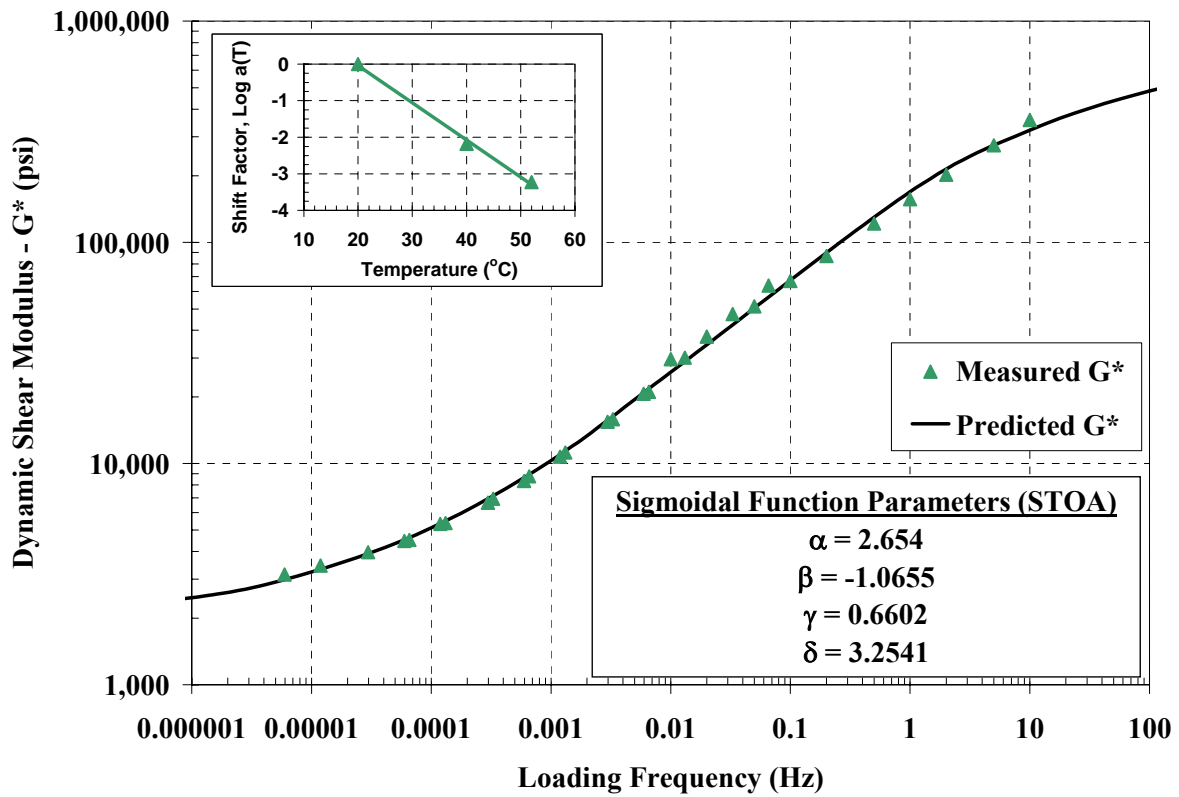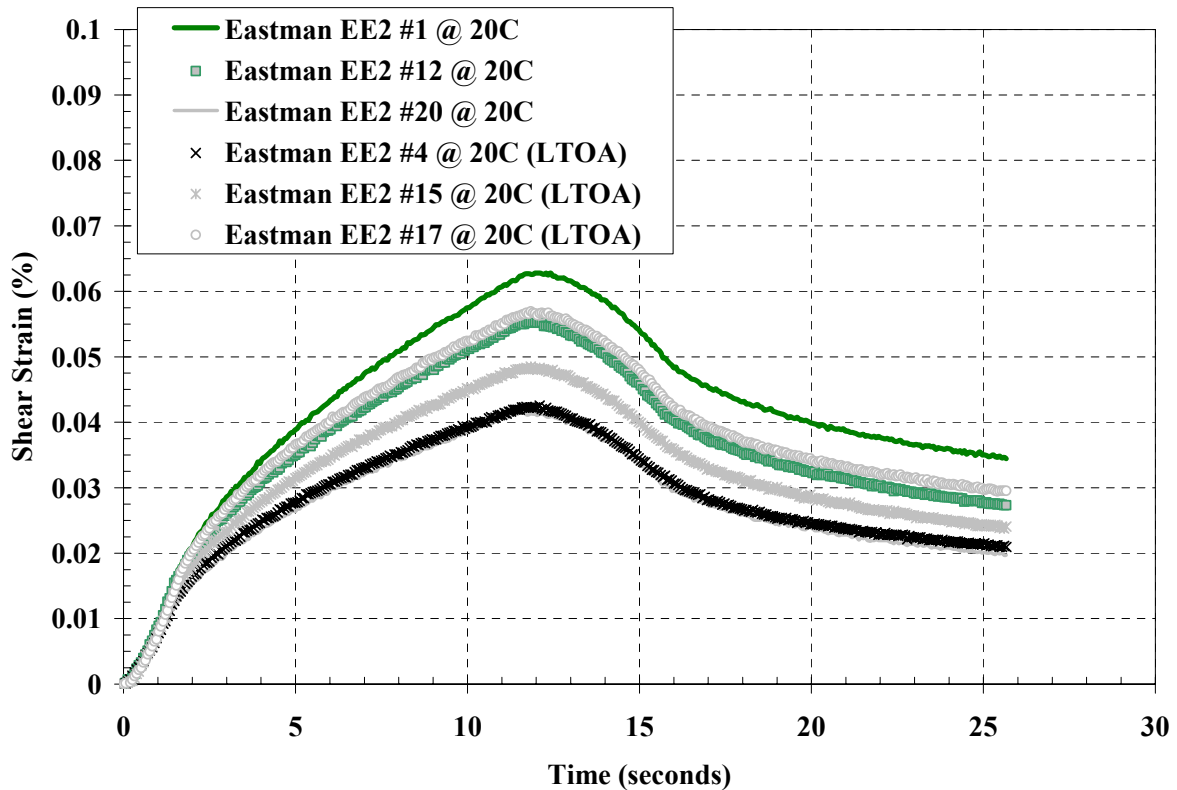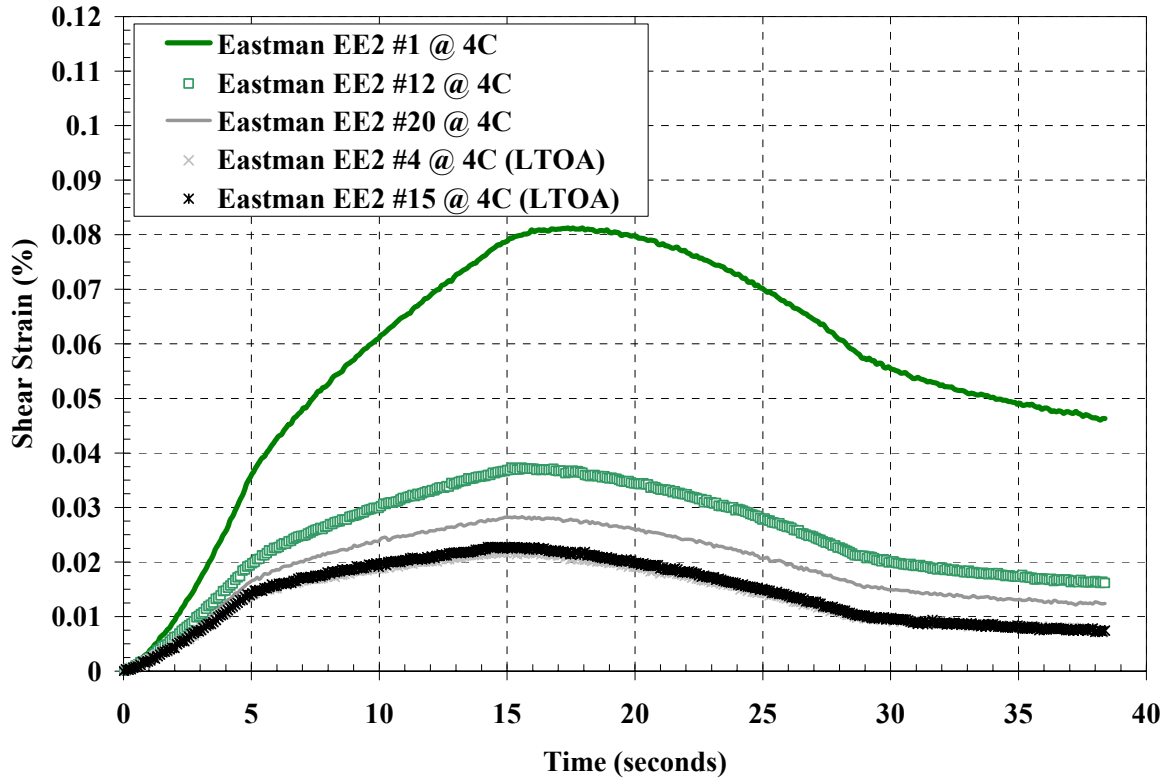Appendix E.5.1 – RSCH for LTOA and STOA Eastman EE-2
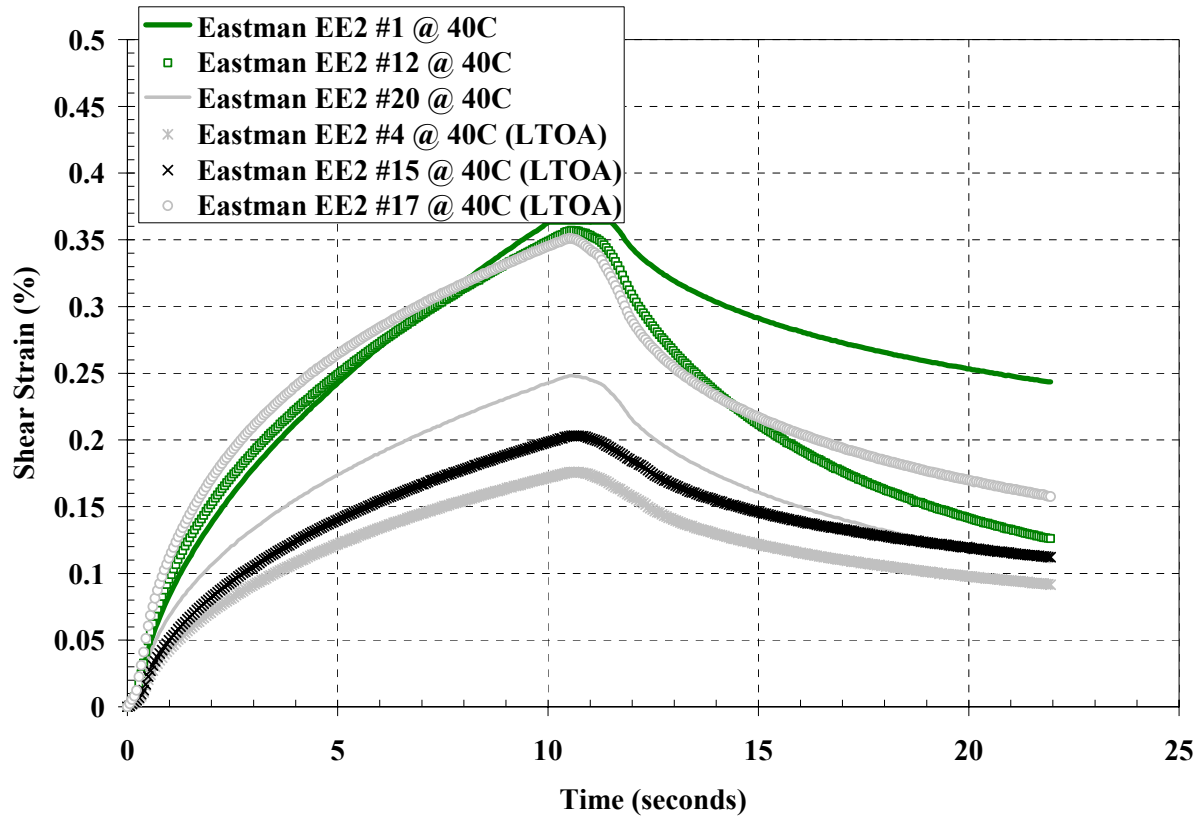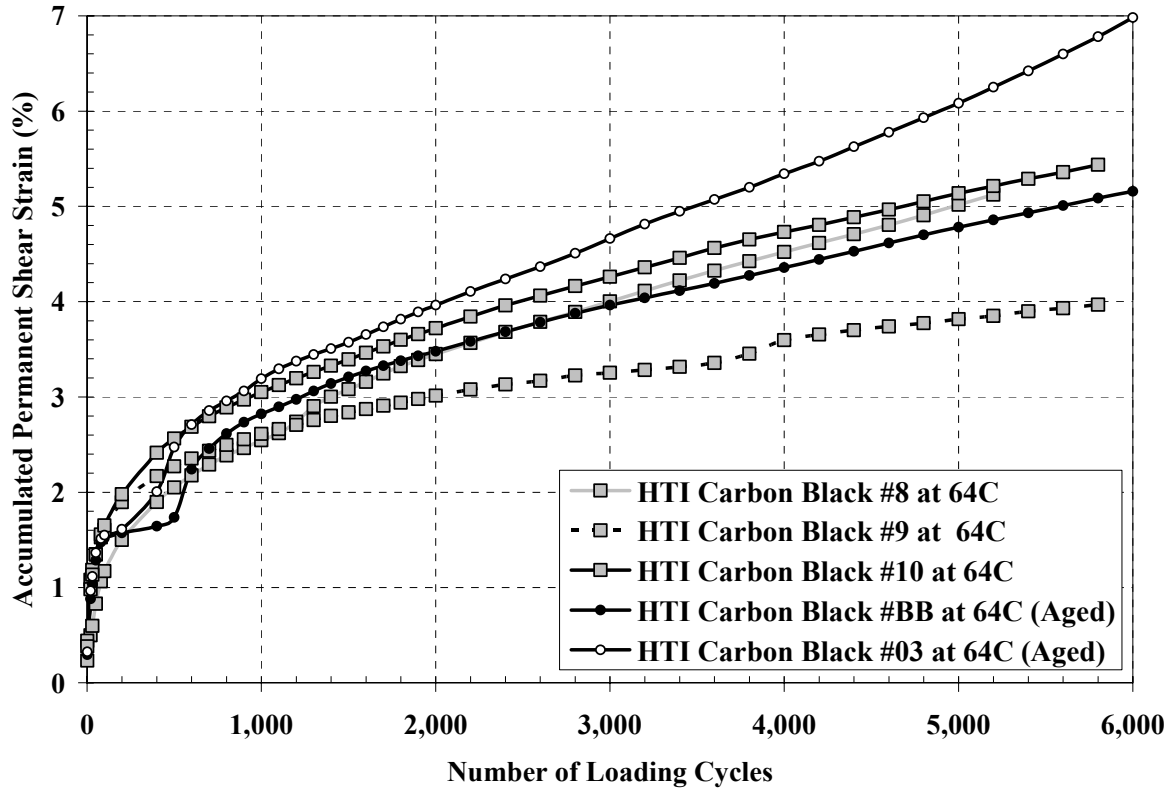
Appendix E.5.2 – FSCH for LTOA and STOA Eastman EE-2
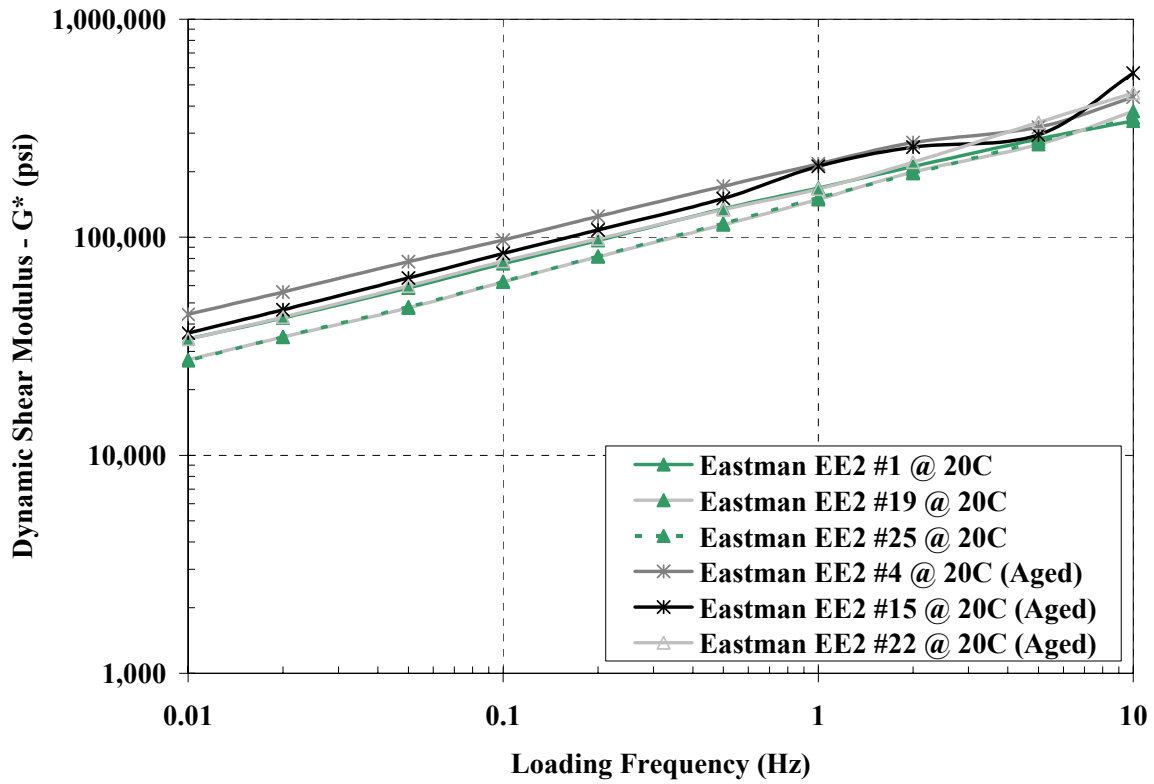
Appendix E.5.3 – SSCH for LTOA and STOA Eastman EE-2

Appendix E.6.1 – RSCH for LTOA and STOA HTI Carbon Black
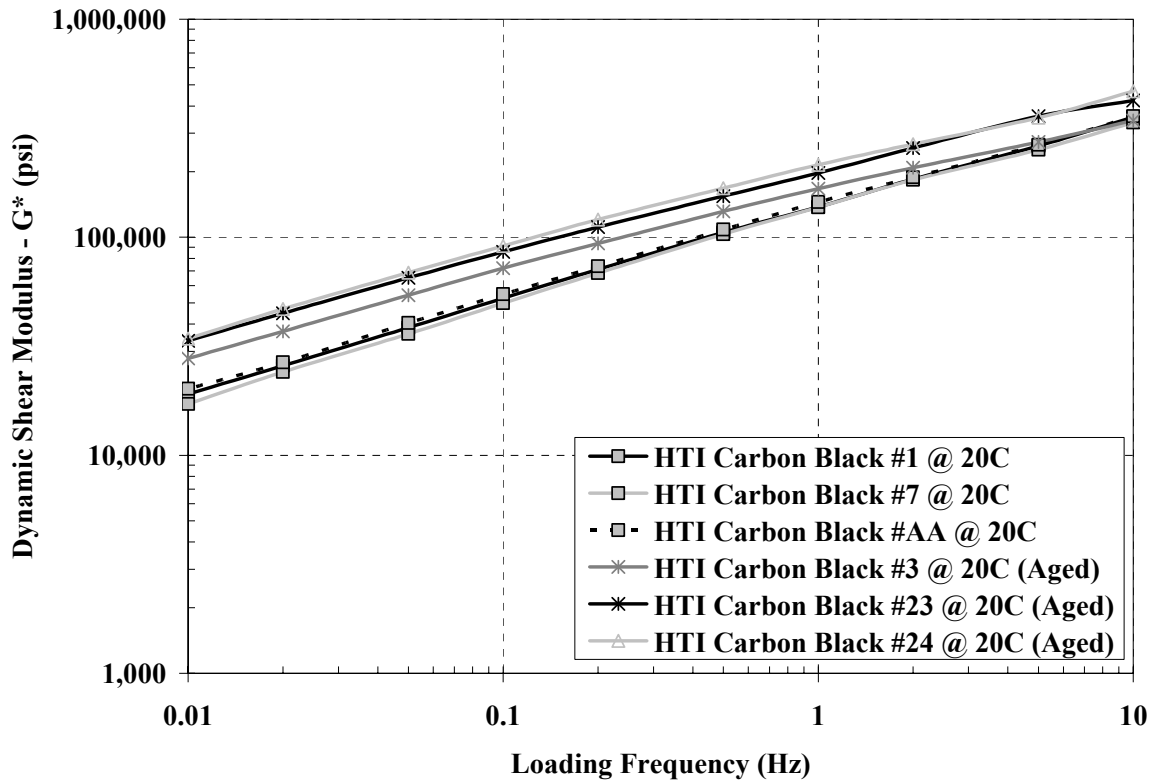
Appendix E.6.2 – FSCH for LTOA and STOA HTI Carbon Black
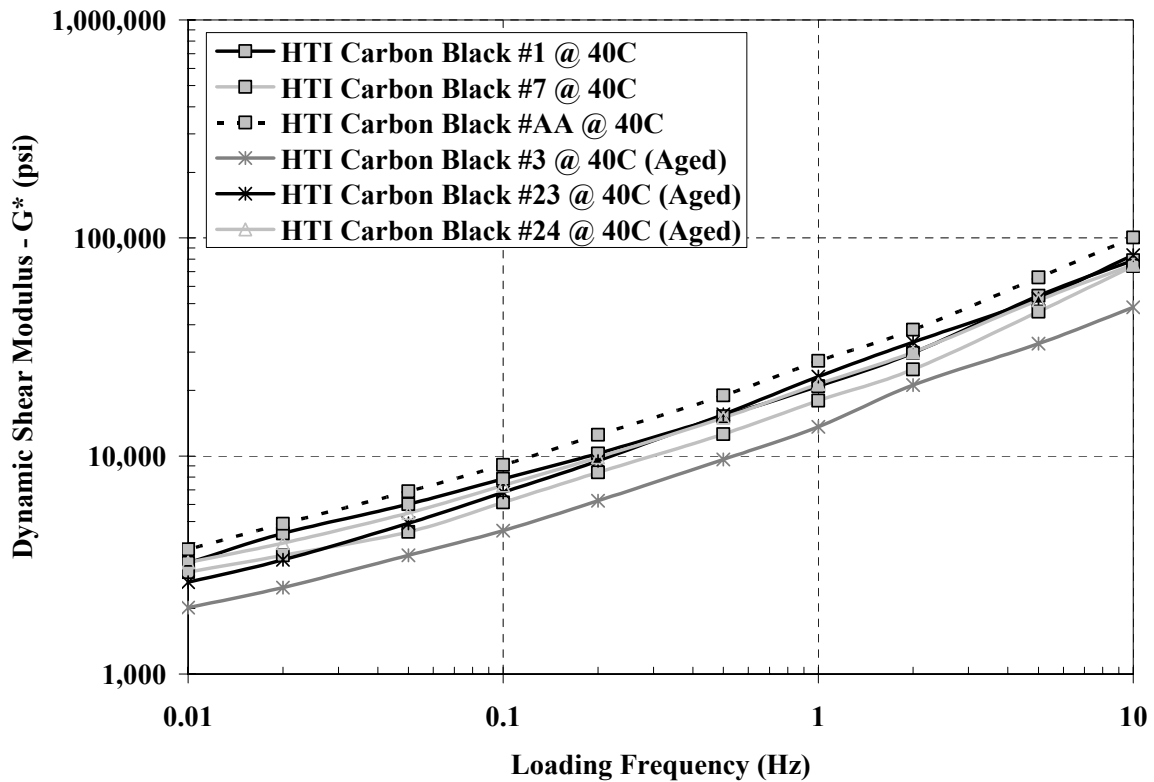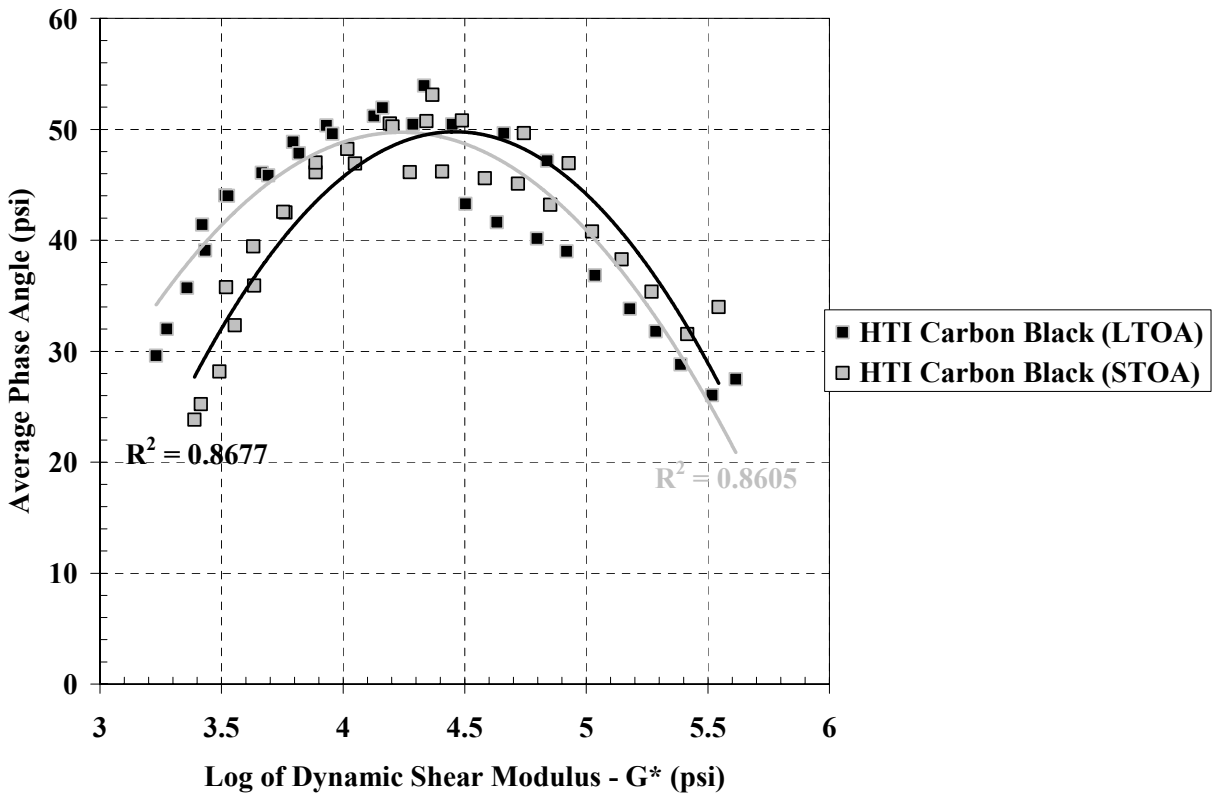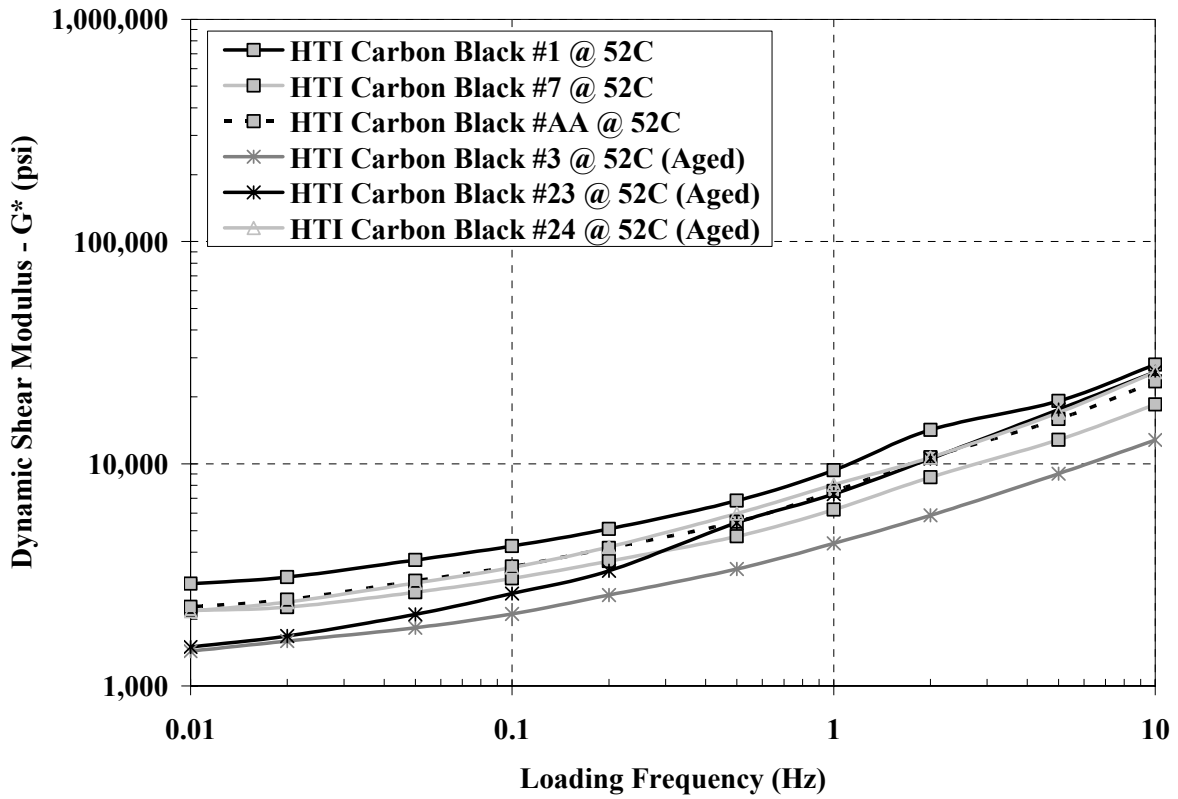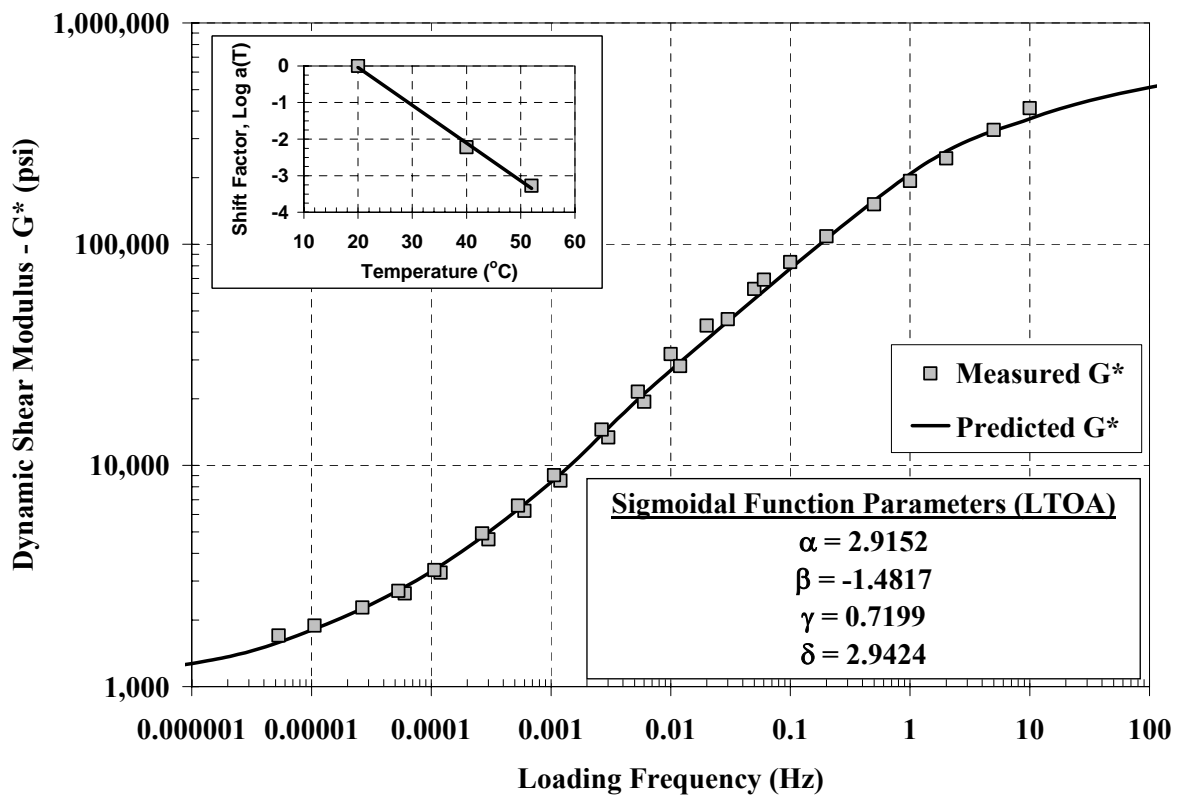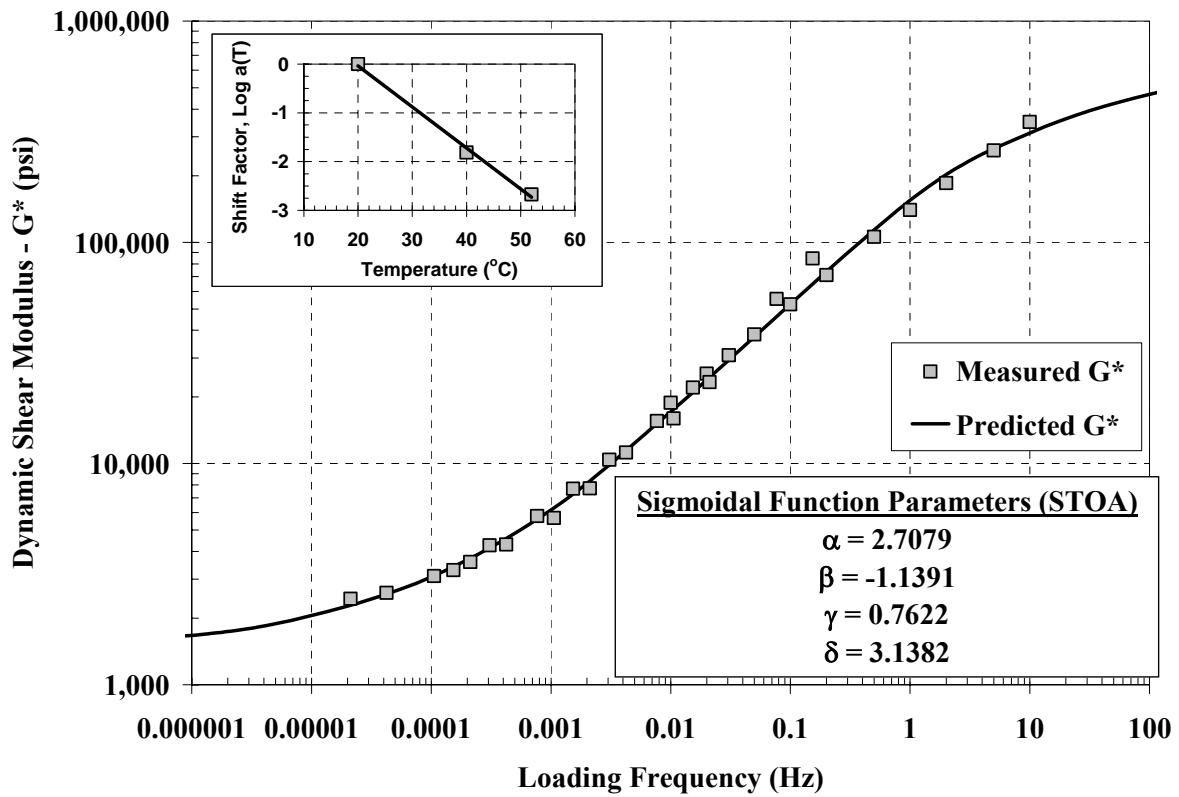
Appendix E.6.3 – SSCH for LTOA and STOA HTI Carbon Black
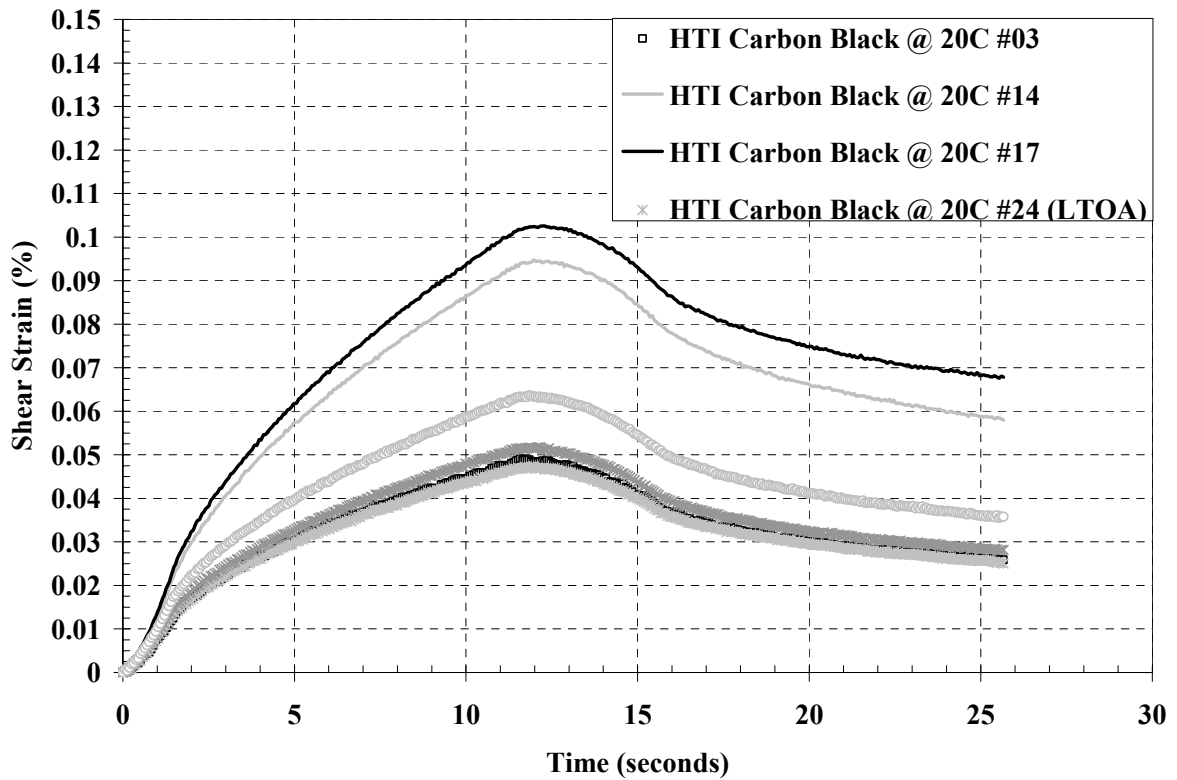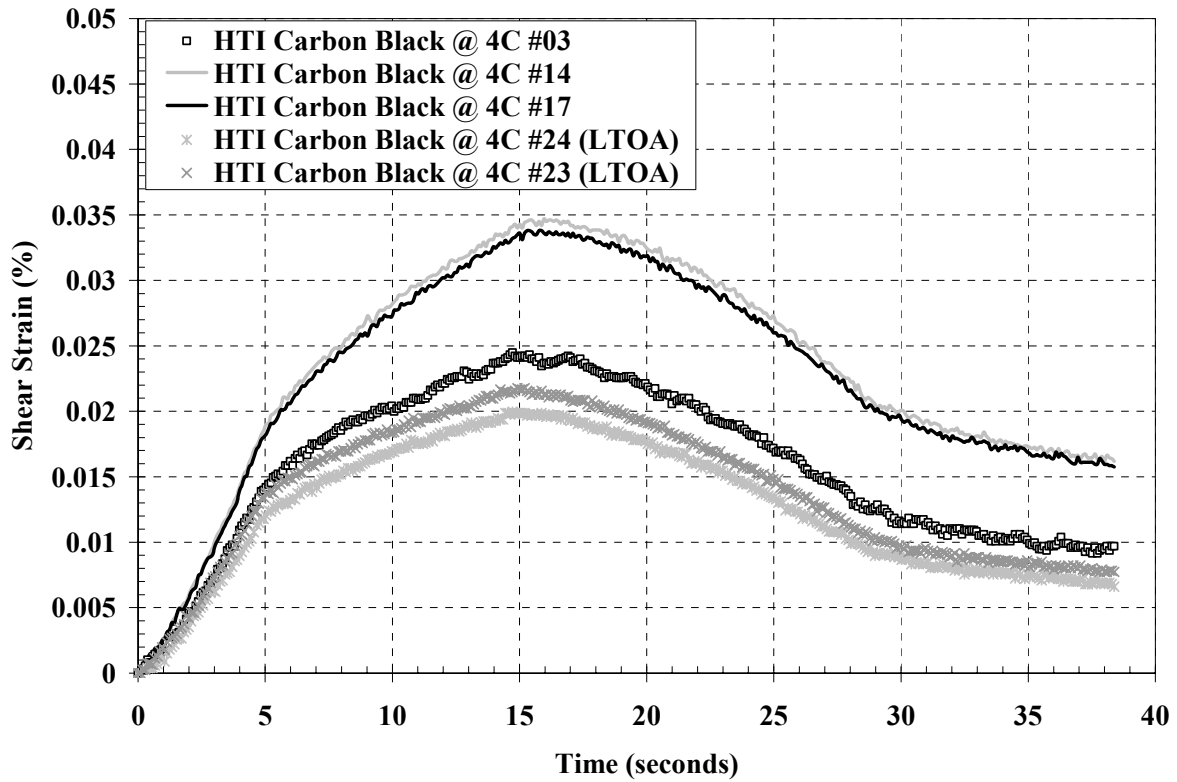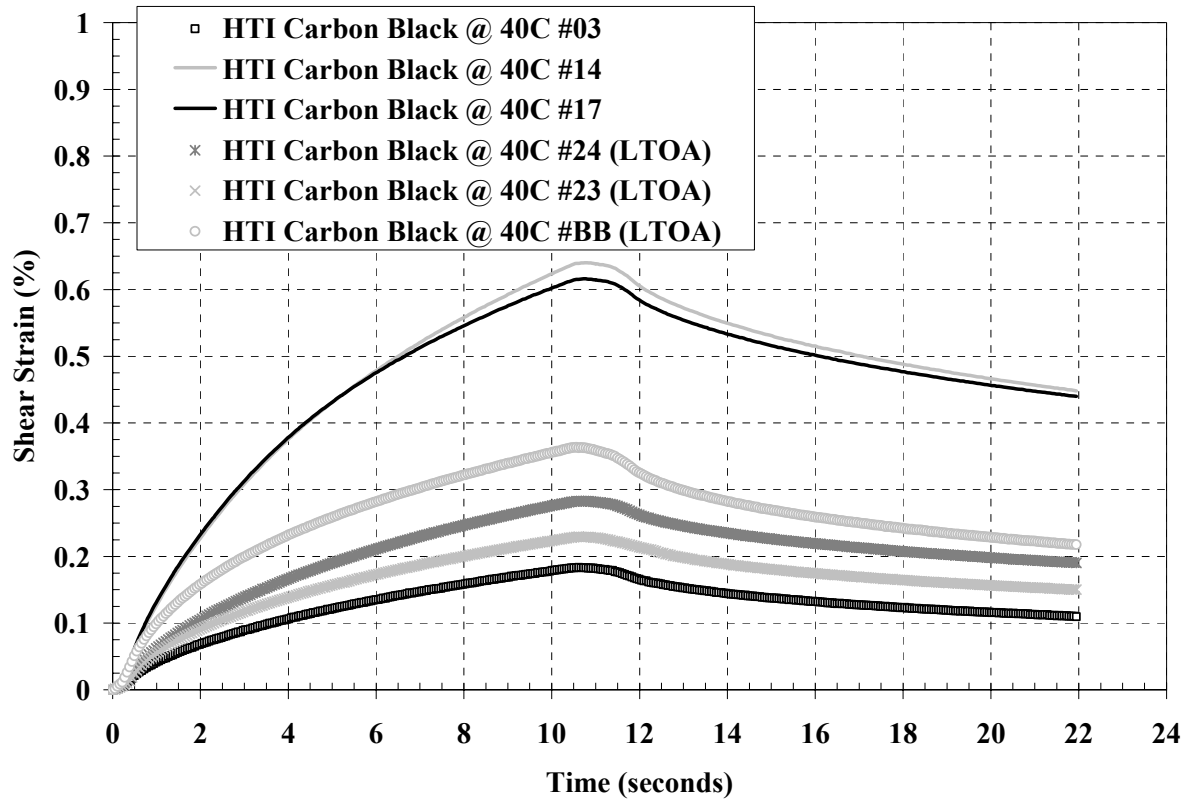
APPENDIX F – PROPOSED NJDOT TEST PROCEDURE

Proposed Test Procedure for Evaluating HMA Mixes Modified with Asphalt Modifiers

1. Scope

1.1 This test method covers procedures for preparing and testing asphalt concrete mixtures to determine effects the addition of an asphalt binder modifier has on a HMA mixture properties.

1.2 This standard is applicable to laboratory prepared specimens of mixtures with nominal maximum size aggregate less than or equal to 25 mm (1.0 in).

1.3 *This standard may involve hazardous material, operations, and equipment. This standard does not purport to address all safety problems associated with its use. It is the responsibility of the user of this procedure to establish appropriate safety and health practices and to determine the applicability of regulatory limitations prior to use.*

2. Referenced Documents

2.1 AASHTO Standards

T312 Method for Preparing and Determining the Density of Hot Mix Asphalt (HMA) Specimens by Means of the Superpave Gyratory Compactor.

PP2 Practice for Mixture Conditioning of Hot Mix Asphalt (HMA).

T166 Bulk Specific Gravity of Compacted Bituminous Mixtures.

T209 Maximum Specific Gravity of Bituminous Paving Mixtures.

T269 Percent Air Voids in Compacted Dense and Open Bituminous Paving Mixtures.

TP7-01 Standard Test Method for Determining the Permanent Shear Strain and Stiffness of Asphalt Mixtures Using the Superpave Shear Tester

3. Significance and Use

3.1 The performance properties of the HMA mixture are determined for both with and without the addition of the asphalt binder modifier. HMA performance testing is conducted to provide both fundamental and simulative loading

conditions on the HMA sample. The fundamental properties evaluated are shear creep and small strain shear stiffness, while the simulative properties are resistance to repeated shear loading. To further investigate materials for which the NJDOT does not have any prior experience with, an evaluation of the effect of aging on the HMA is also conducted.

3.2 The values of Repeated Shear may be used with the SHRP models to predict the field rutting versus applied ESAL's.

4. Apparatus

4.1 Bi-axial Test System – A bi-axial loading test system consisting of a testing machine, environmental chamber, and a data acquisition and control system. It shall accommodate test specimens 150 mm in diameter and 50 mm in height.

    4.1.1 *Testing Machine* – The loading device shall be capable of simultaneously applying both a vertical and horizontal load to the specimen. It shall also be capable of applying static, ramped (increasing or decreasing), and repetitive loads of various wave forms. As a minimum, the loading device shall be capable of applying horizontal shear load pulses in a haversine wave form with a load duration of 0.1 seconds and 0.6 seconds between load pulses. The loading shall be provided by two hydraulic actuators (one each for the horizontal and vertical) and shall be controlled by closed-loop feedback using either stress or strain control throughout the entire range of frequencies and temperatures. The loading device shall be capable of meeting the minimum requirements specified in Table 1.

    4.1.2 *Environmental Chamber* – A chamber for controlling the test specimen at the desired temperature. The environmental chamber shall be capable of controlling the temperature of the specimen over a temperature range from 0 to 70 ^{o}C (32 to 158 ^{o}F) to an accuracy of $\pm$ 0.5 ^{o}C (1 ^{o}F). The chamber shall be large enough to accommodate the test specimen and a dummy specimen with thermocouple mounted at the center for temperature verification.

    4.1.3 *Data Acquisition and Control System* – The data acquisition and control system shall automatically control user-selected measurement parameters, within the accuracy specified in Table 1, during the testing sequence, and shall record load cycles, applied horizontal and vertical loads, specimen deformation in two directions (vertical and horizontal), environmental conditions, and the required frequency of data sampling. At the conclusion of the test, the data acquisition and control shall procide all applicable test data.

4.2 *Platen-Specimen Assemby Device (Optional)* – The platen-specimen assembly device is used to facilitate bonding the specimen to the loading platens with adhesive. The device shall maintain the platens in parallel position (relative to each other) during the gluing operation. The platens must remain parallel so the stresses do not develop in the specimen when the specimen-platen assembly is clamped in the test system. The device shall accommodate test specimens 150 mm in diameter with a height of 50 mm.

4.3 *Aluminum End Platens* - Top and bottom aluminum loading platens at least 6.35 mm or greater in diameter than the diameter of the specimen to be tested and at least 20 mm thick. The bearing face of each platen shall be plane to 0.025 mm.

4.4 Adhesive – A quick-set adhesive with a minimum hardened stiffness modulus of 200 MPa for bonding the platens to the specimen ends.

Note 1 – Devcon^{TM} Plastic Steel Epoxy Cement is satisfactory

4.5 *Saw* – A machine for sawing test specimens ends to the appropriate length is required. The saw shall have a diamond cutting edge and shall be capable of cutting specimens to the prescribed dimensions without excessive heating or shock.

Note 2 – A diamond masonry saw greatly facilitates the preparation of test specimens with smooth, parallel ends. Adequate blade stiffness is also important to control flexing of the blade during thin cuts.

5. Sampling and Specimen Preparation

5.1 Three specimens for each HMA mix are required; six specimens if age hardening is to be evaluated. The same three test specimens will be used for Simple Shear, Frequency Sweep and Repeated Shear at Constant Height testing.

5.2 Laboratory Mixed, Laboratory Compacted (LMLC) Specimens – Sample asphalt binder and aggregates in accordance with AASHTO T40 and T2, respectively. Use the appropriate proportions of asphalt binder and aggregates to match the final asphalt mix design.

5.2.1 Prepare aggregate batches of the appropriate size to produce a compacted specimen that will be 150 mm in diameter and 75 to 80 mm in height. Heat the aggregate batches to the appropriate mixing temperature

5.2.2 Heat the asphalt binder to the appropriate mixing temperature. Mix the correct proportions of asphalt binder and combined aggregates to match the asphalt mix design.

5.2.3 After mixing, the asphalt mixture is required a short term conditioning for two hours at the compaction temperature in accordance with the base asphalt binder data sheet.

Note 3 – When mixing is to be done with modifiers, the addition of the modifier should be conducted under the manufacturer's recommended procedure.

5.2.4 After short-term conditioning is complete, the asphalt mixture specimen should be compacted to 7 (+/-) 0.5% air voids. This air void content represents the before cutting air void content of the specimen.

5.2.5 After the compacted sample is cut to the required 50 mm thick specimen, the test specimen typically has an air void content of 5.5 (+/-) 0.5%. The 5.5 (+/-) 0.5% is the target range for all test samples.

Note 4 – Other compaction procedures than the Superpave gyratory compactor (TP4) and other target air void percentages than those specified in this proposed testing procedure may be used. However, caution is needed to prevent comparisons between asphalt mixtures with different target air voids or compaction methods. The test procedures and analyses are sensitive to both the percentage of air voids and the compaction procedure.

5.2.6 Allow the compacted mixture specimens to cool completely to room temperature. Cut the specimens to the proper test dimensions stated earlier. The cut faces should be parallel to within 2 mm of each other.

5.2.7 Determine the percentage of air voids in the test specimens in accordance with AASHTO T166, T209, and T269. Determine the height of the test specimens in accordance with ASTM D3549.

5.3 Field Mixed, Laboratory Compacted (FMLC) Specimens – Obtain HMA samples in accordance with AASHTO T168. Compact specimens using AASHTO TP4 to the appropriate percentage of air voids (see Section 5.2.4 and Note 4)

5.3.1 Allow the compacted mixture specimens to cool completely to room temperature. Cut the specimens to the proper test dimensions. Cut faces should be parallel to within 2 mm of each other.

5.3.2 Determine the percentage of air voids int eh test specimens in accordance with AASHTO T166, T209, and T269. Determine the height of the test specimens in accordance ASTM D3549.

5.4 Field Mixed, Field Compacted (FMFC) Specimens – Obtain asphalt pavement specimens having a diameter of 150 mm and a minimum thickness of 38 mm in accordance with ASTM D5361.

5.4.1 Cut the specimens to the proper test dimensions. Cut faces should be parallel to within 2 mm of each other.

5.4.2 Determine the percentage of air voids in the test specimens in accordance with AASHTO T166, T209, and T269. Determine the height of the test specimens in accordance ASTM D3549.

5.5 Preparing the Specimens for Testing – The following steps discuss the bonding of the test specimen to the platens for testing in the shear tester.

5.5.1 Ensure the platens are clean, aligned, and clamped into place in the platen-specimen assembly device (optional) or shear test device.

5.5.2 Proportion and mix the epoxy resin and hardener together in accordance with the manufacturer's instructions (Note 1).

Note 5 – If using the Devcon™ Plastic Steel Epoxy, laboratory experience has shown a total mixed weight of 150 grams provides sufficient epoxy for proper bonding. A mixing ratio of 125 grams of epoxy resin to 25 grams of hardener works well.

5.5.3 Apply a thin coating of the epoxy cement to the top of the test specimen and to the bottom platen. Half of the epoxy should be used on the top of the specimen with the other half applied to the bottom platen. Center the test specimen on the bottom platen and lower the top platen onto the specimen. Rotate the specimen slightly to ensure good bonding.

5.5.4 Apply a light pressure, approximately 35 kPa, to the specimen for bonding. During the application of this pressure, remove excess epoxy from the sides of the test specimen by trimming as soon as the light pressure is applied. The time of the applied load will depend on the epoxy's setting time.

5.5.5 After the setting time has been reached, remove the test assembly (specimen with attached platens) from the platen-specimen assembly device (optional) and allow the epoxy to cure for the minimum time recommended by the manufacturer.

6. General Test/Specimen Set-up

6.1   Turn on the hydraulic system at least one hour before starting the test to allow sufficient warm-up time.   Warm-up the actuators and hydraulic oil by using a sinusoidal waveform in deformation control.

6.2   Determine the lowest test temperature at which the specimen will be tested and pre-condition the test specimens for two to four hours (Note 6) at the required test temperature +/- 0.5^{o}C. Set the temperature for the environmental chamber of the shear device at the required test temperature.

> Note 6 – The use of a dummy sample instrumented with a temperature probe provides the best method to ensure that the test specimen reaches the required test temperature. The dummy sample should be a sample of similar properties (density, air voids, etc.) and have a hole drilled into the center of the specimen. The drilled hole should be only slightly larger than the temperature probe.   The temperature probe should measure the sample temperature at the center of the test specimen.   The use of a vegetable oil to be placed inside the hole with the temperature probe can aid in proper specimen temperature measurements if the drilled hole is larger than the temperature probe.

> Note 7 – A conditioning chamber is preferred since it allows the shear test device to be free to perform tests rather than be occupied for temperature conditioning.

6.3   After the conditioning period, remove the specimen (attached to the platens) from the conditioning chamber. Open the environmental chamber of the shear tester and quickly attach the shear and vertical LVDT's to the specimen platens (Note 8). Ensure that the LVDT's are plugged into the proper data acquisition ports within the shear tester's environmental chamber. Zero the shear and vertical LVDT's.

> Note 8 – The LVDT's should be plugged into the data acquisition system, with the data acquisition on, for at least 1 hour. This ensures the LVDT's are warmed up and ready to be used.

6.4   Confirm that the vertical test system heads are positioned to allow the platen-specimen assembly to slide between the bottom horizontal and top vertical heads. Confirm that the horizontal test head is positioned such that the top and bottom test heads are aligned vertically.   Center the specimen between the heads and secure the platens to the head by activating the hydraulic clamps. Close the environmental chamber and lock it in place.

6.5   Confirm that the environmental chamber temperature control is activated and on the proper setting to maintain the required test temperature with a tolerance

of +/- 0.5^{o}C. Allow the specimen to stabilize for a minimum of 20 minutes and a maximum of 60 minutes. This stabilization time allows the specimen to reacquire the proper test temperature (lost during LVDT instrumentation and specimen set-up) and for the LVDT's to stabilize after the temperature change.

7. NJDOT Quick Procedure

7.1   The Quick Procedure uses a total of six specimens for testing. The first three specimens are baseline samples (samples that contain the un-modified asphalt binder), while the remaining three samples contain the asphalt binder modifier added to the same asphalt binder used in the baseline samples. The NJDOT Quick Procedure is meant to be used on materials that the NJDOT have some type of experience with and is not concerned with any age hardening effects.

7.2   There are three different tests used in this procedure to determine three distinct sample characteristics: 1) Frequency Sweep at Constant Height to determine the specimen's small strain stiffness, 2) Simple Shear at Constant Height to determine the creep properties of the specimen, and 3) Repeated Shear at Constant Height to determine the material's ability to resist permanent deformation (rutting).

7.3   Two test temperatures are used in the NJDOT Quick Procedure; 40 and 64°C. The set-up and stabilization of chamber and sample temperatures should conform with Section 6.2 and Note 6 and 7.

7.4   To minimize the amount of damage to the specimen, testing must be conducted in a manner where the test temperatures are applied from lowest to highest, with the imposed deformation on the specimen also applied from lowest to highest. Therefore, the testing sequence will utilized the following order: 1) Frequency Sweep at Constant Height tested at 40°C, 2) Simple Shear at Constant Height tested at 40°C, and 3) Repeated Shear at Constant Height tested at 64°C.

7.5   Conduct the Frequency Sweep at Constant Height test.

7.5.1   Frequency Sweep at Constant Height (FSCH) - apply a sinusoidal shear strain of 0.0001 mm/mm (0.01 percent) at each of the following frequencies – 10, 5, 2, 1, 0.5, 0.2, 0.1, 0.05, 0.02, 0.01 Hz. Use fifty cycles each for the 10 and 5 Hz frequencies. Use twenty cucles each for the 2 and 1 Hz frequencies. Use seven cycles each for the 0.5, 0.2, and 0.1 Hz frequencies. Use four cycles each for the 0.05, 0.02, 0.01 Hz frequencies.

7.5.2   During the loading cycles, maintain the specimen height constant, within +/- 0.013 mm by applying sufficient axial stress during the loading cycle.

This is accomplished by controlling the vertical actuator using closed-loop feedback from the axial LVDT.

7.5.3 Record the axial and shear deformations (from the LVDT's) and the axial and shear loads. Record at a minimum rate of 50 data points per second for the number of cycles specified for each frequency in Section 7.5.

7.5.4 At the conclusion of the test, release the loads and return the actuators to the pre-test position. Switch the control back to the actuators (from the LVDT's) and make sure no residual loading is being applied to the sample. Allow the sample to rest for 30 minutes.

7.6 Simple Shear at Constant Height (SSCH) – After the sample has rested 30 minutes from the FSCH test, the test specimen will be tested in the simple shear mode.

7.6.1 Prior to testing the sample, check the environmental chamber to ensure that the chamber temperature is 40°C (+/-) 0.5°C.

7.6.2 Perform the test by increasing the shear stress at a rate of 70 kPa/sec until 35 +/- 1 kPa is reached. Maintain the stress at the specified level for 10 +/- 1 seconds. Reduce the shear stress to 0 kPa at a rate of 25 +/- 1 kPa/second. Continue the test at 0 kPa for an additional 10 +/- 1 seconds. During the test, maintain the specimen height constant, within +/- 0.013 mm by applying sufficient axial stress during the loading and un-loading cycle. This is accomplished by controlling the vertical actuator using closed-loop feedback from the axial LVDT.

7.6.3 Record the axial and shear deformations (from the LVDT's) and axial and shear loads. Record at a minimum rate of 50 data points per second, as shown in Table 2.

7.6.4 At the conclusion of the test, release the loads and return the actuators to the pre-test position. Switch the control back to the actuators (from the axial LVDT) and make sure no residual loading is being applied to the sample.

7.7 Once the simple shear has completed, the environmental chamber should be set to 64°C. Use a dummy sample to ensure that the test specimen has reached equilibrium (64°C) with the environmental system.

7.8 Conduct the Repeated Shear at Constant Height test.

7.8.1 Apply a repeated haversine shear stress to the test specimen consisting of 69 +/- 7 kPa (approximately 1220 N shear load for a 150 mm diameter specimen) for 0.1 seconds followed by a 0.6 second rest period. During

the loading cycle, maintain the specimen height constant, with +/- 0.013 mm by applying sufficient axial stress during the loading cycle.

7.8.2 Continue the test sequence until 5,000 cycles or until the shear LVDT exceeds it range (usually at 2.5 mm for 5 percent shear strain).

7.8.3 Record the axial and shear deformations (from the LVDT's) and axial and shear loads. Record at a minimum rate of 50 data points per second during the intervals specified in Table 2.

7.8.4 At the conclusion of the test, release the loads and return the actuators to the pre-test position. Switch the control back to the actuators (from the axial LVDT) and disconnect the LVDT's.

7.8.5 Remove the specimen from the test chamber. Remove the specimen from the platens by placing the specimen-platen assembly in an oven at approximately 135°C for 60 minutes to debond the specimen and epoxy from the platens. Scrape the platens clean with a scraper. Use acetone or other suitable solvents to remove any remaining epoxy.

8. NJDOT Full Procedure

8.1 The Full Procedure should be conducted if the NJDOT has no prior knowledge of performance with the use of the asphalt modifier in question. The Full Procedure is similar to that of the Quick Procedure, however, the Full Procedure involves aging samples to evaluate how the material may perform after years of in-service life. The test procedure also uses a lower test temperature, 4°C, to evaluate the affects of age hardening on the low temperature creep properties of the HMA.

8.2 The procedure uses a total of 18 test specimens. Nine of the test specimens are short term aged in accordance to Section 5.2.3. Two sets of three specimens are used for baseline values with the third set used for the asphalt modifier in question. The first baseline set consists of the identical base asphalt binder to be used with the asphalt modifier. The second baseline set consists of an asphalt binder that has a performance grade higher than the first baseline set. This is to provide a better idea as to the potential increase in performance of the asphalt binder modifier. These samples should follow the procedure in Section 5.

8.3 The second set of nine test samples (6 baseline and 3 asphalt binder modified) are to be long term oven aged (LTOA) using the guidelines in AASHTO PP2. These samples should still follow Section 5 to Section 5.2.4, however, once the samples have been compacted, the samples should be placed in a forced air oven at 85°C for 5 days. Once the five days of conditioning has completed, the oven is turned off and the door opened. Allow the samples to reach room

temperature. Once cooled, the samples should be cut, weighed and measured by Sections 5.2.5 through 5.2.7. At this point, there should be a total of 18 test specimens, nine short term aged and nine long term aged.

8.4   Follow Section 6 for warming up the system, installing the specimens for testing, and set the target temperature on the environmental system to 4°C.

8.5   To minimize the amount of damage to the specimen, testing must be conducted in a manner where the test temperatures are applied from lowest to highest, with the imposed deformation on the specimen also applied from lowest to highest. Therefore, the testing sequence will utilized the following order: 1) Simple Shear at Constant Height tested at 4°C, 2) Frequency Sweep at Constant Height tested at 40°C, 3) Simple Shear at Constant Height tested at 40°C, and 4) Repeated Shear at Constant Height tested at 64°C.

8.6   Check that the environmental system and the dummy sample has reached equilibrium (4°C).

8.7   Conduct the simple shear test at constant height.

   8.7.1   Perform the test by increasing the shear stress at a rate of 70 kPa/sec until 345 +/- 5 kPa is reached. Maintain the stress at the specified level for 10 +/- 1 seconds. Reduce the shear stress to 0 kPa at a rate of 25 +/- 1 kPa/second. Continue the test at 0 kPa for an additional 10 +/- 1 seconds. During the test, maintain the specimen height constant, within +/- 0.013 mm by applying sufficient axial stress during the loading and un-loading cycle. This is accomplished by controlling the vertical actuator using closed-loop feedback from the axial LVDT.

   8.7.2   Record the axial and shear deformations (from the LVDT's) and axial and shear loads. Record at a minimum rate of 50 data points per second, as shown in Table 2.

   8.7.3   At the conclusion of the test, release the loads and return the actuators to the pre-test position. Switch the control back to the actuators (from the axial LVDT) and make sure no residual loading is being applied to the sample.

8.8   Follow Section 7.3 until the Section 7.8.5.

8.9   The Full Procedure should then be conducted on the aged samples. Again, follow Section 8 until all test temperatures (4, 40, and 64°C) and tests (Simple Shear, Frequency Sweep and Repeated Shear) have been conducted.